Middle Rio Grande Escondida Reach:

Morpho-dynamic Processes and Silvery Minnow Habitat
from Escondida Bridge to US-380 Bridge
(1918-2018)

August 2020
Master of Science
Plan B Technical Report

Prepared by:
Tori Beckwith

Prepared for:
Dr. Pierre Julien
Dr. Peter Nelson
Dr. Tracy Perkins

Colorado State University
Engineering Research Center
Department of Civil and
Environmental Engineering
Fort Collins, Colorado 80523

Abstract

The Escondida reach spans approximately 16 miles of the Middle Rio Grande (MRG), from the Escondida Bridge to the US HWY 380 Bridge near San Antonio, New Mexico. This reach report focuses on the morpho-dynamic processes within the Escondida reach. The reach is divided into five subreaches (E1, E2, E3, E4, and E5) to illustrate the spatial and temporal trends of the channel geometry and morphology of the dynamic river, still changing in response to anthropogenic impacts over the last century (Posner, 2017).

Discharge and sediment data from the United States Geological Survey were used to identify the seasons of peak discharge and sediment load in the reach. While spring snowmelt leads to peak discharge volumes, monsoonal thunderstorms often transport the greatest amount of suspended sediment. Since 2009, the average discharge has been about 0.48 million acre-ft/yr with an average suspended sediment load of about 7,000 tons per day during the period of available data.

Digitized planforms created from aerial photographs dating back to 1918 were analyzed through geographic information system (GIS) to evaluate the changes in width and sinuosity. Anthropogenic changes and droughts led to significant narrowing throughout the early to mid-1900s, but the width has stabilized between 300 and 500 feet. While the sinuosity of the reach has remained low for most subreaches, it has been increasing since the 1990s. The Escondida reach contains a “pivot point” in which the sand bed river transitions from a degrading channel to an aggrading channel. The upstream subreach has degraded about 2 feet between the years 1962 and 2012, while the downstream subreach has aggraded approximately 1 foot.

Application of Massong et al.’s 2010 geomorphic conceptual model for the Middle Rio Grande was used to classify the Escondida subreaches as migrating or aggrading stages. The upstream end of the reach has excess transport capacity (leading to degradation), while the downstream subreaches have a sediment supply that exceeds the capacity (leading to aggradation). After analyzing changes to the cross-section geometry and aerial imagery, E1, E2, and E3 have been classified in the migrating stages, while E4 and E5 are in the aggrading stages.

Velocity and depth measurements were estimated through HEC-RAS to identify areas of hydraulically suitable habitat for the endangered Rio Grande Silvery Minnow (RGSM) throughout the Escondida reach. Subreaches E1 and E2 provide the least amount of hydraulically suitable habitat, while subreaches E4 and E5 show the greatest amount of possible habitat. Detailed mapping was performed to illustrate where in the Escondida reach habitable areas exist for the RGSM. The habitat maps indicate that while E5 may contain a large inundated area that meets the RGSM velocity and depth criteria, perching prevents connection to the channel at most discharges. Subreach E4, rather, provides hydraulically suitable habitat that remains connected to the channel, and therefore may be more accessible for the RGSM.

Table of Contents

Abstract I
List of Tables V
List of Figures V
Appendix A List of Figures VIII
Appendix B List of Figures VIII
Appendix C List of Figures VIII
Appendix D List of Figures VIII
Appendix E List of Figures X
Appendix F List of Figures XI
Introduction 1
1.1 Site Description 1
1.2 Aggradation/Degradation Lines and Rangelines 2
1.3 Subreach Delineation 2
2. Precipitation, Flow and Sediment Discharge Analysis 6
2.1 Precipitation 6
2.2 River Flow 8
2.2.1 Cumulative Discharge Curves 11
2.2.2 Flow Duration 13
2.3 Suspended Sediment Load 17
2.3.1 Single Mass Curve 17
2.3.2 Double Mass Curve 19
2.3.3 Monthly Sediment Variation 20
3. Geomorphic and River Characteristics 22
3.1 Wetted Top Width 22
3.2 Width (Defined by Vegetation) 24
3.3 Bed Elevation 25
3.4 Bed Material 28
3.5 Sinuosity 28
3.6 Hydraulic Geometry 29
3.7 Mid-Channel Bars and Islands 32
3.9 Channel Response Models 35
3.10 Geomorphic Conceptual Model 36

4. HEC-RAS Modeling for Silvery Minnow Habitat 48
4.1 Modeling Data and Background 48
4.2 Width Slices Methodology 49
4.3 Width Slices Habitat Results 50
4.4 RAS-Mapper Methodology 55
4.5 RAS-Mapper Habitat Results in 2012 55
4.6 Disconnected Areas 56
5. Time-Integrated Habitat Metric 58
6. Conclusions 60
7. Bibliography 62
Appendix A A-1
Appendix B B-1
Appendix C C-1
Wetted Top Width Plots C-2
Appendix D D-1
Width Slices: Habitat Bar Charts D-2
Stacked Habitat Charts D-10
Appendix E E-1
Appendix F F-1

List of Tables

Table 1 Escondida Subreach Delineation 3
Table 2 List of gages used in this study 8
Table 3 Probabilities of exceedance for both gages 13
Table 4 Julien and Wargadalem channel width prediction 35
Table 5 Rio Grande Silvery Minnow habitat velocity and depth range requirements (from Mortensen et al., 2019) 48

List of Figures

Figure 1 Map with the Middle Rio Grande outlined in blue. It begins at the Cochiti Dam (top) and continues downstream to the Narrows in Elephant Butte Reservoir (bottom). The lime green highlights the Escondida reach. 1
Figure 2 Subreach Delineation: Subreaches E1 (top left), E2 (right), and E3 (bottom left). 4
Figure 3 Subreach Delineation: Subreaches E4 (left) and E5 (right). 5

Figure 4 BEMP data collection sites (figure source: http://bemp.org) 6
Figure 5 Monthly precipitation trends near the Escondida reach 7
Figure 6 Cumulative precipitation near the Escondida reach 7
Figure 7 Raster hydrograph of daily discharge at USGS 08354900 Rio Grande Floodway at San Acacia, NM 9
Figure 8 Raster hydrograph of daily discharge at USGS Station 08355050 near Escondida, NM 9
Figure 9 Raster hydrograph of daily discharge at USGS Station 08355490 near San Antonio, NM 10
Figure 10 Raster hydrograph of daily discharge at USGS Station 0835550 at San Antonio, NM (inactive gage near USGS Station 08355490) 10
Figure 11 Discharge single mass curve at the Escondida and San Antonio gages (top) and San Acacia gage (bottom) 12
Figure 12 Cumulative discharge plotted against cumulative precipitation at the US 380 gage near San Antonio, NM 13
Figure 13 Flow Duration Curve for USGS Gage 08355050 Rio Grande at Bridge Near Escondida, NM (left) and USGS Gage 08355490 Rio Grande at HWY 380 Bridge Near San Antonio, NM (right) using the mean daily flow discharge values 14
Figure 14 Comparison of flow duration curves. The Escondida and San Antonio Gage include data since the year 2005 and the San Acacia curve is based off of data post Cochiti Dam (1975). 14
Figure 15 Number of days over an identified discharge at the Escondida gage 15
Figure 16 Number of days over an identified discharge at the HWY 380 gage 16
Figure 17 Number of days over an identified discharge at the HWY 380 gage including historical gage data 16
Figure 18 Suspended sediment discharge single mass curve for US 380 Bridge USGS gage Near San Antonio, NM (top) and Rio Grande Floodway at San Acacia, NM (bottom) 18
Figure 19 Double Mass Curve for the US HWY 380 Bridge Gage near San Antonio, NM 19
Figure 20 Cumulative suspended sediment (data from the US 380 gage at San Antonio, NM) versus cumulative precipitation at the Lemitar gage. 20
Figure 21 Monthly average suspended sediment and water discharge 21
Figure 22 Monthly average suspended sediment concentration and water discharge 21
Figure 23 Moving cross sectional average of the wetted top width at a discharge 1,000 cfs 22
Figure 24 Moving cross sectional average of the wetted top width at a discharge 3,000 cfs 23
Figure 25 Average top width for E1 (top left), E2 (top right), E3 (middle left), E4 (middle right), and E5 (bottom) at discharges 500 to 5,000 cfs 24
Figure 26 Averaged active channel width by subreach 25

Figure 27 Longitudinal profiles of bed elevation.....26
Figure 28 Degradation and Aggradation by subreach.....27
Figure 29 Median grain diameter size of samples taken throughout the Escondida reach 28
Figure 30 Sinuosity by subreach.....29
Figure 31 HEC-RAS Wetted top width of channel at 1,000 cfs (left) and 3,000 cfs (right).....30
Figure 32 HEC-RAS Hydraulic depth at 1,000 cfs (left) and 3,000 cfs (right) 30
Figure 33 Example cross section indicating that the banks are aggrading in addition to the main channel bed. On average, throughout the reach, there was also a decrease in top wetted width.....31
Figure 34 Wetted Perimeter at 1000 cfs (left) and 3000 cfs (right) 31
Figure 35 Bed Slope.....32
Figure 36 Average number of channels at the agg/deg lines in each subreach.....33
Figure 37 Digitized planform and aerial photograph of subreach E5 when multiple mid-channel bars and islands were present in 2002 (left) and in 2012 (right) after a reduction of mid-channel bars and islands.34
Figure 38 Julien and Wargadalam predicted widths and observed widths of the channel.....36
Figure 39 Planform evolution model from Massong et al. (2010). The river undergoes stages 1-3 first and then continues to stages A4-A6 or stages M4-M8 depending on the sediment transport capacity.....37
Figure 40 Channel evolution of a representative cross section from subreach E1 38
Figure 41 Subreach E1: historical cross section profiles and corresponding aerial images.....39
Figure 42 Channel evolution of a representative cross section from subreach E2 40
Figure 43 Subreach E2: historical cross section profiles and corresponding aerial images.....41
Figure 44 Channel evolution of a representative cross section from subreach E3 42
Figure 45 Subreach E3: historical cross section profiles and corresponding aerial images.....43
Figure 46 Channel Evolution of a representative cross section of subreach E4 44
Figure 47 Subreach E4: historical cross section profiles and corresponding aerial images.....45
Figure 48 Channel evolution of a representative cross section of subreach E5.....46
Figure 49 Subreach E5: historical cross section profiles and corresponding aerial images.....47
Figure 50 Comparing the overbanking discharge values at various years. The dashed line (indicating 25% of cross sections in a reach experiencing overbanking) determines the discharge at which computational levees are removed for habitat analysis. 49
Figure 51 Cross-section with flow distribution from HEC-RAS with 20 vertical slices in the floodplains and 5 vertical slices in the main channel. The yellow and green slices are small enough that the discrete color changes look more like a gradient. 50
Figure 52 Larval RGSM habitat availability throughout the Escondida reach- the scale of the y-axis is lower for the larval habitat to better see the trends in the hydraulically suitable habitat.....51

Figure 53 Juvenile RGSM habitat availability throughout the Escondida reach 51
Figure 54 Adult RGSM habitat availability throughout the Escondida reach 52
Figure 55 Stacked habitat charts to display spatial variations of habitat throughout the Escondida reach in 2012 53
Figure 56 Stacked habitat charts to display spatial variations of habitat throughout the Escondida reach in 2012 54
Figure 57 Hydraulically suitable habitat for each life stage in subreach E4 at 1,500 cfs (left) and 5,000 cfs (right) 56
Figure 58 Example of a disconnected area that contains water, but no access to or from the main channel 57
Figure 59 Disconnected area showing hydraulically suitable habitat for RGSM adult (green), juvenile (yellow cross hatch), and larvae (orange) 57
Figure 60 Correlating the discharge values at the San Acacia (Q_{SA}) and Escondida (Q_{ESC}) gages to create a model to estimate the unknown values at the Escondida gage. 58
Figure 61 Habitat curves at 1992 and 2002 from the width slice method, with remaining curves being interpolated from the sediment rating curve. 59
Figure 62 TIHMs for the Escondida reach. In the legend, the numbers in the parentheses indicate the months for which the habitat is accumulated over based on the life stage cycle of the RGSM. For example, months 5 and 6 (May and June) are the months when the new RGSM enter the larval stage. They enter the juvenile stage around month 7 (July) and the adult stage around month 10 (October). 60

Appendix A List of Figures

Figure A- 1 Width (top) and cumulative width (bottom) throughout the Escondida reach for the years 2002 (orange) and 2012 (blue)..... A-2
Figure A- 2 Depth (top) and cumulative depth (bottom) throughout the Escondida reach for the years 2002 (orange) and 2012 (blue)..... A-3

Appendix B List of Figures

Figure B- 1 Comparison between predicted and measured total sediment load (left) and percent difference vs u*/w (right)..... B-2
Figure B- 2 Total sediment rating curve at the San Acacia gage..... B-3
Figure B- 3 the ratio of measured to total sediment discharge vs depth; and (b) the ratio of suspended to total sediment discharge vs h/ds at the San Acacia gage B-3

Appendix C List of Figures

Figure C- 1 Wetted top width at each agg/deg line throughout the Escondida reach at a discharge of 1,000 cfs C-2
Figure C- 2 Wetted top width at each agg/deg line throughout the Escondida reach at a discharge of 3,000 cfs C-2
Figure C- 3 Example of annual habitat interpolating using the sediment rating curve and alpha technique. C-3

Appendix D List of Figures

Figure D- 1 Subreach E1 larva habitat D-2
Figure D- 2 Subreach E1 juvenile habitat D-2
Figure D- 3 Subreach E1 adult habitat D-3
Figure D- 4 Subreach E2 larva habitat D-3
Figure D- 5 Subreach E2 juvenile habitat D-4
Figure D- 6 Subreach E2 adult habitat D-4
Figure D- 7 Subreach E3 Larva Habitat D-5
Figure D- 8 Subreach E3 Juvenile Habitat D-5
Figure D- 9 Subreach E3 Adult Habitat D-6
Figure D- 10 Subreach E4 Larva Habitat D-6
Figure D- 11 Subreach E4 Juvenile Habitat D-7
Figure D- 12 Subreach E4 Adult Habitat D-7
Figure D- 13 Subreach E5 Larva Habitat D-8
Figure D- 14 Subreach E5 Juvenile Habitat D-8
Figure D- 15 Subreach E5 Adult Habitat D-9
Figure D- 16 Stacked habitat charts to display spatial variations of habitat throughout the Escondida reach in 1962 ..... D-10
Figure D- 17 Stacked habitat charts to display spatial variations of habitat throughout the Escondida reach in 1972. ..... D-11
Figure D- 18 Stacked habitat charts to display spatial variations of habitat throughout the Escondida reach in 1992 ..... D-12
Figure D- 19 Stacked habitat charts to display spatial variations of habitat throughout the Escondida reach in 2002 ..... D-13

Figure D- 20 Life stage habitat curves for subreach E1 at the years 1962 (top), 1972 (middle), and 1992 (bottom). D-14
Figure D- 21 Life stage habitat curves for subreach E1 for the years 2002 (top) and 2012 (bottom). ... D-15
Figure D- 22 Life stage habitat curves for subreach E2 at the years 1962 (top), 1972 (middle), and 1992 (bottom). D-16
Figure D- 23 Life stage habitat curves for subreach E2 for the years 2002 (top) and 2012 (bottom). ... D-17
Figure D- 24 Life stage habitat curves for subreach E3 at the years 1962 (top), 1972 (middle), and 1992 (bottom) D-18
Figure D- 25 Life stage habitat curves for subreach E3 for the years 2002 (top) and 2012 (bottom) D-19
Figure D- 26 Life stage habitat curves for subreach E4 at the years 1962 (top), 1972 (middle), and 1992 (bottom). D-20
Figure D- 27 Life stage habitat curves for subreach E4 for the years 2002 (top) and 2012 (bottom). ... D-21
Figure D- 28 Life stage habitat curves for subreach E5 at the years 1962 (top), 1972 (middle), and 1992 (bottom). D-22
Figure D- 29 Life stage habitat curves for subreach E5 for the years 2002 (top) and 2012 (bottom). ... D-23

Appendix E List of Figures

Figure E- 1 RGSM Habitat in subreach E1 at 1500 cfs with hydraulically suitable areas labeled for larvae (green), juvenile (orange), and adult (light blue) and unsuitable inundated areas in dark blue. E-2
Figure E- 2 RGSM Habitat in subreach E2 (upstream portion part a) at 1500 cfs with hydraulically suitable areas labeled for larvae (green), juvenile (orange), and adult (light blue) and unsuitable inundated areas in dark blue. E-3
Figure E- 3 RGSM Habitat in subreach E2 (downstream portion part b) at 1500 cfs with hydraulically suitable areas labeled for larvae (green), juvenile (orange), and adult (light blue) and unsuitable inundated areas in dark blue. E-4
Figure E- 4 RGSM Habitat in subreach E3 at 1500 cfs with hydraulically suitable areas labeled for larvae (green), juvenile (orange), and adult (light blue) and unsuitable inundated areas in dark blue. E-5
Figure E- 5 RGSM Habitat in subreach E4 at 1500 cfs with hydraulically suitable areas labeled for larvae (green), juvenile (orange), and adult (light blue) and unsuitable inundated areas in dark blue. E-6
Figure E- 6 RGSM Habitat in subreach E5 at 1500 cfs with hydraulically suitable areas labeled for larvae (green), juvenile (orange), and adult (light blue) and unsuitable inundated areas in dark blue. E-7
Figure E- 7 RGSM Habitat in subreach E1 at 3000 cfs with hydraulically suitable areas labeled for larvae (green), juvenile (orange), and adult (light blue) and unsuitable inundated areas in dark blue. E-8

Figure E- 8 RGSM Habitat in subreach E2 (upstream portion part a) at 3000 cfs with hydraulically suitable areas labeled for larvae (green), juvenile (orange), and adult (light blue) and unsuitable inundated areas in dark blue. E-9
Figure E- 9 RGSM Habitat in subreach E2 (downstream portion part b) at 3000 cfs with hydraulically suitable areas labeled for larvae (green), juvenile (orange), and adult (light blue) and unsuitable inundated areas in dark blue. E-10
Figure E- 10 RGSM Habitat in subreach E3 at 3000 cfs with hydraulically suitable areas labeled for larvae (green), juvenile (orange), and adult (light blue) and unsuitable inundated areas in dark blue. At 3,000 cfs, computational levees have not been removed from th E-11
Figure E- 11 RGSM Habitat in subreach E4 at 3000 cfs with hydraulically suitable areas labeled for larvae (green), juvenile (orange), and adult (light blue) and unsuitable inundated areas in dark blue. .. E-12
Figure E- 12 RGSM Habitat in subreach E5 at 3000 cfs with hydraulically suitable areas labeled for larvae (green), juvenile (orange), and adult (light blue) and unsuitable inundated areas in dark blue. At 3,000 cfs, computational levees have not been removed from th E-13
Figure E- 13 RGSM Habitat in subreach E1 at 5000 cfs with hydraulically suitable areas labeled for larvae (green), juvenile (orange), and adult (light blue) and unsuitable inundated areas in dark blue. .. E-14
Figure E- 14 RGSM Habitat in subreach E2 (upstream portion part a) at 5000 cfs with hydraulically suitable areas labeled for larvae (green), juvenile (orange), and adult (light blue) and unsuitable inundated areas in dark blue. E-15
Figure E- 15 RGSM Habitat in subreach E2 (downstream portion part b) at 5000 cfs with hydraulically suitable areas labeled for larvae (green), juvenile (orange), and adult (light blue) and unsuitable inundated areas in dark blue. E-16
Figure E- 16 RGSM Habitat in subreach E3 at 5000 cfs with hydraulically suitable areas labeled for larvae (green), juvenile (orange), and adult (light blue) and unsuitable inundated areas in dark blue. .. E-17
Figure E- 17 RGSM Habitat in subreach E4 at 5000 cfs with hydraulically suitable areas labeled for larvae (green), juvenile (orange), and adult (light blue) and unsuitable inundated areas in dark blue ... E-18
Figure E- 18 RGSM Habitat in subreach E5 at 5000 cfs with hydraulically suitable areas labeled for larvae (green), juvenile (orange), and adult (light blue) and unsuitable inundated areas in dark blue. .. E-19

Appendix F List of Figures

Figure F- 1 Geomorphology and habitat connections collage for subreach E1 ..... F-2
Figure F- 2 Geomorphology and habitat connections collage for subreach E2 ..... F-3
Figure F- 3 Geomorphology and habitat connections collage for subreach E3 ..... F-4

Figure F- 4 Geomorphology and habitat connections collage for subreach E4 ..... F-5
Figure F- 5 Geomorphology and habitat connections collage for subreach E5 ..... F-6

Introduction

The purpose of this reach report is to evaluate the morpho-dynamic conditions of the Middle Rio Grande (MRG) which extends from the Cochiti Dam to the Narrows in Elephant Butte Reservoir. The report focuses on the Escondida reach, which begins at a bridge near Escondida, New Mexico, and continues downstream to the US 380 Bridge near San Antonio, New Mexico (Figure 1).

This report focuses on understanding trends of the physical conditions of the Escondida reach. Specific objectives include:

- Summarize the flow and sediment discharge conditions and trends for the period of record available from United States Geological Survey (USGS) gages;
- Analyze geomorphic characteristics at a subreach level (sinuosity, width, bed elevation, bed material, and other hydraulic parameters);
- Link changes in the river geomorphology with shifts in sediment and flow trends;
- Classify subreaches using a geomorphic conceptual model; and
- Characterize Rio Grande Silvery Minnow habitat throughout the Escondida reach.

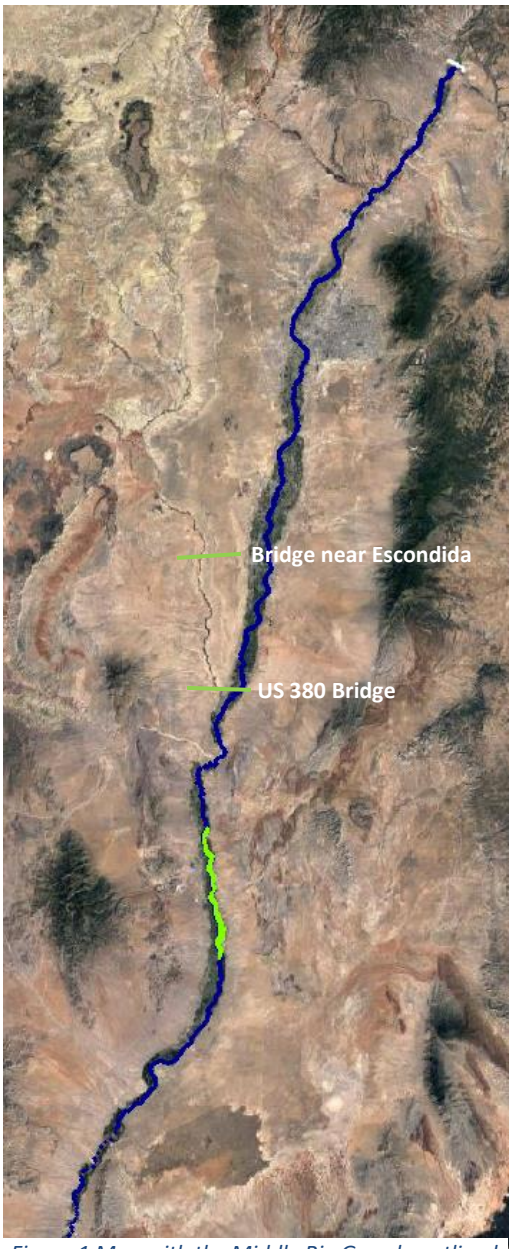

Figure 1 Map with the Middle Rio Grande outlined in blue. It begins at the Cochiti Dam (top) and continues downstream to the Narrows in Elephant Butte Reservoir (bottom). The lime green highlights the Escondida reach.

1.1 Site Description

The Rio Grande begins in the San Juan mountain range of Colorado and continues into New Mexico. It follows along the Texas-Mexico border before reaching the Gulf of Mexico. The Middle Rio Grande is the stretch from the Cochiti Dam to Elephant Butte Reservoir. The MRG has historically been affected by periods of drought and large spring flooding events due to snowmelt. These floods often caused large scale shifts in the course of the river and rapid aggradation (Massong et al., 2010). Floods helped maintain aquatic ecosystems by enabling connection of water between the main channel and the floodplains (Scurlock, 1998), but consequently threatened human establishments that were built near the Rio Grande. Beginning in the 1930s, levees were installed to prevent flooding. Beginning in the 1950s, the USBR undertook a significant channelization effort involving jetty jacks, river straightening and other techniques. Upstream dams built in the 1950s were used to store and regulate flow in the river. While

these efforts enabled agriculture and large-scale human developments to thrive along the MRG, they also fundamentally changed the river, which led to reduced peak flows and sediment supply while altering the channel geometry and vegetation (Makar, 2006). In parts of the MRG, narrowing of the river continues, with channel degradation due to limited sediment supply and the formation of vegetated bars that encroach into the channel (Varyu, 2013; Massong et al., 2010). Farther downstream, closer to Elephant Butte Reservoir, aggradation and sediment plugs have been observed. These factors have created an ecologically stressed environment, as seen in the decline of species such as the Rio Grande Silvery Minnow (Mortensen et al., 2019).

The Escondida reach is a part of the Middle Rio Grande located in central New Mexico. This reach begins at a bridge that crosses the Rio Grande near Escondida and continues approximately 15.7 miles downstream to the US HWY 380 Bridge near San Antonio, New Mexico. Eight small tributaries enter the Escondida reach- most of these arroyos contributing greatly to the sediment load throughout the reach (Larsen, 2007).

1.2 Aggradation/Degradation Lines and Rangelines

Aggradation/degradation lines (agg/deg lines) are "spaced approximately 500-feet apart and are used to estimate sedimentation and morphological changes in the river channel and floodplain for the entire MRG" (Posner, 2017). Each agg/deg line is surveyed approximately every 10 years, when the USBR performs monitoring, and is established as a cross-section in the Rio Grande HEC-RAS models. The most recent entire MRG survey was performed in 2012. Cross-sectional geometry at each agg/deg line is available from models developed by the Technical Service Center (Varyu,2013). Models are available for 1962, 1972, 1992, 2002 and 2012. The 2012 model was developed from LiDAR data, but models prior to 2012 used photogrammetry techniques. All models use the NAVD88 vertical datum. In addition to agg/deg lines, rangelines are used as location identifiers in this analysis. The rangelines, created prior to the use of agg/deg lines, were determined in association with geomorphic factors, such as migrating bends, incision, or river maintenance issues. Repeat surveys are implemented along these cross-section lines, as well as bed material samples.

1.3 Subreach Delineation

To analyze the hydraulic trends, the Escondida reach was divided into five sections. These subreaches were primarily delineated by large confluences, structures or cumulative plots of hydraulic variables such as channel top width and flow depth. Subreaches were designated when there was a noticeable change in the slope of the cumulative plots. All cumulative plots used in the delineations can be found in Appendix A. These plots were developed using a HEC-RAS model with the 2002 and 2012 geometry provided by the USBR. A flow of 3,000 cfs was selected for cumulative plots of hydraulic variables to be consistent with previous reach reports (LaForge et al., 2019; Yang et al., 2019). This is the nominal discharge that fills the main channel without overbanking. The daily percent exceedance for 3,000 cfs is approximately 4.6% at the bridge near Escondida, NM, at the upstream end of the reach.

Subreach Escondida 1 (E1) extends from the Escondida Bridge (agg/deg line 1313) downstream to a low radius bend (agg/deg line 1345). Subreach E2 continues from the low radius bend and ends at a confluence with the Arroyo De Las Cañas (agg/deg line 1397). E3 continues until a change in the cumulative width of the river (agg/deg line 1420), where the river gets wider. The beginning of E4 is at the expansion and continues until a narrowing of the river (agg/deg line 1448). This narrowing is due to

pumping from the Low Flow Conveyance Channel (LFCC) that waters vegetation at the nearby site. The final subreach, E5, begins at the contraction of the river and continues until the US HWY 380 Bridge (agg/deg line 1475), which also marks the end of the entire Escondida reach. The subreaches are shown in Figures 2 and 3. The subreach delineation is summarized in Table 1.

Table 1 Escondida Subreach Delineation

Escondida Reach		
Subreach	**Agg/deg lines**	**Justification**
E1	1313-1345	Start: Escondida Bridge End: Low Radius Bend
E2	1345-1397	Start: Low Radius Bend End: Confluence with Arroyo De Las Cañas
E3	1397-1420	Start: Confluence with Arroyo De Las Cañas End: Change in cumulative width (wider)
E4	1420-1448	Start: Change in cumulative width (wider) End: Change in cumulative width (narrower)
E5	1448-1475	Start: Change in cumulative width (narrower) End: US 380 Bridge near San Antonio, NM

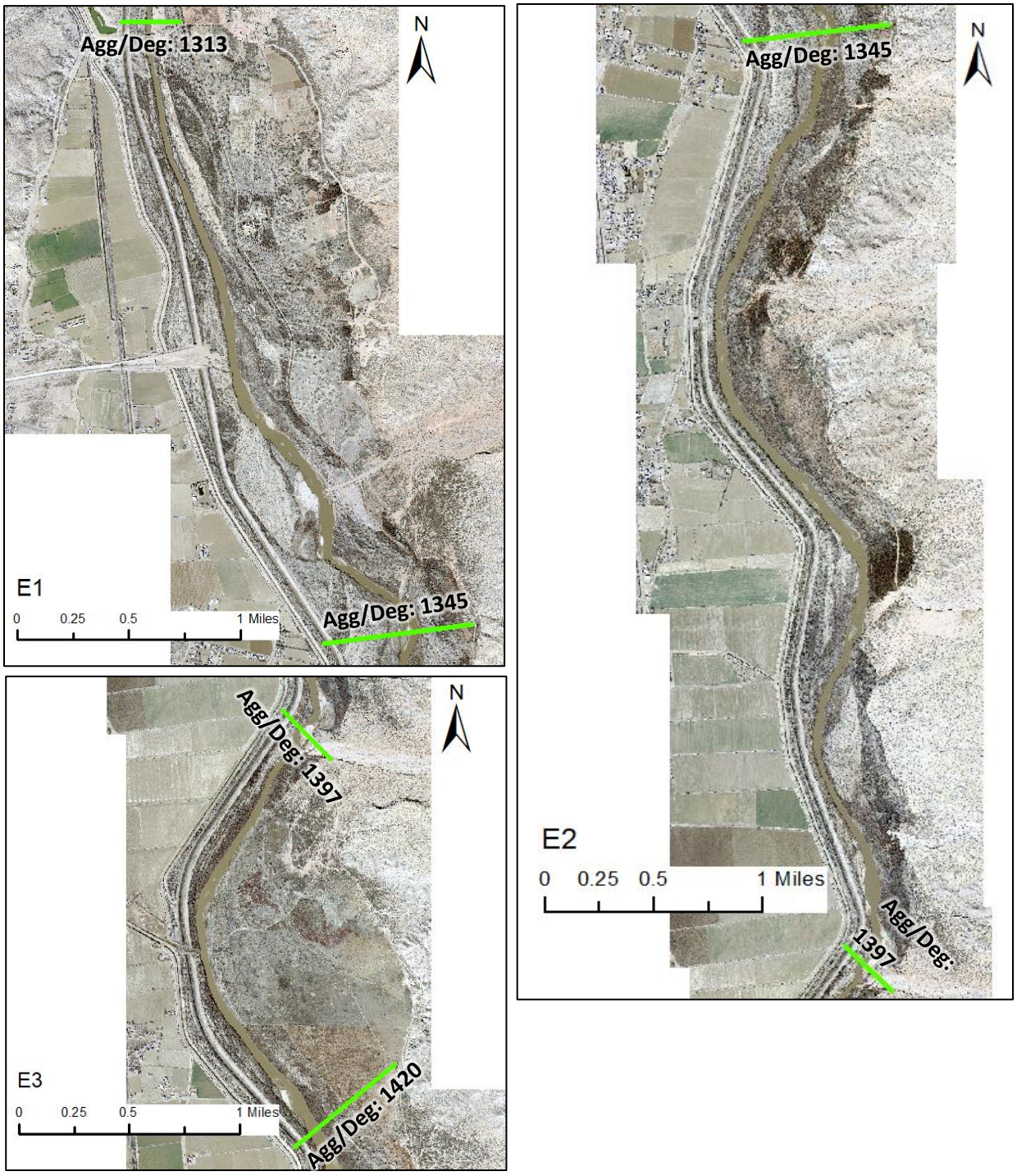

Figure 2 Subreach Delineation: Subreaches E1 (top left), E2 (right), and E3 (bottom left).

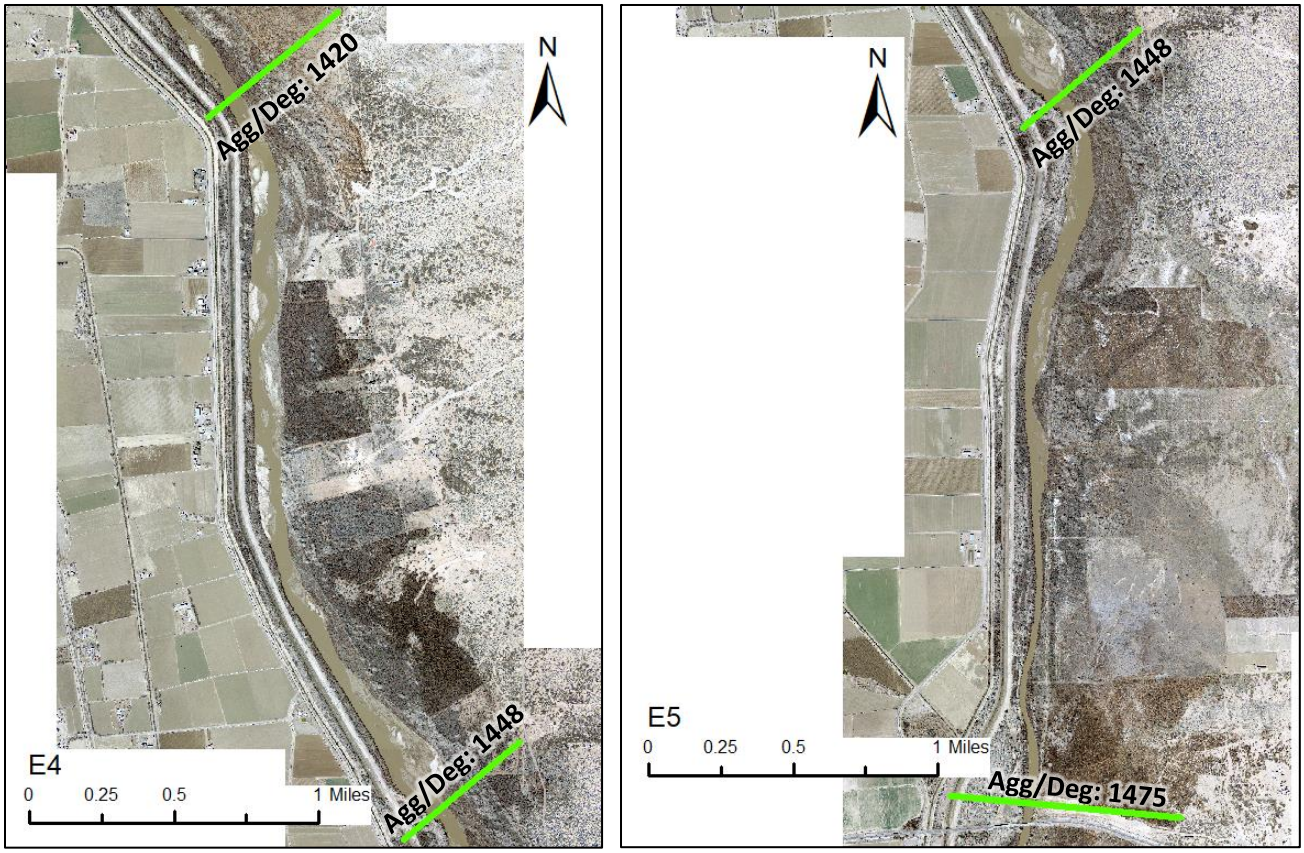

Figure 3 Subreach Delineation: Subreaches E4 (left) and E5 (right).

2. Precipitation, Flow and Sediment Discharge Analysis

2.1 Precipitation

Precipitation data are collected along the MRG by the Bosque Ecosystem Monitoring Program from University of New Mexico (BEMP Data, 2017). The locations of the data collection are shown in Figure 4. The Sevilleta site is near the San Acacia Diversion Dam, and the Lemitar site is North of Escondida, just outside of Lemitar, New Mexico. Both sites were used in the precipitation analysis.

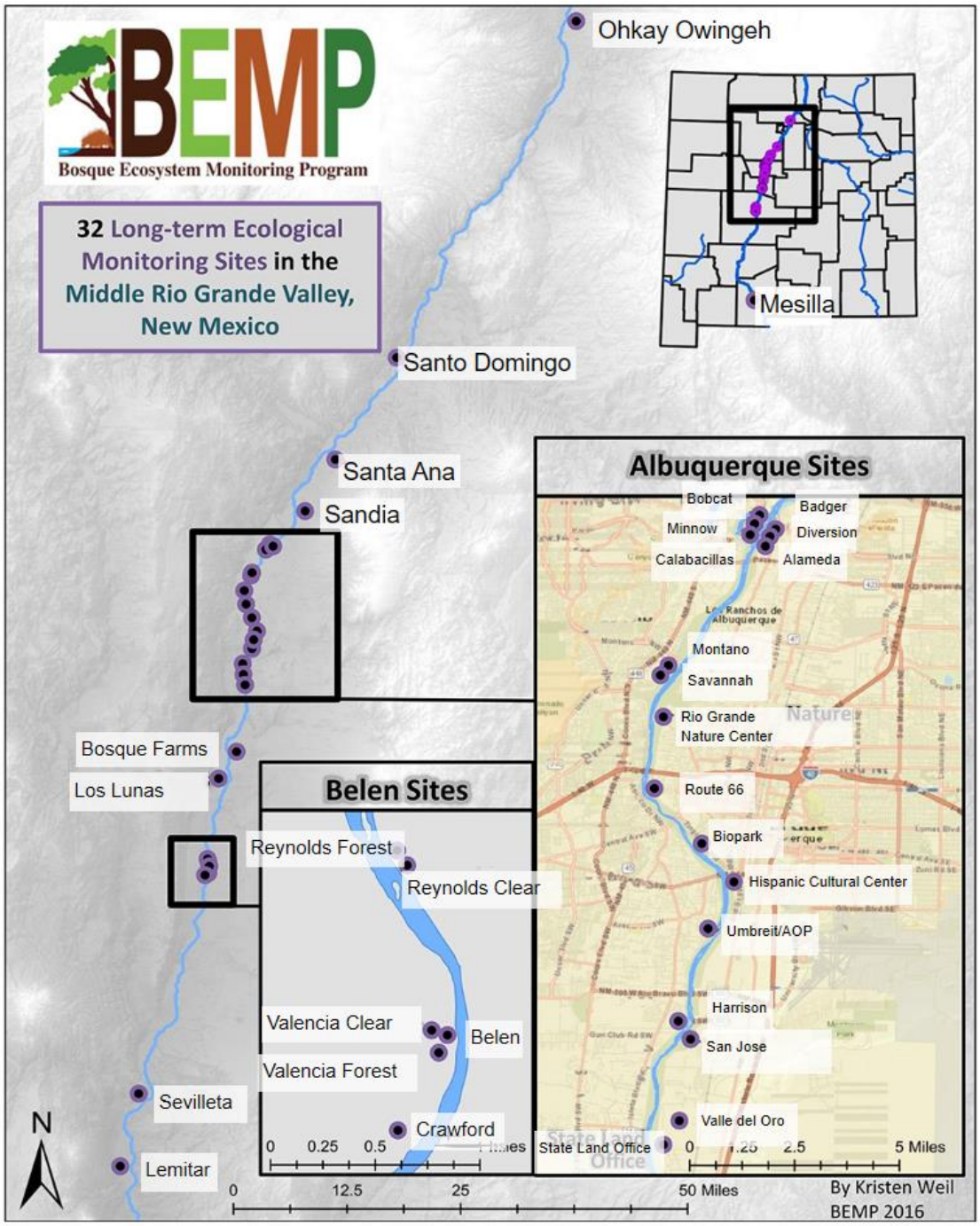

Figure 4 BEMP data collection sites (figure source: http://bemp.org)

The precipitation data are shown in Figure 5. The highest precipitation peak occurred in August of 2006 at the Lemitar gage, with 5.5 inches of rainfall. A general trend was observed with highest precipitation values occurring during monsoon season (late July through early September). A cumulative plot of rainfall (Figure 6) shows that individual rain events can greatly affect the overall trend of the data. It further highlights the monsoonal rains, which create a "stepping" pattern with higher rainfall in August and September, and lower levels throughout the rest of the year. The comparison of the cumulative precipitation at the two sites also shows that the Lemitar gage recieves more precipitation than the Sevilleta gage throughout the time observed.

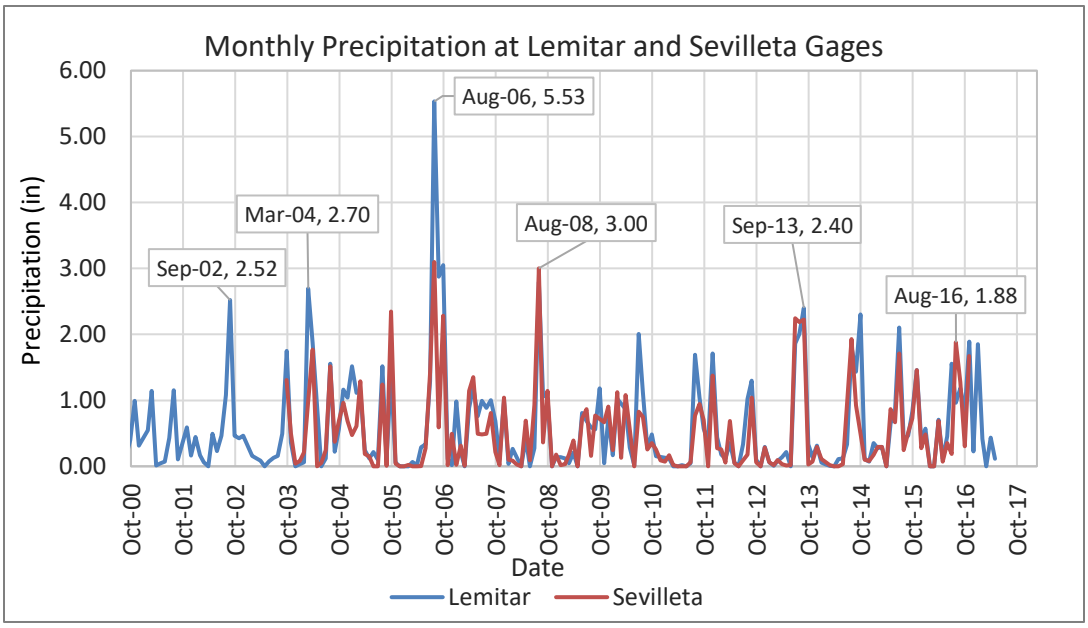

Figure 5 Monthly precipitation trends near the Escondida reach

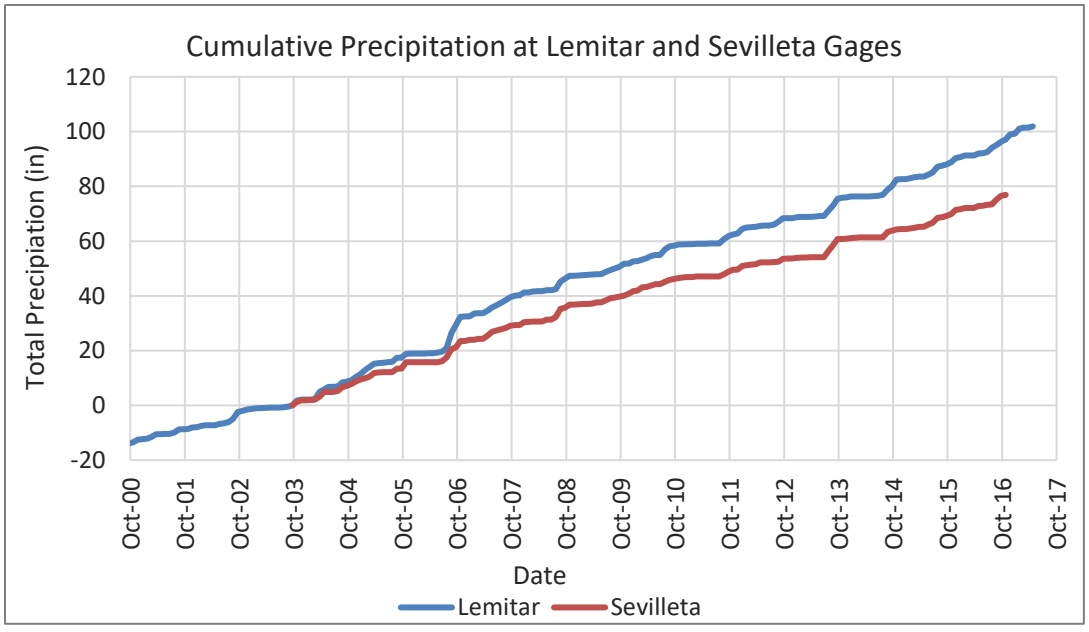

Figure 6 Cumulative precipitation near the Escondida reach

2.2 River Flow

Information regarding river flow was gathered from the United States Geological Survey (USGS) National Water Information System. The gages in the area relevant to the study are included in Table 2.

Table 2 List of gages used in this study

Station	Station Number	Mean Daily Discharge	Suspended Sediment
Rio Grande Floodway at San Acacia	08354900	October 1, 1958 to present	January 5, 1959 to September 30, 2018
Rio Grande at Bridge Near Escondida, NM	08355050	September 30, 2005 to present	No data
Rio Grande above US HWY 380 near San Antonio, NM	08355490	September 30, 2005 to present	October 1, 2011 to September 30, 2018
Rio Grande at San Antonio, NM (Inactive Site)	08355500	April 1, 1951 to June 30, 1957	No data

The gage at San Acacia (08354900) was included in this reach report to provide data for a longer period of time. Further analysis of the San Acacia reach can be found in the reach report "Middle Rio Grande San Acacia Reach: Morphodynamic Processes and Silvery Minnow Habitat from San Acacia Diversion Dam to Escondida Bridge" (Doidge, 2019). The raster hydrographs of the daily discharge at the Rio Grande Floodway at San Acacia (08354900), Rio Grande at the bridge near Escondida (08355050), and US HWY 380 near San Antonio (08355490) gages are shown in Figures 7, 8 and 9, respectively. The raster hydrograph from the inactive site at San Antonio (08355500), which only recorded data between 1951 and 1957, is shown in Figure 10.

The figures show seasonal flow patterns, with peak flow often occurring from snowmelt runoff April through June, low flow throughout the rest of the summer (except for strong summer thunderstorms), and medium flow from November onwards representing the end of the irrigation season.

The raster hydrograph at San Acacia shows much lower flows between 1960 and 1980. While there were periods of drought in the 1960s and 1970s, the severe lack of water at the San Acacia gage in this time period was primarily due to the usage of a Low Flow Conveyance Channel diverting the water away from the main channel.

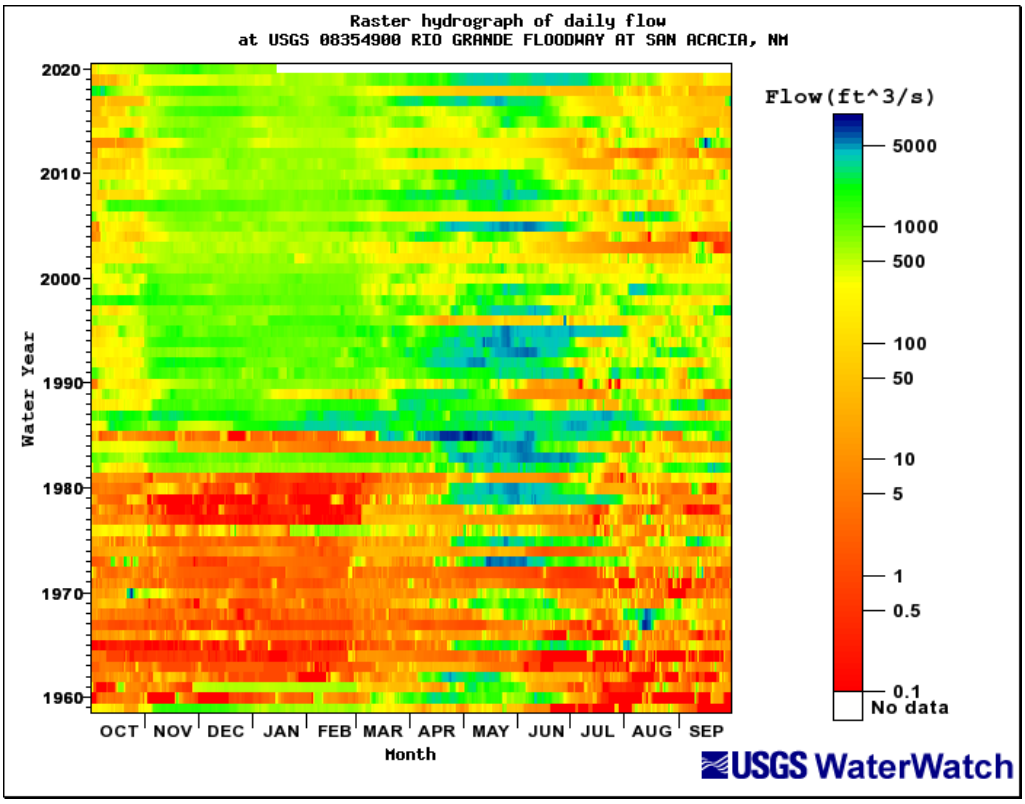

Figure 7 Raster hydrograph of daily discharge at USGS 08354900 Rio Grande Floodway at San Acacia, NM

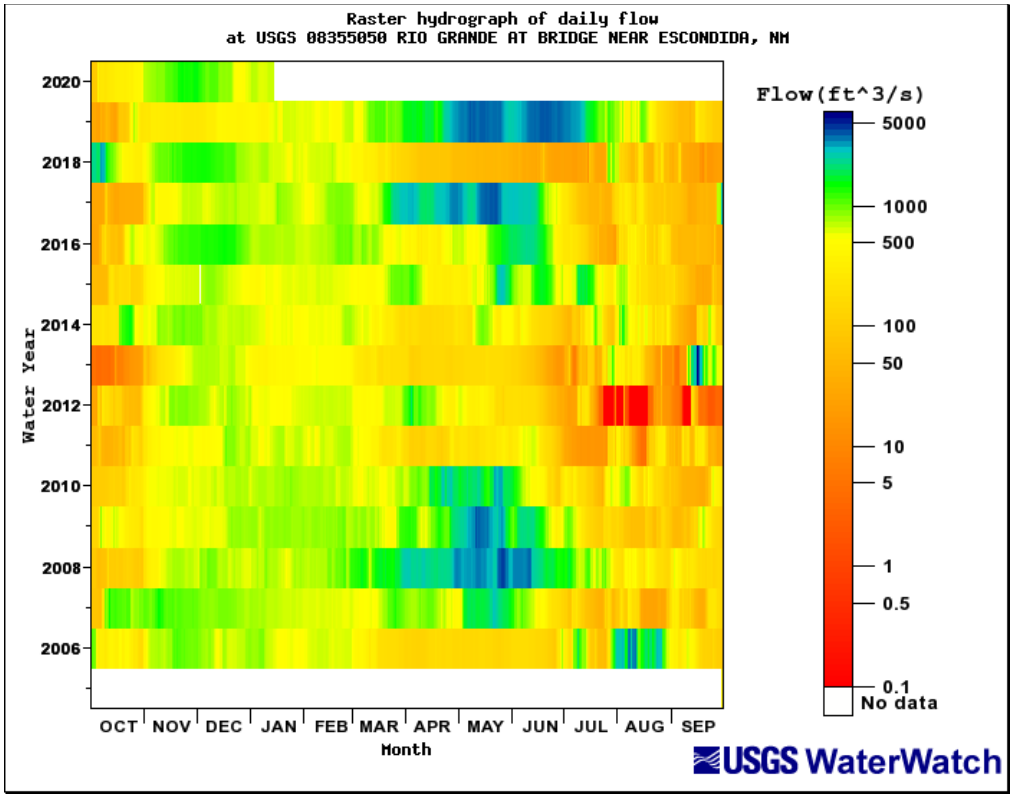

Figure 8 Raster hydrograph of daily discharge at USGS Station 08355050 near Escondida, NM

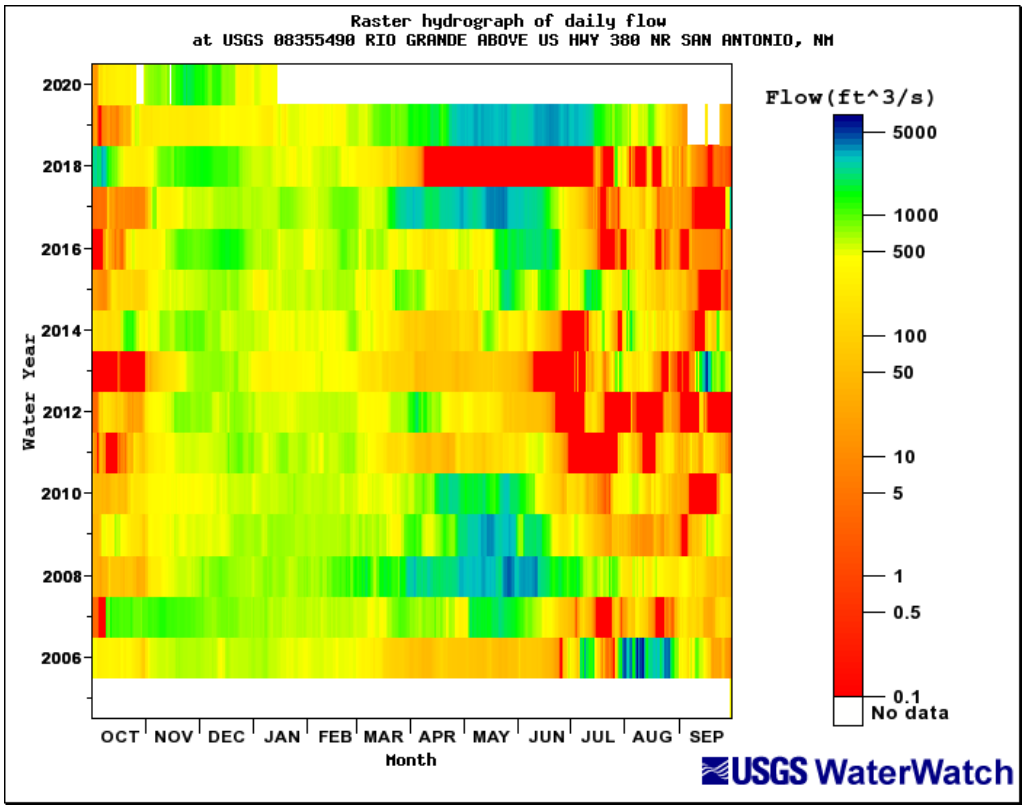

Figure 9 Raster hydrograph of daily discharge at USGS Station 08355490 near San Antonio, NM

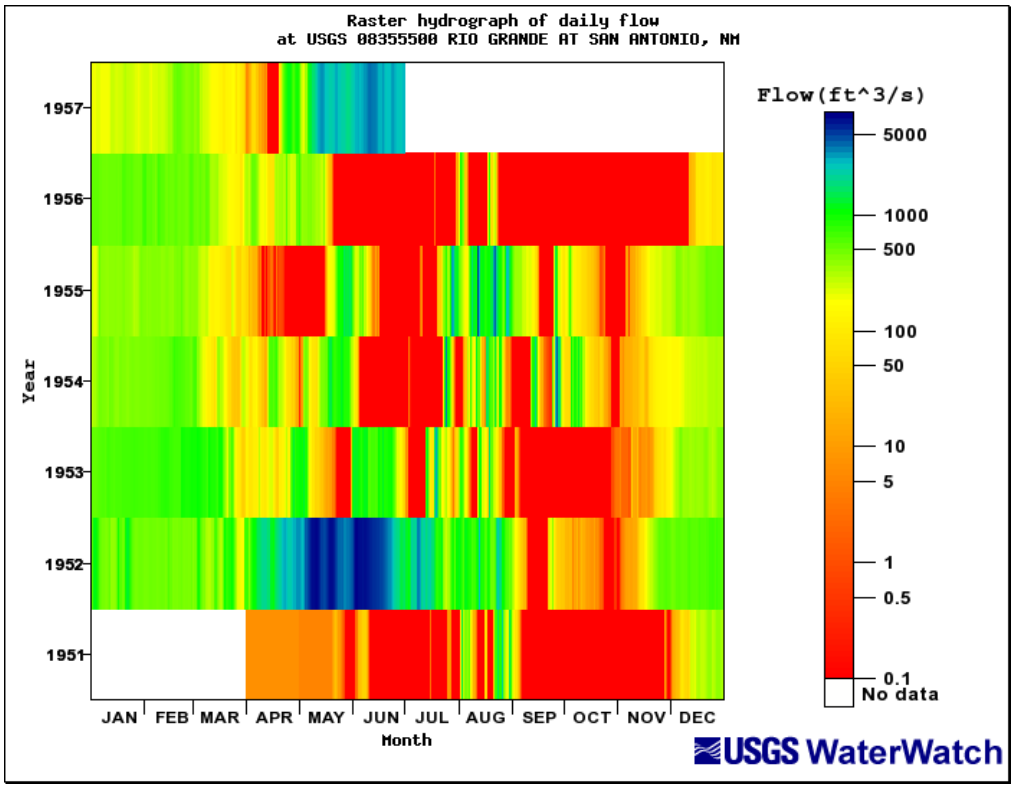

Figure 10 Raster hydrograph of daily discharge at USGS Station 0835550 at San Antonio, NM (inactive gage near USGS Station 08355490)

2.2.1 Cumulative Discharge Curves

Cumulative discharge curves show changes in annual flow volume over a given time period. The slope of the line of the mass curve gives the mean annual discharge, while breaks in the slope show changes in flow volume. Figure 11 shows the mass curves of the gages near Escondida and San Antonio. The mass curves were divided into time periods of similar slopes to analyze long term patterns in discharge. A one-week moving average was used to determine significant breaks in slope. The data callout points represent changes in slope that were greater than the 97.5^{th} percentile of moving-average slope values. This helps to depict the times in which the greatest increase in cumulative discharge occurred. These large increases typically occur between April and June (likely from snowmelt), although noticeable increases can also occur in late August or September from seasonal thunderstorms.

Figure 11 also includes a mass curve created from data at the Rio Grande Floodway gage near San Acacia, NM. This gage has data for a much longer period of record which can help in identifying long term trends. The single mass curve was developed for the time period since the installation of the Cochiti Dam in 1975. Based on the San Acacia single mass curve, there were a few periods where the discharge volume in the river was higher, such as in the mid to late 1980s and again in the early to mid-90s. Given the longer time period analyzed, the detail for many specific events gets washed out. However, an increase in the cumulative discharge can be seen in the year 2017, which was also seen in the Escondida and San Antonio gages. Similar to the cumulative discharge plots at the gages in the Escondida reach, the steeper slopes at the San Acacia gage often occur in the spring months, indicating that snowmelt may have the greatest impact on increasing the flow in the Middle Rio Grande.

Figure 12, which relates the cumulative precipitation and cumulative monthly discharges, can further demonstrate the time periods that experience higher discharges due to snowmelt. A steeper slope indicates that the discharges are increasing with relatively little precipitation. This increase in discharge could occur from snowmelt or possibly controlled release of water from a dam. As seen in Figure 12, many of these increases in discharge with little precipitation occur between February and May. However, there are several noticeable increases in November or October, which could be due to regulated water being released from a dam upstream.

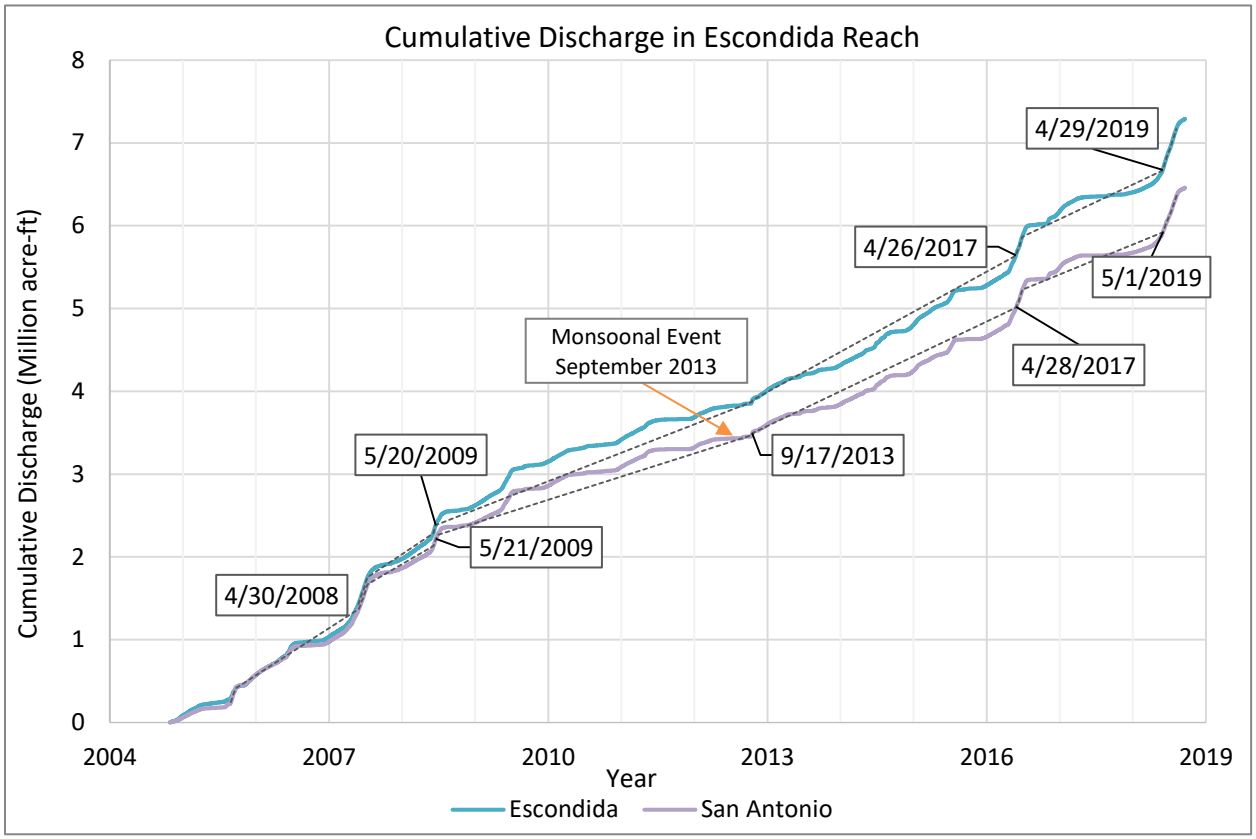

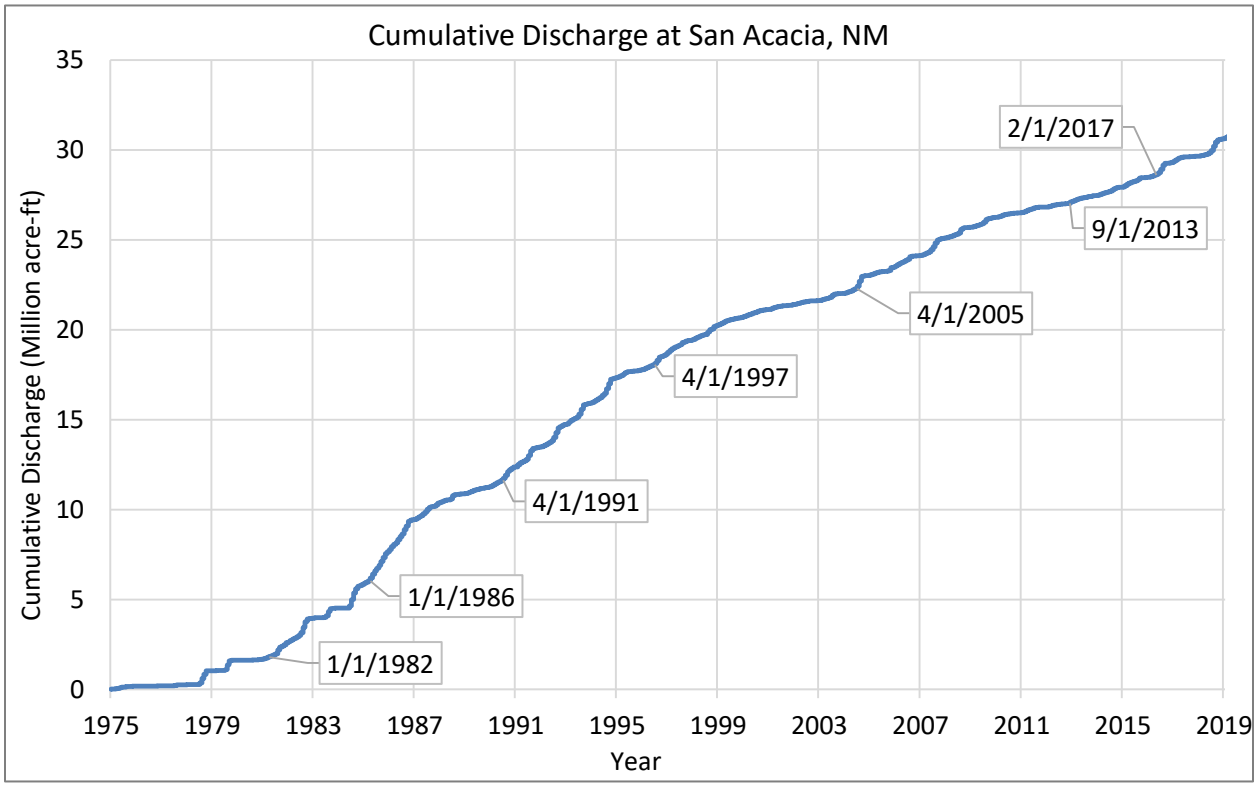

Figure 11 Discharge single mass curve at the Escondida and San Antonio gages (top) and San Acacia gage (bottom)

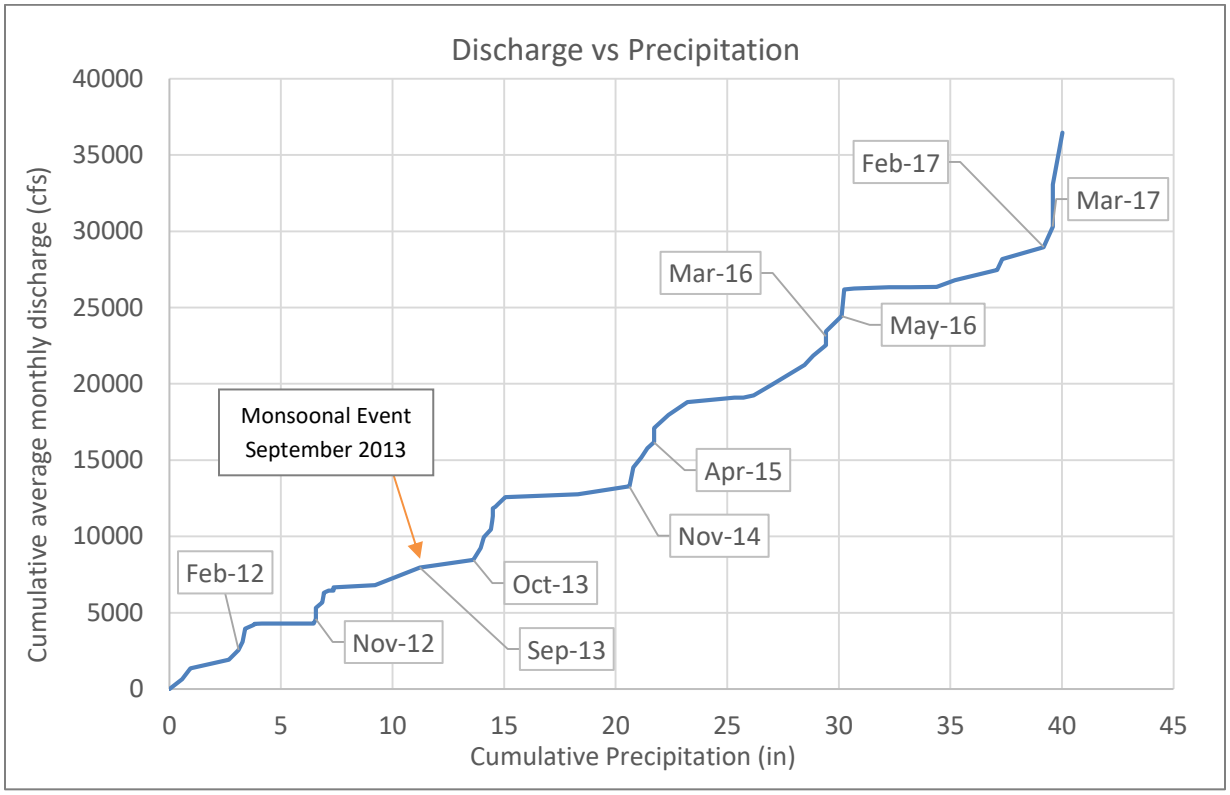

Figure 12 Cumulative discharge plotted against cumulative precipitation at the US 380 gage near San Antonio, NM

2.2.2 Flow Duration

Flow duration curves were developed using the mean daily flow discharge values for the Escondida and San Antonio gages for the complete record (years 2005 to 2019) and for the San Acacia gage since the completion of the Cochiti Dam in 1975. The curves are shown in Figures 13 and 14. Table 3 shows exceedance values calculated from the flow duration curves. The values for the San Antonio gage are slightly lower at every exceedance percentage.

Table 3 Probabilities of exceedance

	Discharge (cfs)		
Probability of Exceedance	08355050 Rio Grande At Bridge Near Escondida, NM (September 30, 2005 - present)	08355490 Rio Grande At HWY 380 Bridge Near San Antonio, NM (September 30, 2005 - present)	08354900 Rio Grande Floodway at San Acacia, NM (October 1, 1975- present)
1%	3900	3730	5270
10%	1640	1600	2580
25%	831	724	1110
50%	570	465	539
75%	170	83	83
90%	55	5	3.2

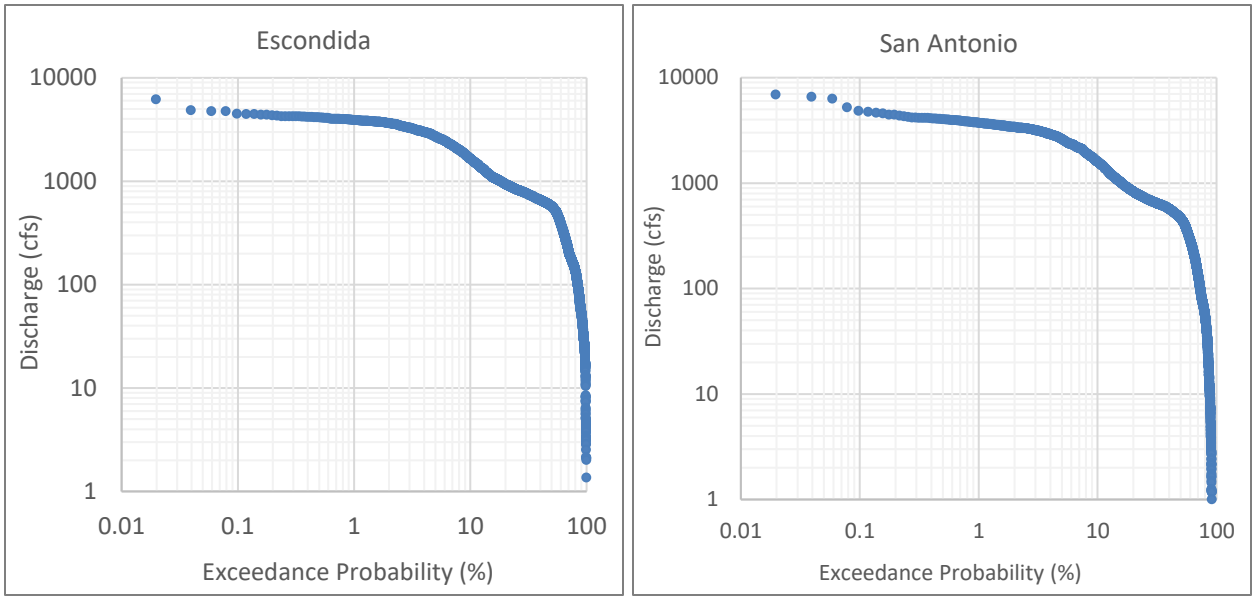

Figure 13 Flow Duration Curve for USGS Gage 08355050 Rio Grande at Bridge Near Escondida, NM (left) and USGS Gage 08355490 Rio Grande at HWY 380 Bridge Near San Antonio, NM (right) using the mean daily flow discharge values

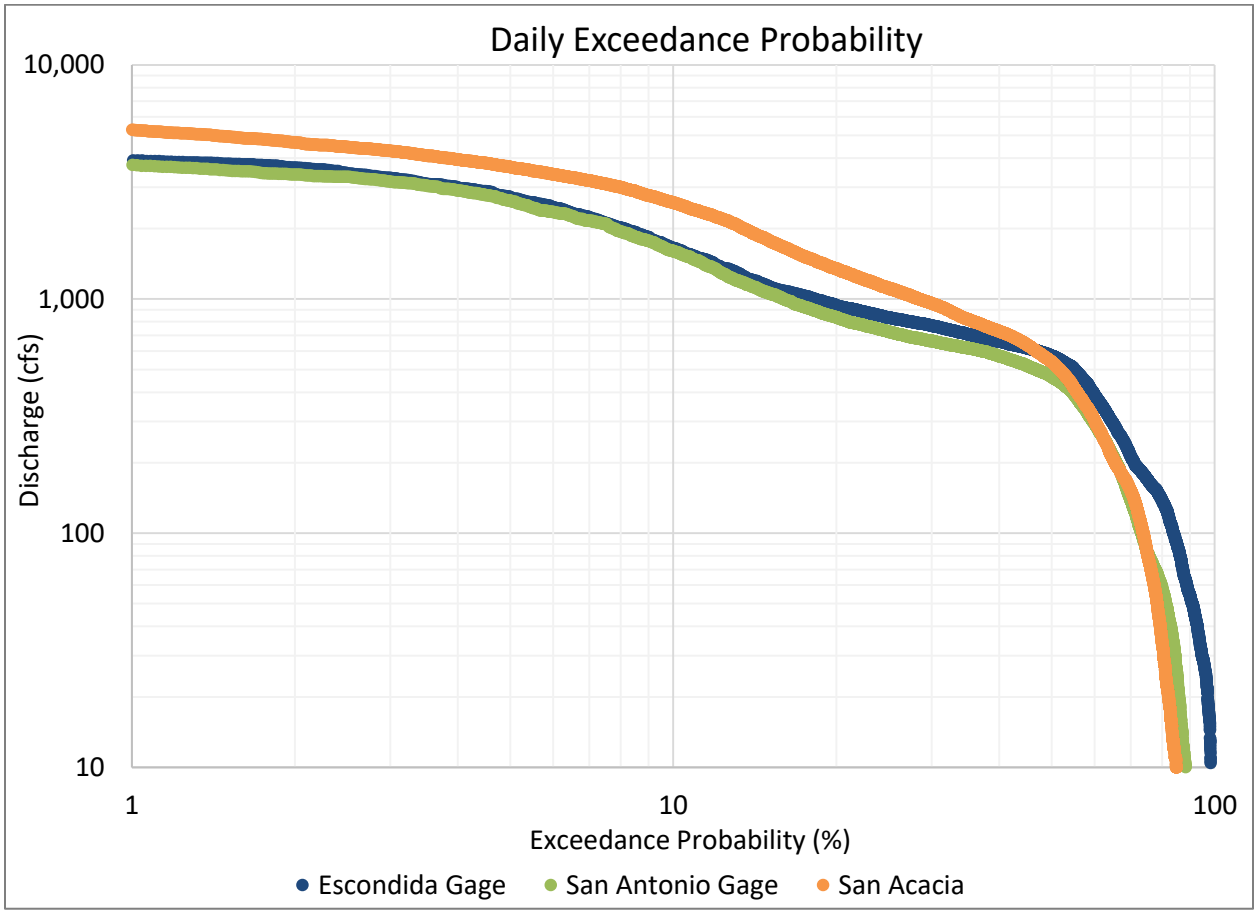

Figure 14 Comparison of flow duration curves. The Escondida and San Antonio Gage include data since the year 2005 and the San Acacia curve is based off of data post Cochiti Dam (1975).

In addition to flow duration curves, the number of days in the water year exceeding identified flow values at each gage was analyzed. This is purely a count of days and does not consider consecutive days. Analysis was performed for the entire record for both the Escondida and San Antonio gages. The data are displayed in Figure 15 and Figure 16, where a period of lower flow can clearly be seen from 2011 to 2013. The year 2013 is particularly interesting in that the fewest number of days over 500 cfs occurred, while the greatest number of days over 6000 cfs occurred. These high outlier values are associated with a monsoonal storm event that occurred in September of 2013. Remnants of two hurricanes pushed warm humid air north, which clashed with a cold front, resulting in heavy rainstorms throughout Colorado and New Mexico. Figures 15 and 16 also show that the Escondida gage has at least a small amount of water in the channel year-round, whereas the gage at San Antonio has years that will go several months without any water.

Figure 17 shows the current US 380 gage data near San Antonio along with the data recorded at the inactive site in the 1950s. Although the record was relatively short, it appears that prior to the Cochiti dam and operation of the Low Flow Conveyance Channel, there were more days that exceeded 6000 cfs (or higher discharge values in general).

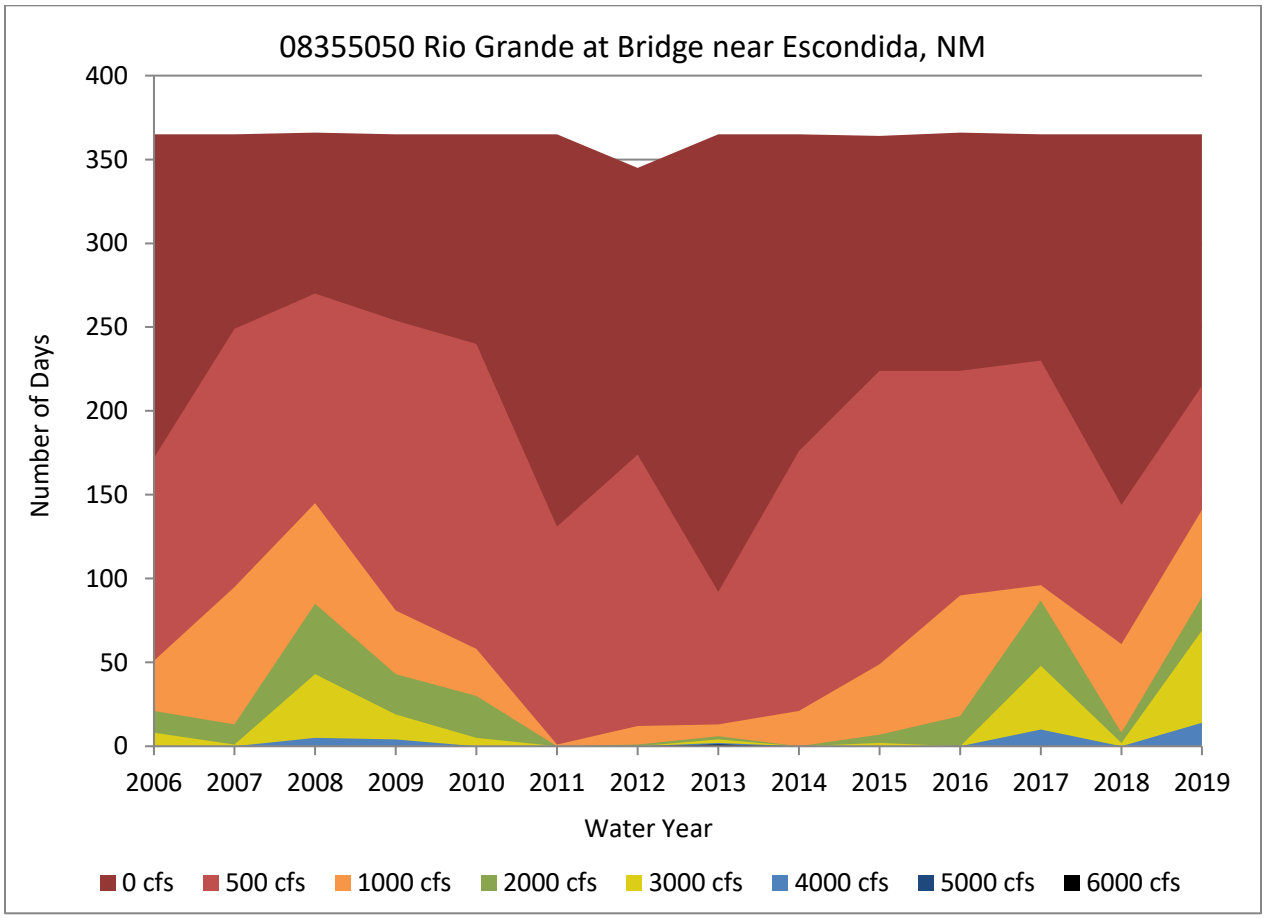

Figure 15 Number of days over an identified discharge at the Escondida gage

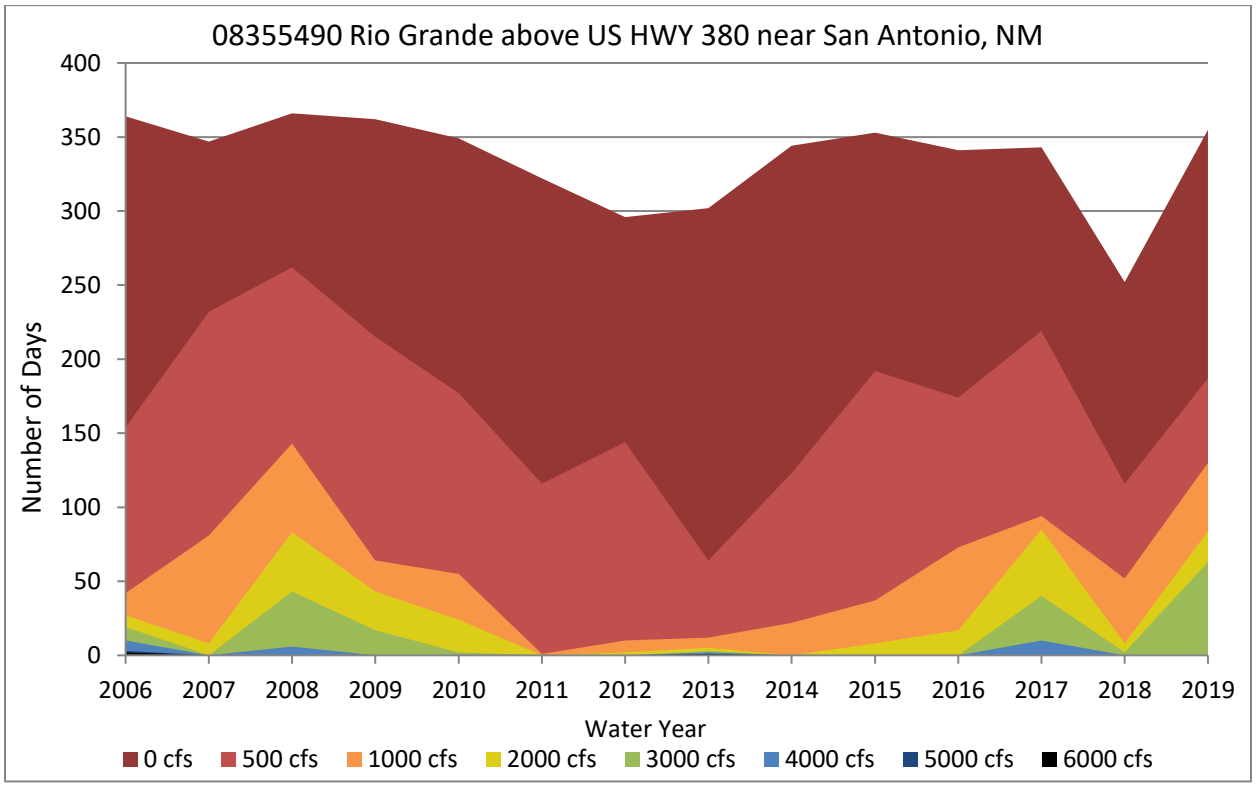

Figure 16 Number of days over an identified discharge at the HWY 380 gage

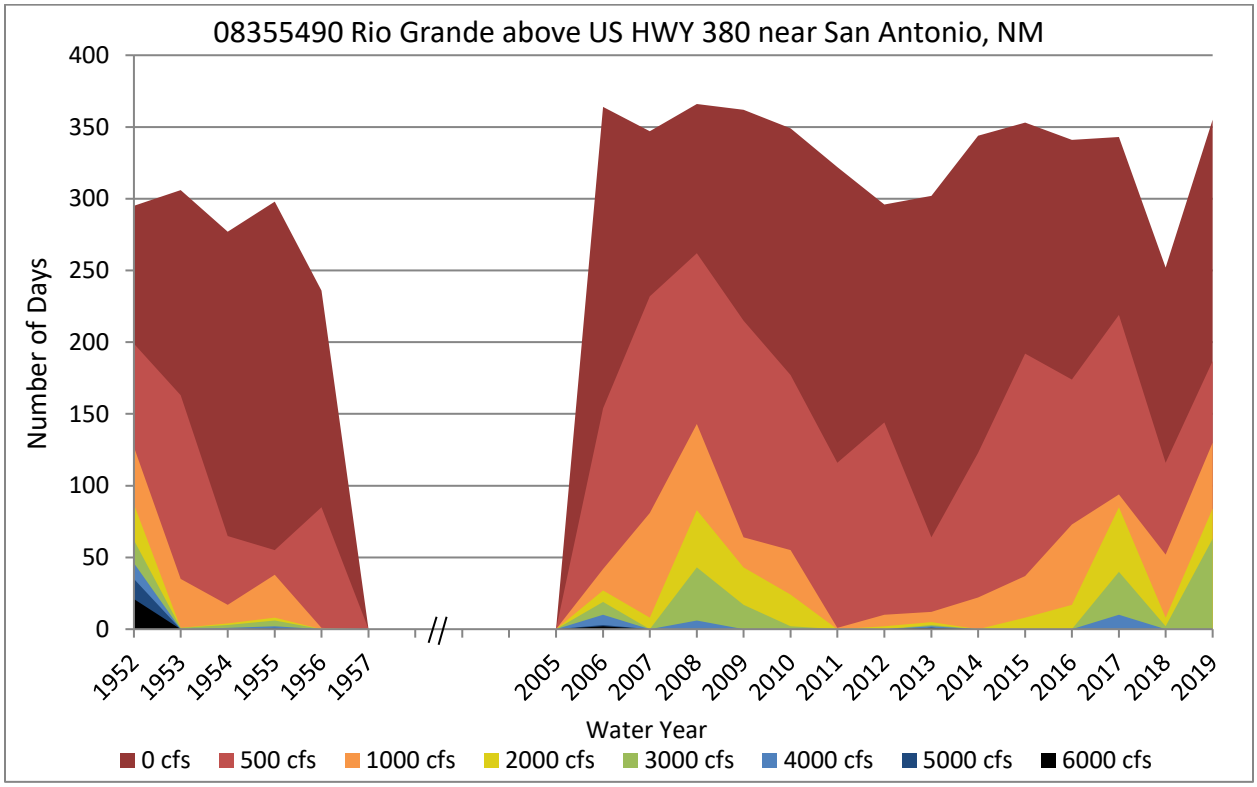

Figure 17 Number of days over an identified discharge at the HWY 380 gage including historical gage data

2.3 Suspended Sediment Load

2.3.1 Single Mass Curve

Single mass curves of cumulative suspended sediment (in millions of tons) at the San Antonio gage and the San Acacia gage are shown in Figure 18. Data comes from the USGS gage near US HWY 380 in San Antonio, NM (08355490) and the USGS gage at the Rio Grande Floodway at San Acacia, NM (08354900). There is no sediment monitoring at the USGS gage at Escondida. For the San Antonio single mass curve, the analysis was performed in water years beginning in 2011, when the collection of suspended sediment data began. The dashed line was created using the same technique as the previous cumulative discharge plot. A one-week moving average was used to determine the 97.5th percentile of slope changes. If a slope change is greater than this value, a point is created along the line indicating a time with one of the greatest increases in sediment transport.

The breaks in slope along the single mass curve show the changes in sediment flux. As previously determined from the cumulative discharge plot in Section 2.2.1, the large increases in flow in the Escondida reach occurred in the spring from snowmelt, with some increases in the summer from seasonal thunderstorms. However, the cumulative sediment discharge curve shows that the greatest increases in sediment occur during the monsoonal storms that occur in the summer. The monsoonal event mentioned earlier is seen by the large increase in suspended sediment in September of 2013. The second largest increase in sediment flux occurred as a result of a series of heavy thunderstorms in the summer of 2014.

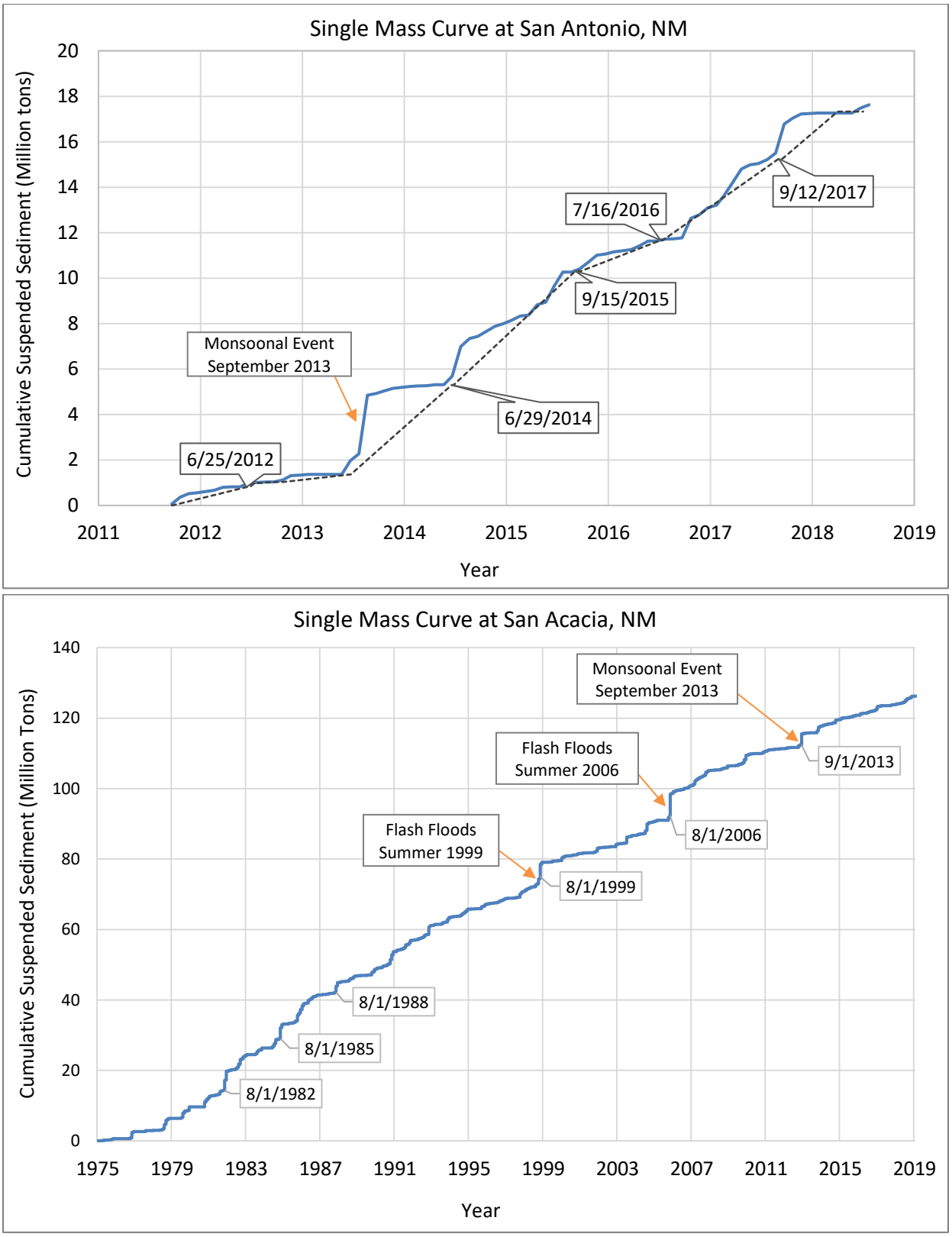

Figure 18 Suspended sediment discharge single mass curve for US 380 Bridge USGS gage Near San Antonio, NM (top) and Rio Grande Floodway at San Acacia, NM (bottom)

2.3.2 Double Mass Curve

Double mass curves show how suspended sediment volume relates to the daily discharge volume. The slope of the double mass curve represents the mean sediment concentration. The double mass curve in Figure 19 is for USGS gage at San Antonio (08355490). The greatest changes in cumulative sediment load with respect to cumulative discharge typically occur during the summer months between June and September when thunderstorms are more prevalent, indicating that the thunderstorms have a greater impact on sediment load than the spring snowmelt.

Figure 20 relates the cumulative average monthly suspended sediment at the San Antonio gage to the cumulative precipitation at the Lemitar gage to further demonstrate the effects of monsoon-related sediment transport. A steeper slope indicates that there was an increase in suspended sediment with very little change in the cumulative precipitation. Specific monsoon events can clearly be seen in the figure, such as the monsoonal event from August 2013 to September 2013 and a series of thunderstorms from July 2014 to August 2014. These events impact the suspended sediment in the Escondida reach.

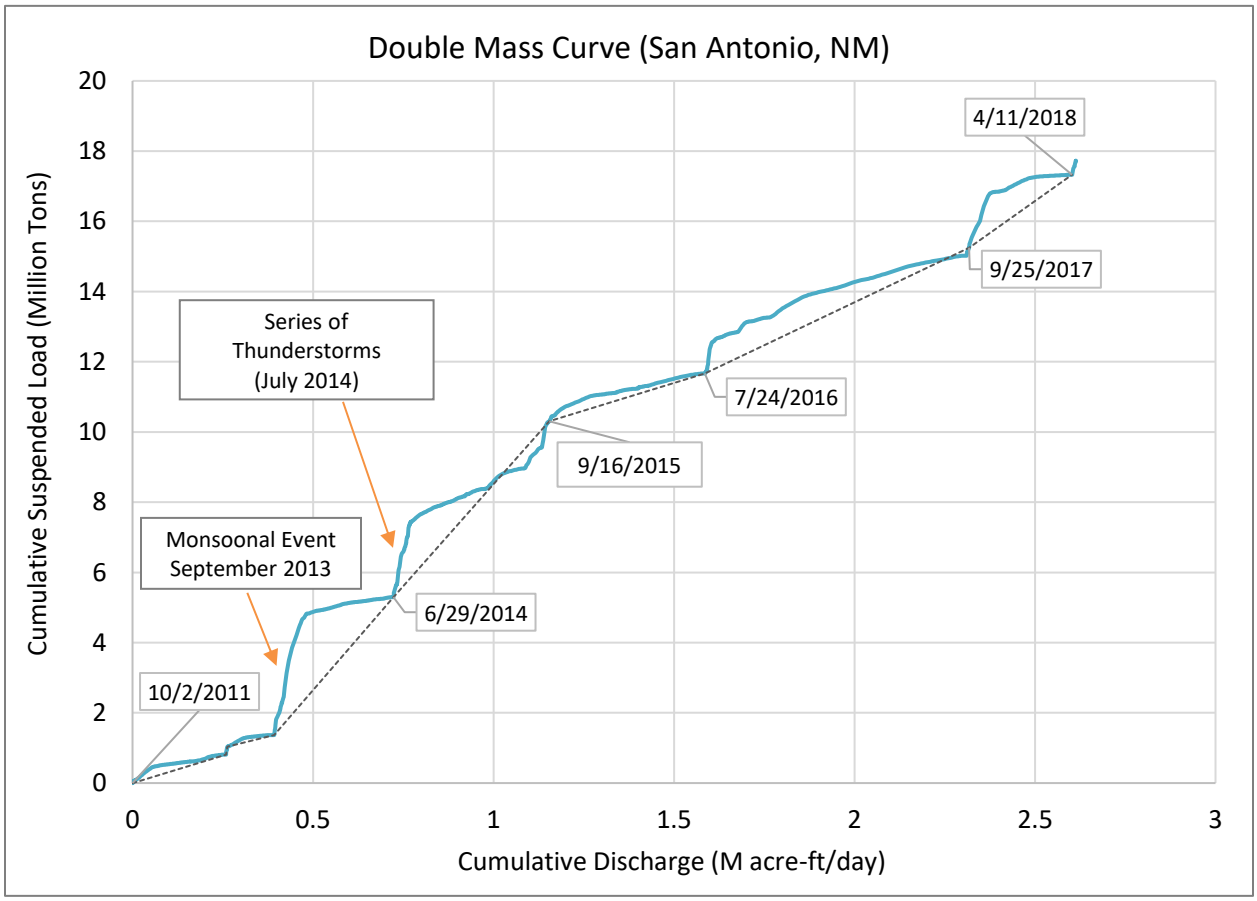

Figure 19 Double Mass Curve for the US HWY 380 Bridge Gage near San Antonio, NM

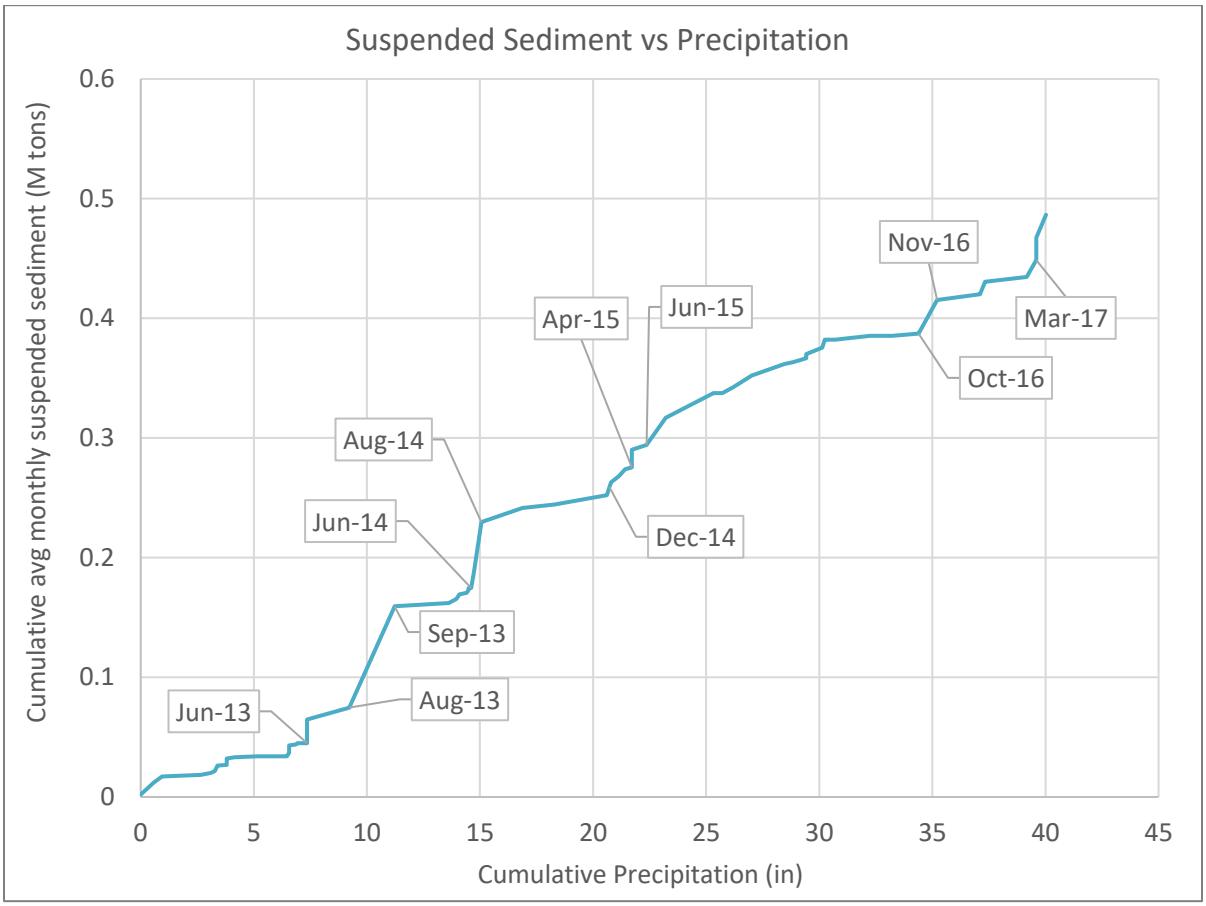

Figure 20 Cumulative suspended sediment (data from the US 380 gage at San Antonio, NM) versus cumulative precipitation at the Lemitar gage.

2.3.3 Monthly Sediment Variation

A plot of monthly average discharge and suspended sediment was created for the San Antonio gage to help reveal any important seasonal trends. Figure 21 and Figure 22 show the seasonal trends of suspended sediment load and concentration, respectively, along with the discharges that correspond with the years. As seen previously, although the spring snowmelt brings some of the larger discharge volumes, the increased flows from the intense thunderstorms or monsoon seasons are what transport the most sediment. A SEMEP analysis of total sediment load in the MRG can be found in Appendix B.

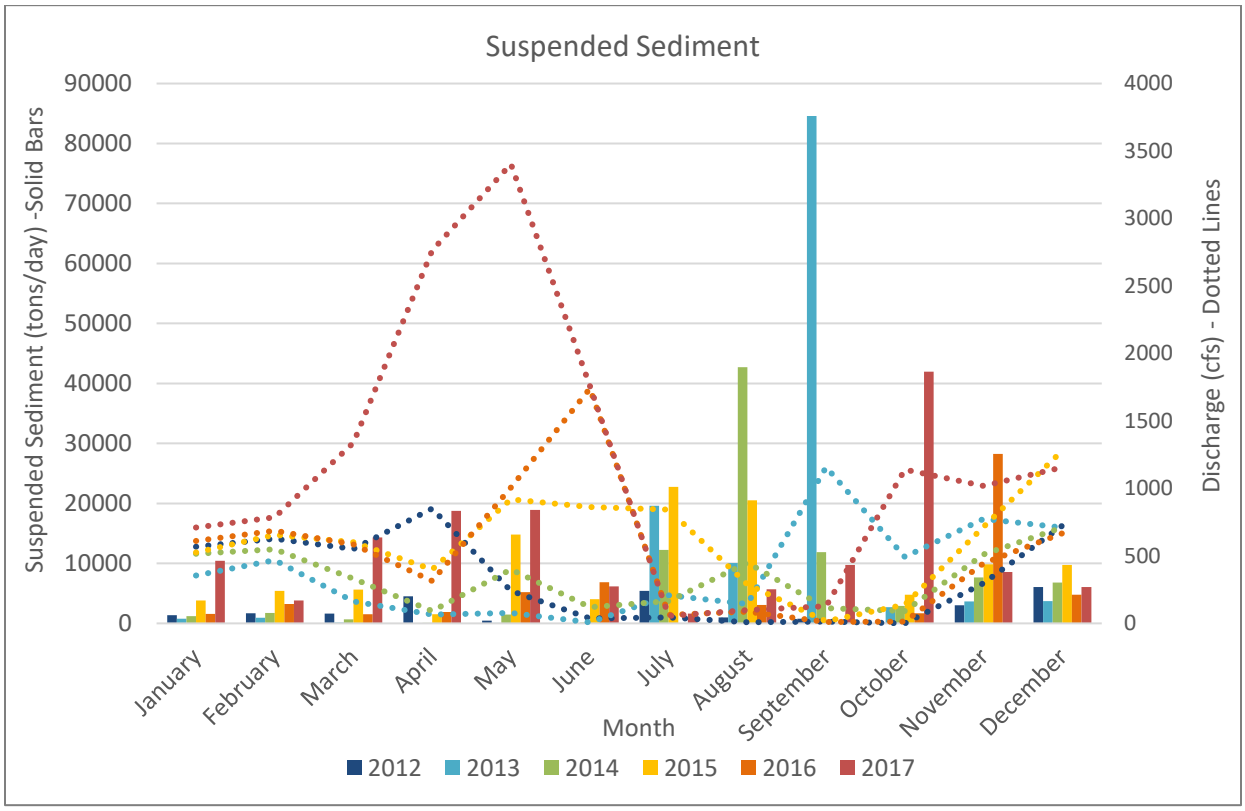

Figure 21 Monthly average suspended sediment and water discharge

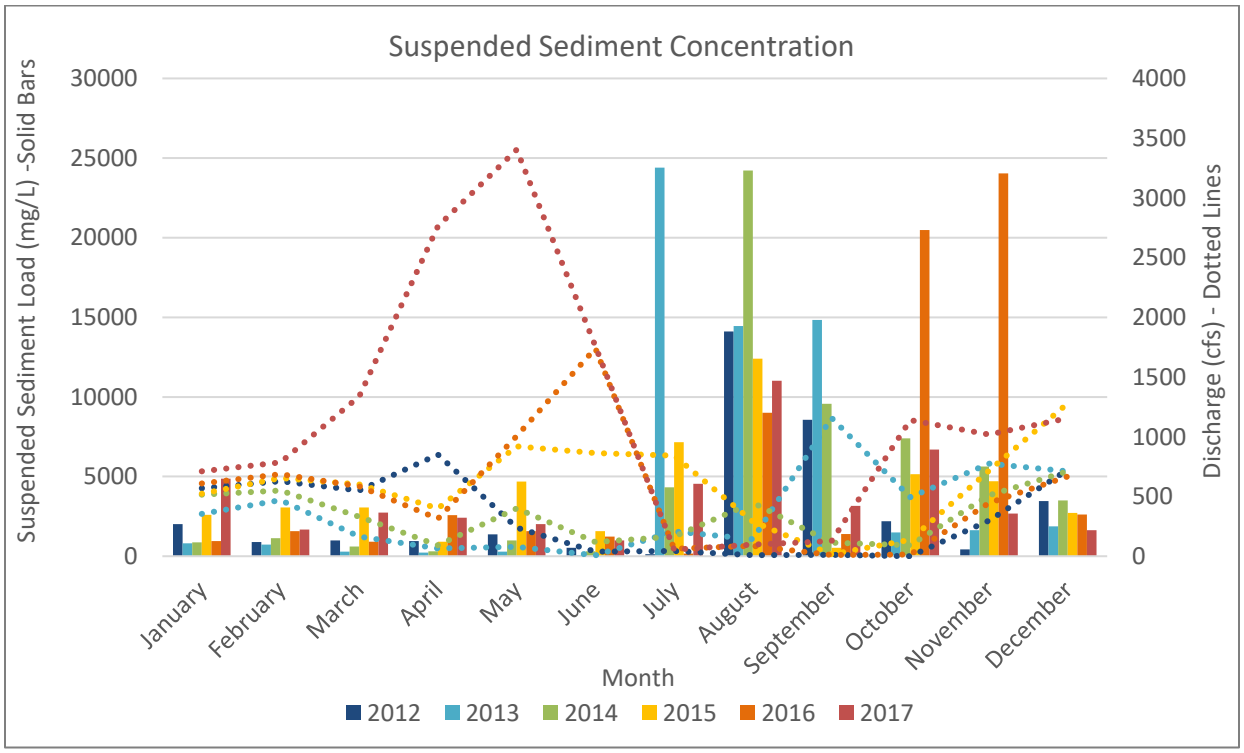

Figure 22 Monthly average suspended sediment concentration and water discharge

3. Geomorphic and River Characteristics

3.1 Wetted Top Width

Wetted top width can provide significant insight into at-a-station hydraulic geometry. Typically, wetted top width in a compound trapezoidal channel would slowly increase as discharge values increase until there is a connection with the floodplain. At this point, the top wetted width would quickly increase as the water spills onto the floodplains. Then, the gradual increase in width would continue. Analysis of the wetted top width can be used to help understand bankfull conditions and how they vary spatially and temporally in the Escondida reach. A HEC-RAS model was created to analyze a variety of top width metrics. An increment of 500 cfs up to 10,000 cfs was used in the top width analysis for the years with available data: 1962, 1972, 1992, 2002 and 2012.

Figure 23 and Figure 24 show the moving cross sectional averaged top wetted width at 1,000 cfs and 3,000 cfs from the HEC-RAS model results. The top width shown at each agg/deg line comes from the moving average from five consecutive cross sections: the identified agg/deg line, two upstream agg/deg lines, and two downstream agg/deg lines. Based on the analysis, subreach E5 has experienced the most dramatic change in width, which occurred between the years 1962 and 1972. Subreach E1 and the first half of subreach E2 also experienced narrowing at that time. The average top wetted width in subreaches E3 and E4 has increased in the most recent time intervals. Additional figures from this analysis can be found in Appendix C, including plots with the corresponding top width for each agg/deg line rather than the moving average.

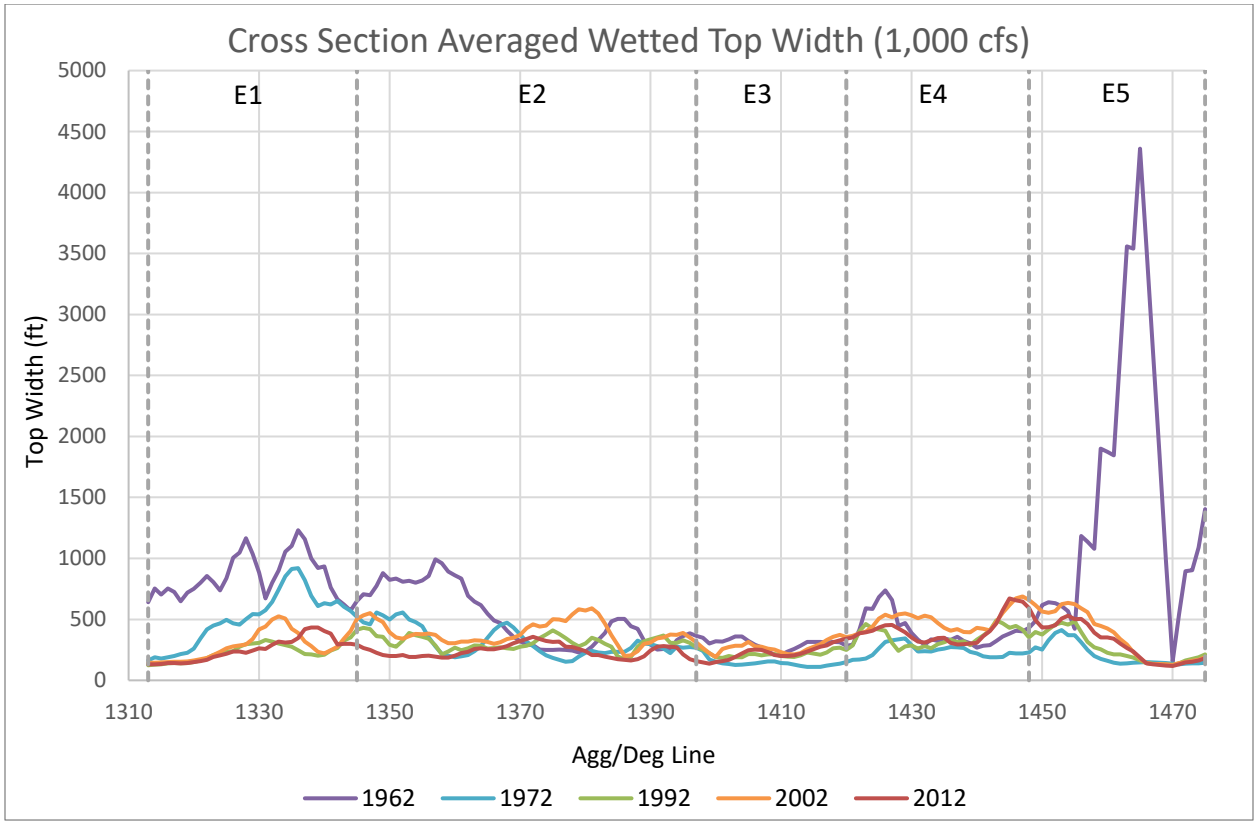

Figure 23 Moving cross sectional average of the wetted top width at a discharge 1,000 cfs

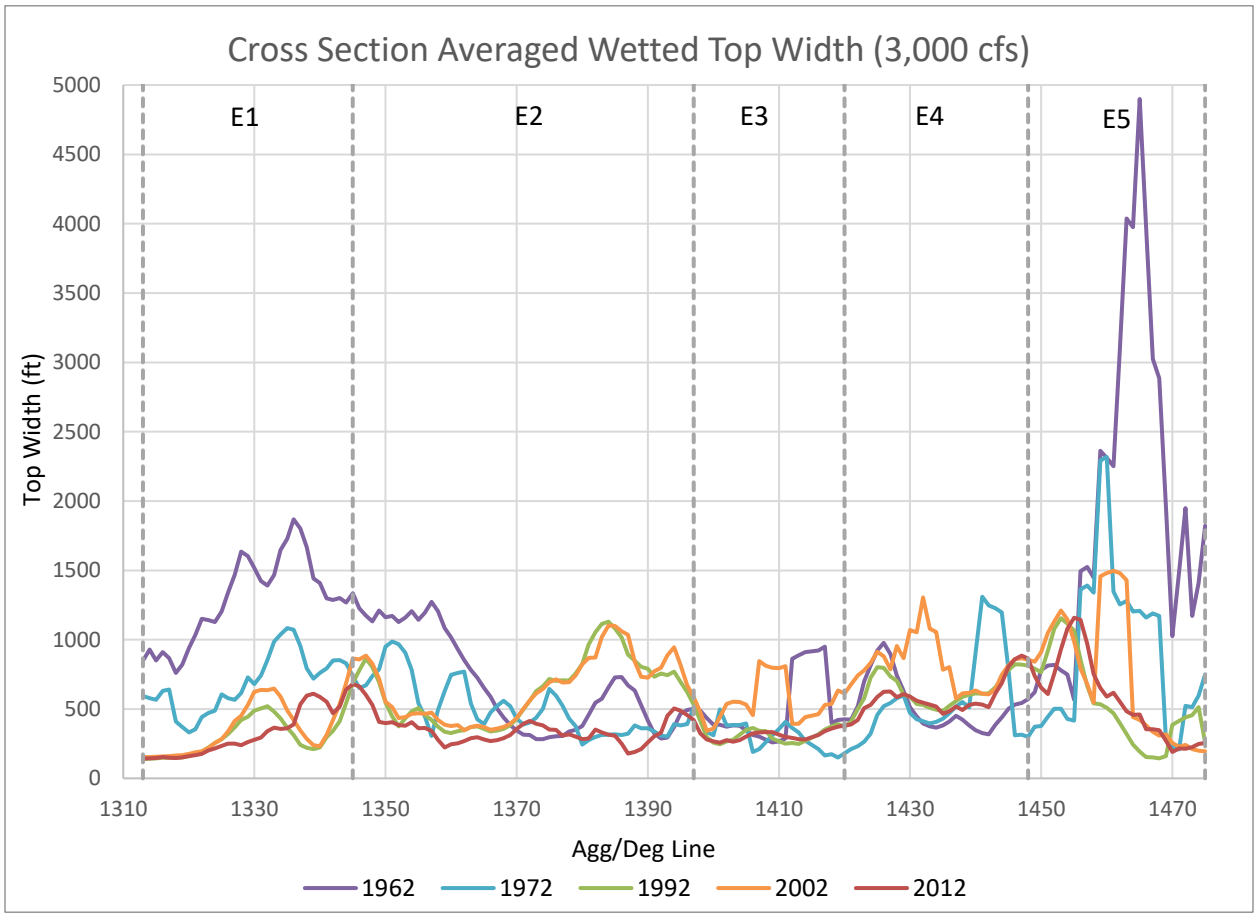

Figure 24 Moving cross sectional average of the wetted top width at a discharge 3,000 cfs

In 1962, subreach E5 has a much larger wetted top width than the other subreaches. This width comes from the perching of the channel. Water would quickly fill the channel in subreach E5 and spill out onto the floodplains. Because many of the cross sections are perched in this subreach, the width quickly increases to values between 3,500 feet to almost 5,000 feet. Degradation occurred in subreach E5 between the years 1962 and 1972, which resulted in fewer cross sections experiencing overbanking at these discharges, and therefore fewer cross sections having a large predicted top wetted width.

The average top width for each subreach was also plotted for the years analyzed in Figure 25 for discharges up to 5,000 cfs. The average top width decreased the most in subreach E1 between 1972 and 1992. The top widths have not seen any major changes between 1992 and 2012 in subreaches E1, E3, and E4. Subreach E2 has experienced narrowing between 2002 and 2012, and E5 has seen an increase in top width between 1992 and 2012.

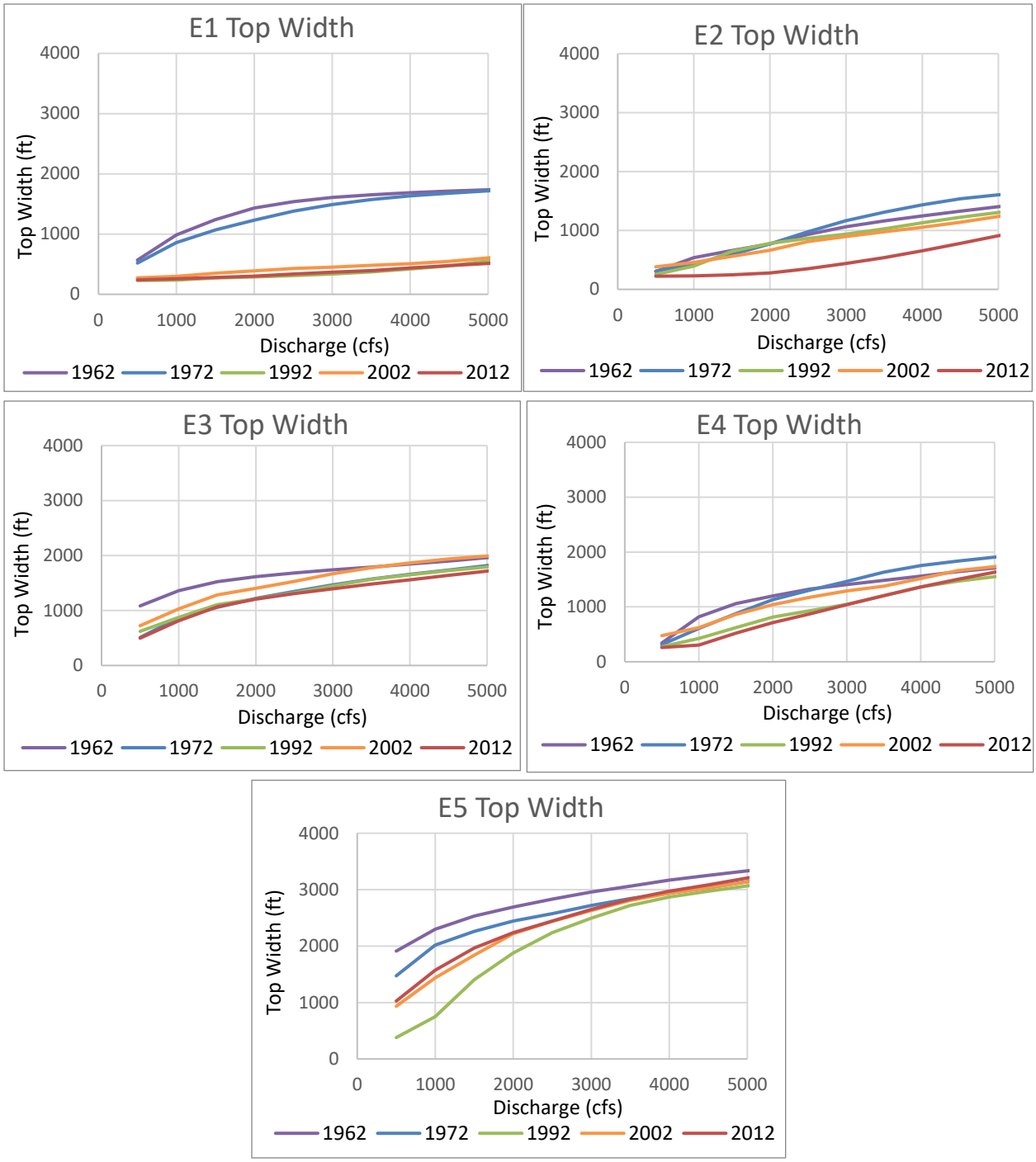

Figure 25 Average top width for E1 (top left), E2 (top right), E3 (middle left), E4 (middle right), and E5 (bottom) at discharges 500 to 5,000 cfs

3.2 Width (Defined by Vegetation)

The width of the active channel, defined as the non-vegetated channel, was found by clipping the agg/deg line to the width of the active channel polygon provided by the USBR's GIS and Remote Sensing Group. The widths of the active channel polygon were exported from ArcMap for each agg/deg line. Then the average width of each subreach was calculated by averaging the width of all agg/deg lines within the

subreach. Aerial photographs and accompanying digital shapefiles were provided for years 1918, 1935, 1949, 1962, 1972, 1985, 1992, 2001, 2002, 2006, 2008, 2012 and 2016. The results are shown in Figure 26.

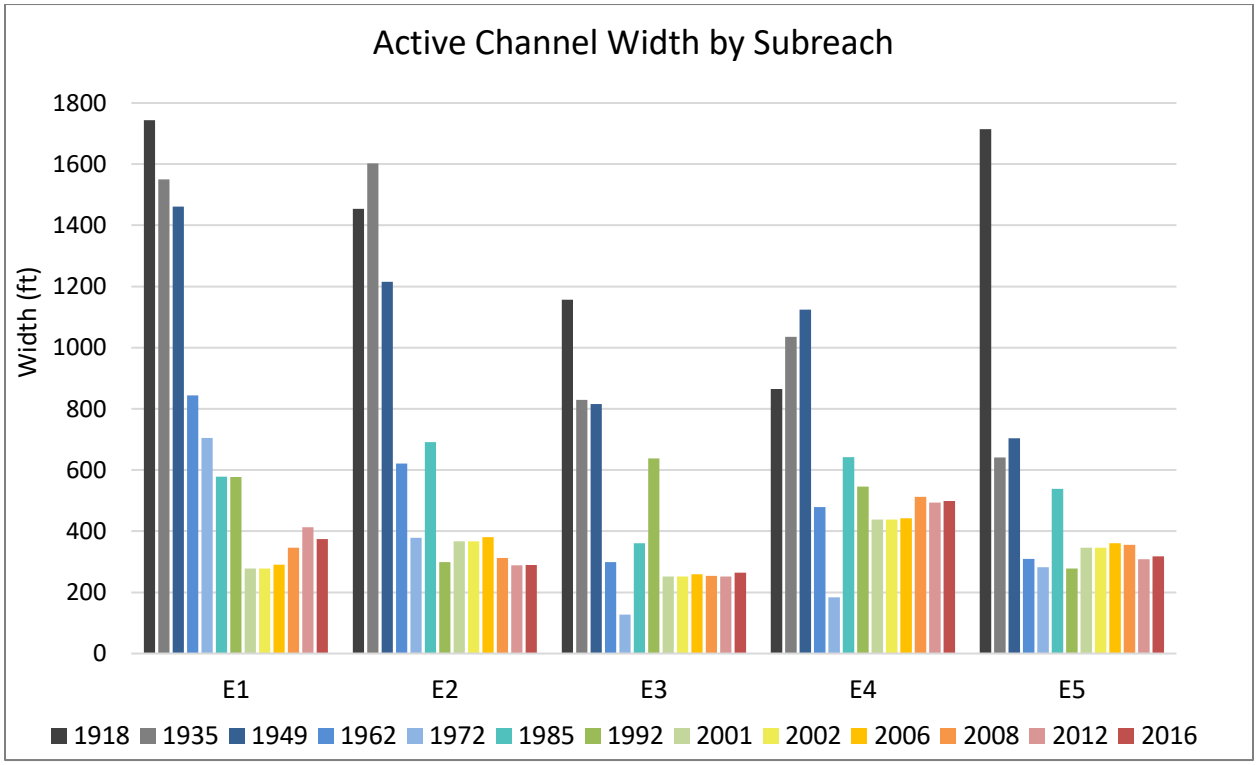

Figure 26 Averaged active channel width by subreach

Figure 26 shows that the active channel width in all subreaches was the greatest between 1918 and 1949 before a sharp decrease in width in the following years. A reduction in peak flows lead to a decline in the active channel width of the river between 1918 and 1949. An extended period of drought beginning in the 1940s and installation of jetty jacks in the 1950s resulted in additional narrowing of the active channel (Scurlock, 1998). Upstream dams and reservoir storage also lead to a decrease in peak flows. Furthermore, installation of the Low Flow Conveyance Channel reduced the discharges in the Rio Grande by diverting the flow from the 1960s to the 1980s, further decreasing the width as seen in Figure 26. Mowing operations cleared vegetation along the river banks from the 1960s to the 1980s (and into the early 1990s in various locations along the MRG), which played a part in a slight widening of the river between 1972 and 1985, in addition to the increased flows as the period of drought came to an end and operation of the Low Flow Conveyance Channel was stopped (Makar, 2006). After another period of drought from the late 1990s to the early 2000s, the active channel width of the river has decreased once again and has remained stable ever since in each subreach.

3.3 Bed Elevation

The minimum channel bed elevation is used to evaluate the change in the longitudinal profile of the Escondida reach. The bed elevation of the channel comes from an estimate generated by HEC-RAS, which is based on the discharge and the water surface elevation on the day of the aerial photography. Based on national mapping standards, 95% of the points need to be within 6 inches of the true ground

elevation. While the minimum channel elevation points may not be exact, the overall trends can still be identified throughout the Escondida reach. The minimum channel elevation was obtained at each cross-section from the HEC-RAS geometry files to generate a plot of the bed elevation throughout the reach, as seen in Figure 27.

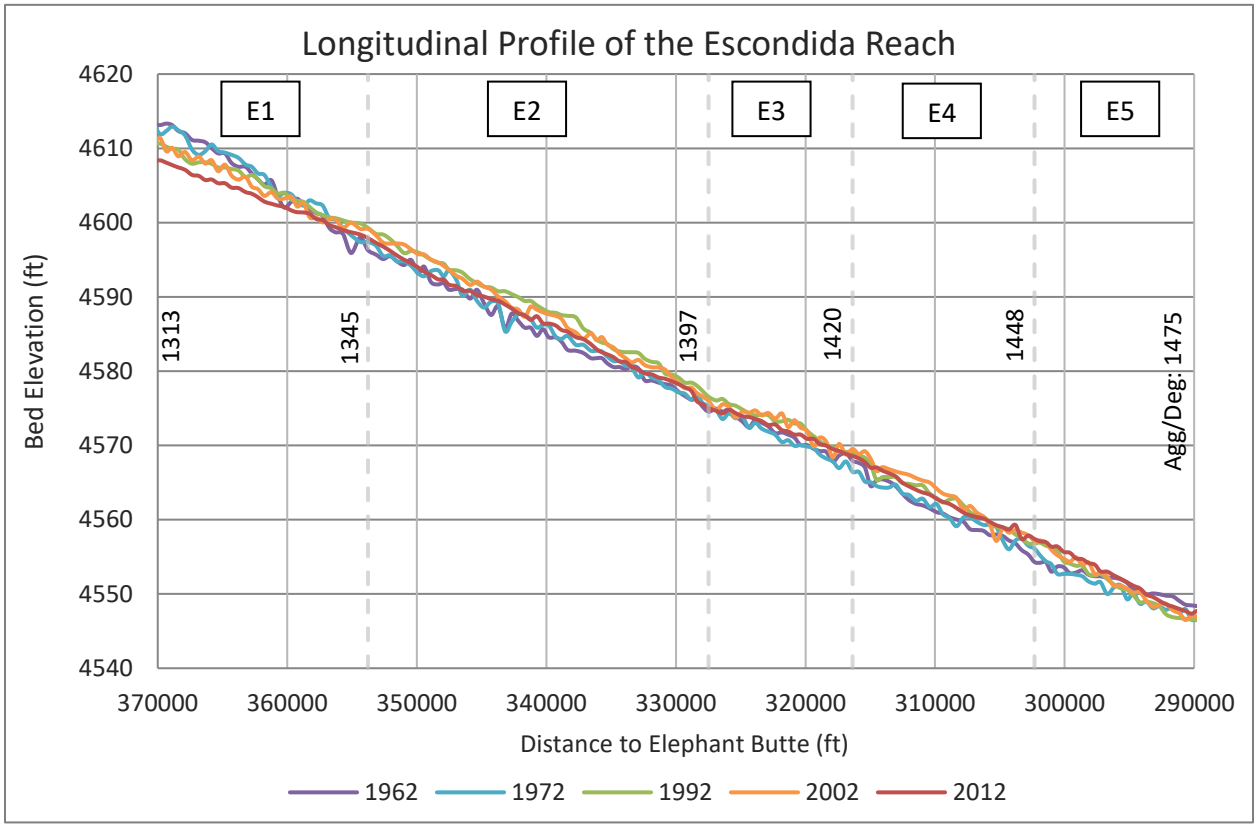

Figure 27 Longitudinal profiles of bed elevation

The Escondida reach is an interesting reach in that it contains a "pivot point" of where the MRG switches from a degrading channel to an aggrading channel. Upstream of the Escondida reach, sediment is being picked up and transported, leading to an incising river. Downstream of the Escondida reach, large amounts of sediment are being deposited leading to an aggrading bed and sediment plugs. The Escondida reach contains the section of river at which this transition occurs. At the upstream end of the reach, degradation has occurred as shown in Figure 27 and Figure 28 by the overall decrease in bed elevation from 1962 to 2012. However, further down the reach aggradation can be seen by the overall increase in bed elevation since 1962. From the earlier section on active channel width, the downstream end of the Escondida reach is stabilizing at a greater width than the upstream end of the reach. This could be because more sediment is being deposited at this location leading to a wider and shallower river.

Figure 28 shows the main channel aggradation and degradation of each subreach, which was found by first finding the average minimum channel elevation for each subreach and then subtracting the average bed elevation of the earlier year from the later year. A positive number indicates aggradation and a negative number indicates degradation. Subreach E1 has been degrading since approximately 1972 and subreach E5 has been aggrading since 1972, which supports the idea that Escondida contains an aggradation and degradation "pivot point" of the MRG. Figure 28 also shows that degradation may be

shifting downstream. In subreach E1, the channel has been degrading since the time interval spanning the years 1972 to 1992. In subreach E2, the degradation began between 1992 and 2002. The channel has also been degrading in subreach E3 since 1992 to 2002, it is possible that since there has been less degradation, it began within that time interval closer to the year 2002. In subreach E4, degradation began most recently, between the years 2002 and 2012.

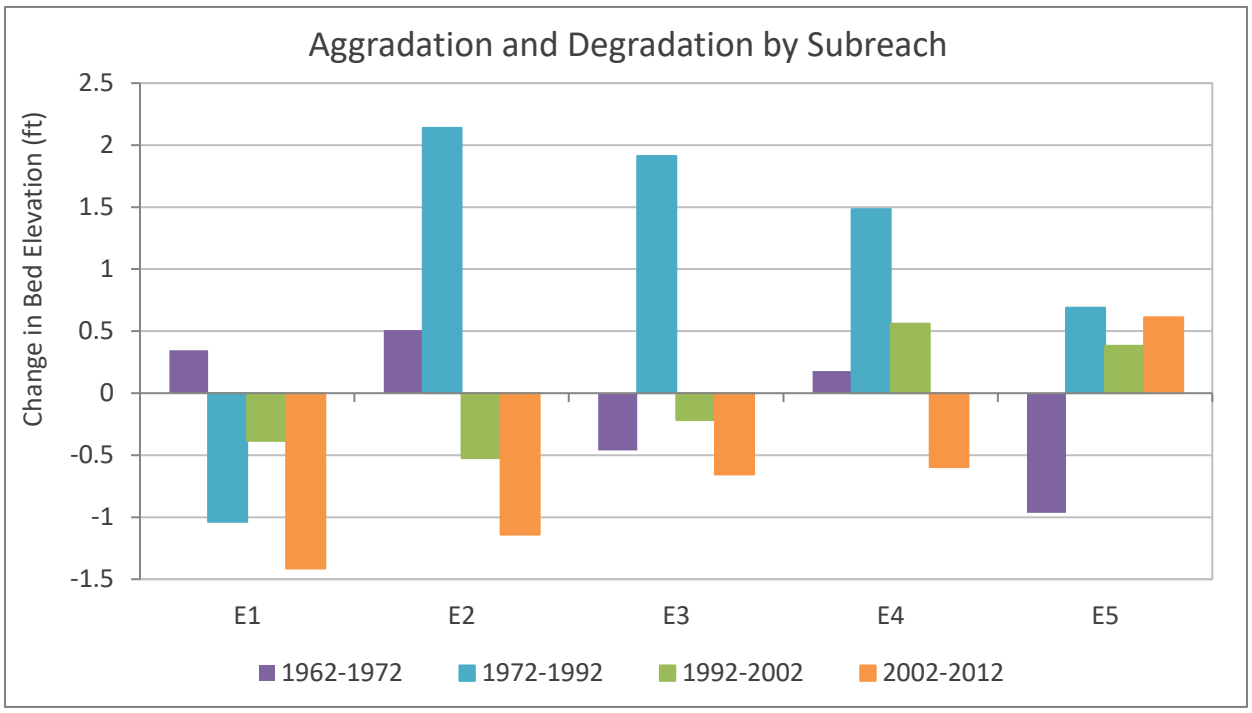

Figure 28 Degradation and Aggradation by subreach

3.4 Bed Material

Bed material samples were collected at various rangelines in the channel. There are bed material samples available for analysis of the Escondida reach from the years 1991 to 2002. Figure 29 shows the median grain diameter of each sample versus the distance downstream of the Escondida Bridge (i.e. the start of the Escondida reach).

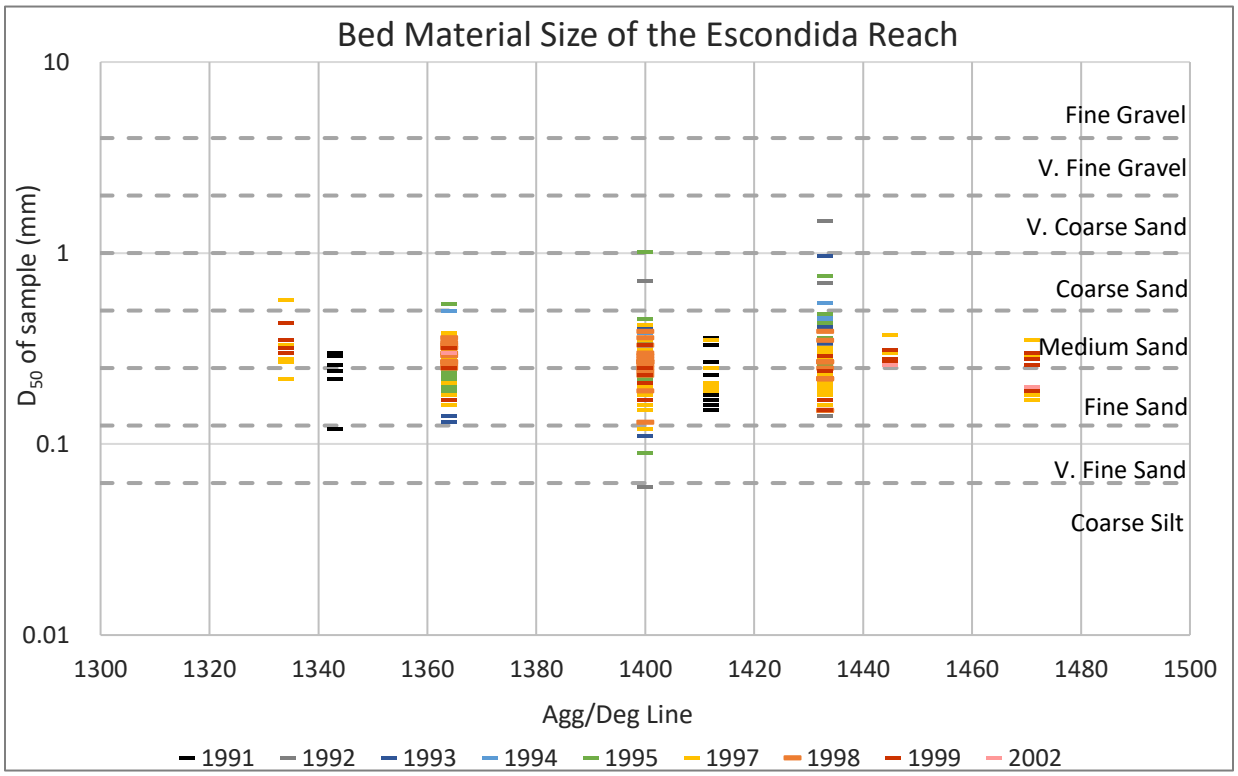

Figure 29 Median grain diameter size of samples taken throughout the Escondida reach

Throughout the reach the median diameter size of the samples is typically between 0.1 millimeter and 1 millimeter for the years in which data were collected. These grain size diameters correspond with classifications of fine sand to coarse sand, emphasizing that the Escondida reach of the MRG is a sand-bed river.

3.5 Sinuosity

The sinuosity was calculated at each subreach using digitized channel centerlines provided by the USBR's GIS and Remote Sensing Group. Aerial photographs and accompanying digital shapefiles were provided for the years 1918, 1935, 1949, 1962, 1972, 1985, 1992, 2001, 2002, 2006, 2008, 2012 and 2016. To analyze the sinuosity of each subreach, the centerlines were split at each subreach boundary. Then, for each subreach, the length of the centerline (channel length) was divided by the valley length to get the sinuosity value.

Overall, the sinuosity values in the Escondida reach are low, measuring just above 1 throughout the reach, as seen in Figure 30. There has been a slight increase in sinuosity in subreaches E1 and E2. The sinuosity in E3 dropped slightly in 1972 but has remained relatively constant since and remains the most sinuous

subreach in the Escondida reach. The sinuosity in E4 has been fluctuating throughout the time that data has been recorded and has not seen any significant changes. E5, on the other hand, had a significant decrease in sinuosity between 1918 and 1935 and it has remained low ever since.

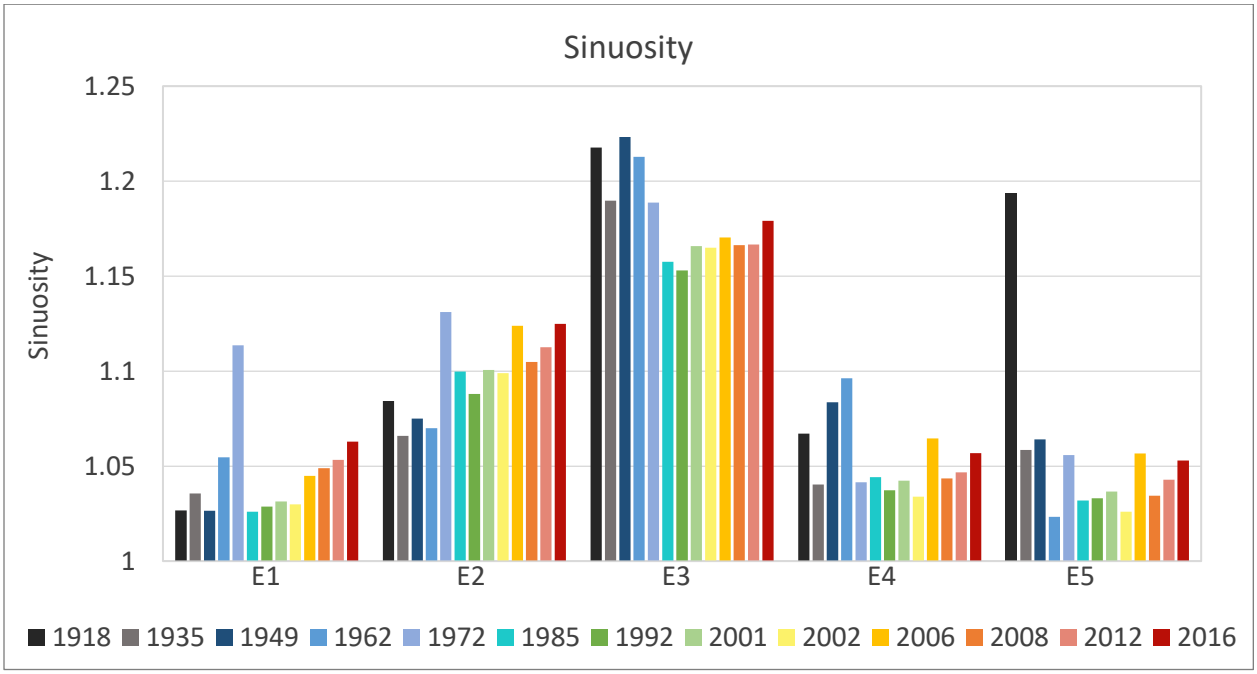

Figure 30 Sinuosity by subreach

3.6 Hydraulic Geometry

Flow depth, velocity, width, wetted perimeter of the main channel, and bed slope are obtained using HEC-RAS 5.0.3 with a discharge of 3,000 cfs, which was selected based on the fact that this discharge represents bankfull conditions with limited likelihood of overbanking (LaForge et al., 2019 and Yang et al., 2019). A discharge of 3,000 cfs has a daily exceedance of 4.6% at the upstream end of the Escondida reach. Therefore, the same hydraulic geometry variables were analyzed for a discharge more commonly seen in this reach: 1,000 cfs, which has a daily exceedance of about 16%. For the plots of the hydraulic geometry variables, the values were averaged by subreach.

The HEC-RAS results (Figure 31) show a decrease in the wetted top width from the years 1962 to 1972 due to the divergence of flow into the Low Flow Conveyance channel and a period of drought, which matches the findings from section 3.2 Width (Defined by Vegetation). Figure 31 also shows a slight increase in width for most of the Escondida reach between 1972 and 2002, which is likely from increased discharge values in the MRG and the mowing operations that cleared vegetation along the banks of the MRG.

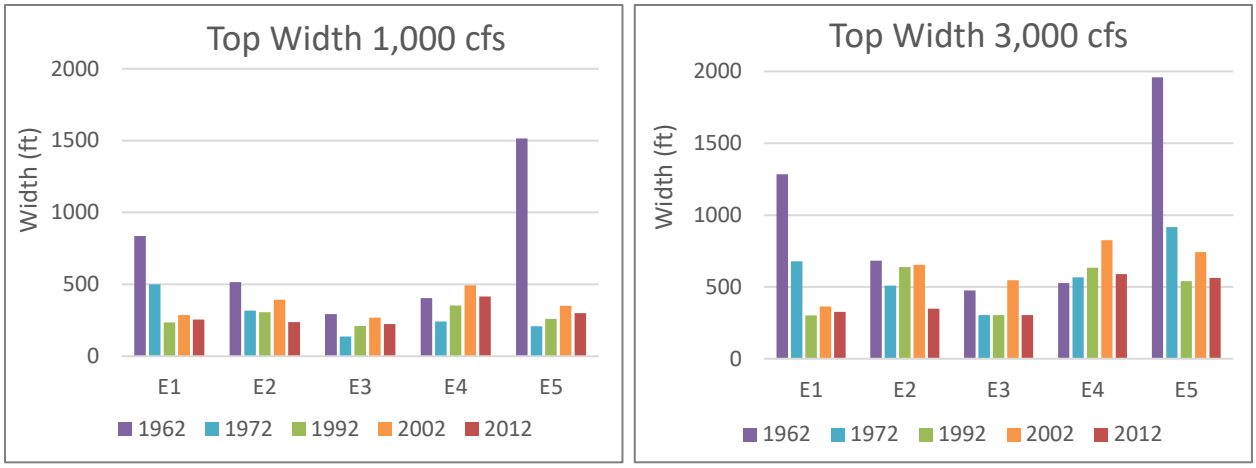

Figure 31 HEC-RAS Wetted top width of channel at 1,000 cfs (left) and 3,000 cfs (right)

Because the upstream end of the Escondida reach is narrowing and degrading, an increase in flow depth would be expected. Figure 32 shows the HEC-RAS calculated hydraulic depths at discharges of 1,000 cfs and 3,000 cfs. Subreaches E1 and E2 show the greatest increase in hydraulic depth between 1962 and 2012, whereas the end of the subreach shows fluctuations resulting in only a small change in hydraulic depth of 4-7 inches. Although the downstream end of the reach is aggrading, there was also narrowing since 1962 as seen in Figure 31, which accounts for the slight increase in hydraulic depth.

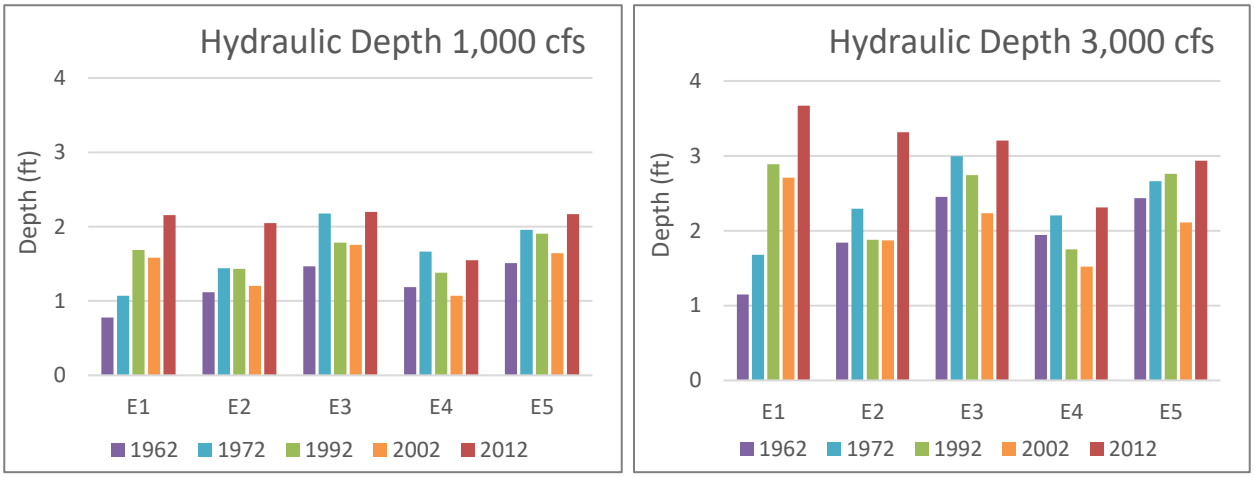

Figure 32 HEC-RAS Hydraulic depth at 1,000 cfs (left) and 3,000 cfs (right)

Figure 33 shows one cross section in Subreach E5. This example shows that although the main channel has aggraded, the banks have aggraded as well. In the downstream end of subreach E5, several cross sections have exhibited this pattern in which the banks are aggrading faster than the main channel, which is another factor leading to an average increase in the hydraulic depth.

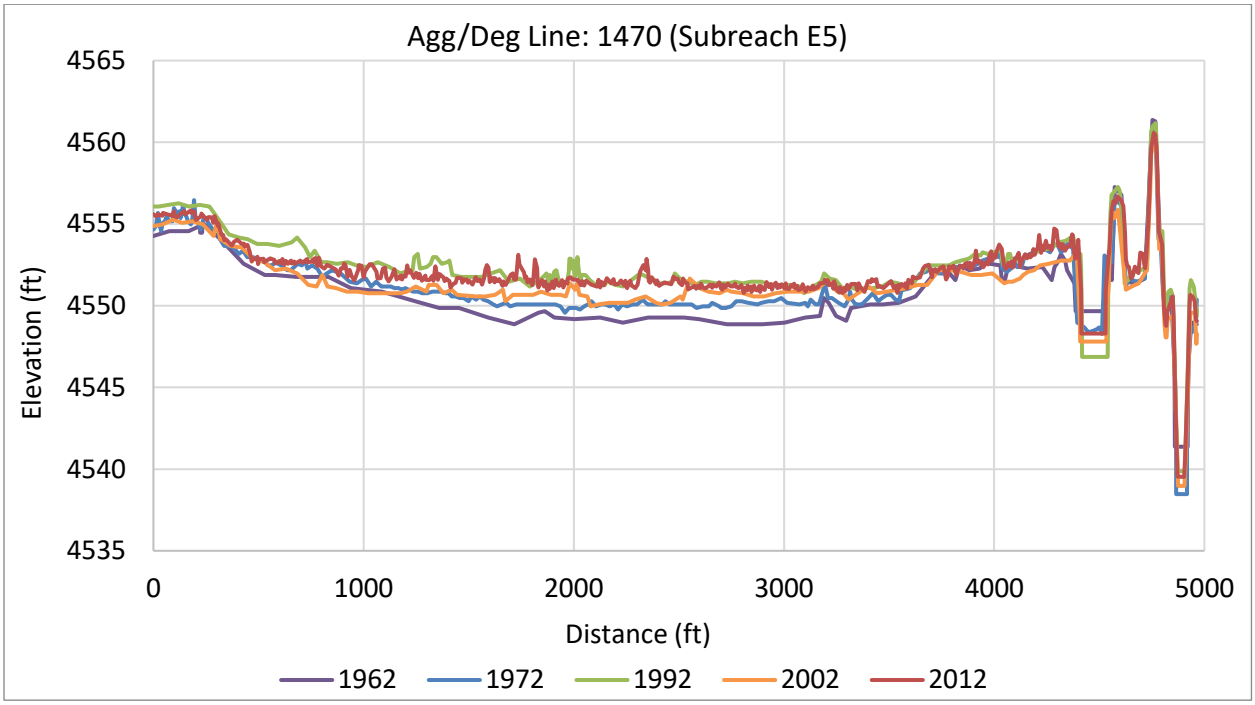

Figure 33 Example cross section indicating that the banks are aggrading in addition to the main channel bed. On average, throughout the reach, there was also a decrease in top wetted width.

The wetted perimeter of the main channel was also obtained from HEC-RAS for each of the years analyzed, as shown in Figure 34. Generally, the wetted perimeter follows a similar trend to the top width. The perching and water inundation of the floodplains led to high top widths in 1962 in subreach E5. The wetted perimeter obtained is specifically for the main channel, so the wetted perimeter does not begin at those large values. A significant decrease in the wetted perimeter of the main channel occurs for subreach E1 between 1962 and 2012. While the decrease is not as great as E1, the wetted perimeter is also reduced for subreach E2 between 1962 and 2012. Subreaches E3, E4, and E5 have fluctuations in the wetted perimeter values throughout the time period analyzed but have nearly the same wetted perimeter in 1962 and 2012.

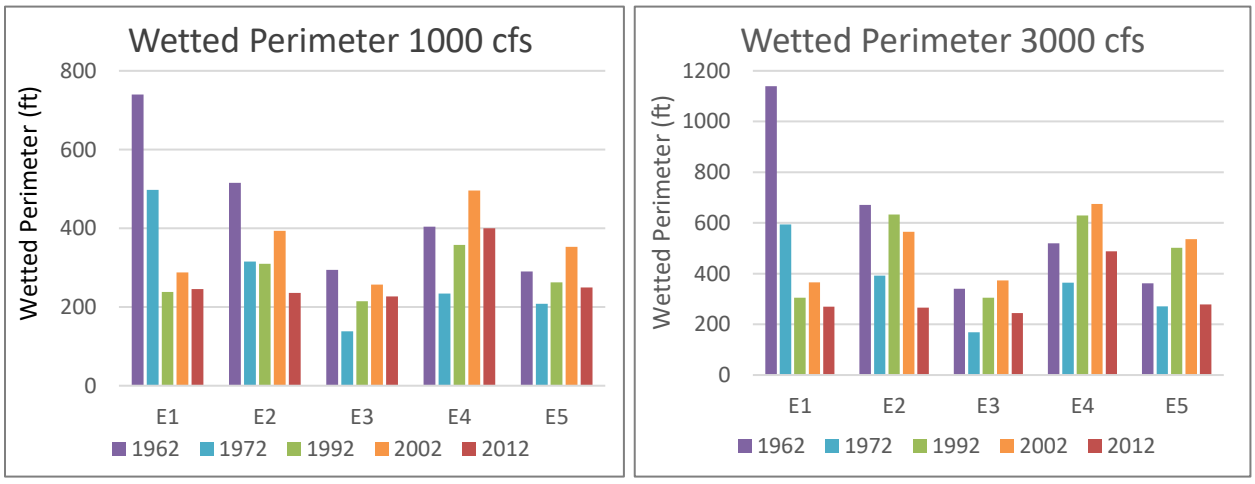

Figure 34 Wetted Perimeter at 1000 cfs (left) and 3000 cfs (right)

The bed slope was calculated between each agg/deg line and averaged by subreach. A bar chart of the bed slope is shown in Figure 35. The plot shows a decrease in the bed slope for subreach E1 since 1962. Subreach E5 had an increase in bed slope between 1962 and 1992 but has stabilized around 0.0008. The other three subreaches had slight changes in slope but have remained relatively stable for the years analyzed. Subreach E3 has remained the subreach with the lowest bed slope. Changes in flow depth and slope often have an inverse relationship. As slope decreases, the flow depth increases. This trend can be seen in the Escondida reach, particularly in subreach E1. The bed slope has decreased between the years 1962 and 2012 (except for a small increase in 2002), and the hydraulic depth has increased since 1962 (except for a small decrease in 2002).

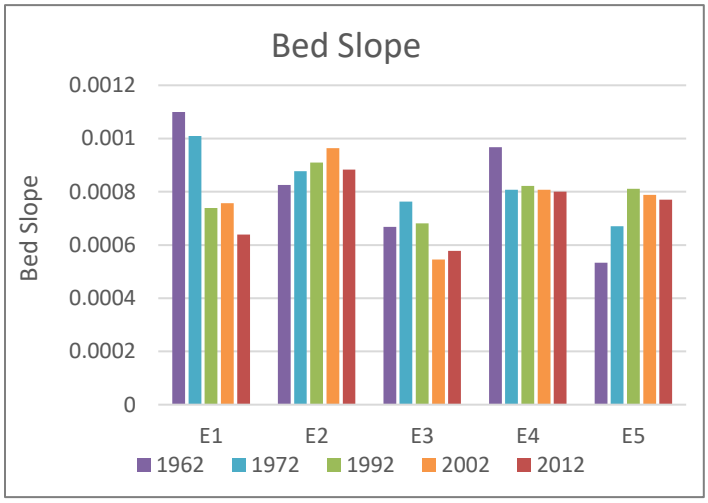

Figure 35 Bed Slope

3.7 Mid-Channel Bars and Islands

At low flows, the number of mid-channel bars and islands at each agg/deg line is measured from digitized planforms from the aerial photographs provided by the USBR. In some locations, multiple channels were present at one agg/deg line due to a vegetated bar or island bifurcating the flow. The number of channels at each agg/deg line were averaged throughout each subreach and the results are presented in Figure 36. E1 typically has a slightly higher average number of mid-channel bars and islands which may indicate that subreach E1 is migrating. In contrast, E3 has remained nearly a single-thread channel throughout the time period analyzed. Although there are slight changes by subreach, the average number of mid-channel bars and islands throughout the reach is still only just above 1 for most of the years analyzed.

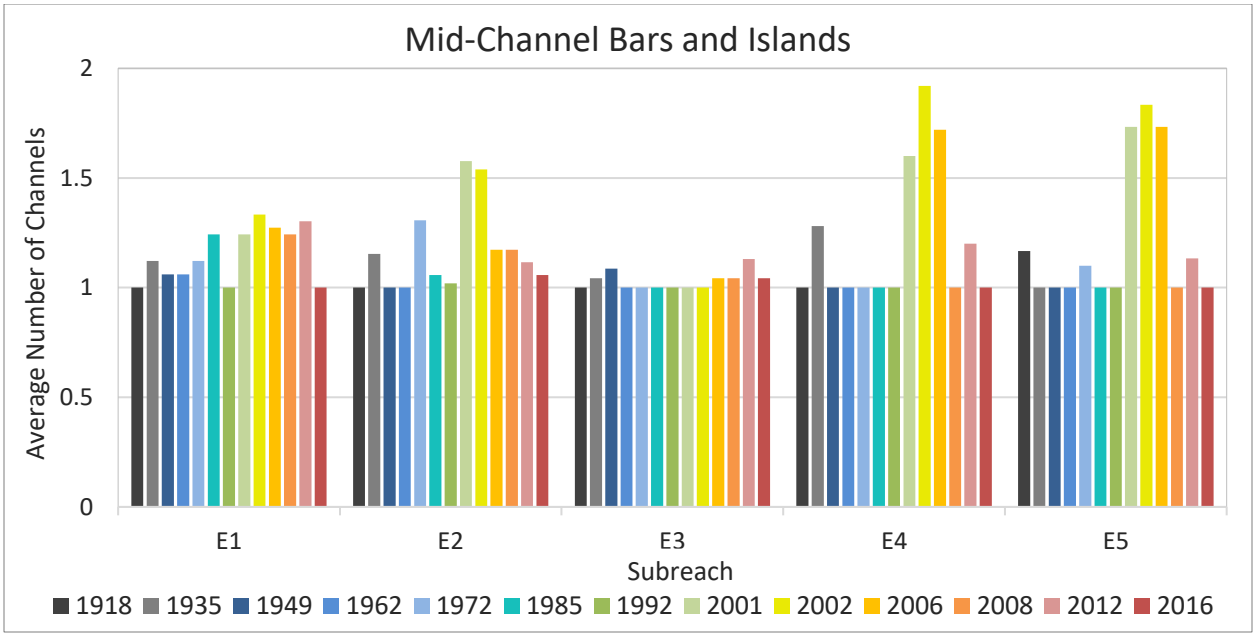

Figure 36 Average number of channels at the agg/deg lines in each subreach

Based on the analysis of the digitized planforms, the years 2001 through 2006 appear to be more braided, which could be from lower peak flows unable to wipe out the vegetation and re-work bars and islands. Figure 37 shows a digitized planform and aerial photograph in 2002, just after an increase in the number of bars and islands, compared to the year 2012. Between 2006 and 2008, the number of bars and islands decreased. The aerial photographs show that the islands had become attached to the banks and supported vegetation growth by the year 2012.

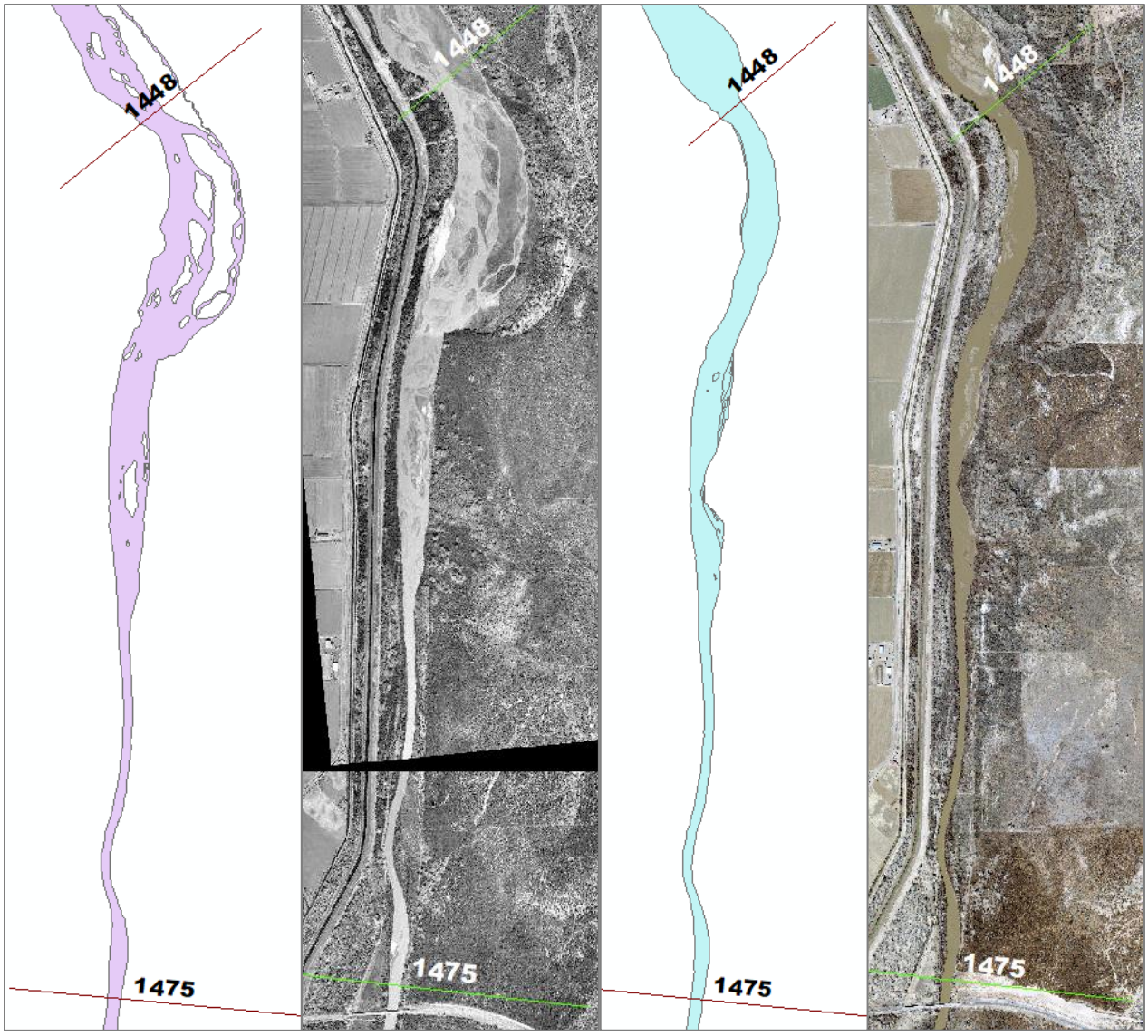

Figure 37 Digitized planform and aerial photograph of subreach E5 when multiple mid-channel bars and islands were present in 2002 (left) and in 2012 (right) after a reduction of mid-channel bars and islands.

3.9 Channel Response Models

The Julien and Wargadalam (JW) equations were used to predict the downstream hydraulic geometry of rivers (Julien and Wargadalam, 1995). These equations were based on empirical analysis of over 700 single-threaded rivers and channels, and predicted the width and depth likely to result from a given discharge, grain size and slope:

$$h = 0.2Q^{\frac{2}{6m+5}}D_s^{\frac{6m}{6m+5}}S^{\frac{-1}{6m+5}}$$

$$W = 1.33Q^{\frac{4m+2}{6m+5}}D_s^{\frac{-4m}{6m+5}}S^{\frac{-1-2m}{6m+5}}$$

Where $m = 1/\left[2.3\log\left(\frac{2h}{D_s}\right)\right]$, h is the flow depth, W is the channel width, Q is the flow discharge, D_s is the median grain size, and S is the slope. A discharge of 3,000 cfs, the same discharge as in the previous HEC-RAS analysis, was used. The values for slope and grain size were obtained from 3.3 Bed Elevation and 3.4 Bed Material, respectively. The median D_{50} of the 1990s was used for 1992, median D_{50} of the 2000s for 2002 and median D_{50} of the 2010s for 2012. The results are compared to the observed active channel widths (from the GIS analysis of the digitized planforms) in Table 4 and plotted in Figure 38. The percent difference was calculated as:

$$\text{Percent Difference} = 100 * \left(\frac{\text{predicted width} - \text{observed width}}{\text{observed width}}\right)$$

Table 4 Julien Wargadalam channel width prediction

Year	Subreach	D_s (mm)	Slope	Predicted Width (ft)	Observed Width (ft)	Percent difference
1992	E1	0.238	0.0007	251.737	326.430	-22.88
	E2	0.259	0.0009	239.370	576.966	-58.51
	E3	0.274	0.0007	250.604	298.608	-16.08
	E4	0.305	0.0009	236.210	637.482	-62.95
	E5	0.206	0.0008	240.071	545.582	-56.00
2002	E1	0.342*	0.0007	248.797	290.880	-14.47
	E2	0.300	0.0009	237.910	380.245	-37.43
	E3	0.227*	0.0006	258.455	259.079	-0.24
	E4	0.260	0.0008	240.214	441.868	-45.64
	E5	0.200	0.0008	239.769	360.179	-33.43
2012	E1	0.342*	0.0006	255.557	374.486	-31.76
	E2	0.300*	0.0009	238.400	289.556	-17.67
	E3	0.227*	0.0006	258.696	264.017	-2.02
	E4	0.260*	0.0008	242.624	498.712	-51.35
	E5	0.200*	0.0008	243.413	317.484	-23.33

*For 2002, there were no grain size data available for E1 and E3, so data from 1999 were used in replacement. For 2012, there were no grain size data, so the 2002 data was used.

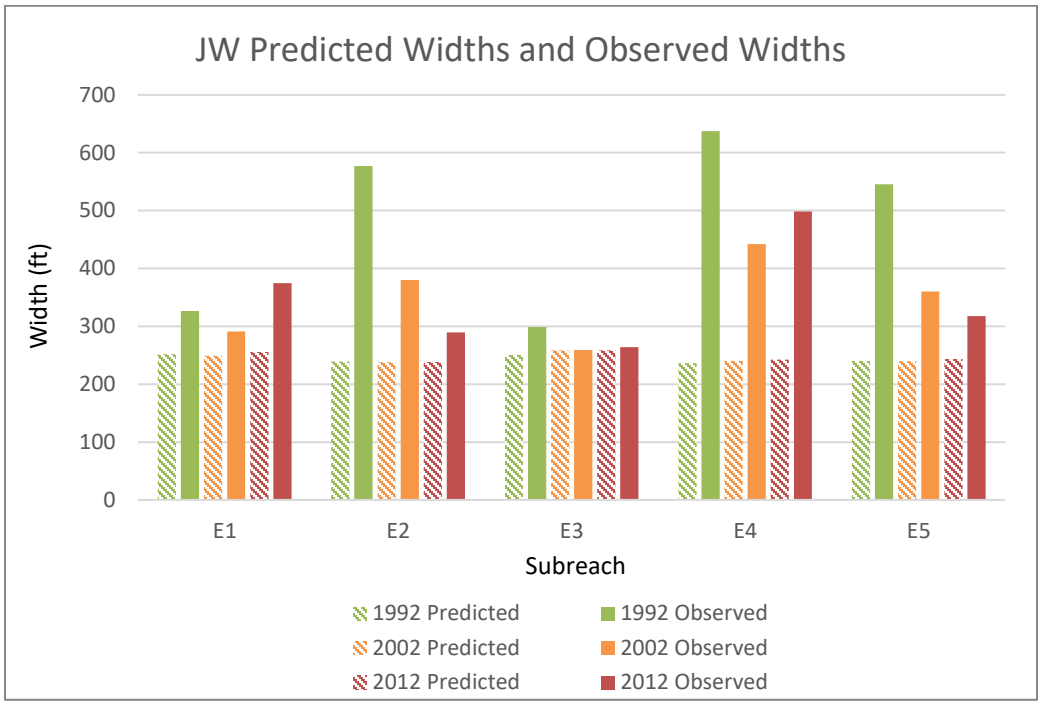

Figure 38 Julien and Wargadalam predicted widths and observed widths of the channel

The predicted widths are narrower than the observed widths for all subreaches but match very closely to the observed widths in subreach E3. The JW equations predict that the channel width for all subreaches will eventually narrow to around 240 to 260 feet. When calculating the predicted width of the river, the bankfull discharge was used when in reality, varying discharges would be occurring in the river. This could lead to the greater variability in the observed width values.

3.10 Geomorphic Conceptual Model

Massong et al. (2010) developed a channel planform evolution model for the Rio Grande based on historic observations. The sequence of planform evolution is outlined in Figure 39. Stage 1 describes a large channel with a high sediment load and large floods, which results in an active channel with constantly changing bars and dunes and little vegetation encroachment. The evolution from dunes to islands and bars transitions the river into Stage 2. As the islands and bars are stabilized by vegetation, they begin to act like floodplains indicating that the river is transitioning to Stage 3. The sediment transport capacity then becomes the determining factor of the future course of the river to either an aggrading river (stages A4-A6) or a migrating river (stages M-4 to M-8). A deficiency in sediment transport capacity, meaning the sediment supply is exceeding the transport capacity, leads to aggradation in the main channel and the flow eventually shifts onto the lower surrounding floodplain. When the sediment transport capacity exceeds the sediment supply, bank material erodes both laterally and vertically, leading to a meandering river. Transition between the M stages and the A stages can occur, but a reset to a Stage 1 requires a large, prolonged flood (Massong et al., 2010).

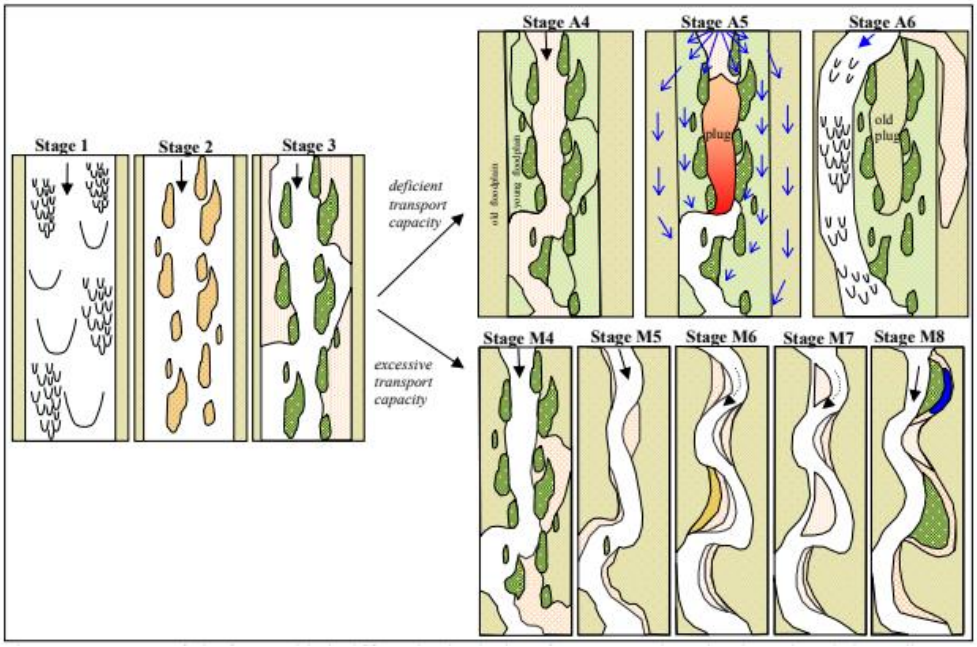

Figure 39 Planform evolution model from Massong et al. (2010). The river undergoes stages 1-3 first and then continues to stages A4-A6 or stages M4-M8 depending on the sediment transport capacity.

Comparisons between channel shifts and the channel slope of the MRG have indicated that transitions into the aggrading reach cycle have a slope of less than 0.0007 ft/ft, while transitions through the migrating reach stages have a slope greater than 0.0009 ft/ft (Massong 2010). The Escondida reach has slopes that range between 0.0006 and 0.0009, which has resulted in a river that can transition into either the aggrading or migrating reach stages.

Figure 40 and Figure 41 show the evolution of the channel in the first subreach using a representative cross section of E1 along with aerial photos throughout history. The river's discharge is unknown at the time of the photos. Subreach E1 has become more incised between 1962 and 2012 and the area of the channel has increased. The sediment transport capacity exceeds the sediment supply of the subreach leading to lateral and vertical erosion. From 1992 to 2012, the main channel becomes more dominant, while the side channels become less active, which indicates that the subreach is transitioning from migrating stage M4 to M5.

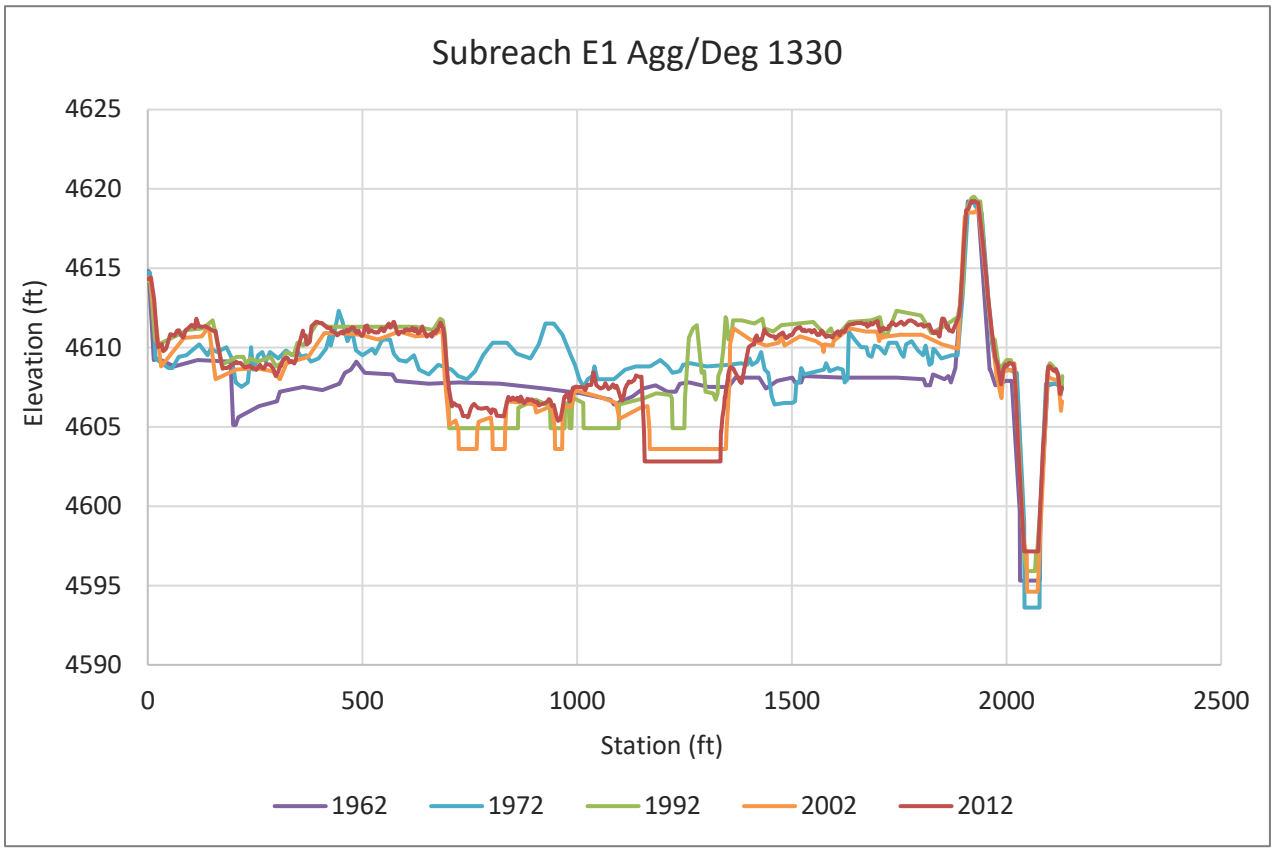

Figure 40 Channel evolution of a representative cross section from subreach E1

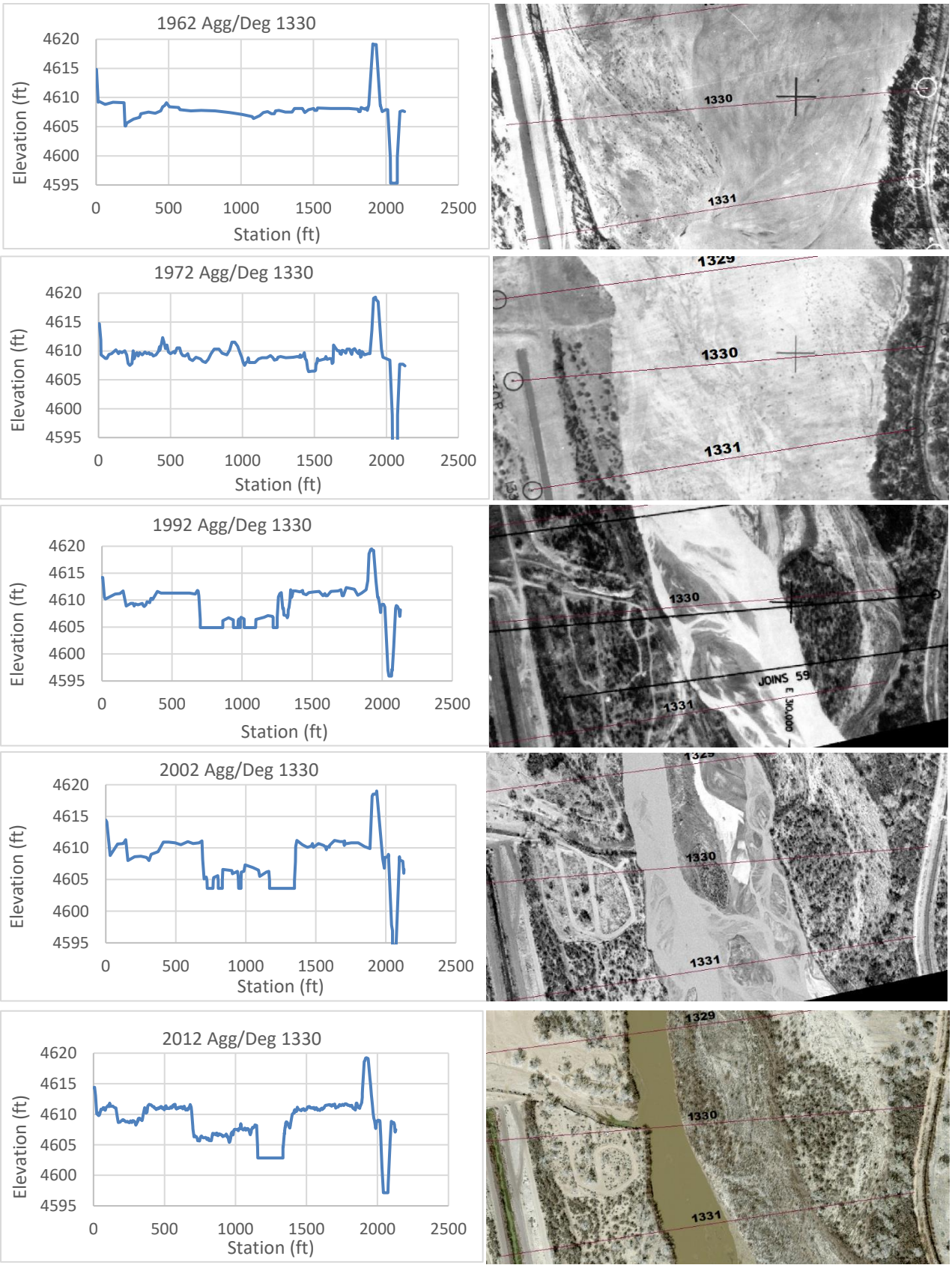

Figure 41 Subreach E1: historical cross section profiles and corresponding aerial images

Subreach E2 appears to have a channel that is constantly shifting laterally but hasn't seen significant aggradation or degradation. Between 2002 and 2012, the channel did not migrate quite as much, but began to incise indicating it could be in the M4 stage, beginning to form a more dominant channel. The cross-section profile is shown in Figure 42 and a side by side view of the cross section and aerial imagery is shown in Figure 43.

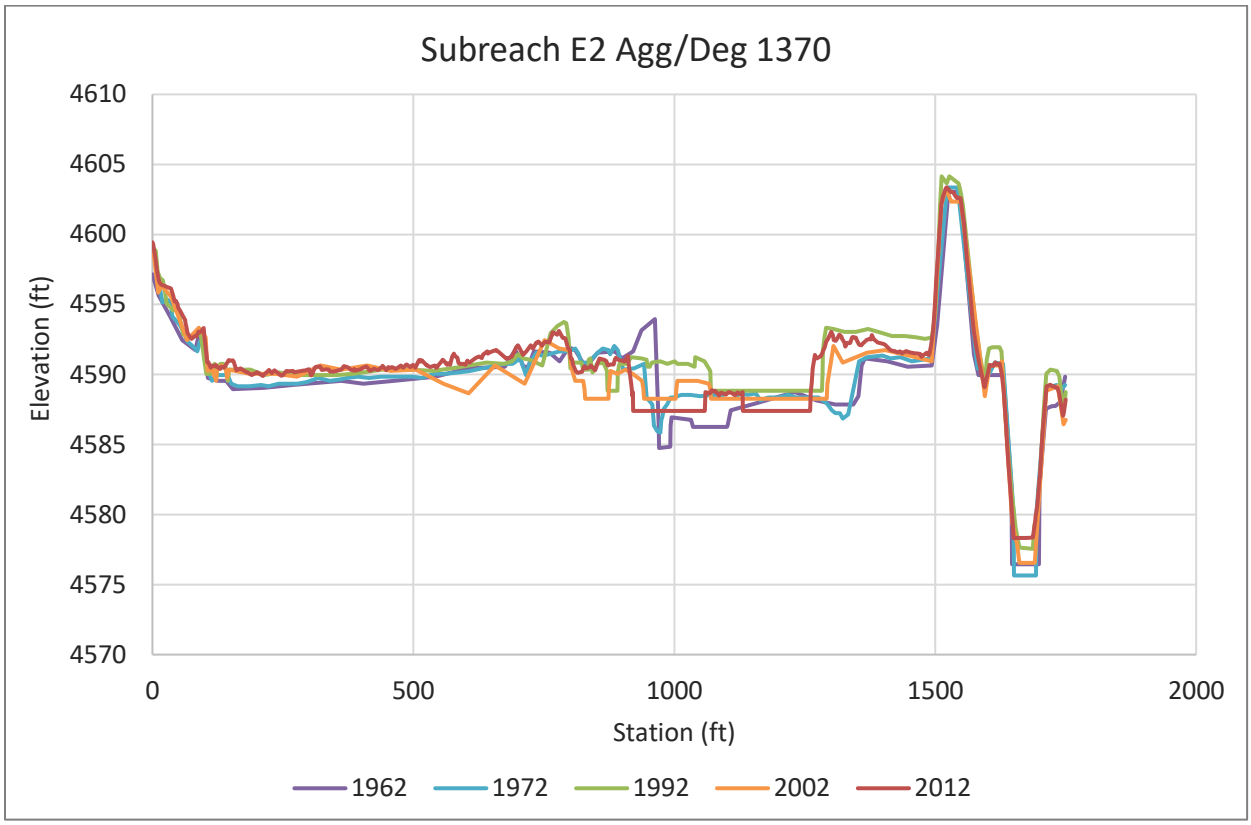

Figure 42 Channel evolution of a representative cross section from subreach E2

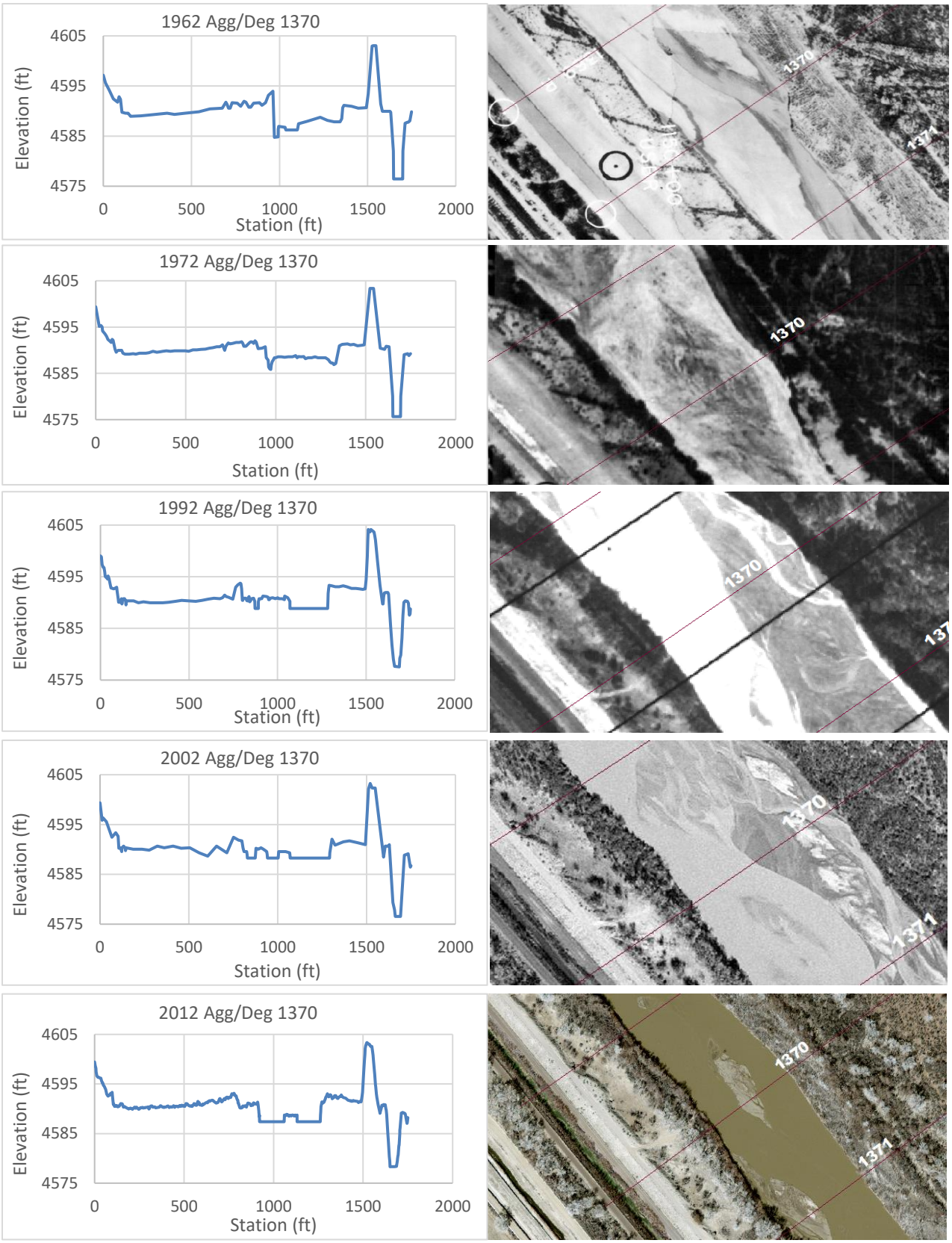

Figure 43 Subreach E2: historical cross section profiles and corresponding aerial images

Subreach E3 appears to be in the M5 stage. Based on the evolution of the cross-section profile throughout the available years (Figure 44), the channel has not changed significantly between 1962 and 2012. There was aggradation that occurred leading up to 1992, but the channel has since degraded to a level like 1962. The channel remains single-threaded and the sinuosity has remained relatively constant between 1918 and 2016 based off of the GIS analysis performed, further indicating that the subreach may be in the M5 stage. Although the channel may be in the migrating stages now, the perched cross sections within subreach E3 indicate that the channel was aggrading at one point. This highlights that the subreach can transition between migrating and aggrading stages depending on the hydrology and sediment trends. Figure 45 shows the cross-section profile for the various years along with a corresponding aerial image of the river.

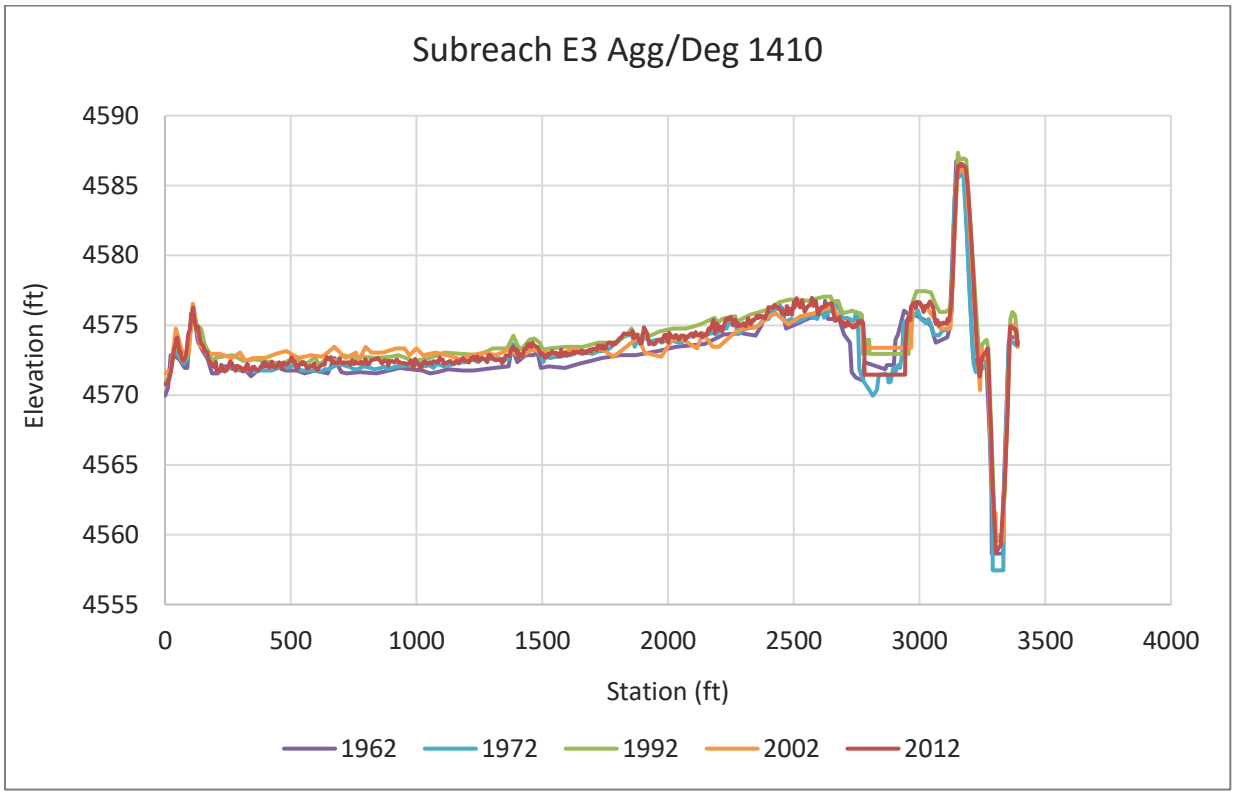

Figure 44 Channel evolution of a representative cross section from subreach E3

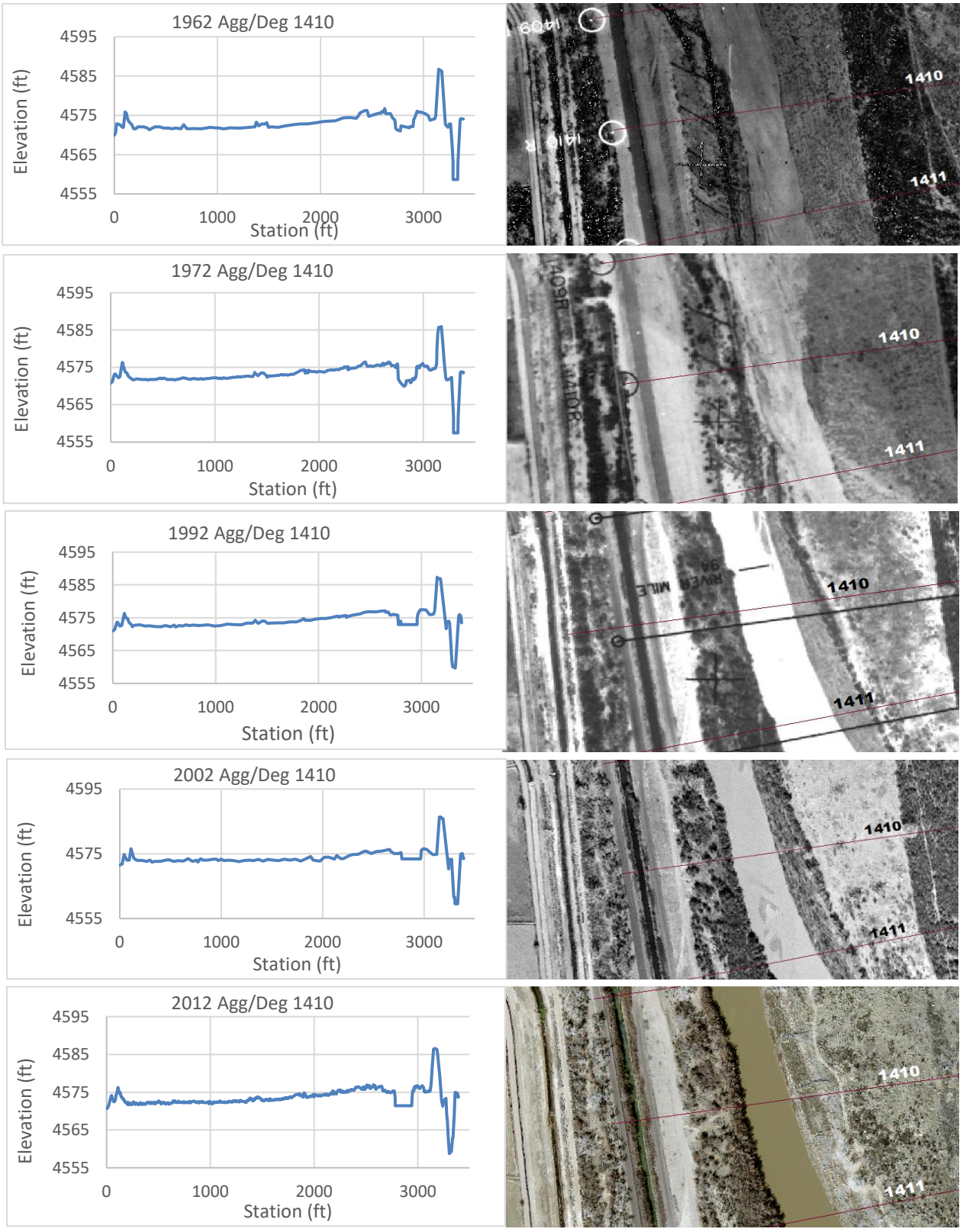

Figure 45 Subreach E3: historical cross section profiles and corresponding aerial images

Subreach E4 would be classified as an aggrading subreach, possibly in the stage A4 in 2012. The sediment supply exceeds the sediment transport capacity, so sediment is being deposited throughout the subreach. As seen in Figure 46 and Figure 47, the channel in 2002 the channel had aggraded, but did not become fully plugged by sediment.

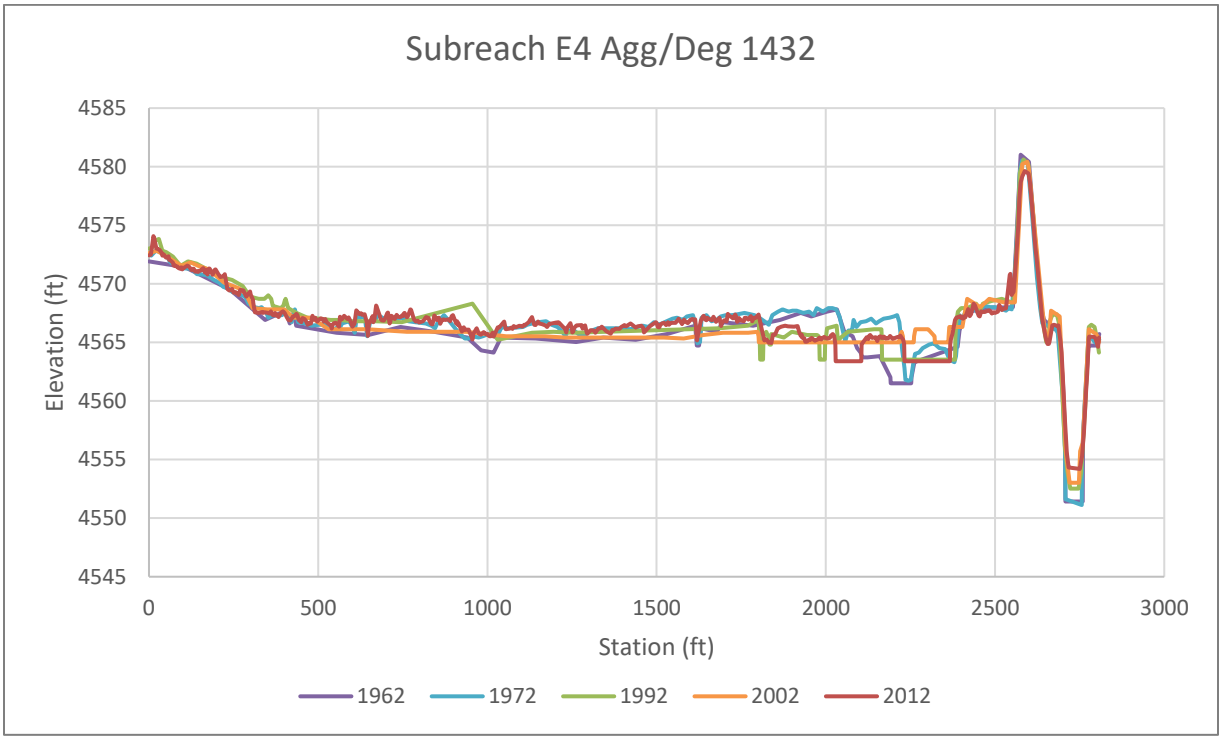

Figure 46 Channel Evolution of a representative cross section of subreach E4

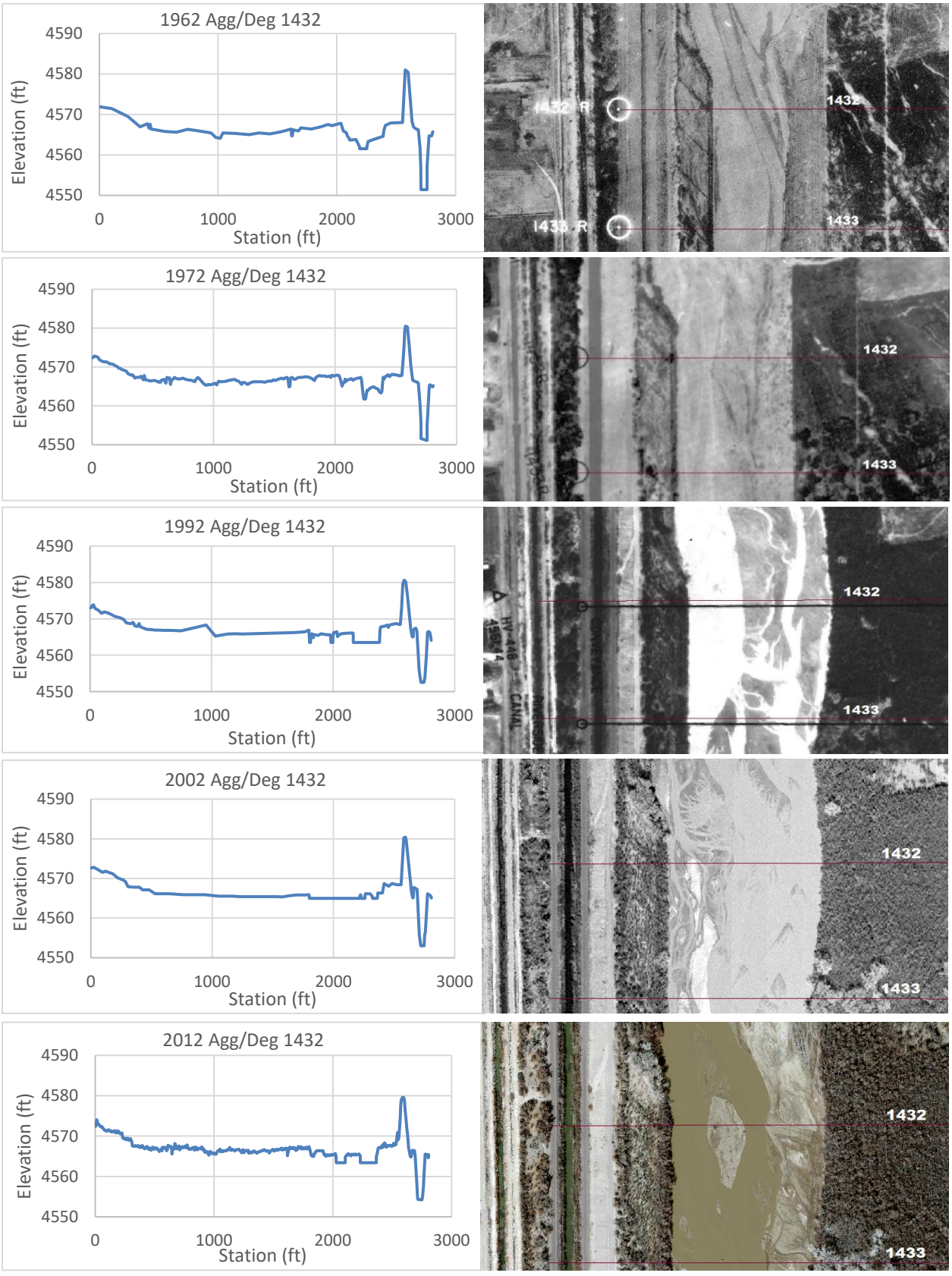

Figure 47 Subreach E4: historical cross section profiles and corresponding aerial images

Subreach E5 is characteristic of having a perched channel for many of the cross sections. This subreach is at the downstream end of the reach, past the "pivot point" of degradation and aggradation. As seen in Figure 48 and Figure 49, the main channel has widened and aggraded from 1962 and 2012. Between 2002 and 2012, the sediment load has exceeded the transport capacity, so sediment is deposited in the channel while the width has remained nearly constant leading to a decrease in channel area. This subreach would be classified as an aggrading reach, A4. At a moderate flow, the water would overtop the banks and spill into the floodplains. While the subreach is aggrading, the aggradation rate has not increased enough to result in a sediment plug.

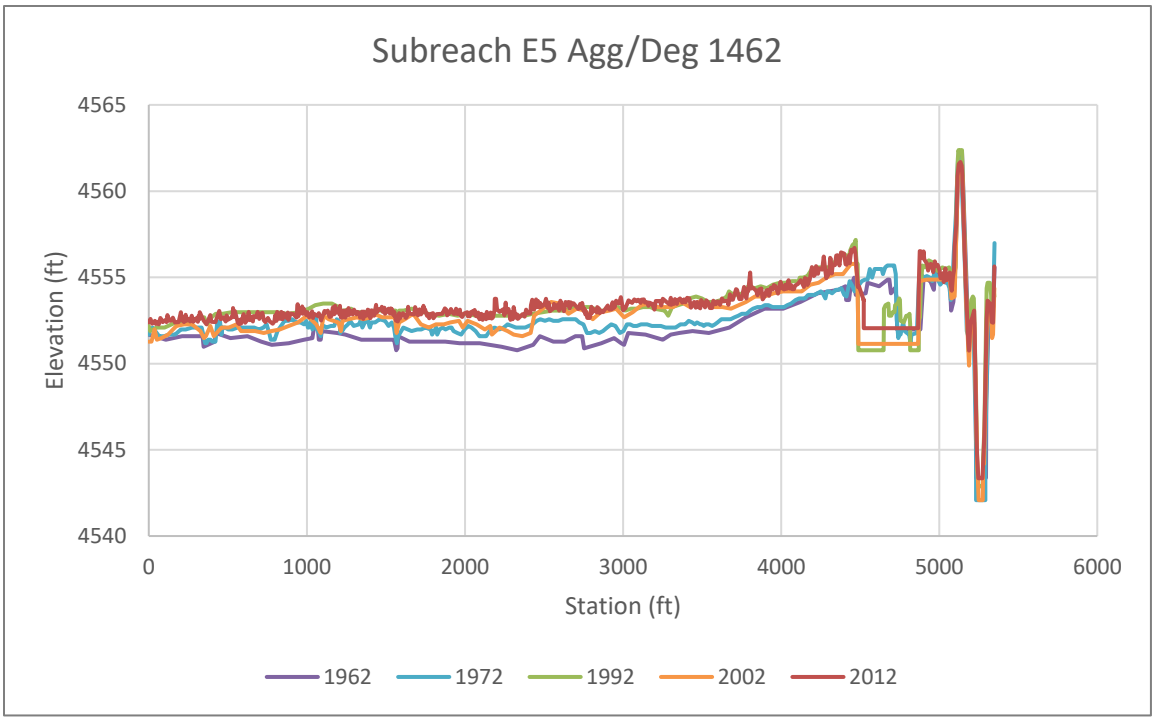

Figure 48 Channel evolution of a representative cross section of subreach E5

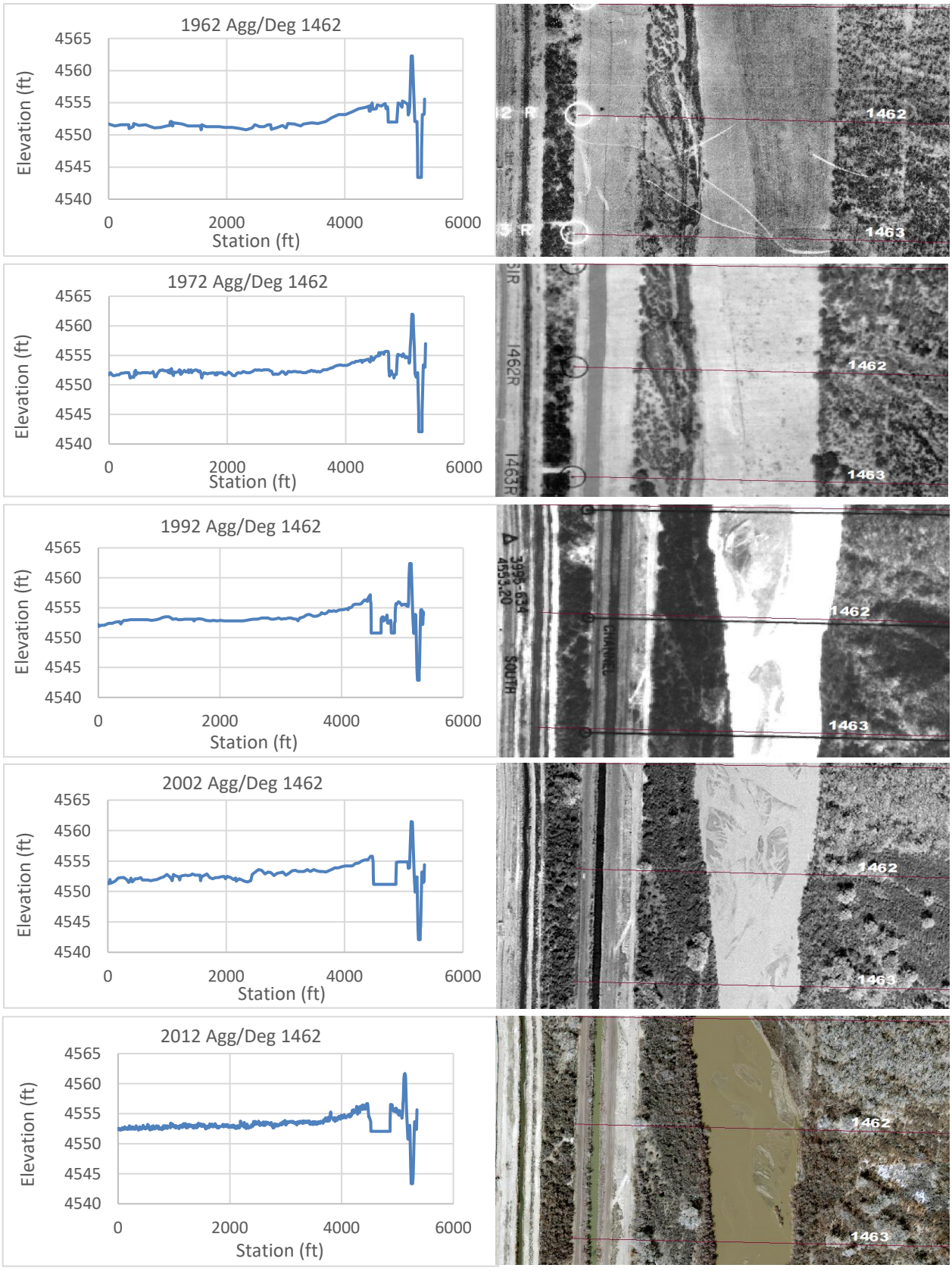

Figure 49 Subreach E5: historical cross section profiles and corresponding aerial images

4. HEC-RAS Modeling for Silvery Minnow Habitat

The Rio Grande Silvery Minnow (RGSM or silvery minnow) is an endangered fish species that is native to the Middle Rio Grande. Currently, it occupies only about seven percent of its historic range (U.S. Fish and Wildlife Service, 2010). It was listed on the Endangered Species List by the US Fish and Wildlife Service in 1994.

One of the most important aspects of silvery minnow habitat is the connection of the main channel to the floodplain. Spawning is stimulated by peak flows in late April to early June. These flows should create shallow water conditions on the floodplains, which is ideal nursery habitat for the silvery minnow (Mortensen et al., 2019). Silvery minnows require specific velocity and depth ranges depending on the life stage that the fish is in. Table 5 outlines these velocity and depth guidelines. Fish population counts are available from 1993 to the present. Therefore, analysis of silvery minnow habitat will not begin prior to 1992. In preparation for the process linkage report, figures relating the geomorphology of the river and RGSM habitat availability are included in Appendix F.

Table 5 Rio Grande Silvery Minnow habitat velocity and depth range requirements (from Mortensen et al., 2019)

	Velocity (cm/s)	Depth (cm)
Adult Habitat	<40	>5 and <60
Juvenile Habitat	<30	>1 and <50
Larvae Habitat	<5	<15

4.1 Modeling Data and Background

The data available to develop these models varies year by year. Cross section geometry was available for the years 1962, 1972, 1992, 2002, and 2012. In 2012, additional LiDAR data of the floodplain was available, which allowed the development of a terrain for RAS-Mapper. Therefore, RAS-Mapper was used in 2012 only, while comparisons across years are done using 1-D techniques.

HEC-RAS distributes water by adding water to a cross section from the lowest elevation up. Much of the MRG is perched, so this can lead to inaccurate predictions of the flow distribution within the cross sections- overpredicting water in the floodplains, therefore overpredicting hydraulically suitable habitat. Computational levees were used in HEC-RAS to keep the water contained in the channel until bankfull is reached. At the discharge that this occurs, the computational levees were removed to allow water to spill out onto the floodplains. The computational levees are removed at the same discharge throughout the entire reach. This method is described by Baird and Holste (2020) and uses a capability in HEC-RAS that determines the “left levee freeboard” and “right levee freeboard” which is the difference between water surface elevation and computational levee elevation. A negative value indicates an overtopping discharge. A sensitivity analysis was completed to determine the percentage of cross sections that should be overtopped before removing the top of bank points in HEC-RAS. For this analysis, when 25% of the cross sections in the reach were experiencing overtopping, signifying 25% had reached bankfull discharge, the computational levees were removed, allowing water to inundate the floodplains. The results from the levee freeboard analysis are shown in Figure 50.

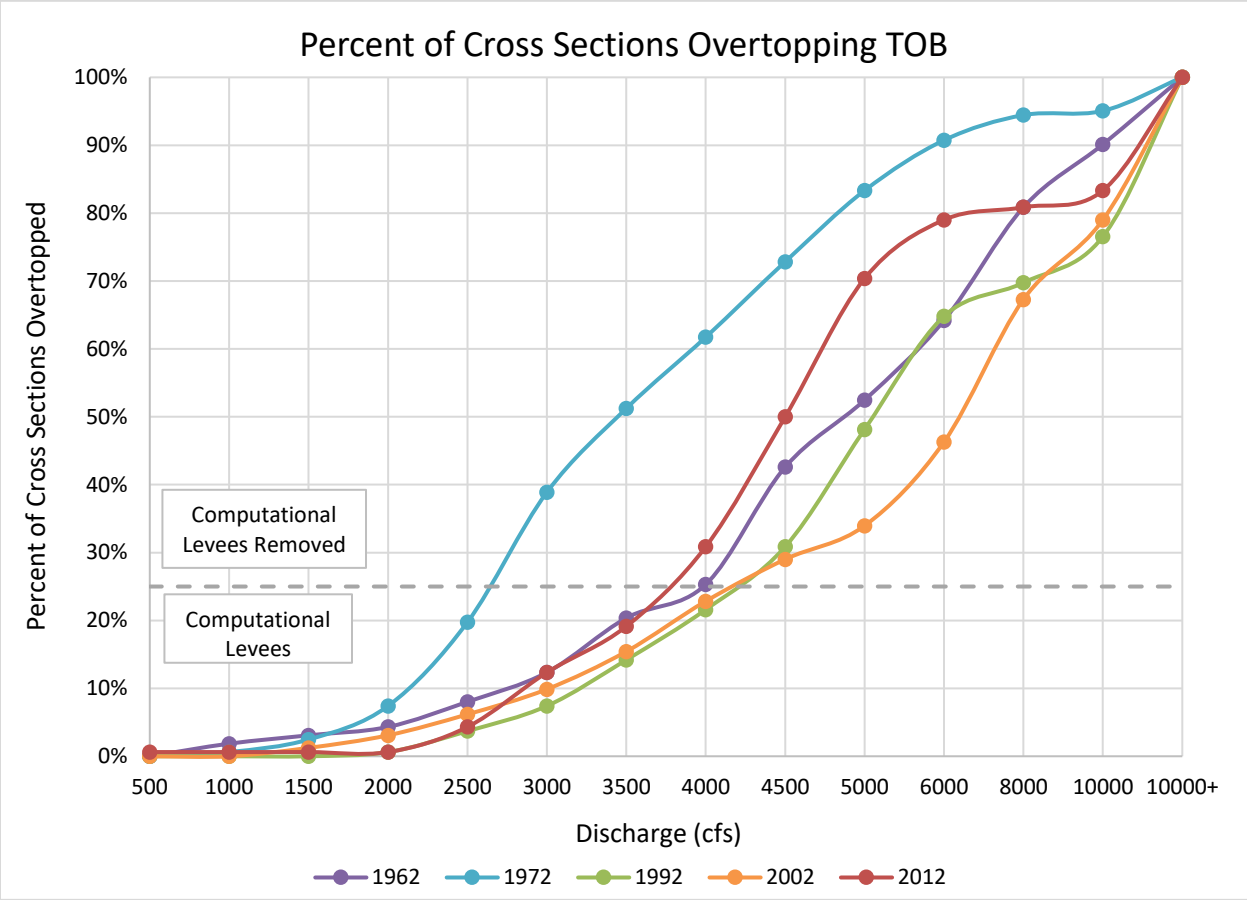

Figure 50 Comparing the overbanking discharge values at various years. The dashed line (indicating 25% of cross sections in a reach experiencing overbanking) determines the discharge at which computational levees are removed for habitat analysis.

4.2 Width Slices Methodology

Without a terrain for 2002 and 1992, additional methods had to be considered to determine a metric of fish habitat. HEC-RAS has the capability to perform a flow distribution analysis to calculate the laterally varying velocities, discharges, and depths throughout a cross section as described in chapter 4 of the HEC-RAS Hydraulic Reference Manual (US Army Corps of Engineers, 2016). HEC-RAS allows each cross-section to be divided into a set number of slices up to 45. Because the RGSM relies heavily on floodplains for habitat (due to higher velocities and depths in the main channel) and the floodplains contain more variability than the main channel, 20 width slices were assigned in each floodplain and 5 width slices in the channel. An example of the flow distribution in a cross-section is shown in Figure 51. The velocity and depth of each slice were analyzed to determine the total width at each agg/deg line that meets the RGSM larval, juvenile, and adult criteria. Because the agg/deg lines are spaced approximately 500 feet apart, the hydraulically suitable widths were multiplied by 500 feet to obtain an area of hydraulically suitable habitat per length of river.

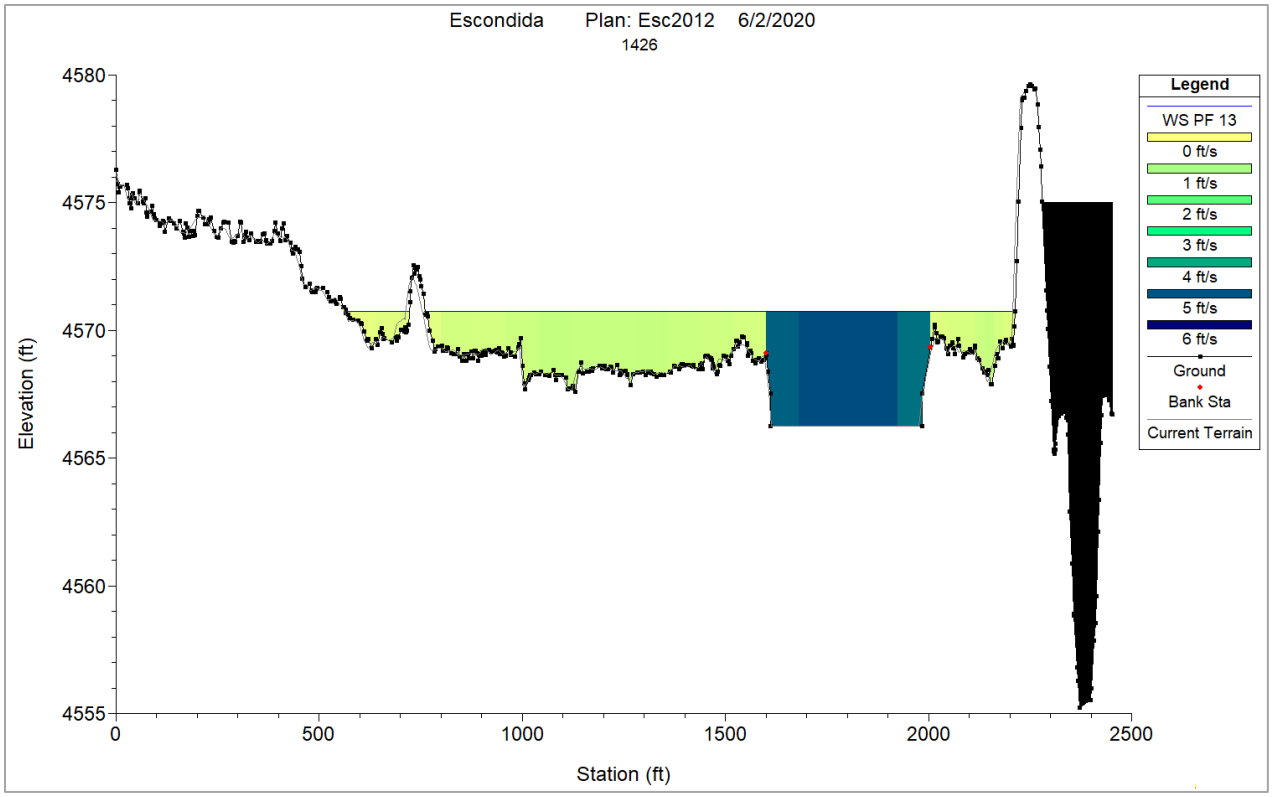

Figure 51 Cross-section with flow distribution from HEC-RAS with 20 vertical slices in the floodplains and 5 vertical slices in the main channel. The yellow and green slices are small enough that the discrete color changes look more like a gradient.

4.3 Width Slices Habitat Results

The width slices method was first used to analyze the habitat availability throughout the Escondida reach at a reach scale for the years of 1962, 1972, 1992, 2002 and 2002. For the discharges at which the water is contained in the main channel, there is less habitat availability. At low discharges, such as 500 cfs, the depth and velocity in the channel remain low enough to provide suitable areas for the RGSM. However, as the discharge increase (but flow is still maintained in the channel) the amount of habitable area that meets the depth and velocity criteria for the Silvery Minnow decreases. When the discharge increases and the water can spill out onto the floodplains, there is suddenly an increase in area where the depth and velocity criteria are met. This is displayed by Figures 52 to 54.

Throughout the Escondida reach, the trend follows the same general pattern for larvae, juvenile, and adult stage habitat. In 1972, the channel was narrow and relatively shallow, making the channel area the smallest out of the years analyzed. The channel would overbank at a much lower discharge, which leads to an earlier spike in habitat availability. Once the depth or velocity becomes too high due to higher discharges, the hydraulically suitable habitat availability decreases.

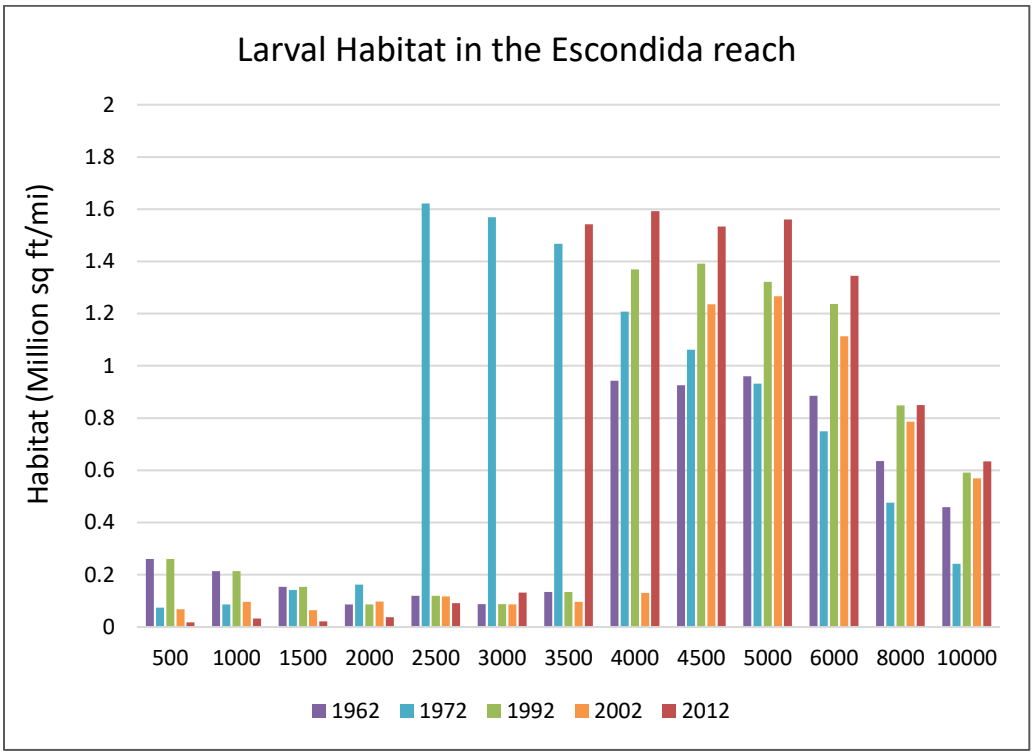

Figure 52 Larval RGSM habitat availability throughout the Escondida reach- the scale of the y-axis is lower for the larval habitat to better see the trends in the hydraulically suitable habitat.

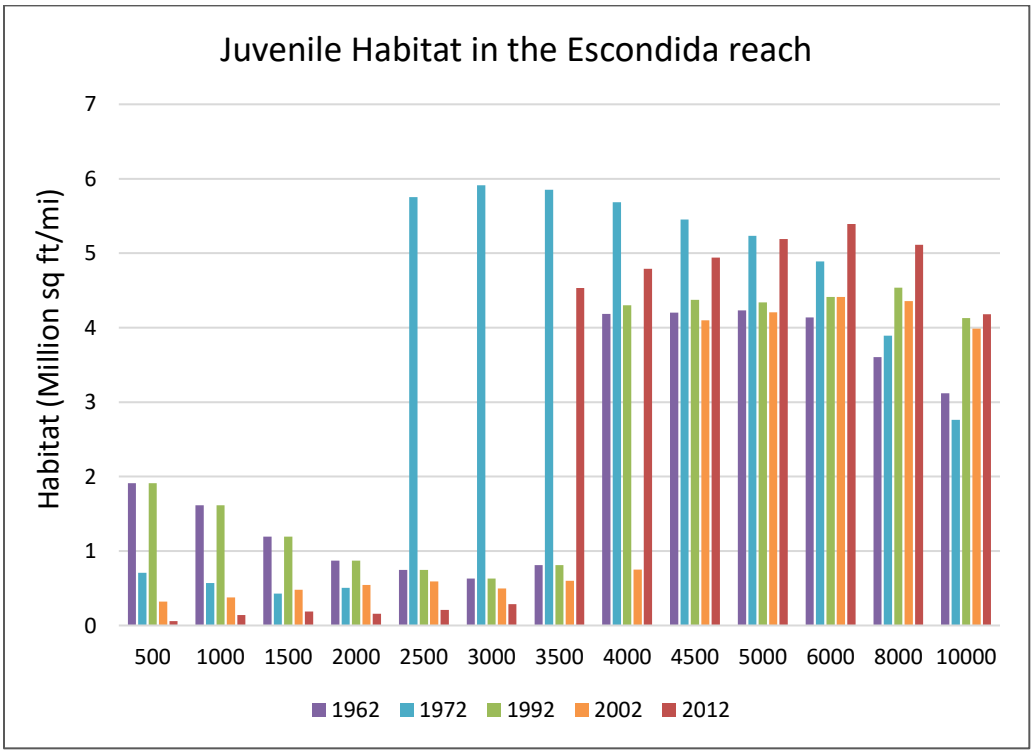

Figure 53 Juvenile RGSM habitat availability throughout the Escondida reach

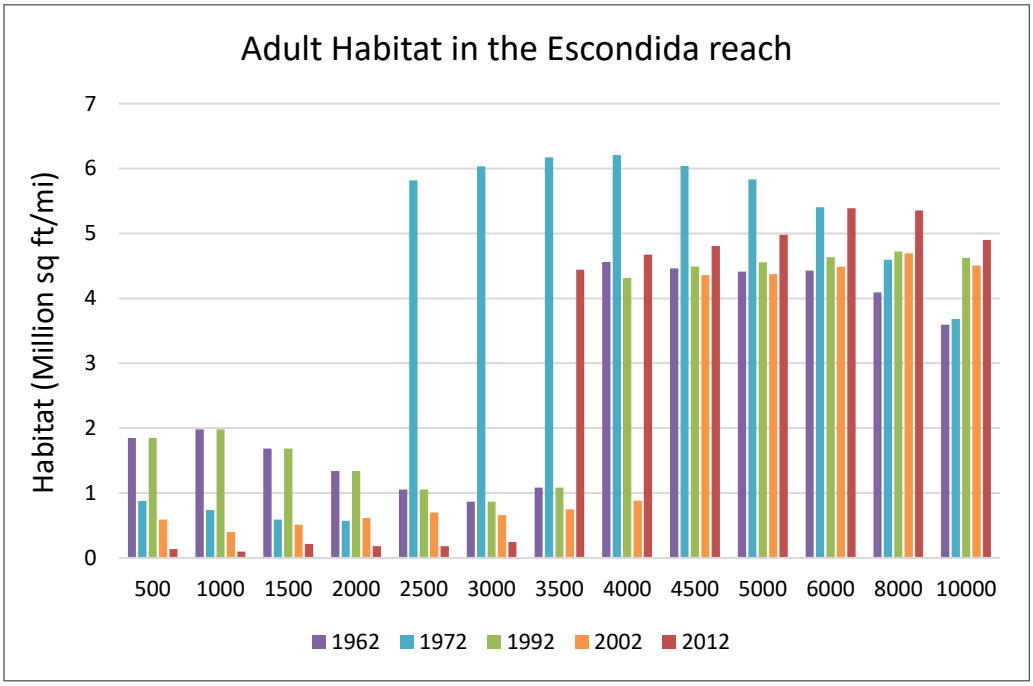

Figure 54 Adult RGSM habitat availability throughout the Escondida reach

The width slices method was also used to analyze the habitat availability throughout the Escondida reach at a subreach level. Based on this method, subreach E5 had the greatest amount of possible habitat at higher discharges. At lower discharges, E1 previously had the greatest amount of hydraulically suitable habitat between 1962 and 1992, but in 2012, subreach E4 had the greatest amount of possible habitat at lower discharges. Additional bar charts for all subreaches are in Appendix D.

Stacked habitat bar charts were also created to portray the spatial variation of hydraulically suitable habitat throughout the Escondida reach. Bar charts displaying width of habitat were created for 1962, 1972, 1992, 2002, and 2012. To convert this to an the area of habitat, these values can be multiplied by 500 feet (the approximate distance between agg/deg lines). There is little available habitat at the lower discharges for the year 2012, so first a plot of 2012 habitat is shown up to 3,000 cfs in Figure 55. The full stacked habitat chart for 2012 is shown in Figure 56, and the other years are included in Appendix D.

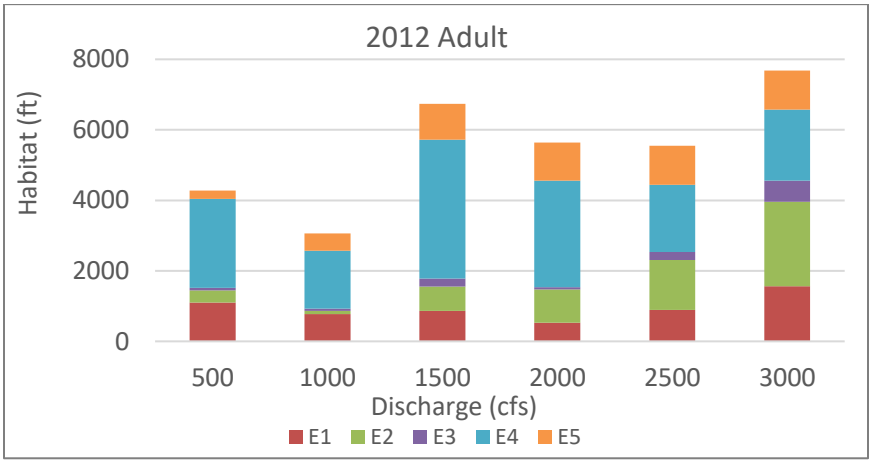

Figure 55 Stacked habitat charts to display spatial variations of habitat throughout the Escondida reach in 2012

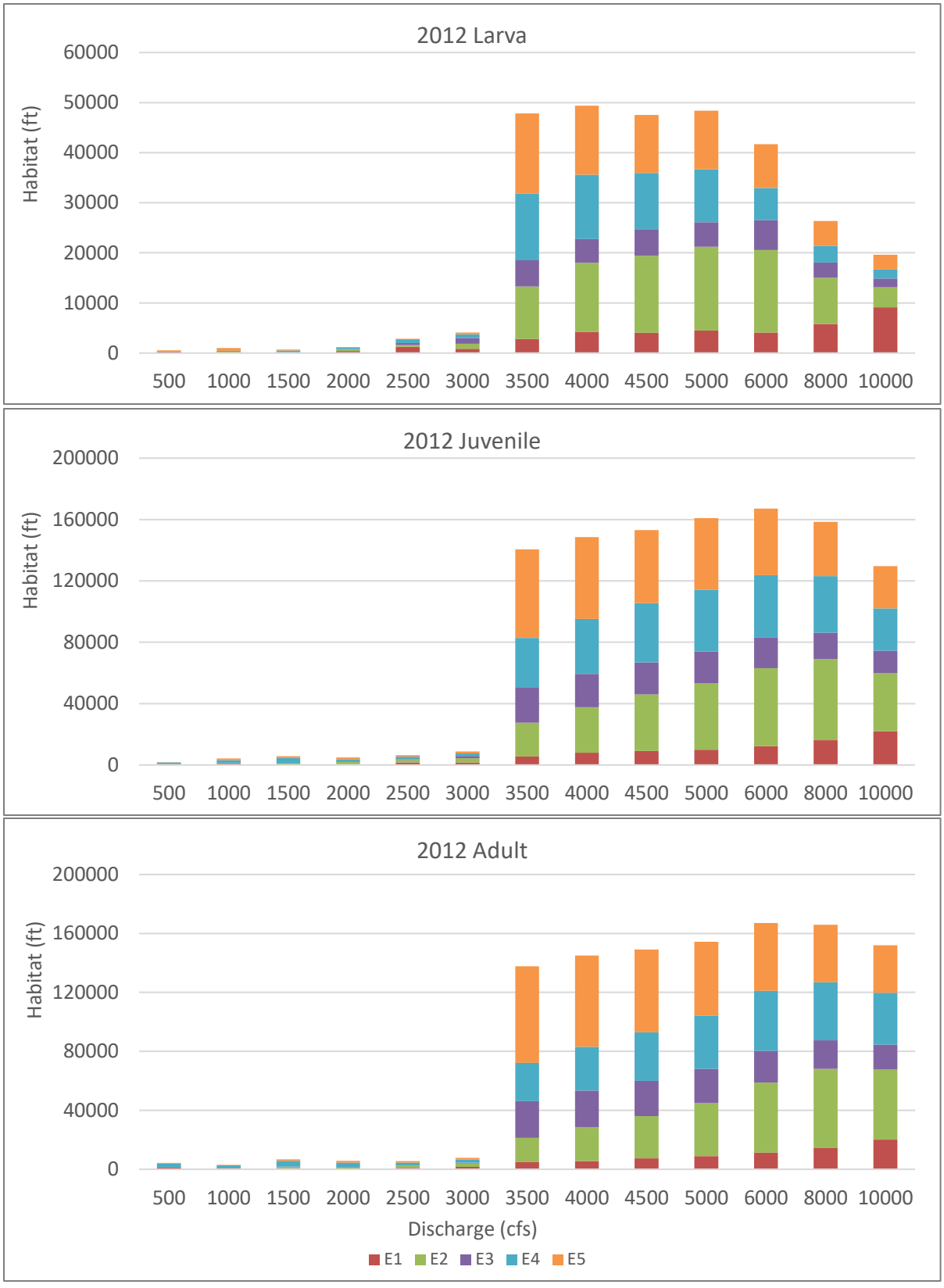

Figure 56 Stacked habitat charts to display spatial variations of habitat throughout the Escondida reach in 2012

4.4 RAS-Mapper Methodology

The goal of RAS-Mapper was to transform the 1-D habitat estimates into pseudo two-dimensional (2-D) results. RAS-Mapper overlays the water onto a prescribed terrain and interpolates the water surface elevation to create an estimate of the location of water inundation, which can then be used to predict locations of hydraulically suitable habitat.

The HEC-RAS geometry data that was necessary for the RAS-Mapper analysis (geo-referenced cross-sections and a LiDAR surface to generate a terrain) was available only for the year 2012. Therefore, only 2012 results were processed in RAS-Mapper. The original 2012 LiDAR data were used to develop a raster on ArcMap software (intellectual property of ESRI), which could be imported as a terrain in RAS-Mapper. The RAS-Mapper application distributes the water throughout the terrain, interpolating between the cross-sections, which results in a more accurate understanding of where water is present in a channel. RAS-Mapper will also predict the flow depth and velocity at a given discharge. ArcMap was used to combine the RAS-Mapper generated rasters for velocity and depth, so the RGSM depth and velocity criteria could be applied to identify the areas of suitable habitat. The results were used to create maps that show the areas of hydraulically suitable habitat for each life stage of the RGSM.

4.5 RAS-Mapper Habitat Results in 2012

While the width slice method quantitatively determined areas with increased potential for habitat, Ras-Mapper was used to spatially depict these areas of potential RGSM habitat throughout the MRG and display the results on a map of the river. The hydraulically suitable habitat for each life stage was mapped at discharges of 1,500 cfs, 3,000 cfs, and 5,000 cfs, which have daily exceedance probabilities of around 11%, 4%, and 0.04%, respectively.

According to the RAS-Mapper results, there is very little Silvery Minnow habitat in the upper portion of the Escondida reach at 1,500 cfs and 3,000 cfs. At a discharge of 5,000 cfs, the amount of hydraulically suitable habitat increases greatly. An example of the habitat maps for subreach E4 at discharges of 1,500 cfs and 5,000 cfs is shown in Figure 57. The habitat maps for the remainder of the subreaches at each discharge can be found in Appendix E.

Although a discharge of 5,000 cfs may not be commonly seen throughout the Escondida reach, maps at this discharge still provide the opportunity to examine possible areas that are more likely to meet the velocity and depth criteria for the RGSM. This can help in identifying which areas may have hydraulically suitable habitat that are connected to the main channel due to backwater or natural formation of pools and which subreaches contain habitat that may be found suitable but are not connected to the main channel. Both instances may be beneficial for the future of the RGSM, but different approaches may be needed in planning restoration efforts.

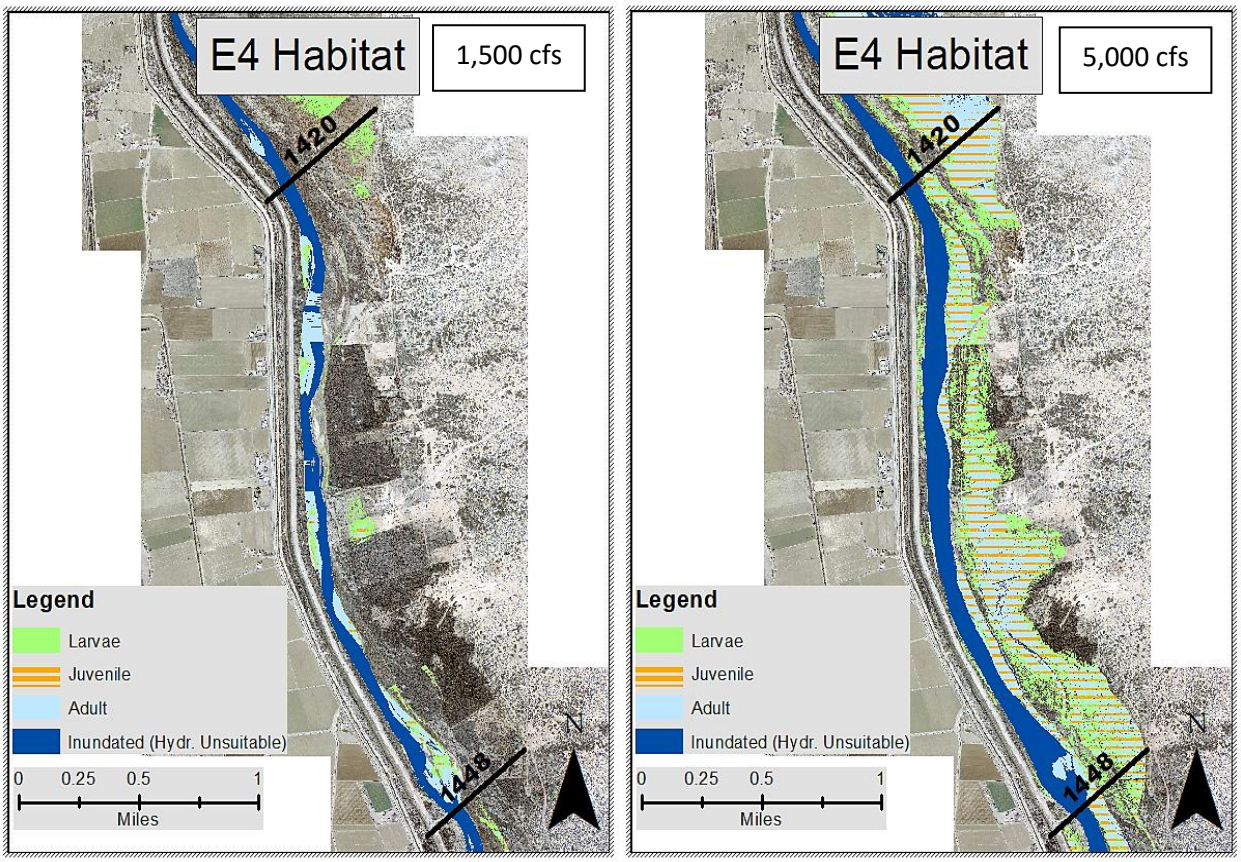

Figure 57 Hydraulically suitable habitat for each life stage in subreach E4 at 1,500 cfs (left) and 5,000 cfs (right)

4.6 Disconnected Areas

RAS-Mapper provides the opportunity to identify areas that likely meet the velocity and depth requirements of the RGSM at specified discharges. RAS-mapper may also be beneficial for identifying areas throughout the reach that may contain water but fail to remain connected to the main channel. These may be possible areas of focus for restoration efforts.

By connecting several of these disconnected areas, the Silvery Minnow may gain a great amount of possible habitat. Figure 58 shows one instance of a disconnected area in the Escondida reach. The disconnected area is emphasized in the zoomed in square on the right. It is possible to see that the main channel is deeper (darker blue) yet the floodplains and low-lying areas may become inundated at higher flows. The disconnected areas could identify problem areas for the RGSM by indicating that there are areas where fish may become stranded in months when the river contains less water and disconnected areas form. Conversely, these areas could become possible restoration sites leading to an increase in hydraulically suitable RGSM habitat.

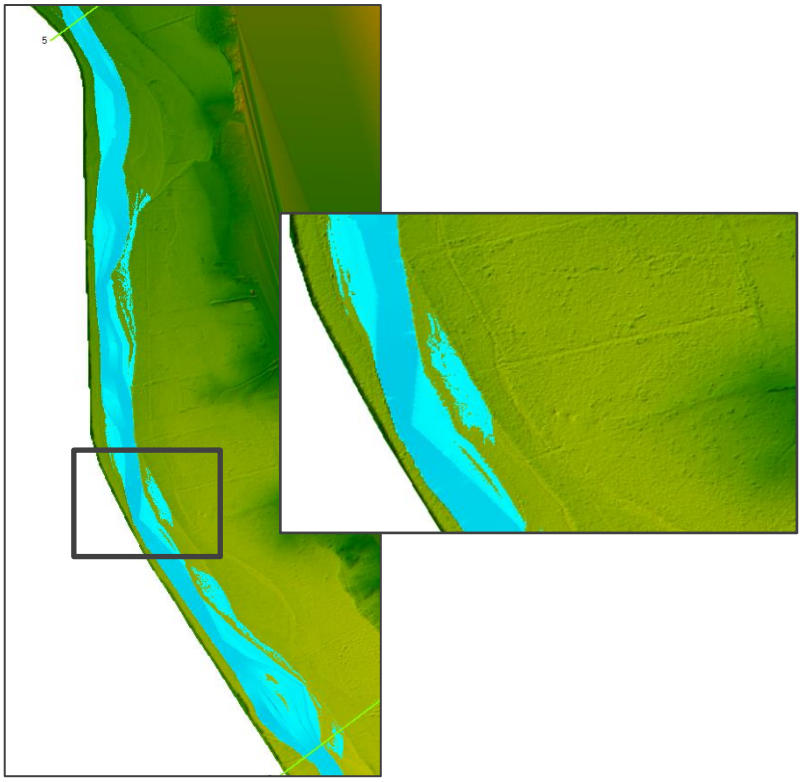

Figure 58 Example of a disconnected area that contains water, but no access to or from the main channel

After calculating the velocity and flow distribution, these disconnected areas often meet the depth and velocity criteria of the RGSM. However, the lack of connectivity eliminates the possibility of RGSM habitat. Figure 59 for example predicts that the shown disconnected areas would be hydraulically suitable for the RGSM extensively for the adult and juvenile life stages, and even show small areas that may support the larval life stage as well.

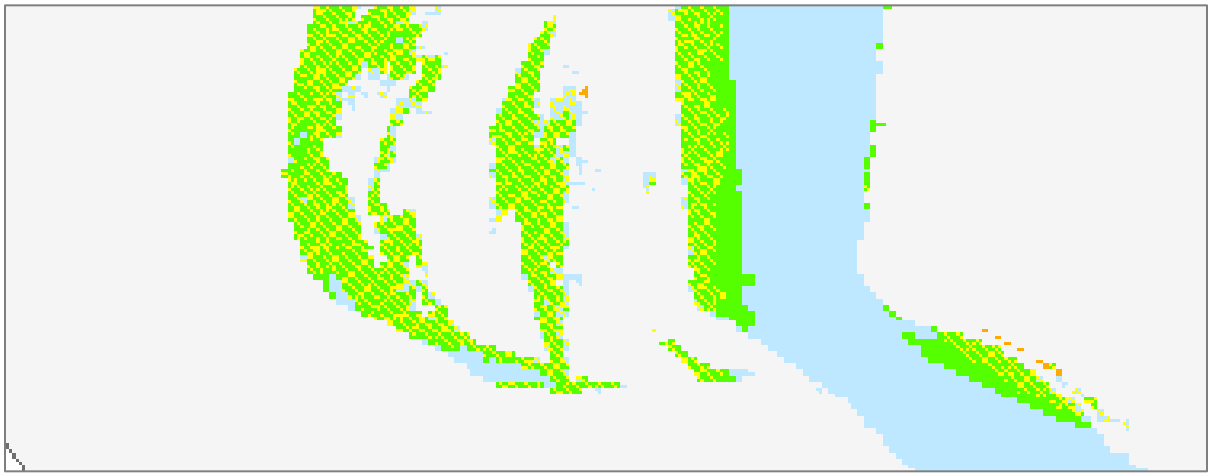

Figure 59 Disconnected area showing hydraulically suitable habitat for RGSM adult (green), juvenile (yellow cross hatch), and larvae (orange)

5. Time-Integrated Habitat Metric

Time-Integrated Habitat Metrics (TIHMs) were developed to estimate the hydraulically suitable habitat annually using the habitat results obtained from the width slice method and considering measured daily discharges in the reach. The TIHMs can be used to "assess the interaction between discharge periods, habitat conditions, and the RGSM population by providing a quantitative basis to compare the availability of suitable habitat area over time to the estimated densities of Rio Grande Silvery Minnow at the reach scale" (Mortensen 2020). The TIHM model requires daily discharge data and yearly habitat data. The gages in the Escondida reach do not have a complete record of discharge data from 1992 to 2012, so the San Acacia gage was used to interpolate the discharge values for the unknown time gaps. Both gages have data from 2005 to 2019, so the values from the two gages were plotted as seen in Figure 60. An equation was determined from the line of best fit that could be used to estimate the values from 1992 to 2005 at the Escondida gage (Q_{ESC}) based on the known San Acacia discharge values (Q_{SA}). This model fits best when applied to San Acacia discharge values that are greater than approximately 15 cfs.

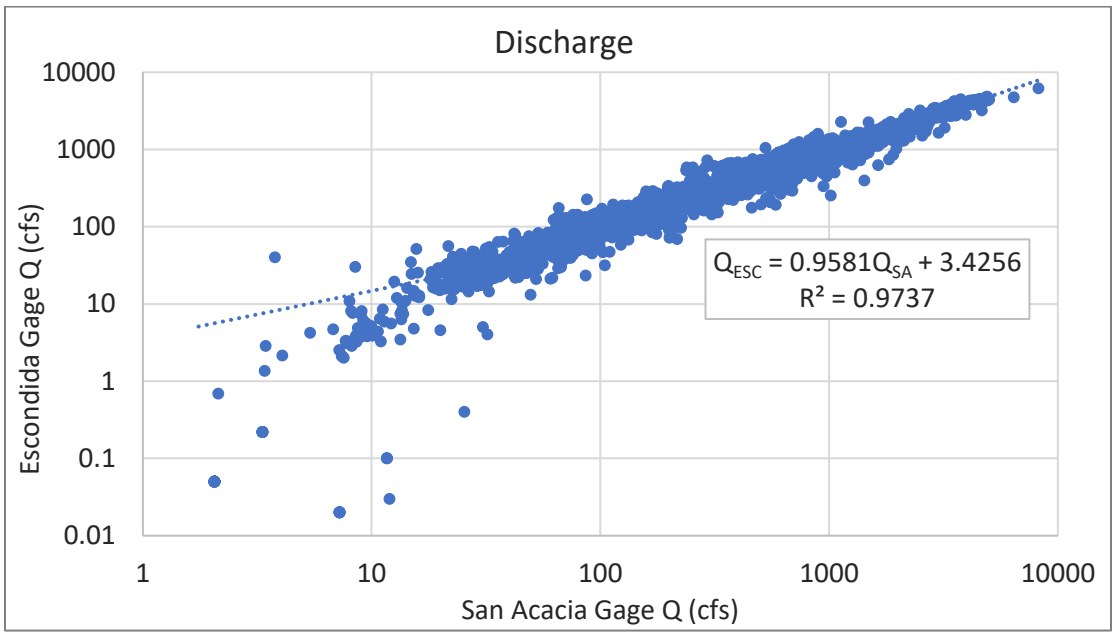

Figure 60 Correlating the discharge values at the San Acacia (Q_{SA}) and Escondida (Q_{ESC}) gages to create a model to estimate the unknown values at the Escondida gage.

Because annual habitat data is also required for the TIHM model, the sediment rating curve was used to interpolate from the previously generated habitat results (for the years 1992, 2002, and 2012) to create a habitat plot for each year between 1992 and 2019 as a function of discharge. For this method, it is assumed that the greatest changes in suspended sediment transport will lead to the greatest changes in geomorphology, and therefore changes in available habitat. The cumulative sediment was determined for each time interval (1992-2002 and 2002-2012). A variable "α", which represents the fraction of cumulative sediment at a given year relative to the cumulative sediment of the time interval, was determined from the sediment rating curve. For example, for the year 1997, alpha would be calculated as:

$$\alpha_{1997} = \frac{\text{cumulative sediment discharge (1997)}}{\text{max cumulative sediment discharge (2002)}}$$

Alpha is used to determine what fraction of the habitat comes from the lower bound curve and what fraction comes from the upper bound curve. Using the 1997 example, the habitat would be calculated as:

$$1997\ \text{Habitat} = (1 - \alpha_{1997}) * 1992\ \text{Habitat} + \alpha_{1997} * 2002\ \text{Habitat}$$

Example figures with the use of alpha from the Isleta reach (Mortensen, 2020) can be found in Appendix C. Figure 61 displays one decade of the interpolated habitat curves between 1992 and 2002 that are used in the TIHM analysis.

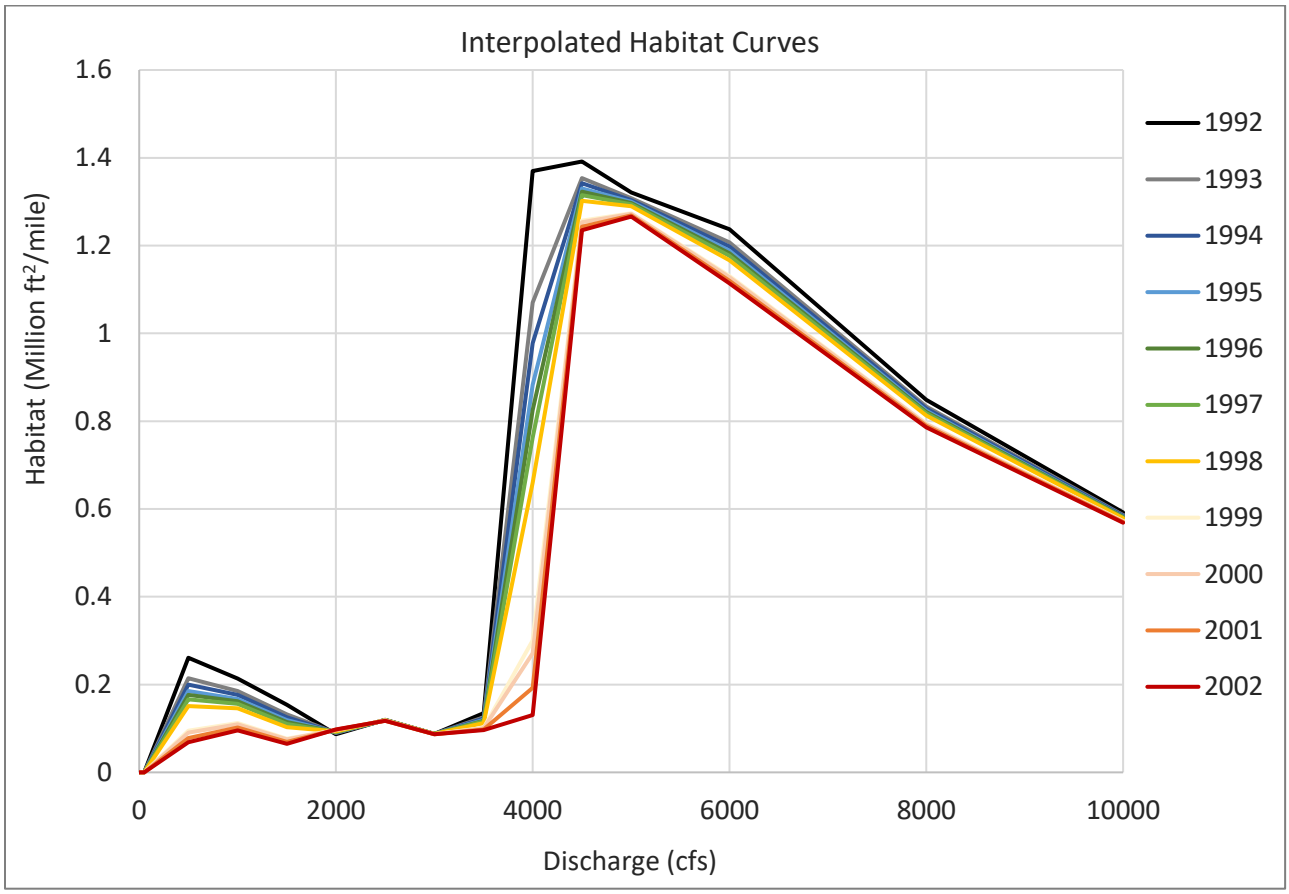

Figure 61 Habitat curves at 1992 and 2002 from the width slice method, with remaining curves being interpolated from the sediment rating curve.

Once a habitat curve is generated for each year of the analysis, the daily habitat can be estimated based off of the hydrograph from a nearby gage. The habitat curves identify hydraulically suitable habitat at discharges between 500 cfs and 5,000 cfs, at 500 cfs increments, and then at 6,000 cfs, 8,000 cfs, and 10,000 cfs. Linear interpolation was used to estimate a habitat value at any discharge up to 10,000 cfs. The daily hydrograph data is used to obtain the hydraulically suitable habitat for each day of the year. Then, the daily available habitat is summed over the representative months of each life stage. The larval fish are present in May and June, so the habitat is summed over those two months. The juvenile fish are present from July to September, and for the remaining months, all fish are considered adults.

The time integrated habitat metrics for the Escondida reach are summarized annually in Figure 62. The bars represent the predicted habitat for each life stage and the black points were measured fish population

densities at the San Acacia monitoring site. Based on the analysis, the larval stage is more dependent on the discharge values of the river, so a bad water year has a larger impact on the larval fish.

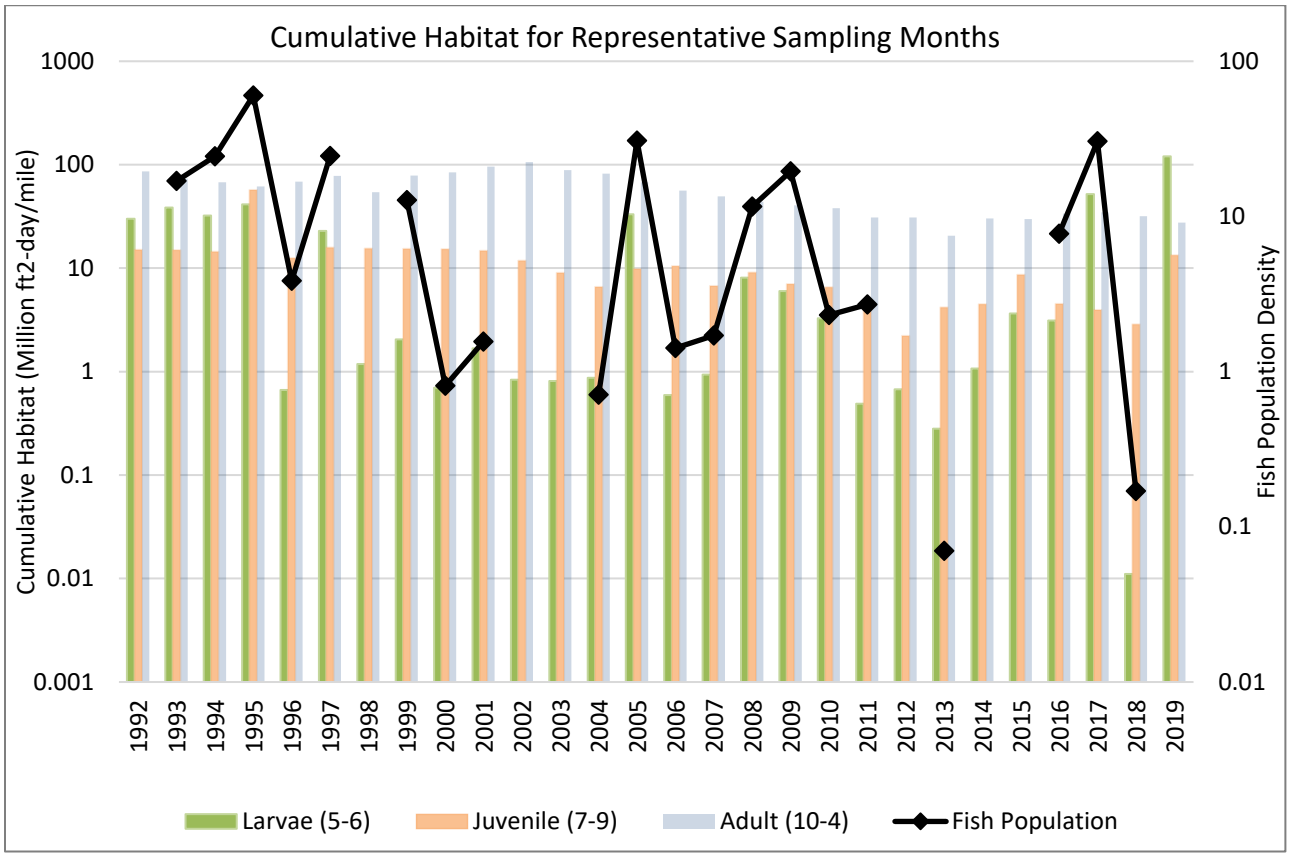

Figure 62 TIHMs for the Escondida reach. In the legend, the numbers in the parentheses indicate the months for which the habitat is accumulated over based on the life stage cycle of the RGSM. For example, months 5 and 6 (May and June) are the months when the new RGSM enter the larval stage. They enter the juvenile stage around month 7 (July) and the adult stage around month 10 (October).

6. Conclusions

The Escondida reach, spanning about 16 miles from the Escondida Bridge near Escondida to the US 380 Bridge near San Antonio, New Mexico, was analyzed for hydrologic, hydraulic and geomorphic trends between 1918 and 2018. HEC-RAS and GIS were used to find geomorphic and river characteristics such as sinuosity, width, bed elevation and other hydraulic parameters. Hydraulically suitable RGSM habitat was determined quantitatively and spatially throughout the reach. Lastly, a time-integrated habitat metric was developed to estimate the annual RGSM habitat based on measured daily discharge values.

Major findings include:

- While spring snowmelt typically brings the largest increases in the discharge volumes in the Escondida reach, summer thunderstorms have a greater impact on the amount of suspended sediment transported. Strong monsoonal storms above Colorado and New Mexico led to flooding of the MRG in September of 2013, resulting in large increases in both cumulative discharge and sediment. Peak discharges topped 6,000 cfs in the Escondida reach on September 16, 2013, with

suspended sediment load measuring 403,000 tons per day on September 14th. Several severe thunderstorms between July 27th August 5th of 2014 also resulted in flooding of the MRG with a peak discharge of about 1,800 cfs on August 4th with suspended sediment transport of 285,000 tons per day on Aug 5th. For both storms the sediment concentration peaked around the same value: 54,000 mg/L. The majority of grain diameter measurements of the bed material from 1991 to 2002 are classified as fine to medium sand.

- Significant narrowing of the channel occurred between 1918 and 1972. Since 2001 the widths have remained relatively stable, with E2, E3, and E5 approaching the theoretical equilibrium width predicted by the JW equations- around 300 feet. The width of subreach E4 has stabilized around 500 feet. Although the sinuosity remains low, it has been increasing in most subreaches. Subreaches E1, E4 and E5 have increased from about 1.03 to 1.06, and E4 has increased from 1.06 to 1.12. Subreach E3 has had a sinuosity of about 1.15 since 1985.
- The Escondida reach contains a "pivot point" in which the sand bed river transitions from a degrading channel to an aggrading channel. Between 1962 and 2012, the upstream subreach E1 degraded about 2 feet while the downstream subreach E5 aggraded approximately 1 foot. Higher peak flows resulted in aggradation throughout most of the Escondida reach between 1972 and 1992. Degradation has been moving downstream in the Escondida reach. The main channel has been degrading since 1972 to 1992 in subreach E1, since 1992 to 2002 in subreaches E3 and E4, and since 2002 to 2012 in subreach E4. In 2012, it took approximately 2,000 cfs less discharge to reach bankfull in 50% of the cross sections than in 2002 and approximately 500 cfs less discharge to reach bankfull in 25% of the cross sections.
- Through observation of the cross-sectional profiles and historical aerial imagery, subreaches E1, E2, and E3 appear to be in the migrating stages of Massong's classification, M4 to M5, while subreaches E4 and E5 appear to be in aggrading stages of Massong's classification, A6 and A4, respectively.
- While the width slices method estimates the greatest amount of hydraulically suitable habitat for subreach E5, the RAS-mapper habitat maps show that much of the habitat is not connected to the main channel at lower discharges. Based on the RAS-mapper habitat maps, Subreaches E2 and E4 provide hydraulically suitable habitat that may be more accessible for the RGSM due to connectivity to the main channel.

7. Bibliography

Baird, D and Holste, N. (2020) "One-Dimensional Numerical Modeling of Perched Channels." U.S. Bureau of Reclamation, Denver, CO.

Bovee, K.D., Waddle, T.J., and Spears, J.M. (2008). "Streamflow and endangered species habitat in the lower Isleta reach of the middle Rio Grande." *U.S. Geological Survey Open-File Report 2008-1323*.

Doidge, S and Julien, P.Y. (2019). Draft Report. *Middle Rio Grande San Acacia Reach: Morphodynamic Processes and Silvery Minnow Habitat from San Acacia Diversion Dam to Escondida Bridge*, Colorado State University, Fort Collins, CO.

Julien, P.Y. (2002). *River Mechanics*, Cambridge University Press, New York

Julien, P. Y., and Wargadalam, J. (1995). "Alluvial channel geometry: theory and applications." *Journal of Hydraulic Engineering*, American Society of Civil Engineers, 121(4), 312–325.

Klein, M., Herrington, C., AuBuchon, J., and Lampert, T. (2018a). *Isleta to San Acacia Geomorphic Analysis*, U.S. Bureau of Reclamation, Reclamation River Analysis Group, Albuquerque, New Mexico.

Klein, M., Herrington, C., AuBuchon, J., and Lampert, T. (2018b). *Isleta to San Acacia Hydraulic Modeling Report*, U.S. Bureau of Reclamation, Reclamation River Analysis Group, Albuquerque, New Mexico.

LaForge, K., Yang, C.Y., Julien, P.Y., and Doidge, S. (2019). Draft Report. *Rio Puerco Reach: Hydraulic Modeling and Silvery Minnow Habitat Analysis*, Colorado State University, Fort Collins, CO.

Larsen, A. (2007). *Hydraulic modeling Analysis of the Middle Rio Grande-Escondida Reach, New Mexico*. M.S thesis, Civil Engineering Department, Colorado State University, Fort Collins, CO.

Makar, P., Massong, T., and Bauer, T. (2006). "Channel Widths Change Along the Middle Rio Grande, NM." *Joint 8th Federal Interagency Sedimentation Conference, Reno, NV, April 2 -April6, 2006.*

Massong, T., Paula, M., and Bauer, T. (2010). "Planform Evolution Model for the Middle Rio Grande, NM." *2nd Joint Federal Interagency Conference, Las Vegas, NV, June 27 - July 1, 2010*.

MEI. (2002). *Geomorphic and Sedimentologic Investigations of the Middle Rio Grande between Cochiti Dam and Elephant Butte Reservoir*, Mussetter Engineering, Inc., Fort Collins, CO, 220 p.

Mortensen, J.G., Dudley, R.K., Platania, S.P., and Turner, T.F. (2019). Draft report. *Rio Grande Silvery Minnow Habitat Synthesis*, University of New Mexico with American Southwest Ichthyological Researchers, Albuquerque, NM.

Mortensen, J.G., Dudley, R.K., Platania, S.P., White, G.C., and Turner, T.F., Julien, P.Y., Doidge, S, Beckwith, T., Fogarty, C. (2020). Draft Report. *Linking Morpho-Dynamics and Bio-Habitat Conditions on the Middle Rio Grande: Linkage Report 1- Isleta Reach Analyses*. Submitted to the U.S. Bureau of Reclamation, Albuquerque, New Mexico.

Posner, A. J. (2017). Draft report. *Channel conditions and dynamics of the Middle Rio Grande River*, U.S. Bureau of Reclamation, Albuquerque, New Mexico.

Scurlock, D. (1998). "From the Rio to the Sierra: an environmental history of the Middle Rio Grande Basin." *General Technical Report RMRS-GTR-5. Fort Collins, CO: US Department of Agriculture, Forest Service, Rocky Mountain Research Station, 440 p.*

Shah-Fairbank, S. C., Julien, P. Y., and Baird, D. C. (2011). "Total sediment load from SEMEP using depth-integrated concentration measurements." Journal of Hydraulic Engineering, 137(12), 1606–1614.

U.S. Bureau of Reclamation. (2012). “Middle Rio Grande River Maintenance Program - Comprehensive Plan and Guide.” Albuquerque Area Office, Albuquerque, New Mexico, 202p.

U.S. Fish and Wildlife Service. (2007). “Rio Grande Silvery Minnow (Hybognathus amarus).” Draft Revised Recovery Plan, Albuquerque, New Mexico, 174 p.

Varyu, D. (2013). *Aggradation / Degradation Volume Calculations: 2002-2012*. U.S. Department of the Interior, Bureau of Reclamation, Technical Services Center, Sedimentation and River Hydraulics Group. Denver, CO.

Varyu, D. (2016). *SRH-1D Numerical Model for the Middle Rio Grande: Isleta Diversion Dam to San Acacia Diversion Dam*. U.S. Department of the Interior, Bureau of Reclamation, Technical Services Center, Sedimentation and River Hydraulics Group. Denver, CO.

Yang, C.Y. (2019). *The Sediment Yield of South Korean Rivers*, Colorado State University, Fort Collins, CO.

Yang, C.Y. and Julien, P.Y. (2019). “The ratio of measured to total sediment discharge.” *International Journal of Sediment Research*, 34(3), pp.262-269.

Yang, C.Y., LaForge, K., Julien, P.Y., and Doidge, S. (2019). Draft Report. *Isleta Reach: Hydraulic Modeling and Silvery Minnow Habitat Analysis*, Colorado State University, Fort Collins, CO.

Appendix A

Cumulative Plots used in the Subreach Delineation

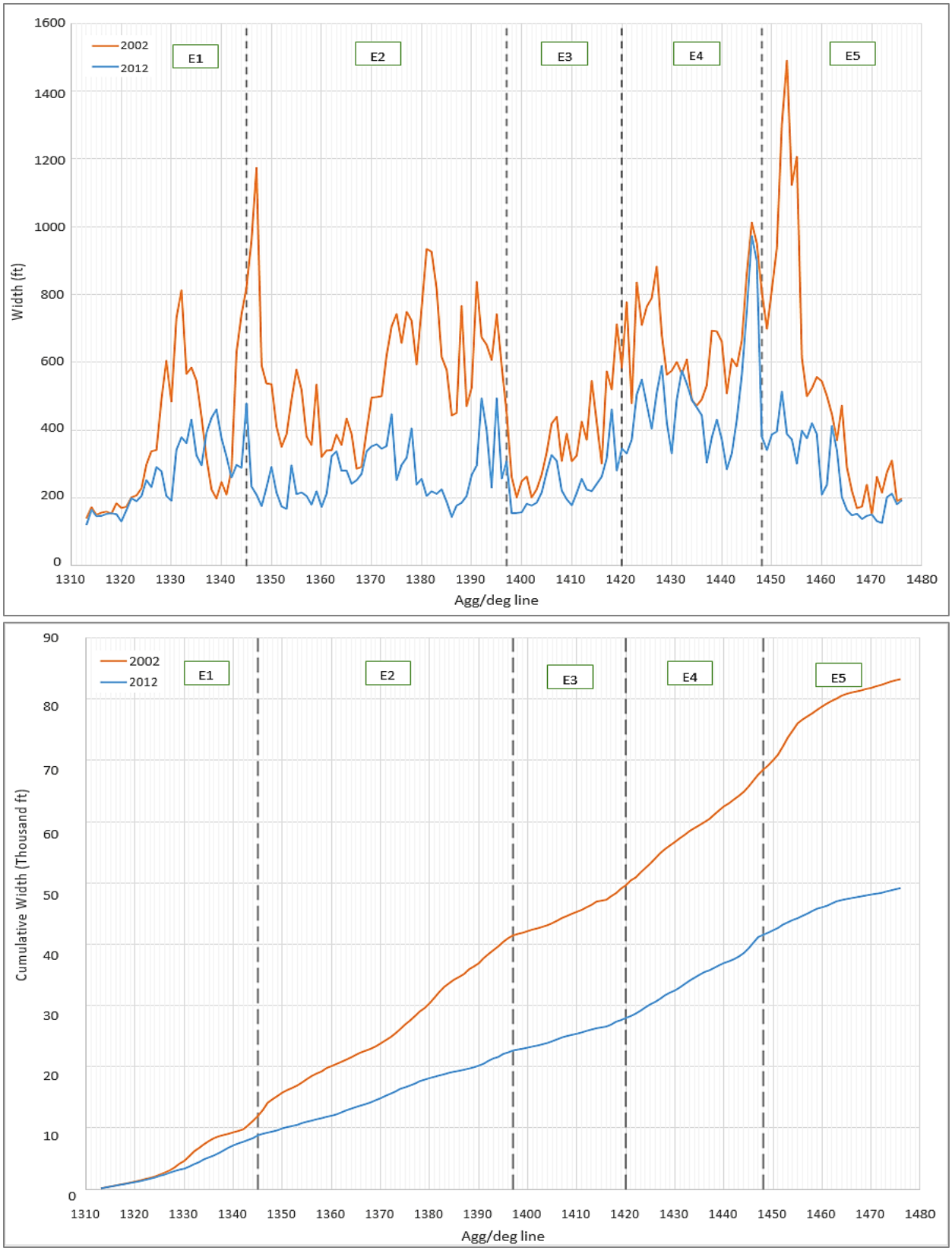

Figure A- 1 Width (top) and cumulative width (bottom) throughout the Escondida reach for the years 2002 (orange) and 2012 (blue).

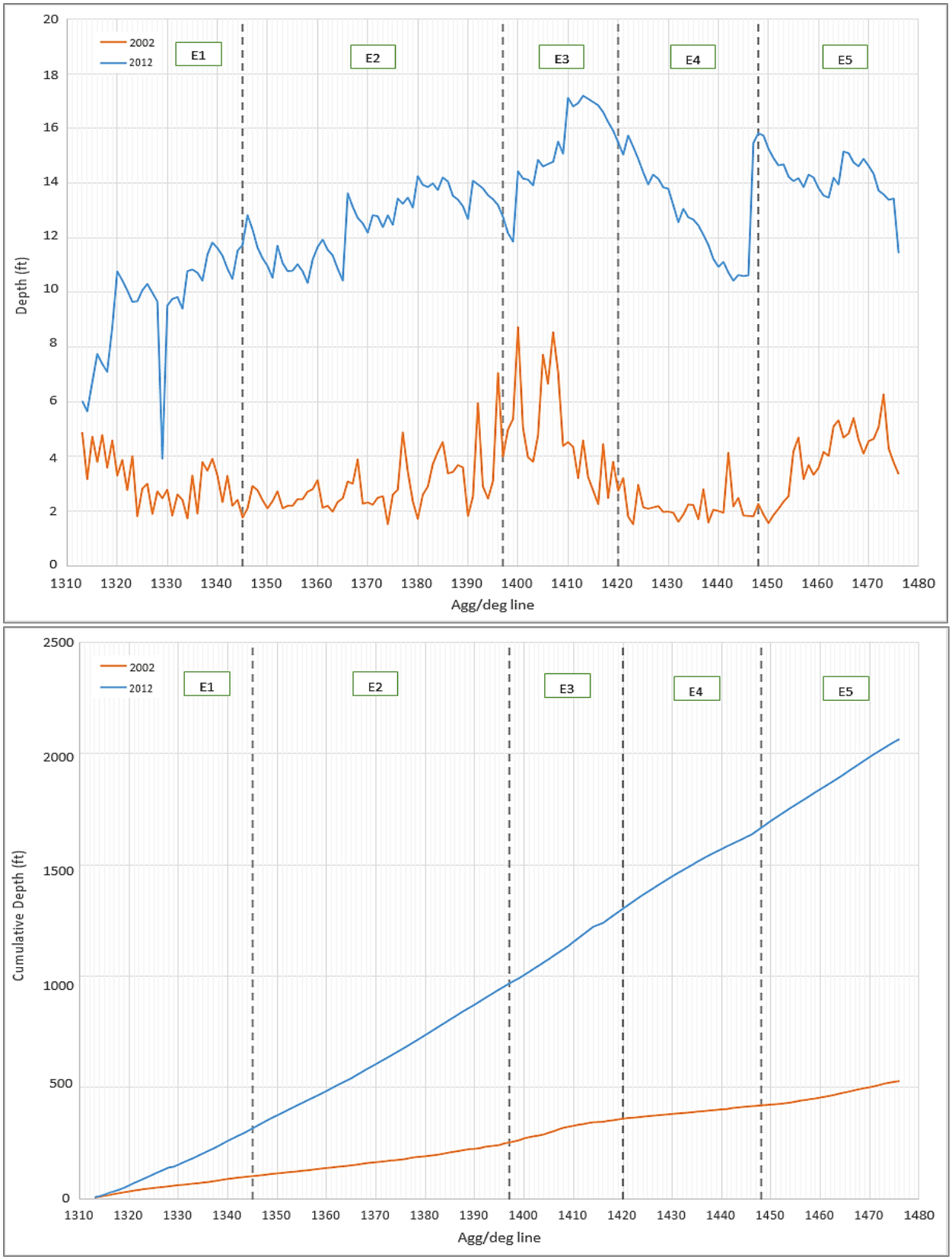

Figure A- 4 Depth (top) and cumulative depth (bottom) throughout the Escondida reach for the years 2002 (orange) and 2012 (blue).

Appendix B

Total Sediment Load using SEMEP Analysis

The Series Expansion of Einstein Procedure (SEMEP) was used in this study to estimate the total sediment load in the Middle Rio Grande (Yang, C.Y. 2019). The method was developed at CSU with the procedure detailed in Shah-Fairbank et al. (2011) as a function of shear velocity u_* and fall velocity ω. In this report, SEMEP is applied at three stations on the Rio Grande, at San Acacia gage 08354900, as well as Albuquerque and Bernardo at gages 08330000 and 08332010. The number of field samples calculated by the SEMEP are 306, 211, and 173, respectively, at gages 08330000, 08332010, and 08354900. For these stations, the values of u_*/ω range from 1.5 to 37,600. According to Shah-Fairbank et al. (2011), SEMEP performs accurately when $u_*/\omega > 5$, so good results are expected from this application.

It can be seen in Figure B-1 that the SEMEP predictions and total sediment load measurements fall close to the 45-degree line of perfect agreement. Figure B-1 also shows the prediction errors between SEMEP calculations and measurements as a function of u_*/ω. The mean absolute percent difference is 27%. Figure B-2 shows the sediment rating curves for total sediment discharges at gage 08354900.

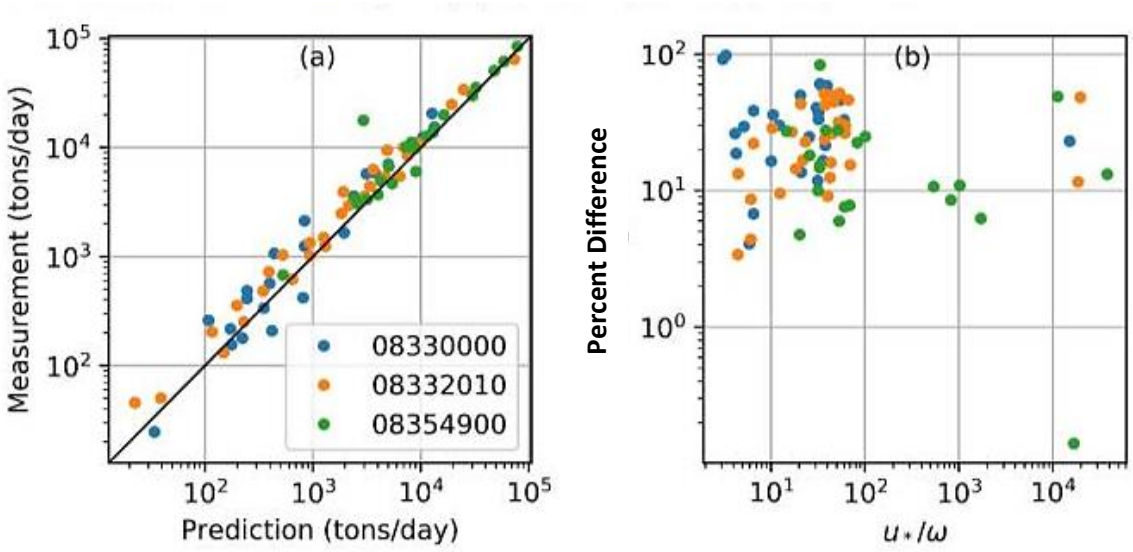

Figure B- 1 Comparison between predicted and measured total sediment load (left) and percent difference vs u/w (right)*

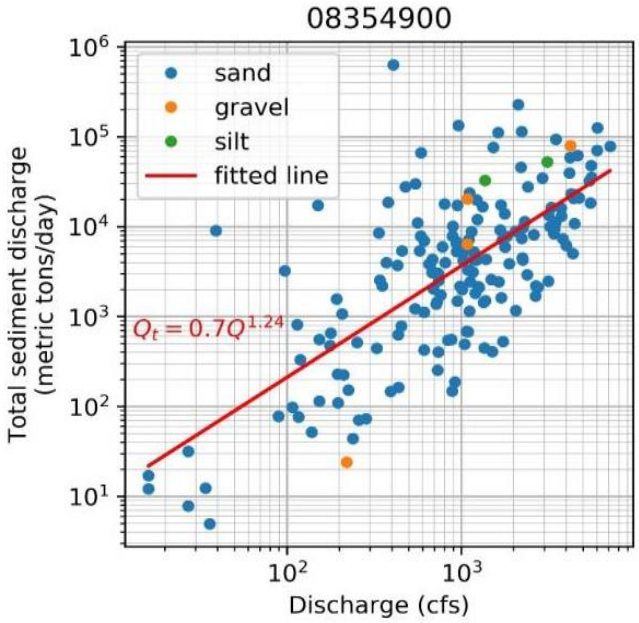

Figure B- 2 Total sediment rating curve at the San Acacia gage

The ratio of measured to total sediment discharge is a function of flow depth h, grain size d_s, and Rouse number Ro (Ro = $\omega/2.5u_*$) according to SEMEP (Shah-Fairbank et al. 2011; Yang and Julien 2019). In addition, the ratio of suspended to total sediment discharge is a function of the ratio h/d_s and Ro. The calculated ratio Q_m/Q_t and the ratio Q_s/Q_t are plotted with the analytical solutions in Figure B-3 for the San Acacia gaging stations, where Q_m is the measured sediment discharge, Q_t is the total sediment discharge, and Q_s is the suspended sediment discharge. As expected, when the value of Ro is low (Ro < 0.3), the ratio Q_s/Q_t is close to 100% during floods when h/d_s > 100. These ratios are also in good agreement with the theory for both sands and gravels.

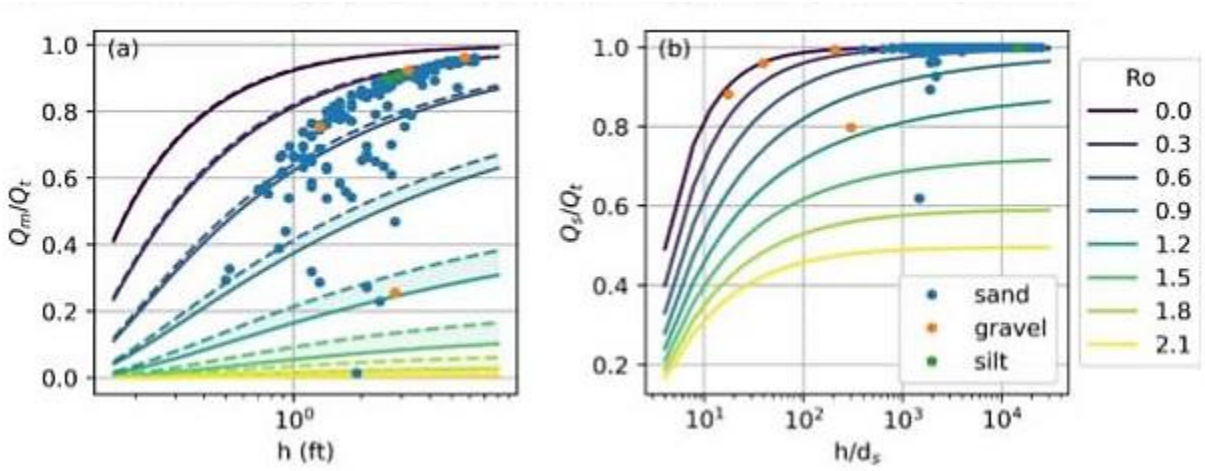

Figure B- 3 the ratio of measured to total sediment discharge vs depth; and (b) the ratio of suspended to total sediment discharge vs h/ds at the San Acacia gage

Appendix C

Additional Figures from Geomorphology Analyses

(Wetted Top Width Plots, Sediment Rating Curve/Alpha Method Example)

Wetted Top Width Plots

In section 3.1, the cross-section moving averaged top width was plotted for all agg/deg lines in the Escondida reach. Figures B-1 and B-2 show each cross-section top width plotted against the agg/deg lines rather than the moving average at discharges of 1,000 cfs and 3,000 cfs.

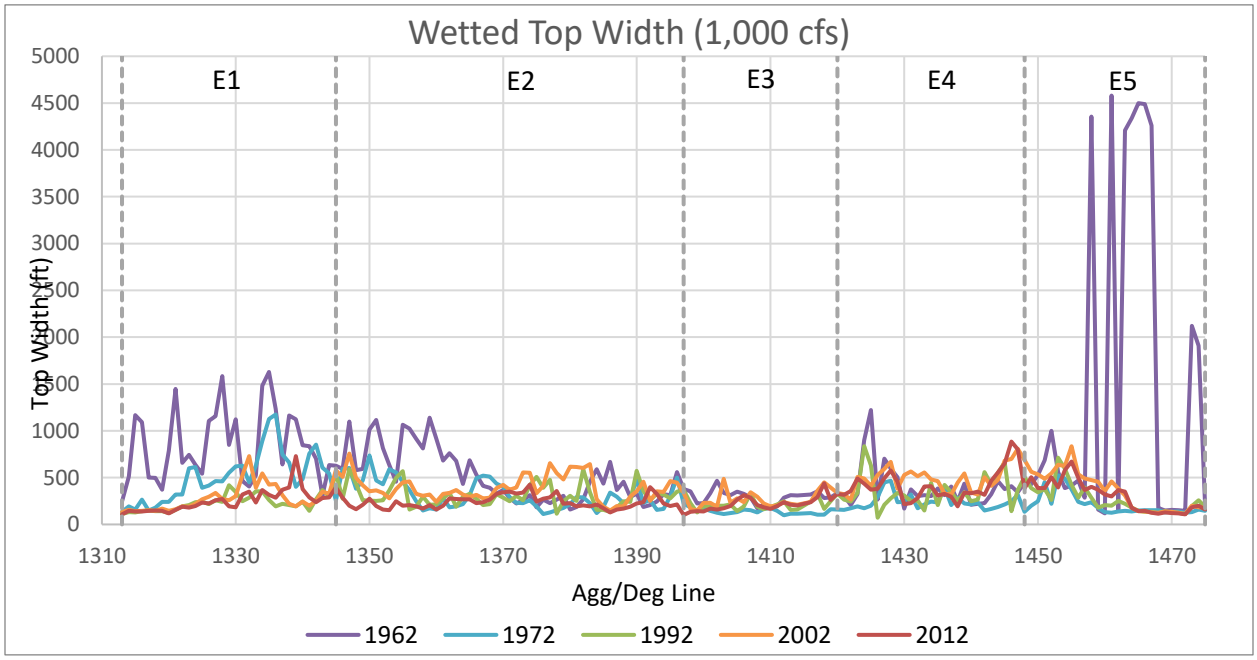

Figure C- 1 Wetted top width at each agg/deg line throughout the Escondida reach at a discharge of 1,000 cfs

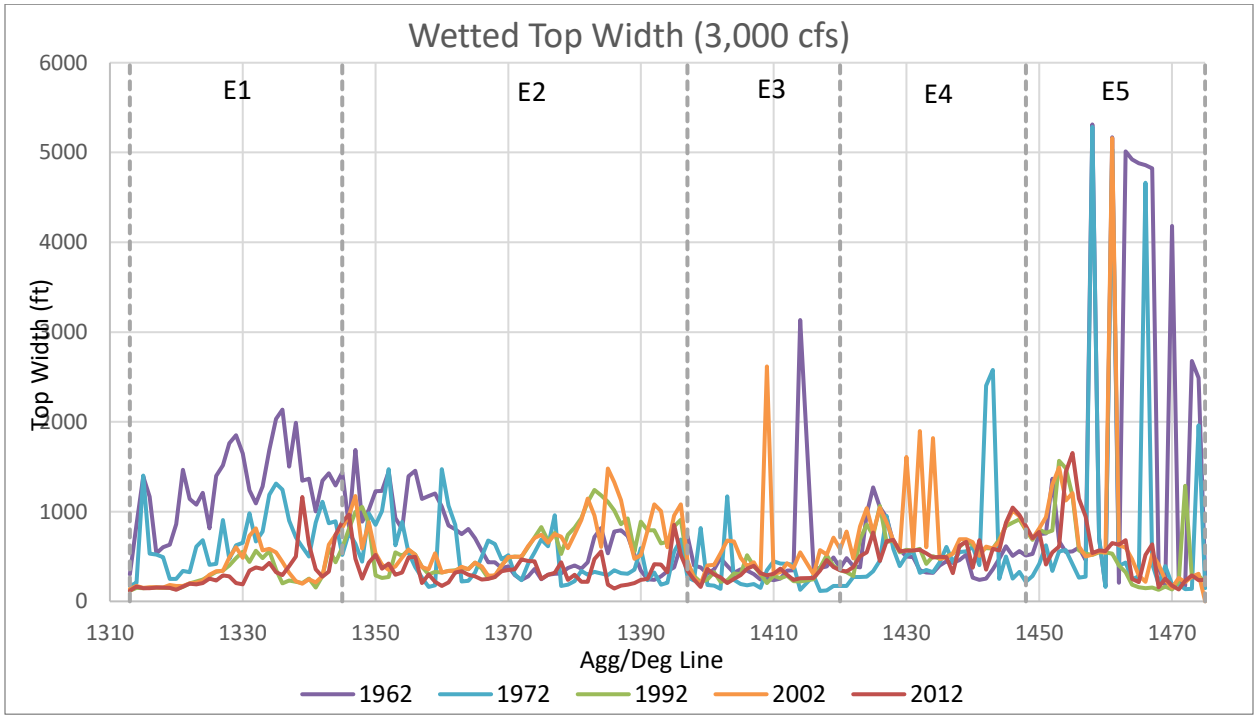

Figure C- 2 Wetted top width at each agg/deg line throughout the Escondida reach at a discharge of 3,000 cfs

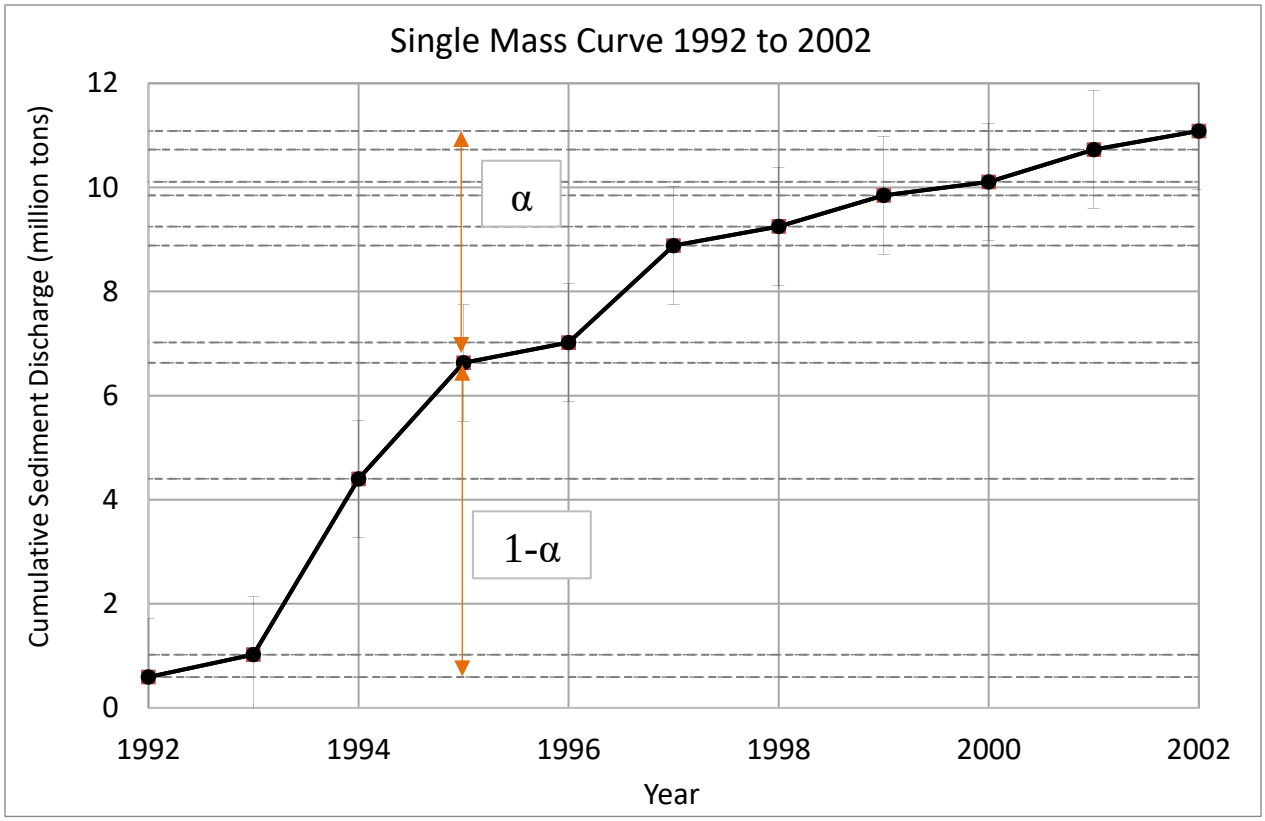

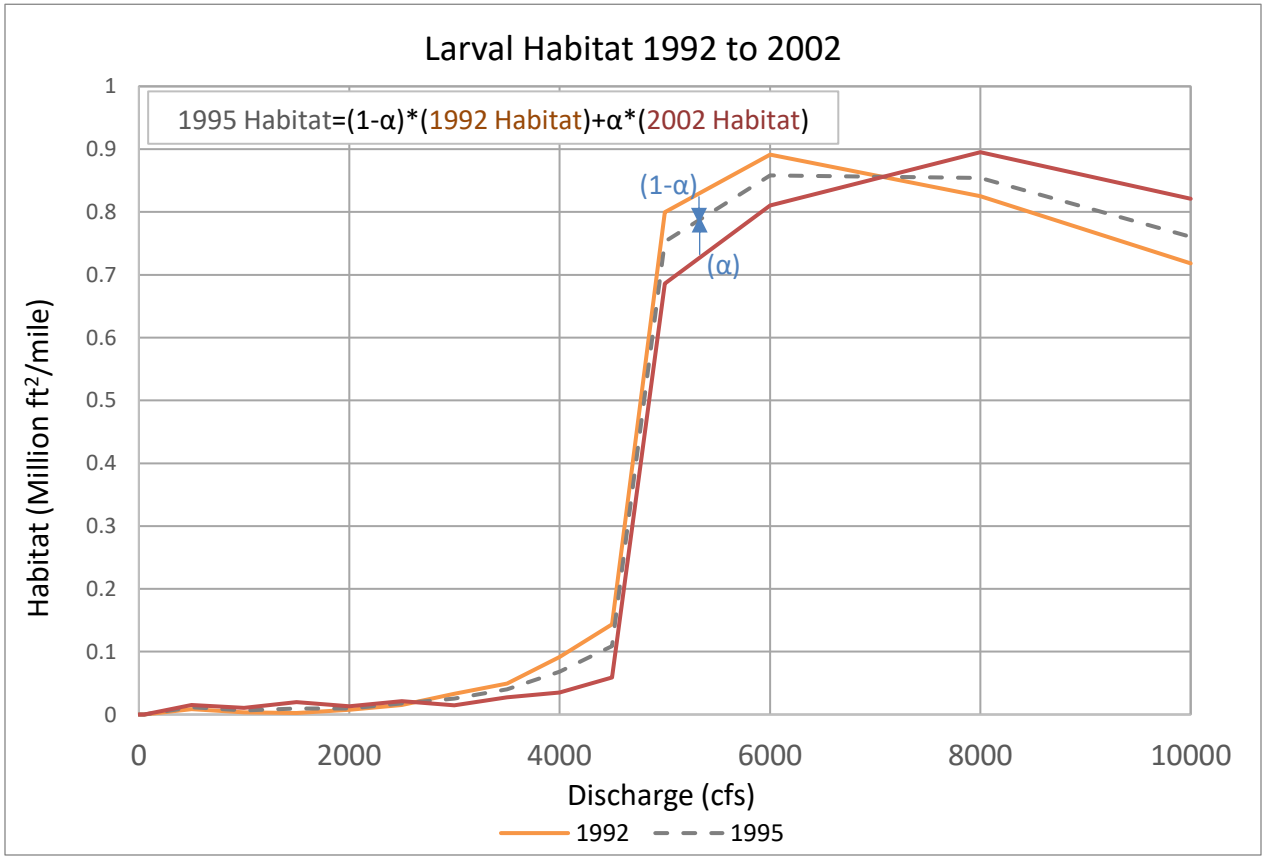

Figure C- 3 Example of annual habitat interpolating using the sediment rating curve and alpha technique.

Appendix D

Additional Figures from Habitat Analyses

(Habitat Charts by Subreach, Spatially Varying Habitat Charts, Habitat Curves)

Width Slices: Habitat Bar Charts

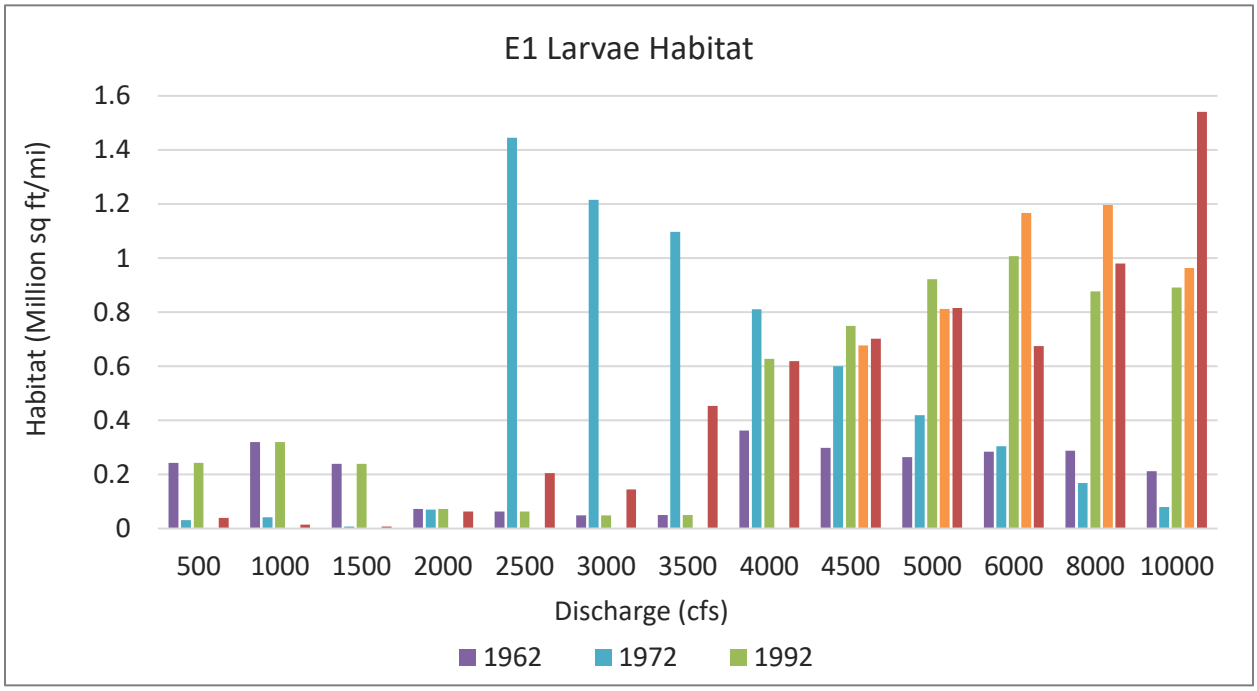

Figure D- 1 Subreach E1 larva habitat

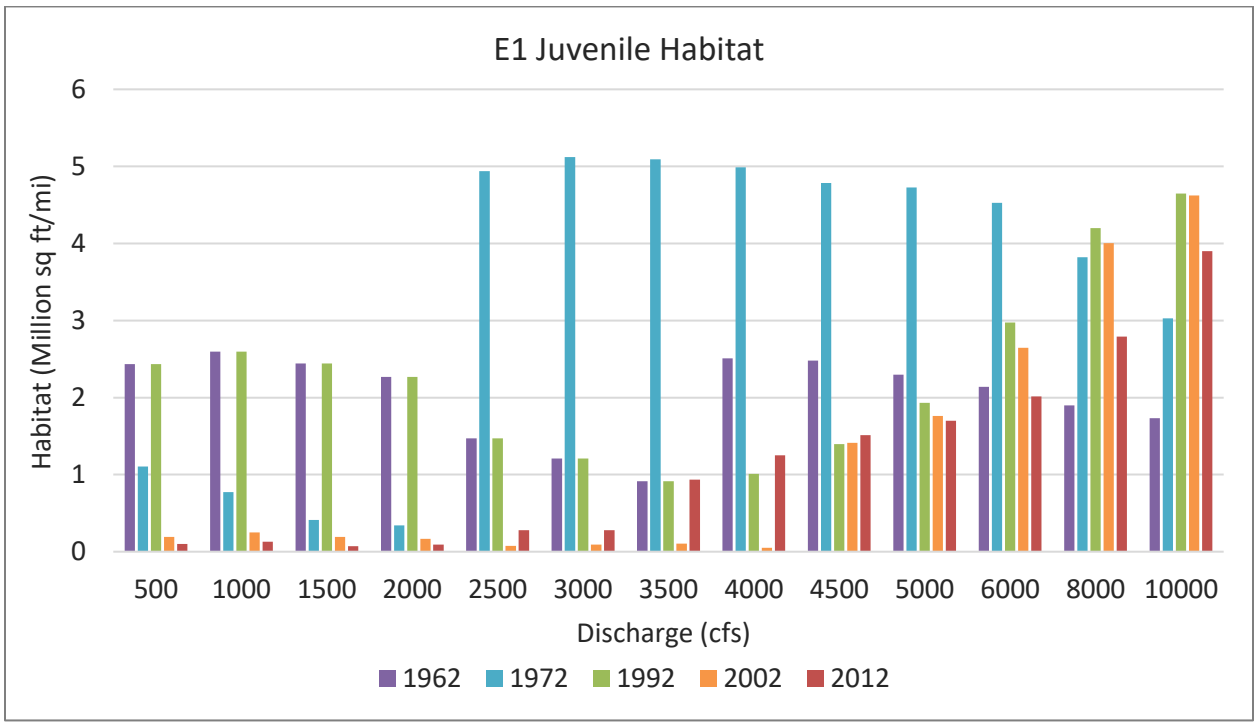

Figure D- 2 Subreach E1 juvenile habitat

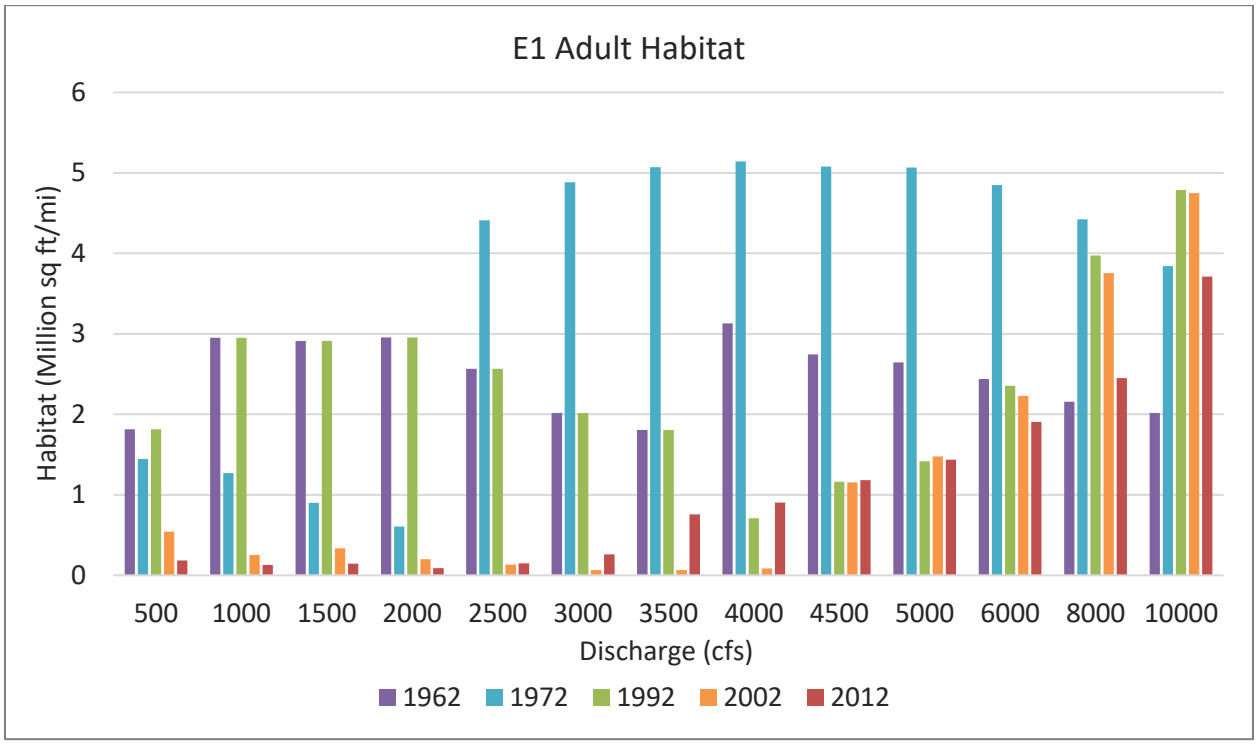

Figure D- 3 Subreach E1 adult habitat

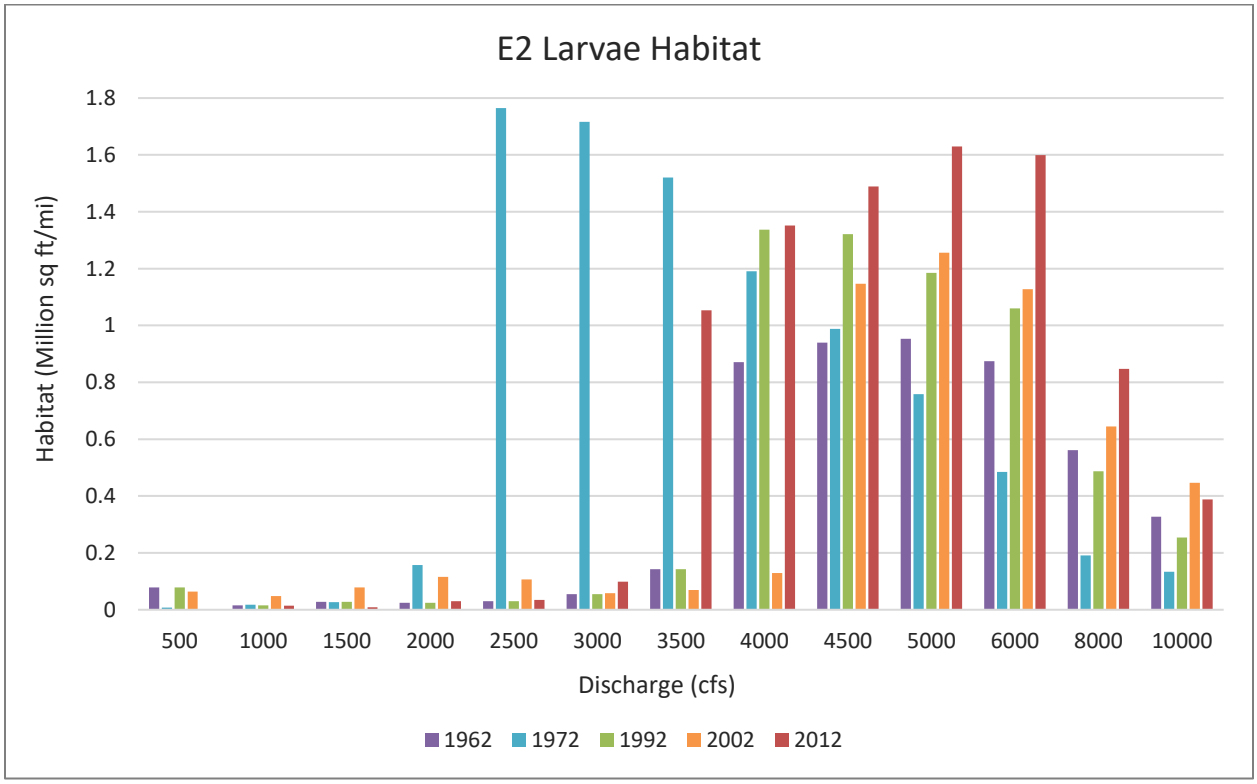

Figure D- 4 Subreach E2 larva habitat

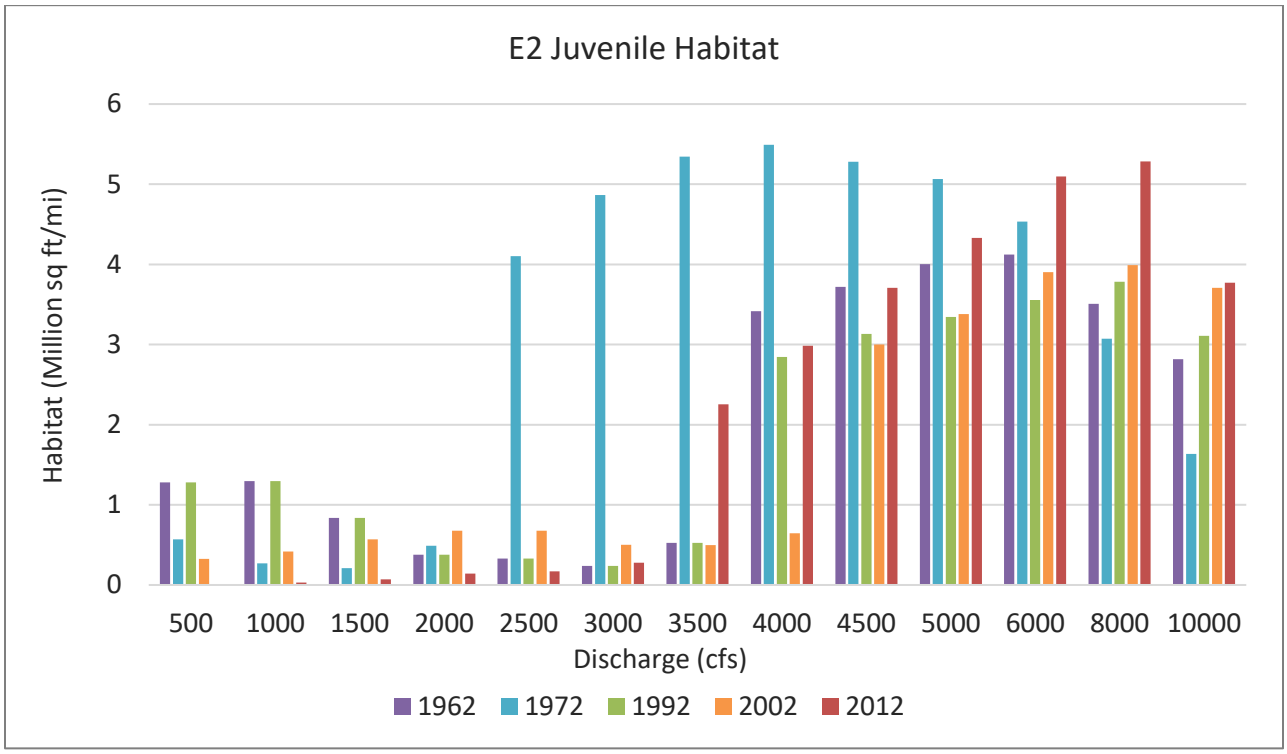

Figure D- 5 Subreach E2 juvenile habitat

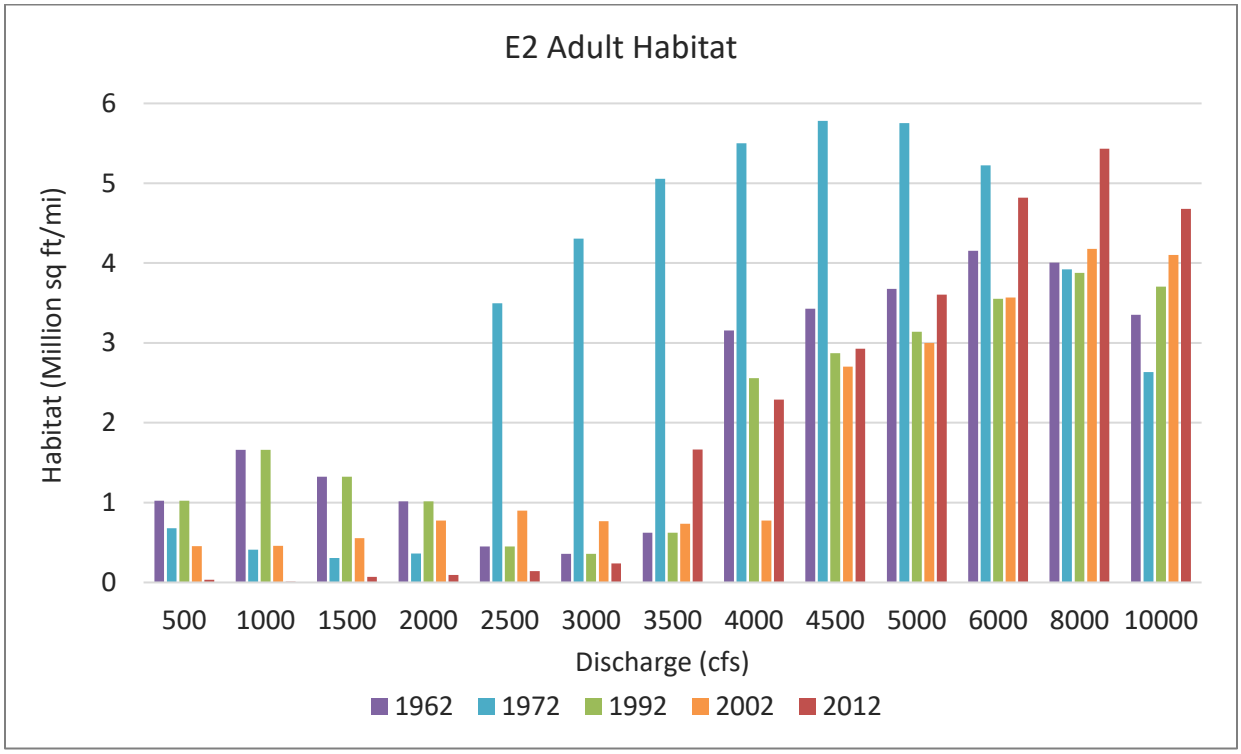

Figure D- 6 Subreach E2 adult habitat

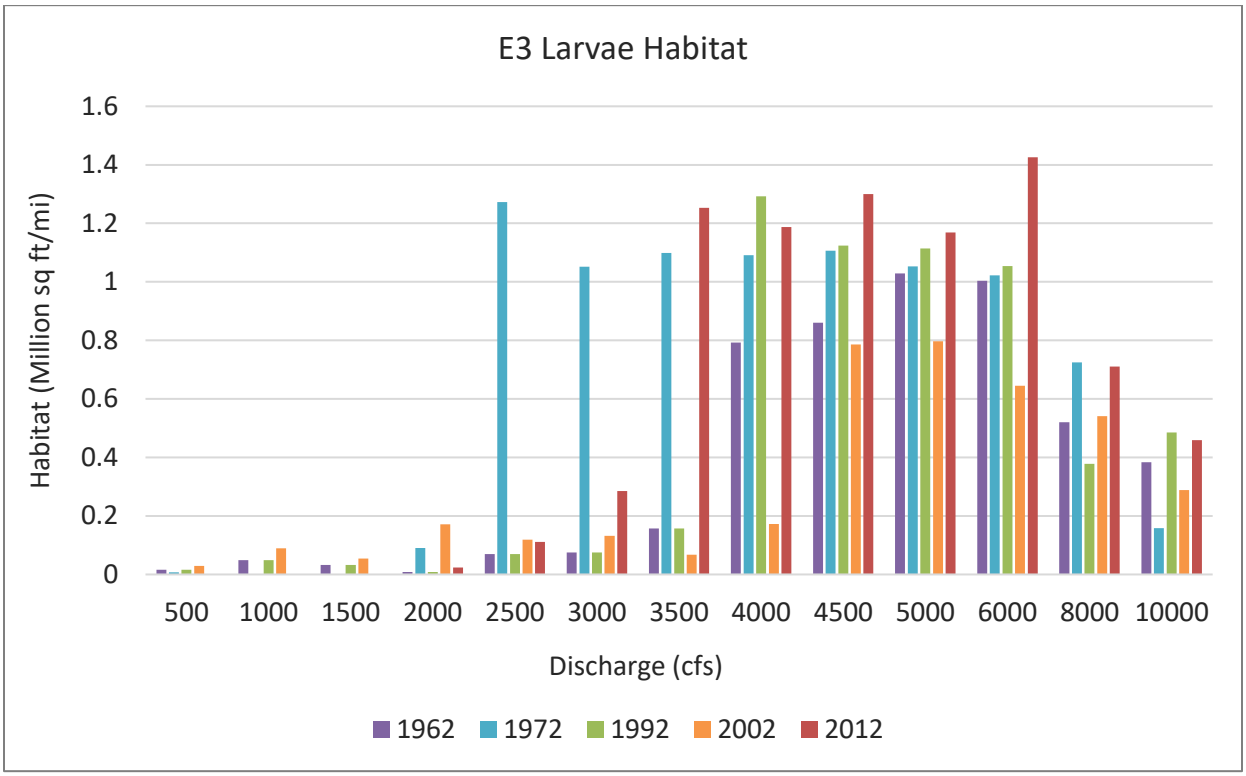

Figure D- 7 Subreach E3 Larva Habitat

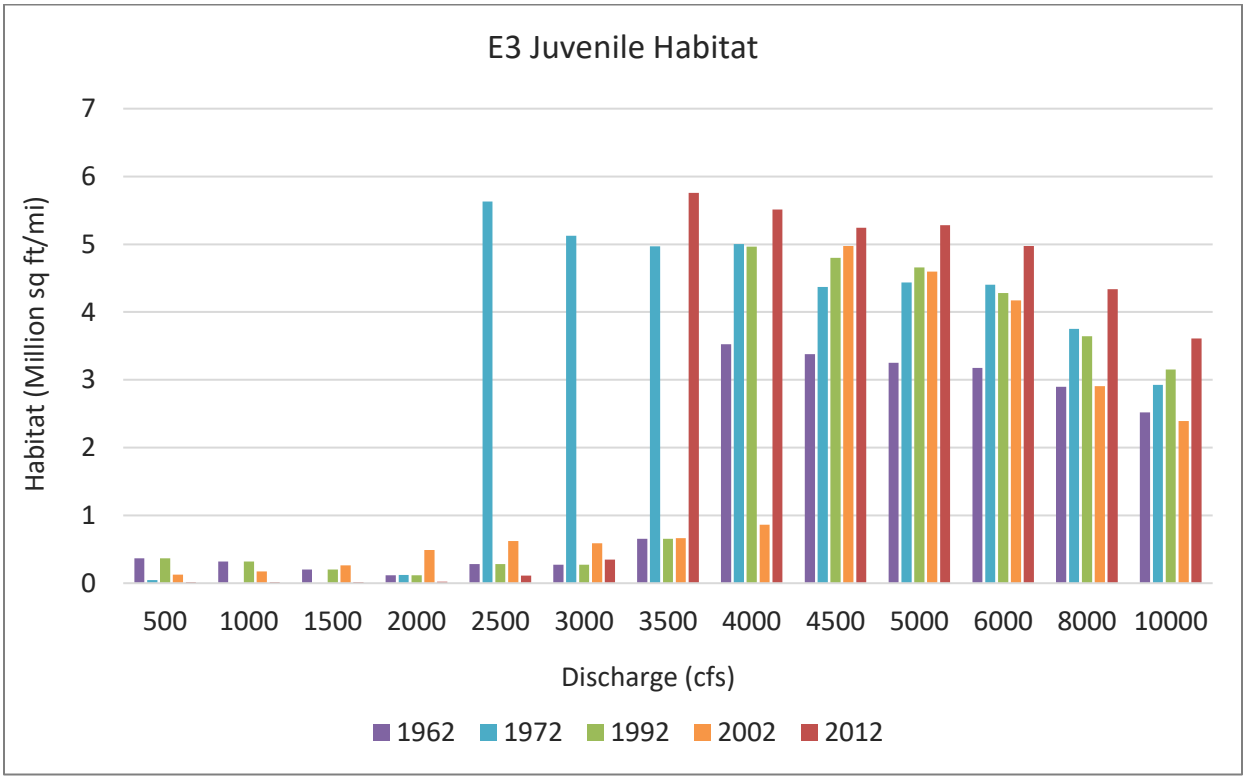

Figure D- 8 Subreach E3 Juvenile Habitat

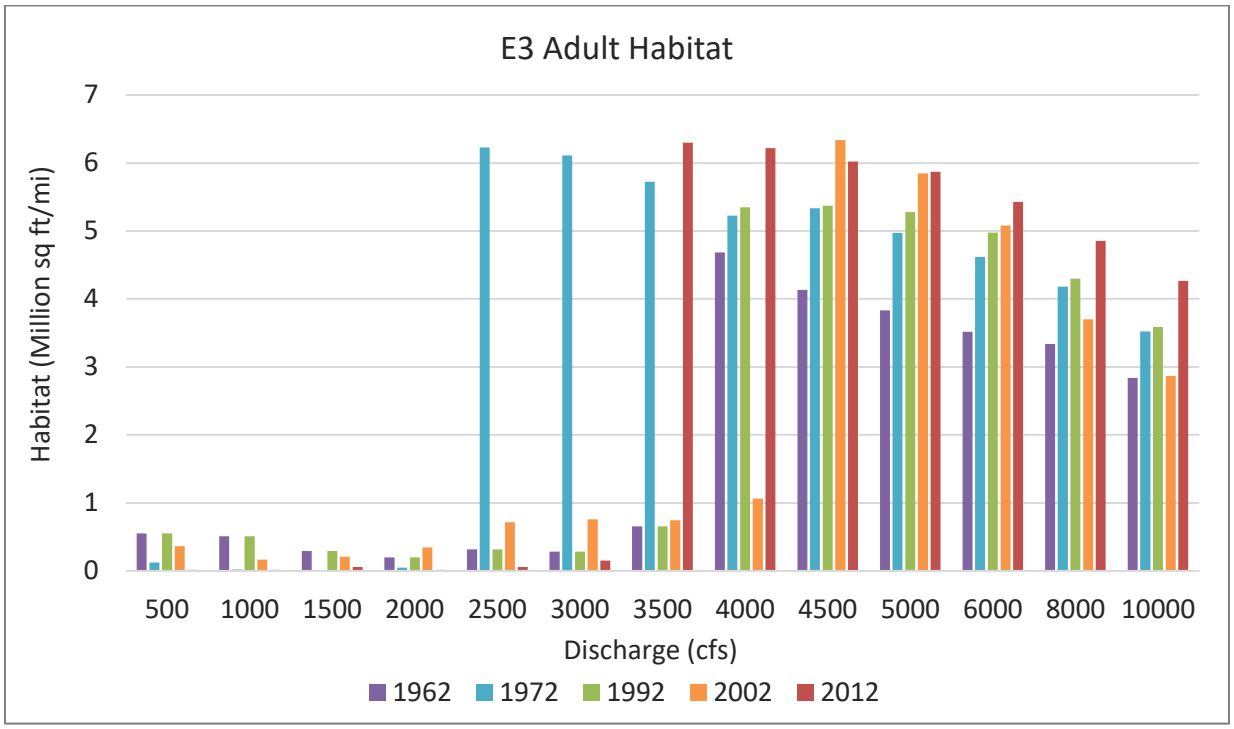

Figure D- 9 Subreach E3 Adult Habitat

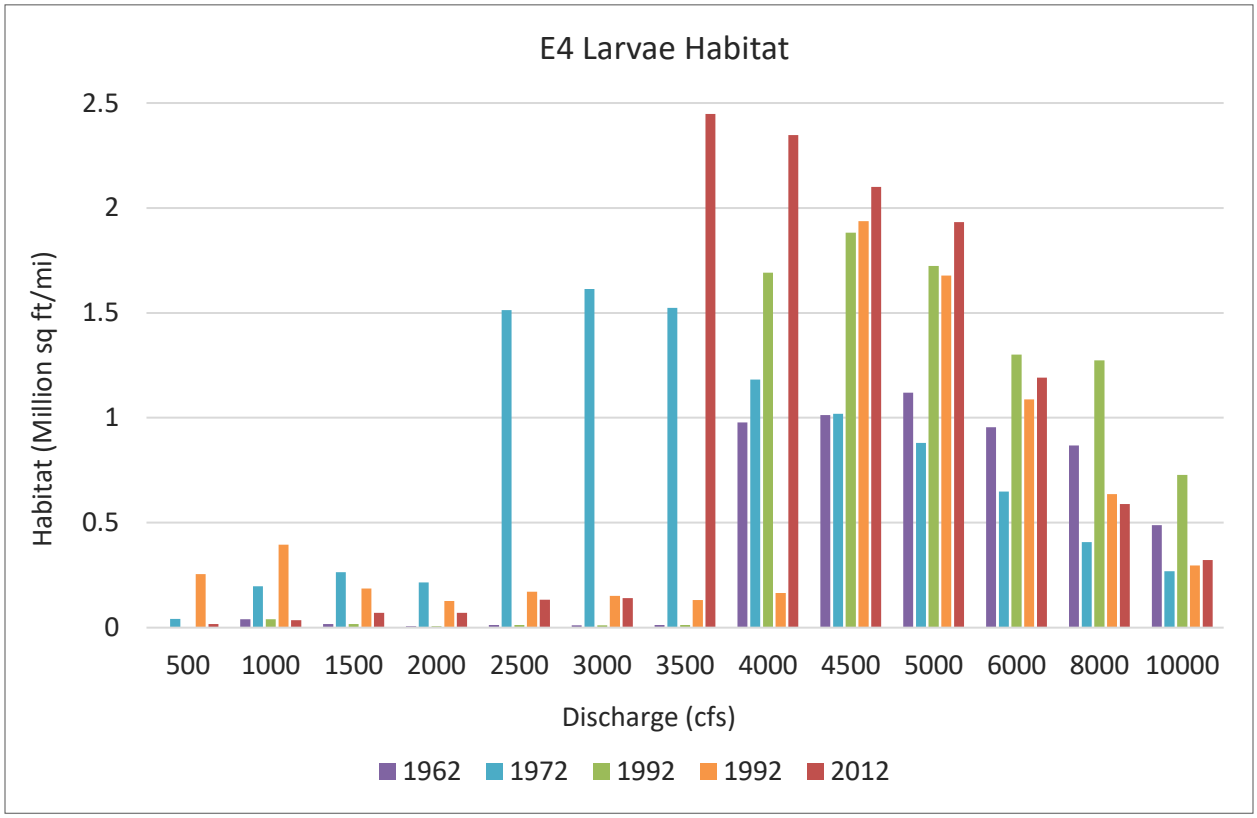

Figure D- 10 Subreach E4 Larva Habitat

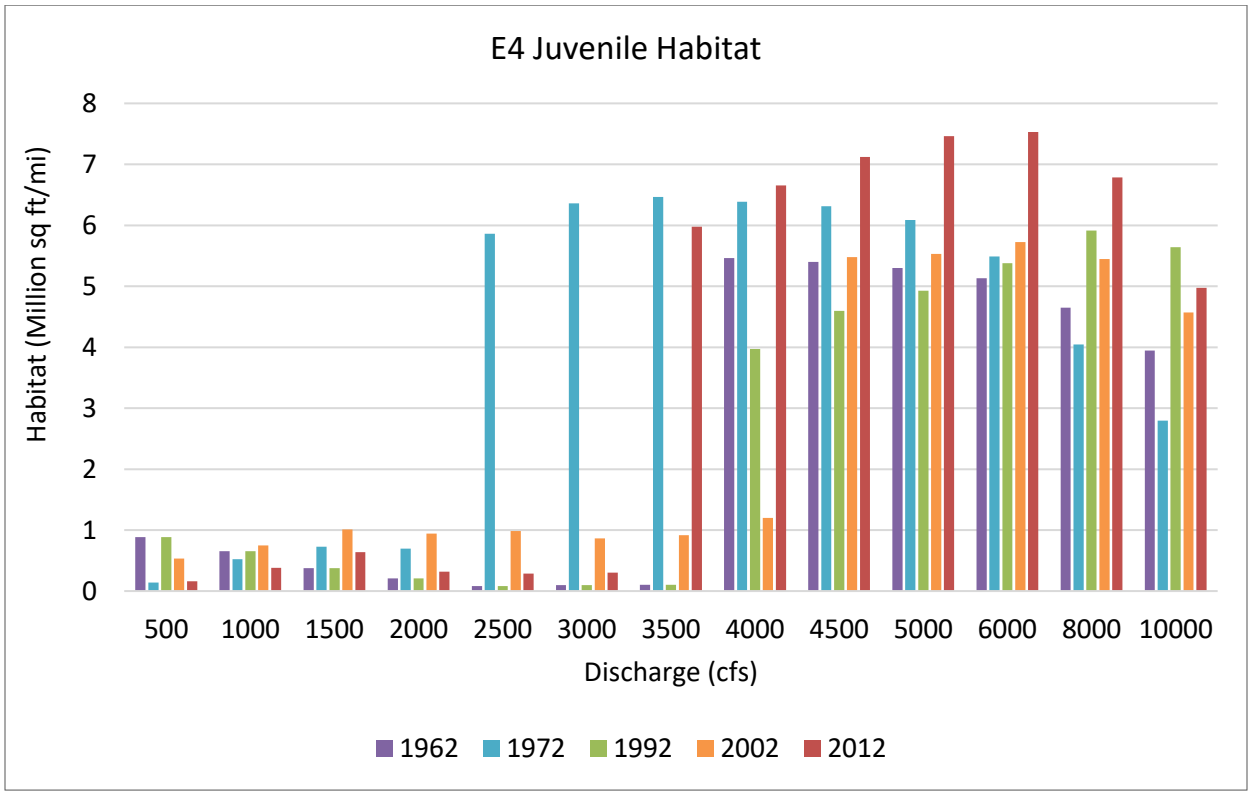

Figure D- 11 Subreach E4 Juvenile Habitat

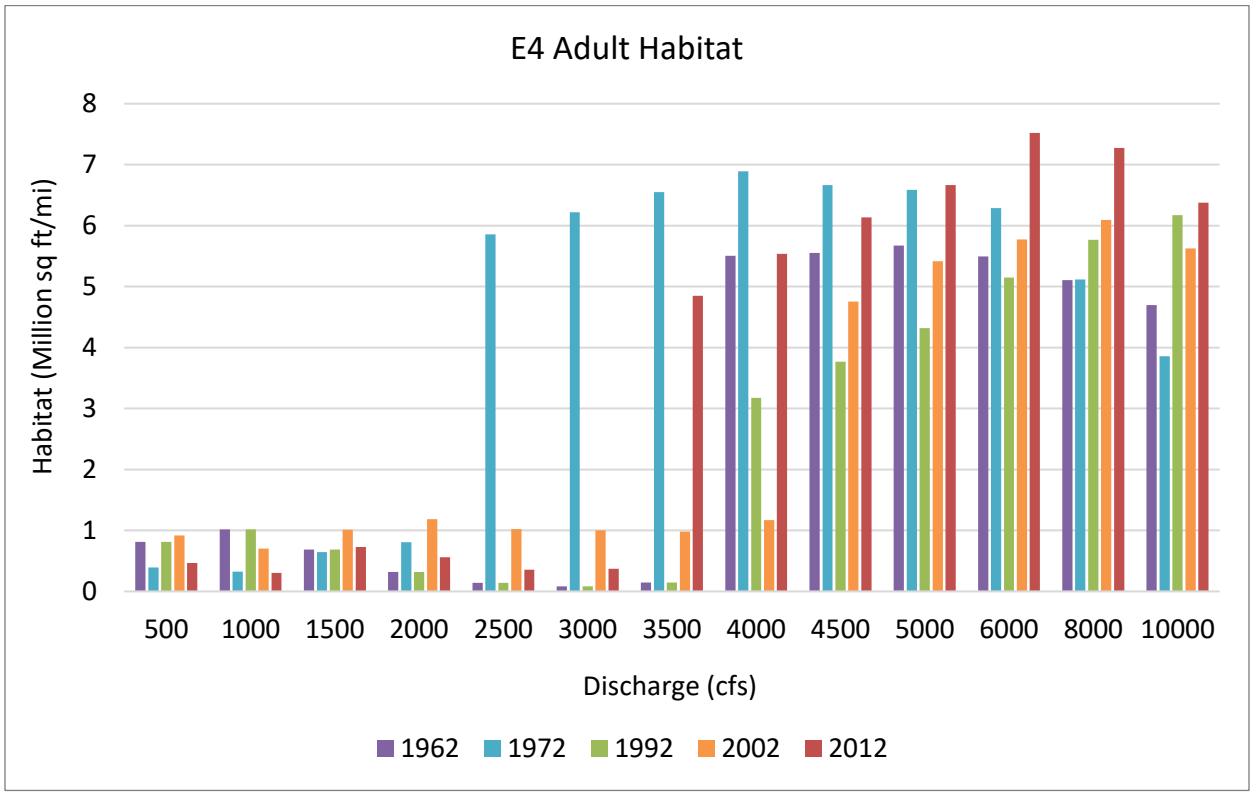

Figure D- 12 Subreach E4 Adult Habitat

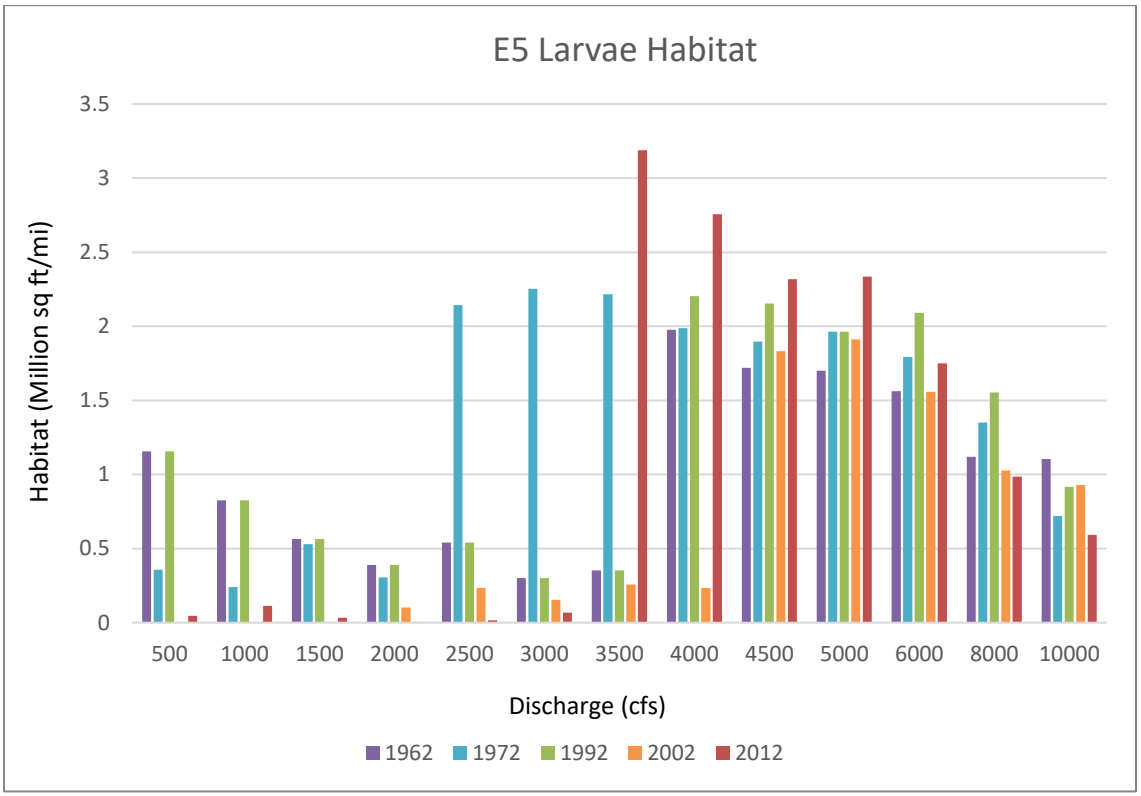

Figure D- 13 Subreach E5 Larva Habitat

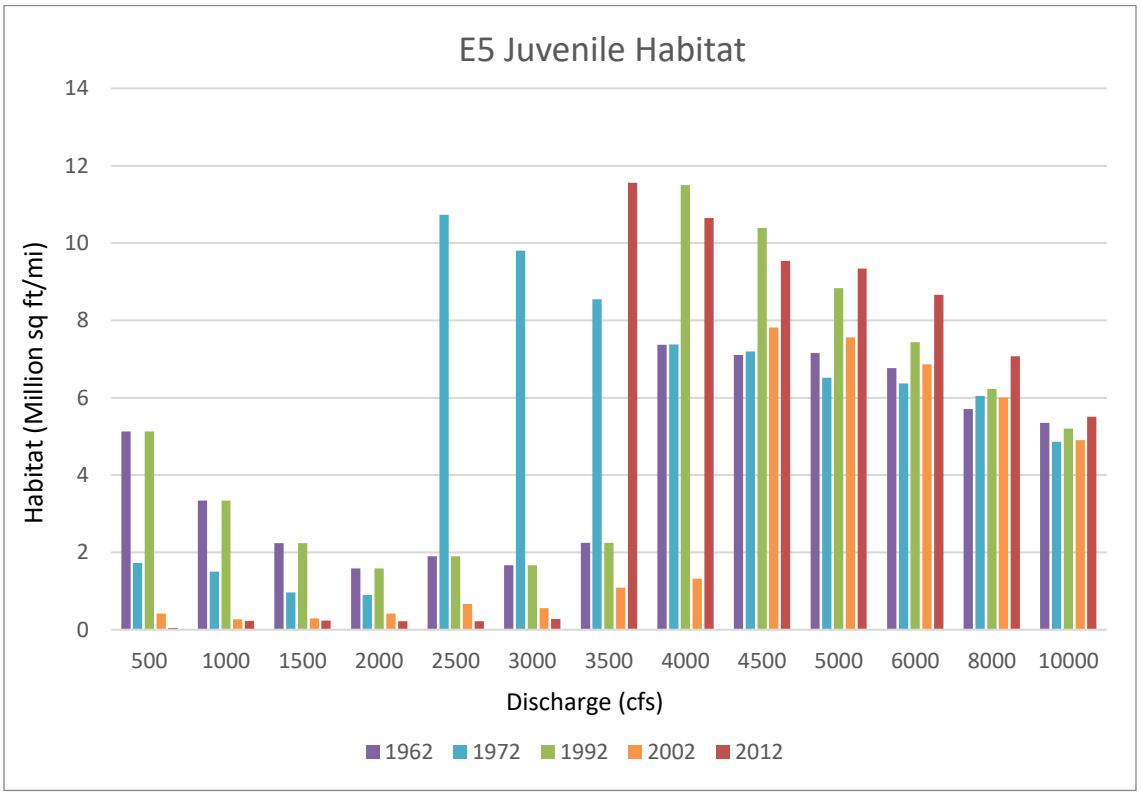

Figure D- 14 Subreach E5 Juvenile Habitat

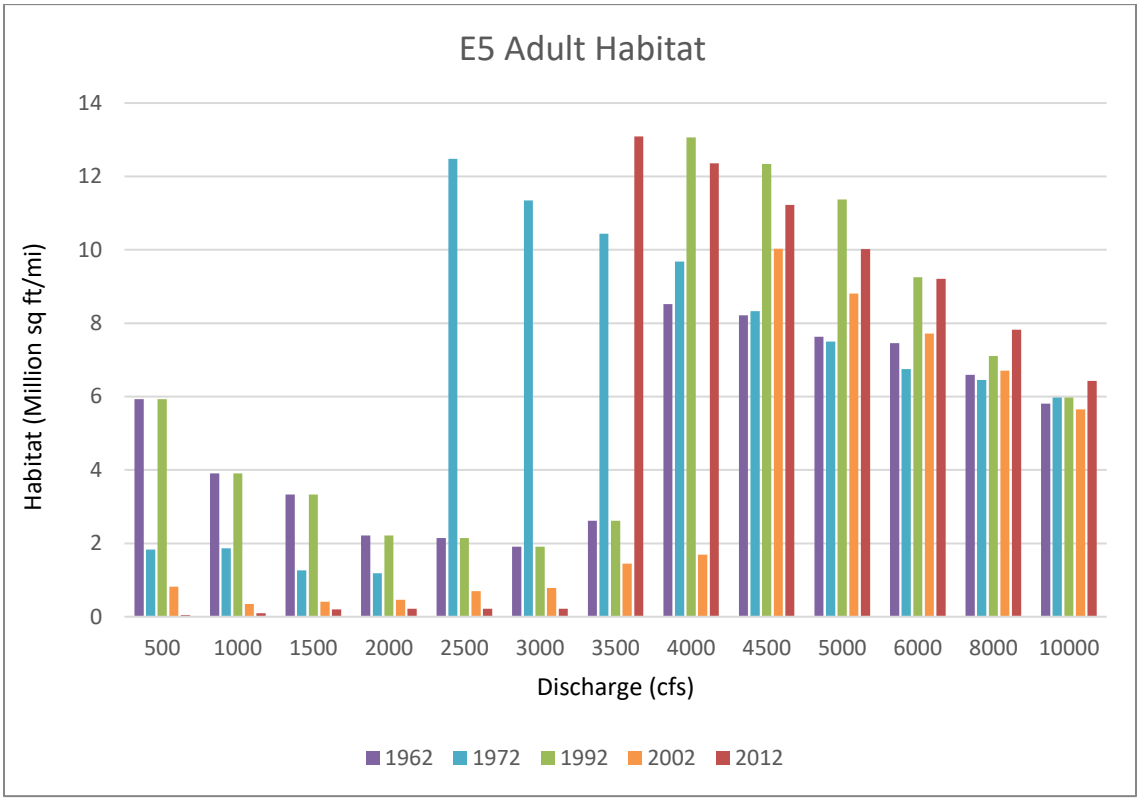

Figure D- 15 Subreach E5 Adult Habitat

Stacked Habitat Charts

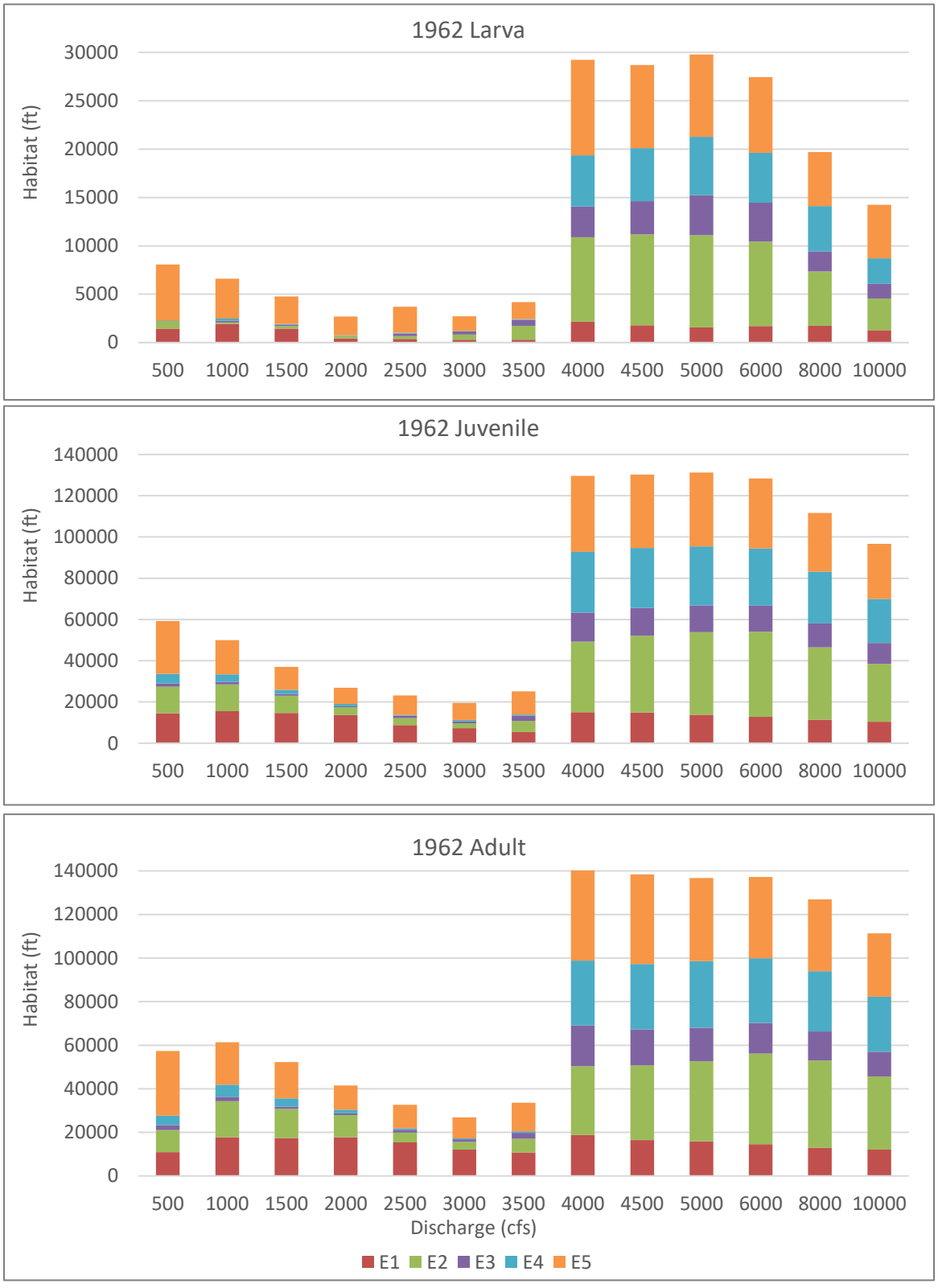

Figure D- 16 Stacked habitat charts to display spatial variations of habitat throughout the Escondida reach in 1962

Figure D- 17 Stacked habitat charts to display spatial variations of habitat throughout the Escondida reach in 1972.

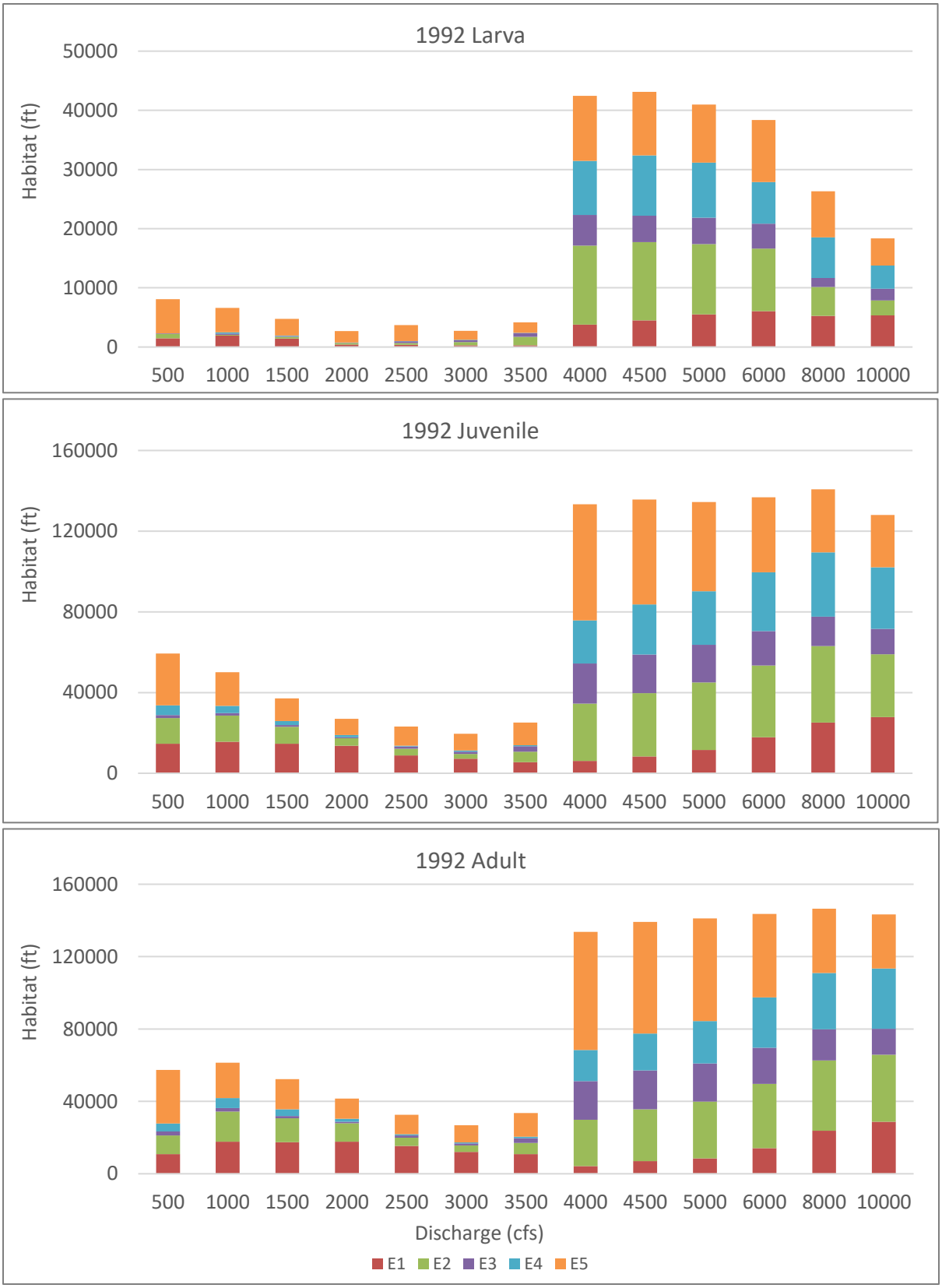

Figure D- 18 Stacked habitat charts to display spatial variations of habitat throughout the Escondida reach in 1992

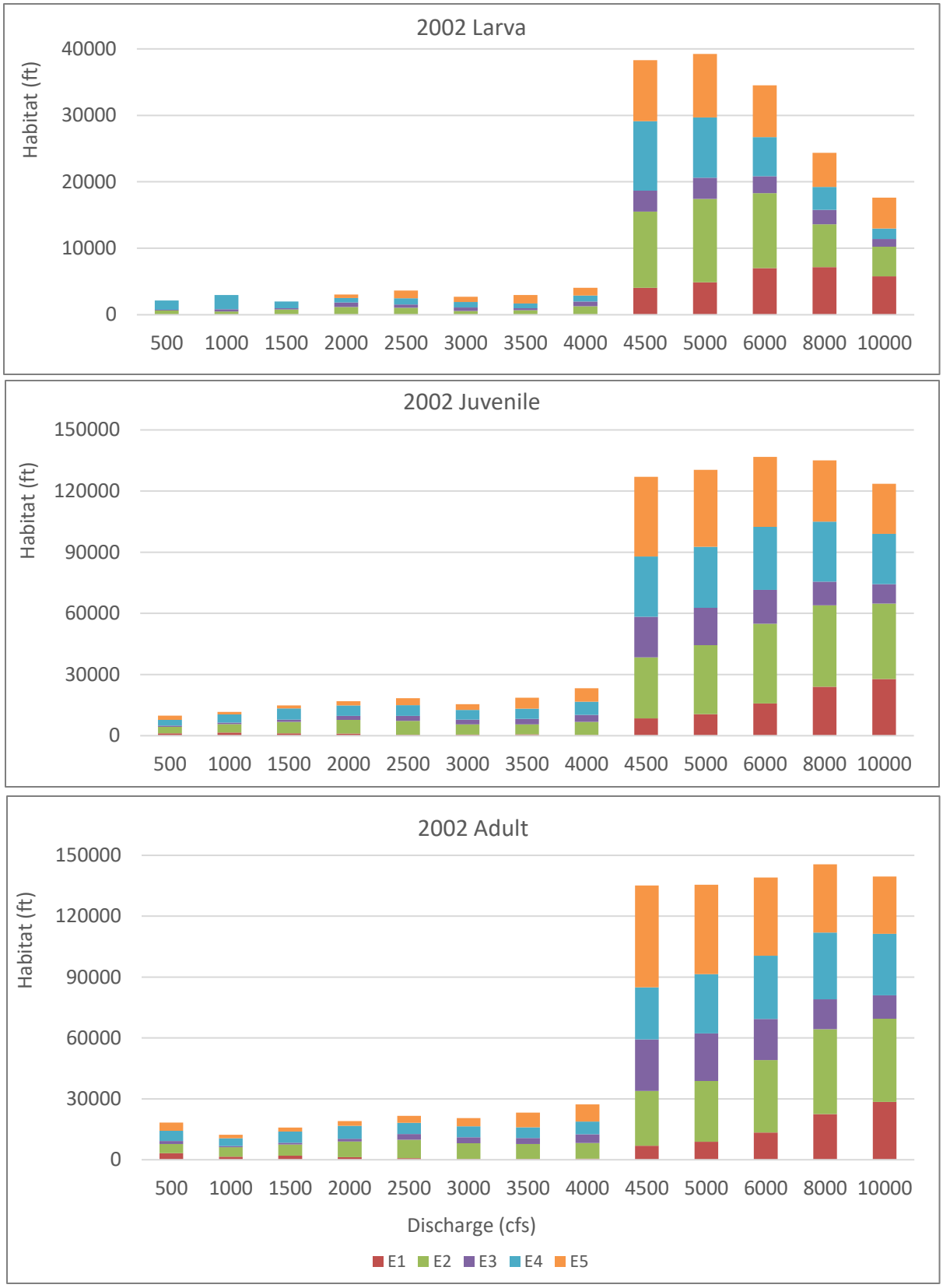

Figure D- 19 Stacked habitat charts to display spatial variations of habitat throughout the Escondida reach in 2002

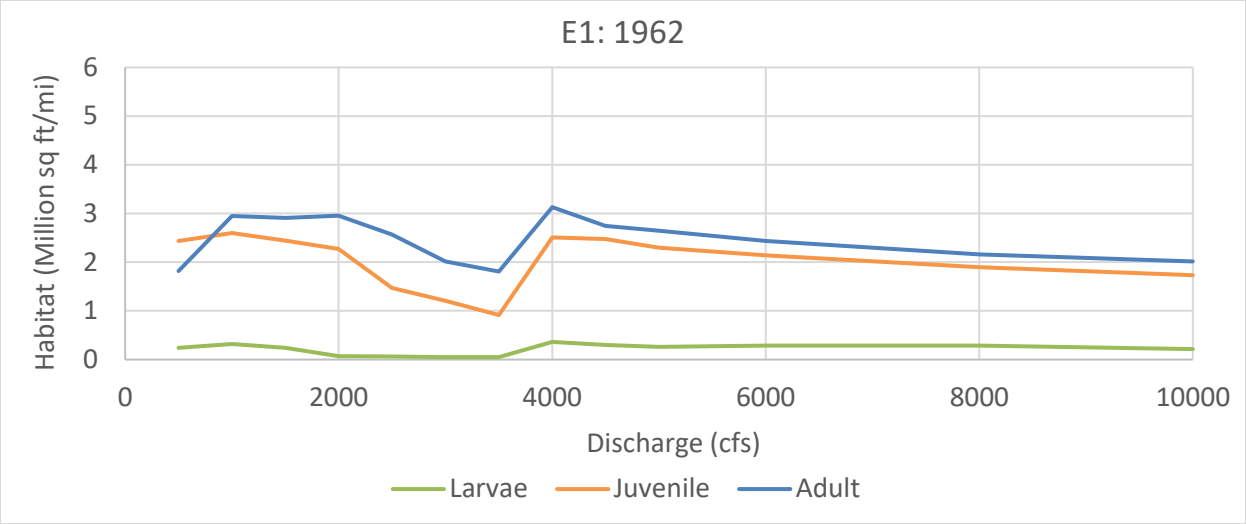

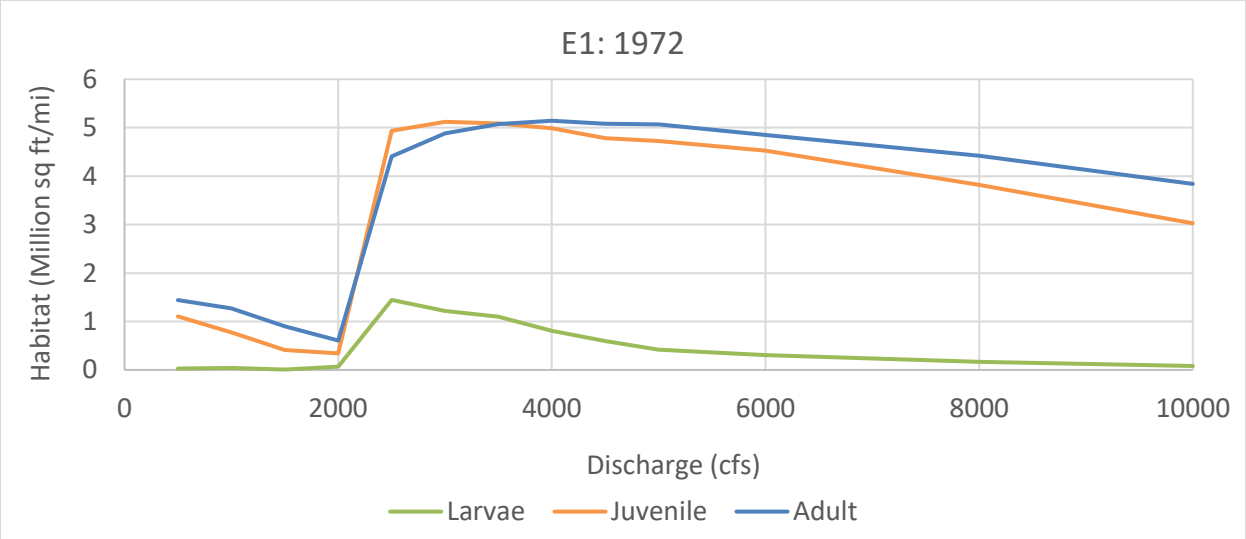

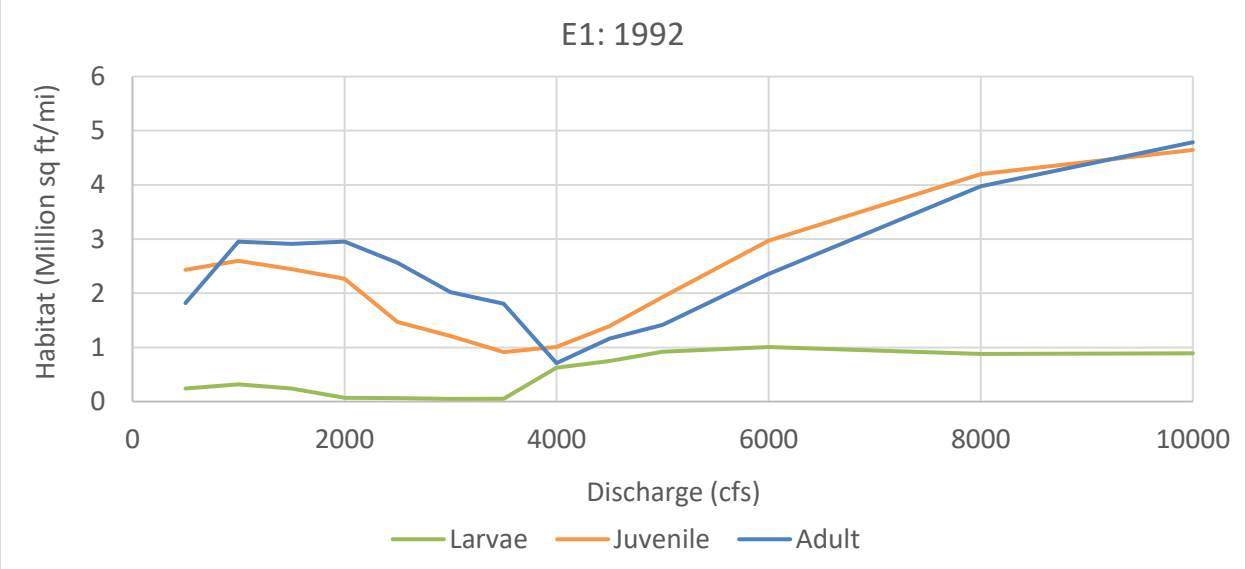

Figure D- 20 Life stage habitat curves for subreach E1 at the years 1962 (top), 1972 (middle), and 1992 (bottom).

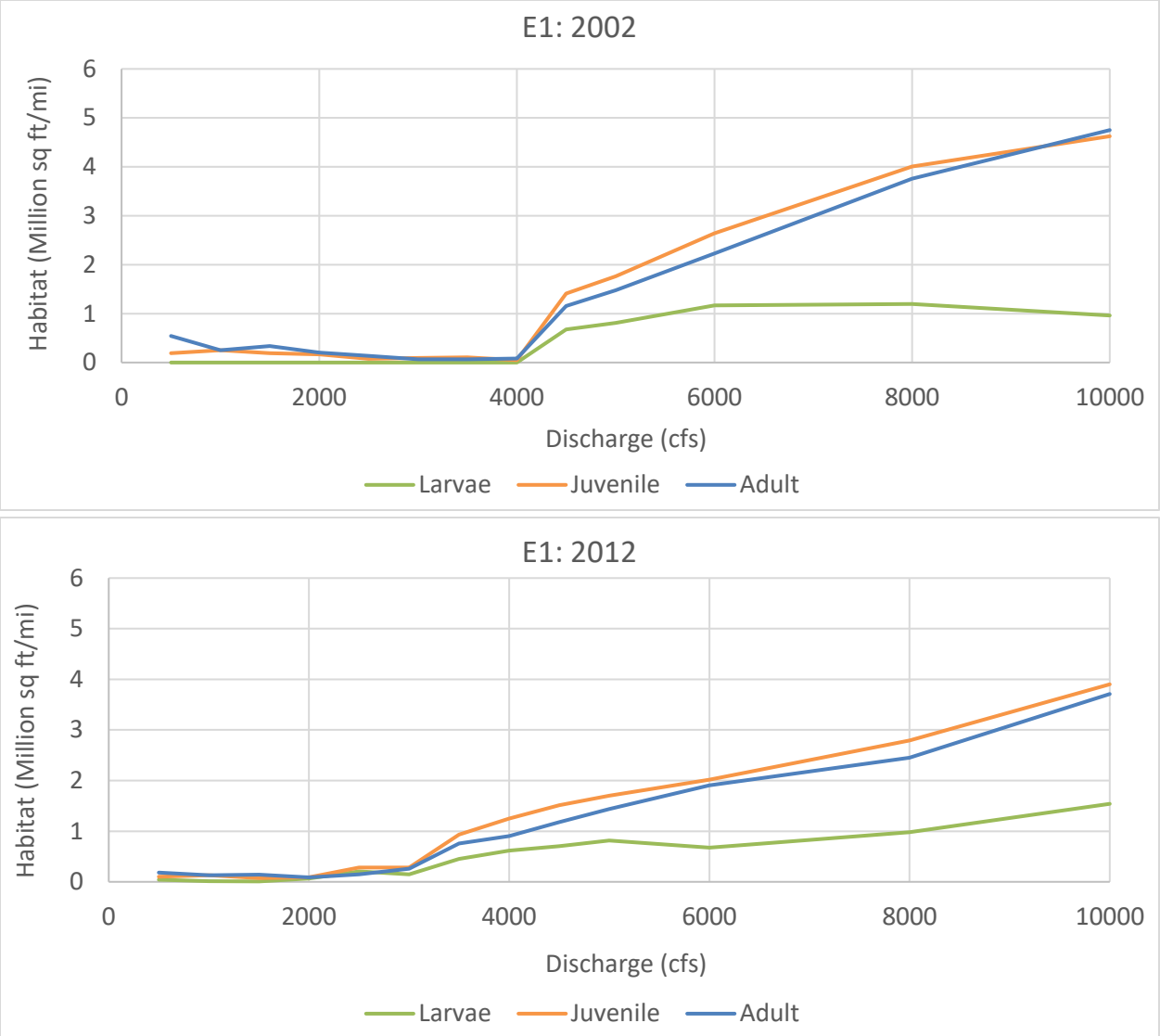

Figure D- 21 Life stage habitat curves for subreach E1 for the years 2002 (top) and 2012 (bottom).

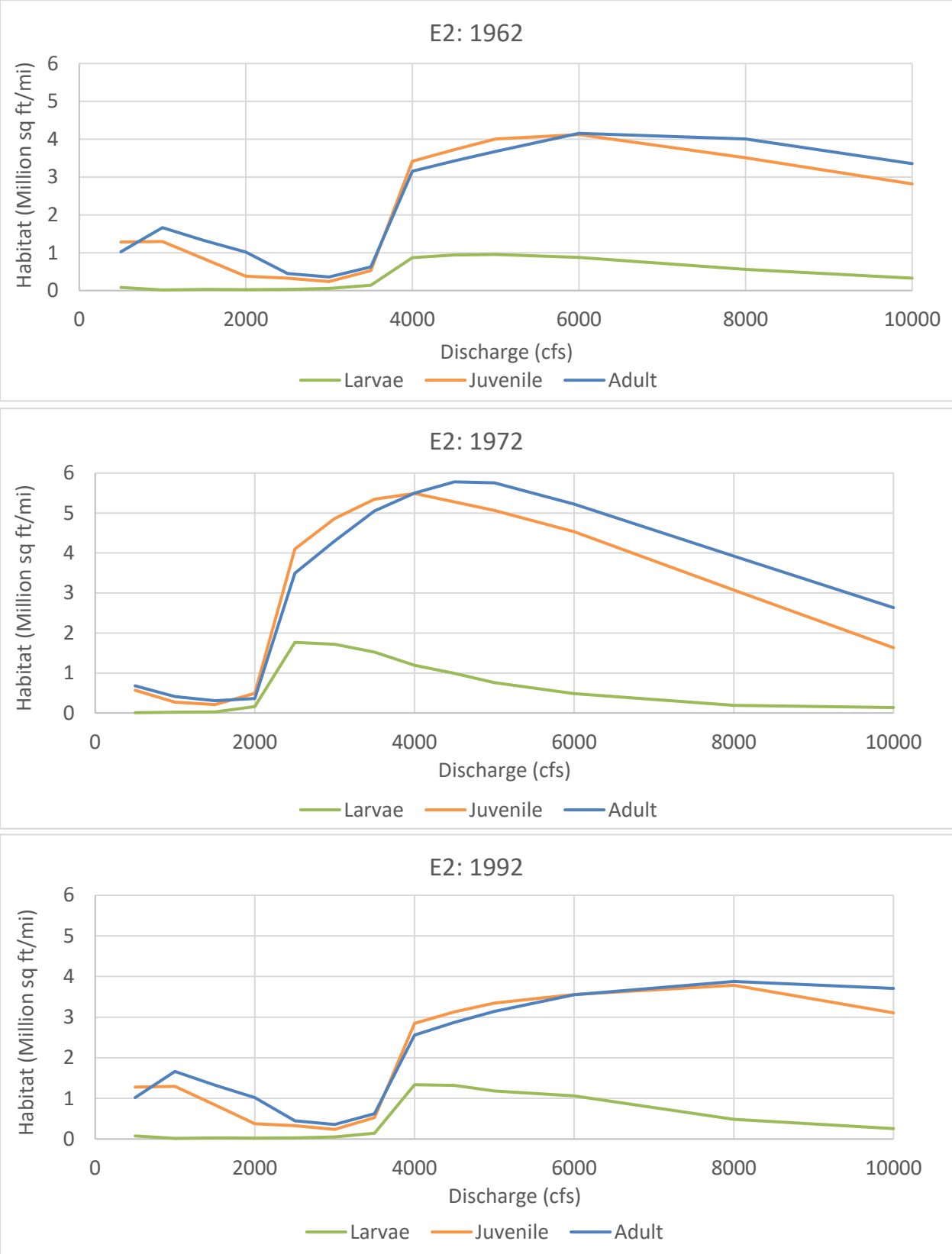

Figure D- 22 Life stage habitat curves for subreach E2 at the years 1962 (top), 1972 (middle), and 1992 (bottom).

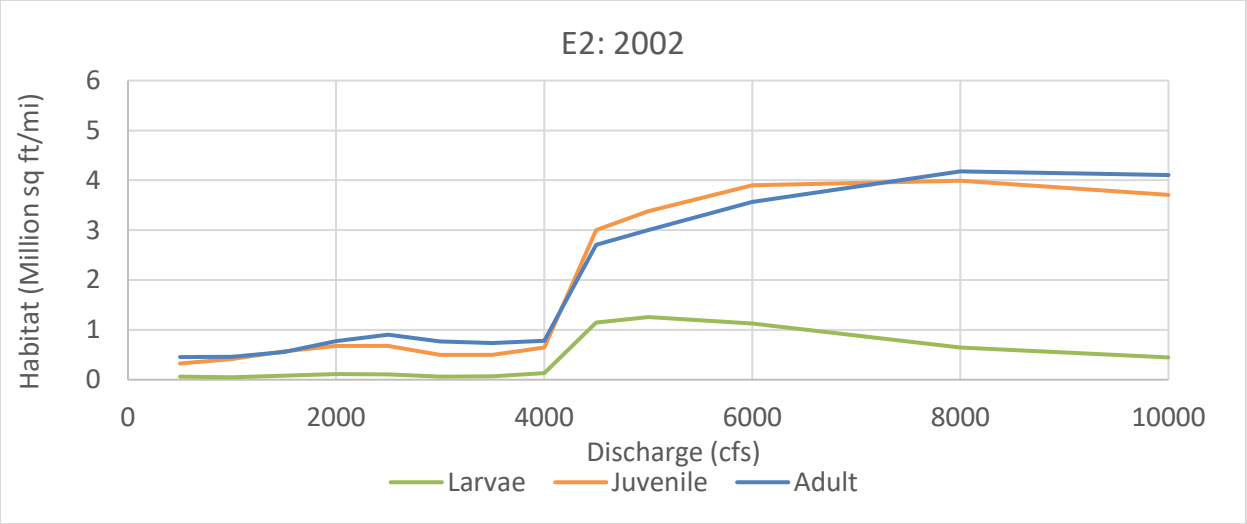

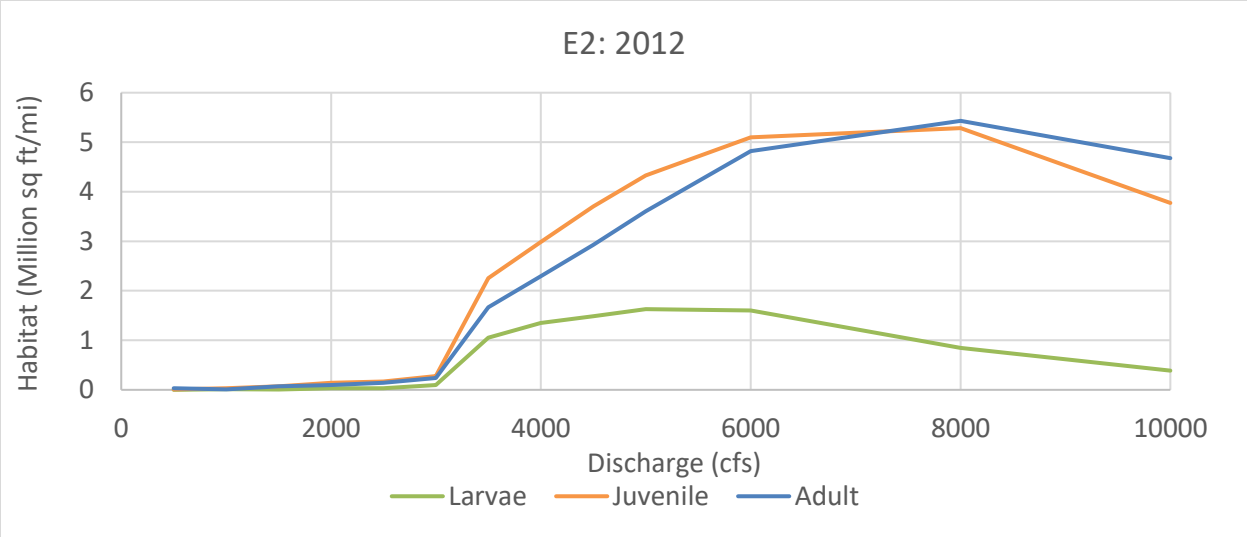

Figure D- 23 Life stage habitat curves for subreach E2 for the years 2002 (top) and 2012 (bottom).

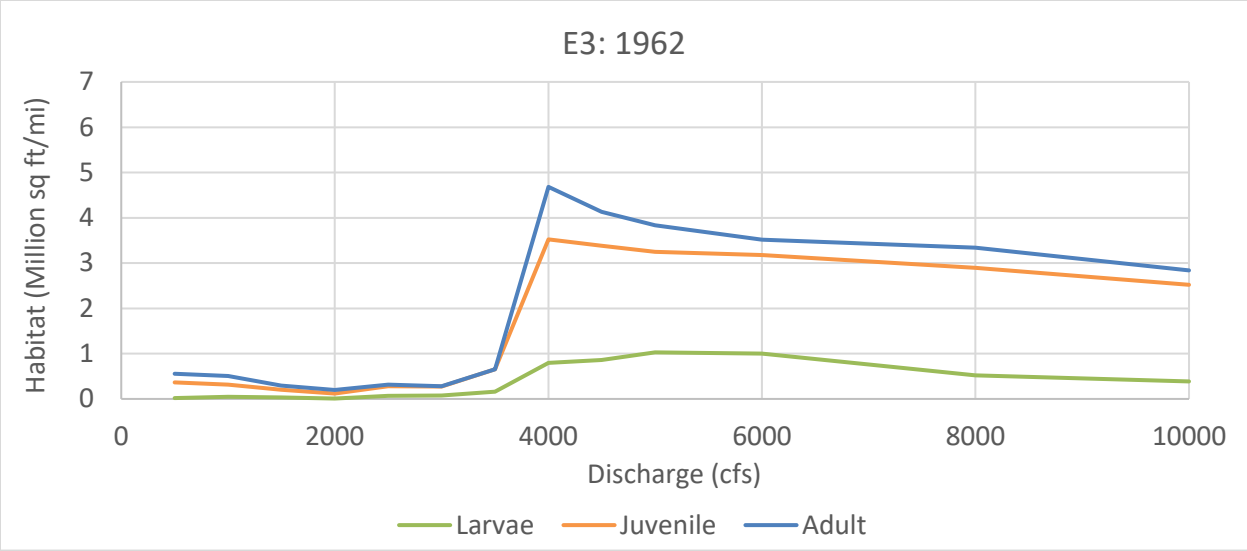

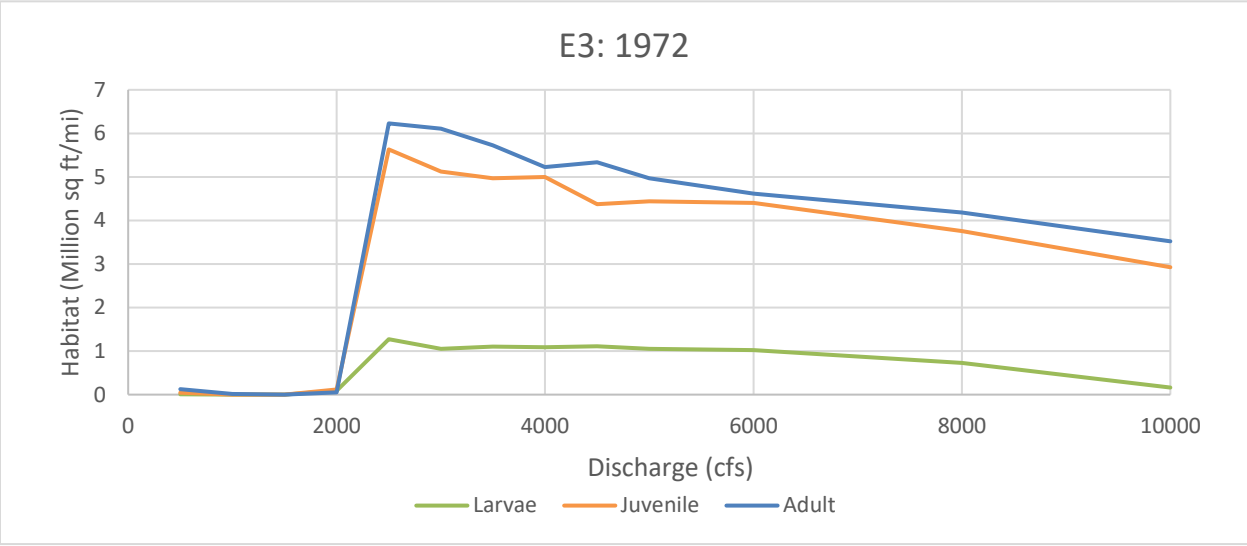

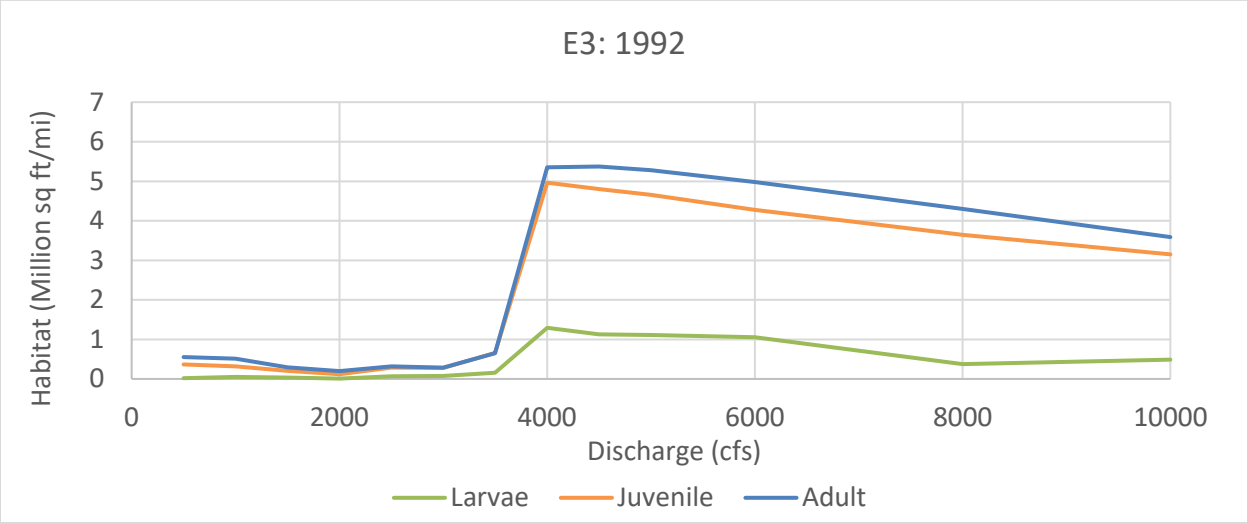

Figure D- 24 Life stage habitat curves for subreach E3 at the years 1962 (top), 1972 (middle), and 1992 (bottom)

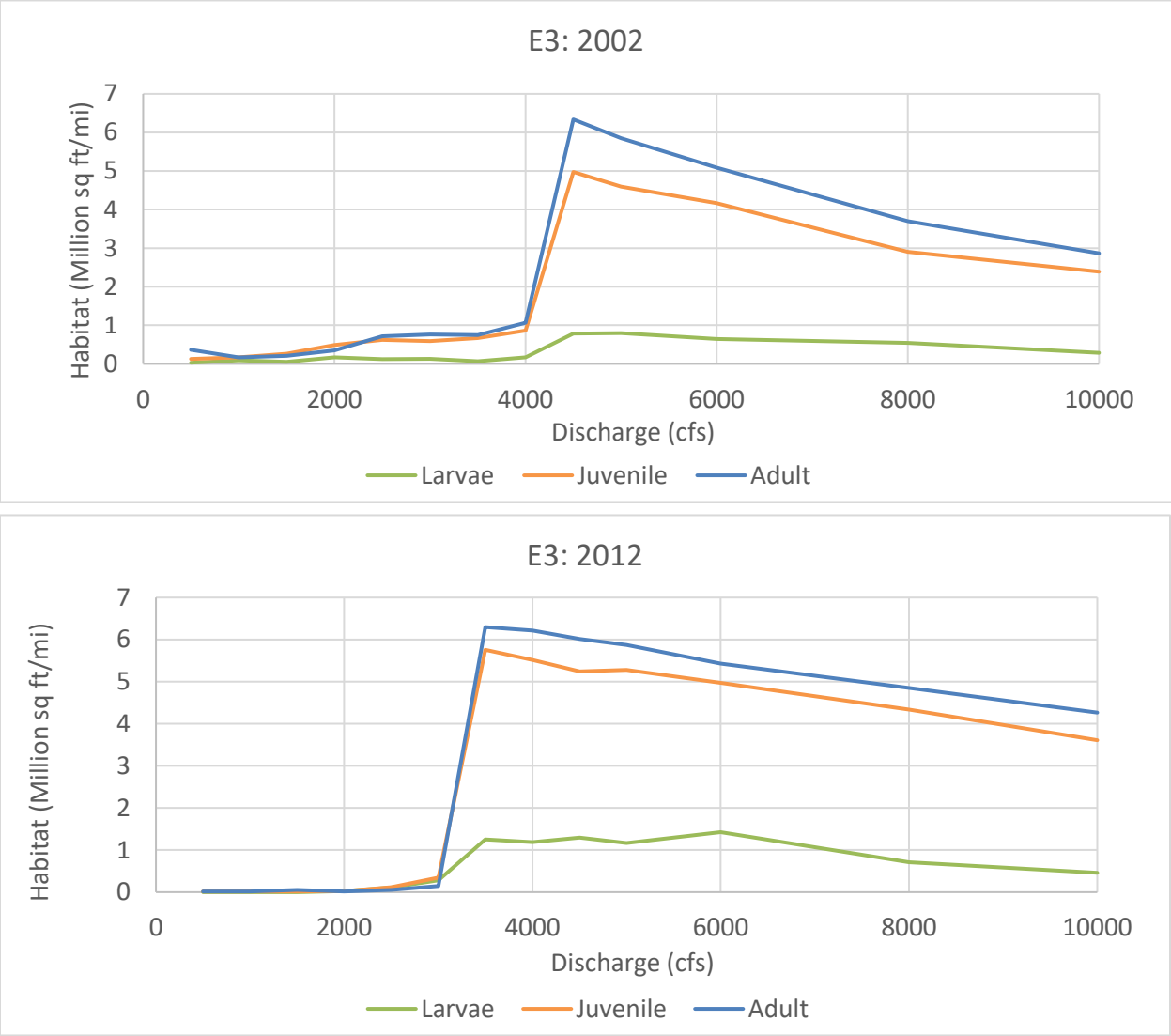

Figure D- 25 Life stage habitat curves for subreach E3 for the years 2002 (top) and 2012 (bottom)

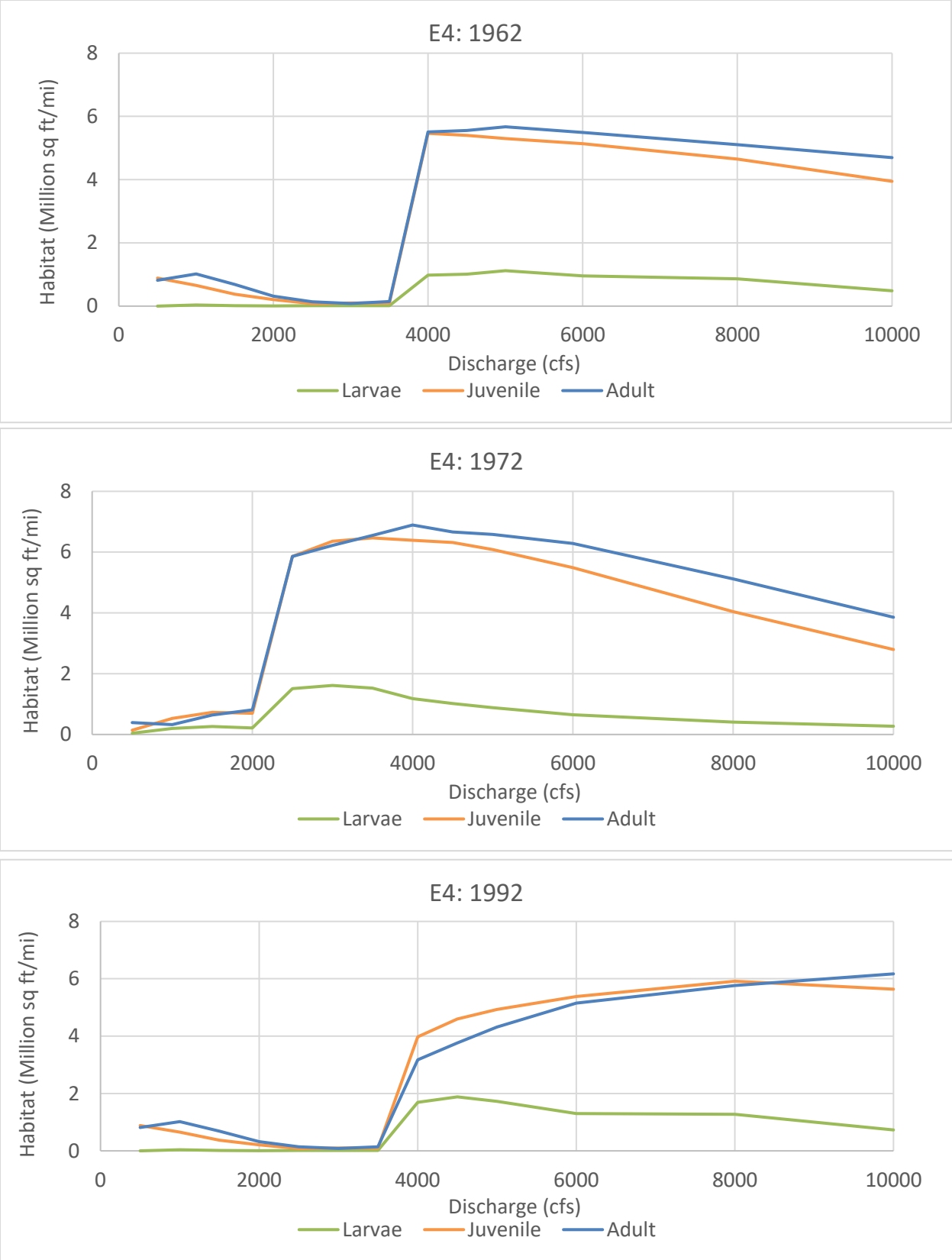

Figure D- 26 Life stage habitat curves for subreach E4 at the years 1962 (top), 1972 (middle), and 1992 (bottom).

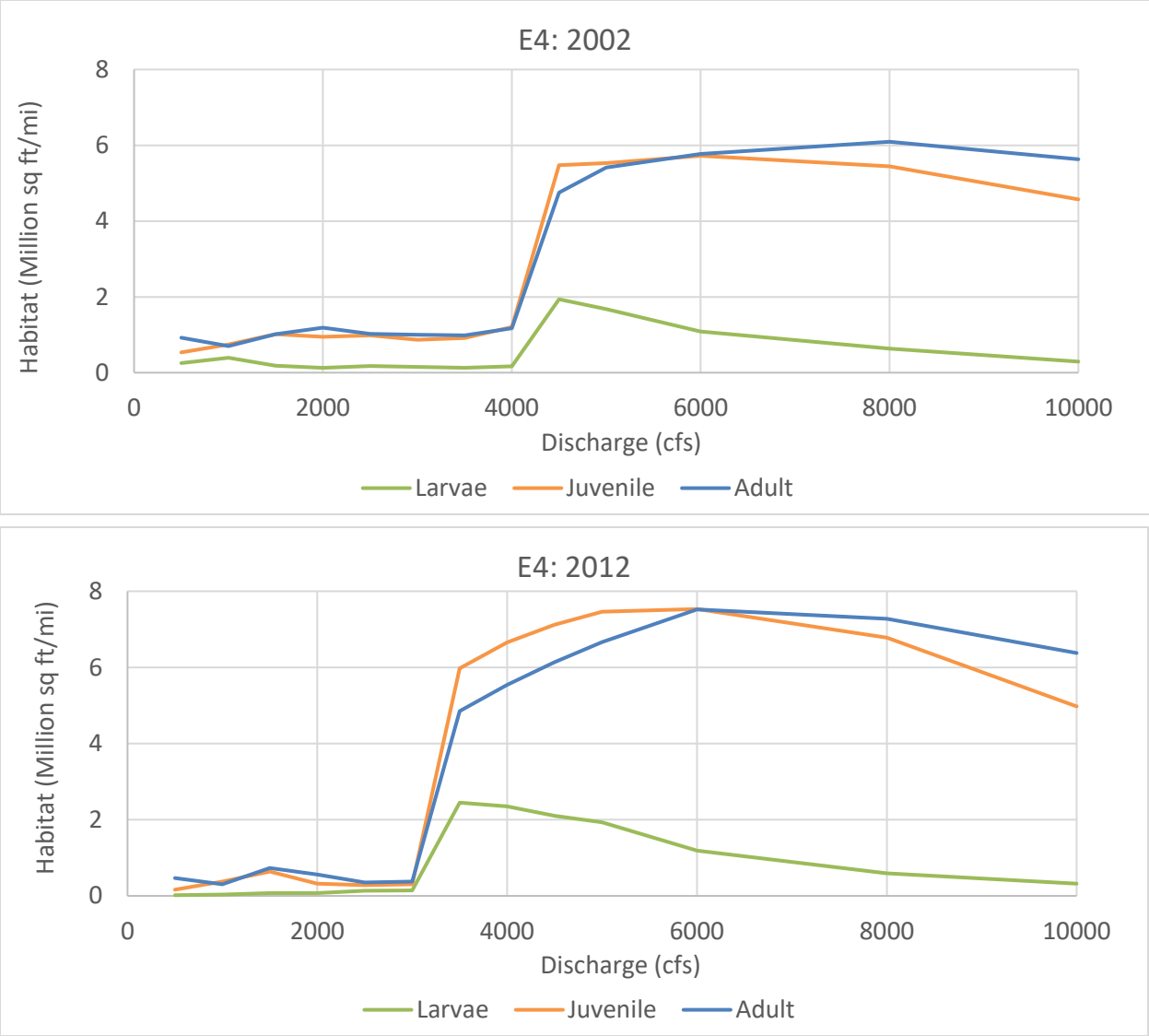

Figure D- 27 Life stage habitat curves for subreach E4 for the years 2002 (top) and 2012 (bottom).

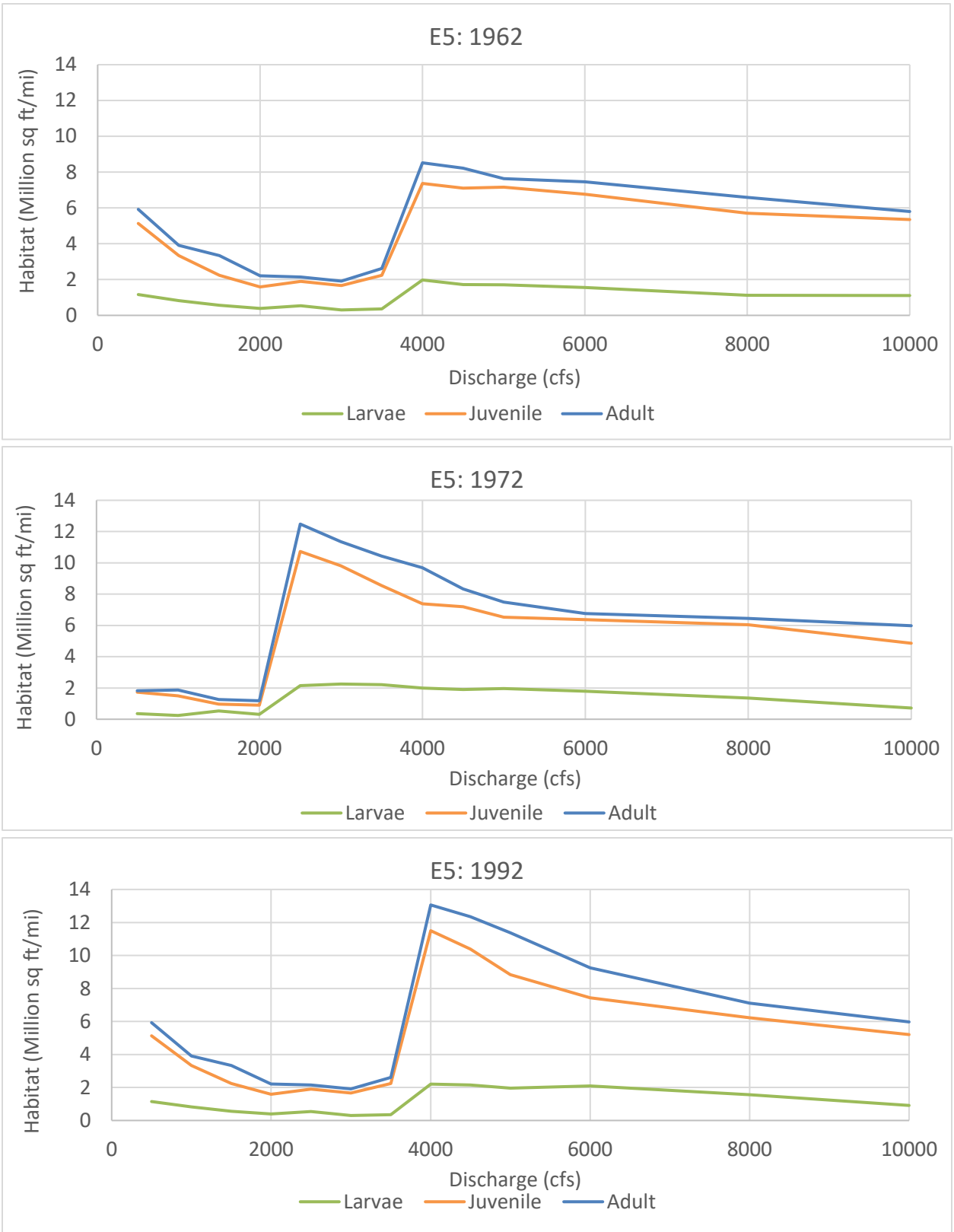

Figure D- 28 Life stage habitat curves for subreach E5 at the years 1962 (top), 1972 (middle), and 1992 (bottom).

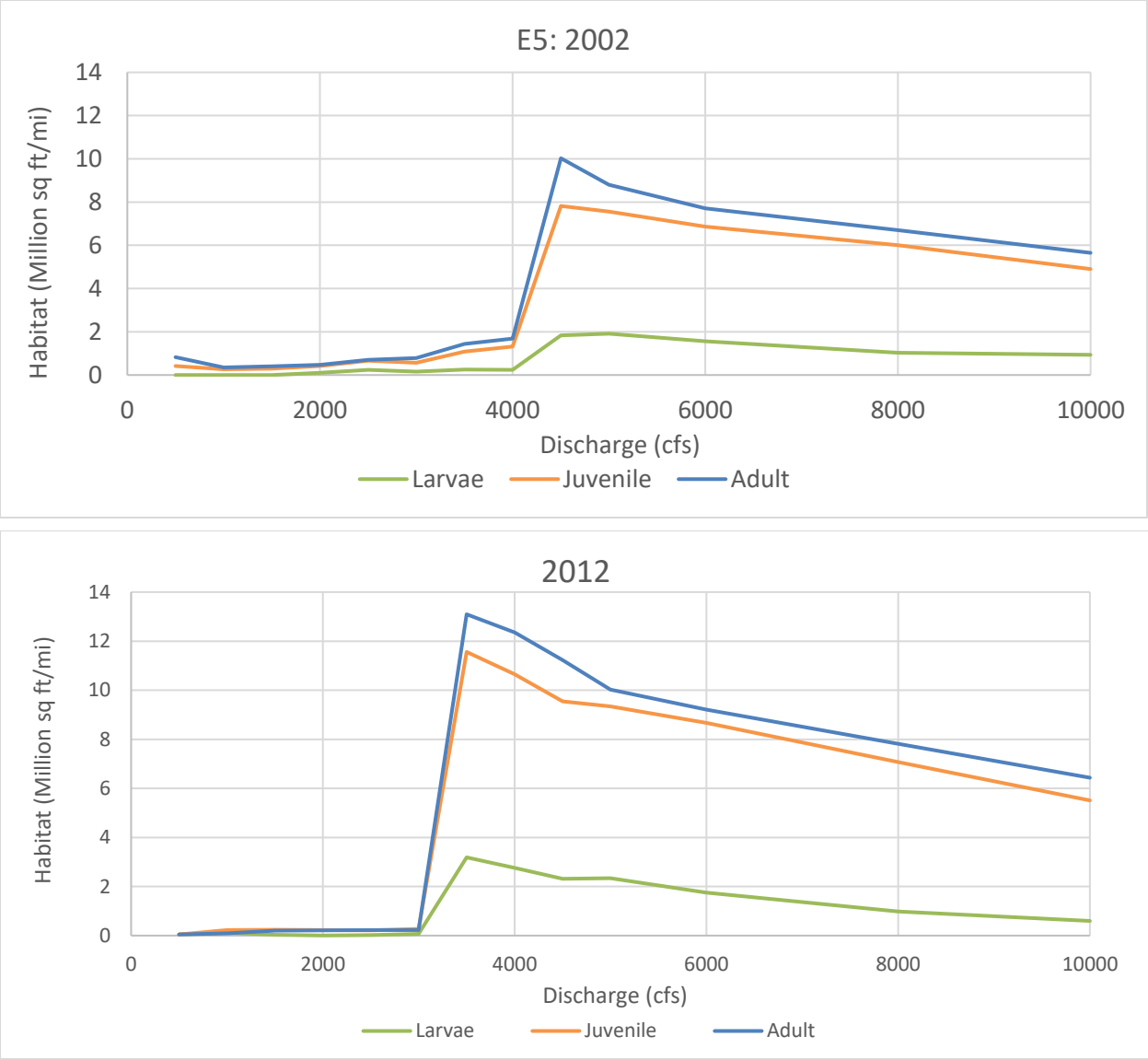

Figure D- 29 Life stage habitat curves for subreach E5 for the years 2002 (top) and 2012 (bottom).

Appendix E

Habitat Maps

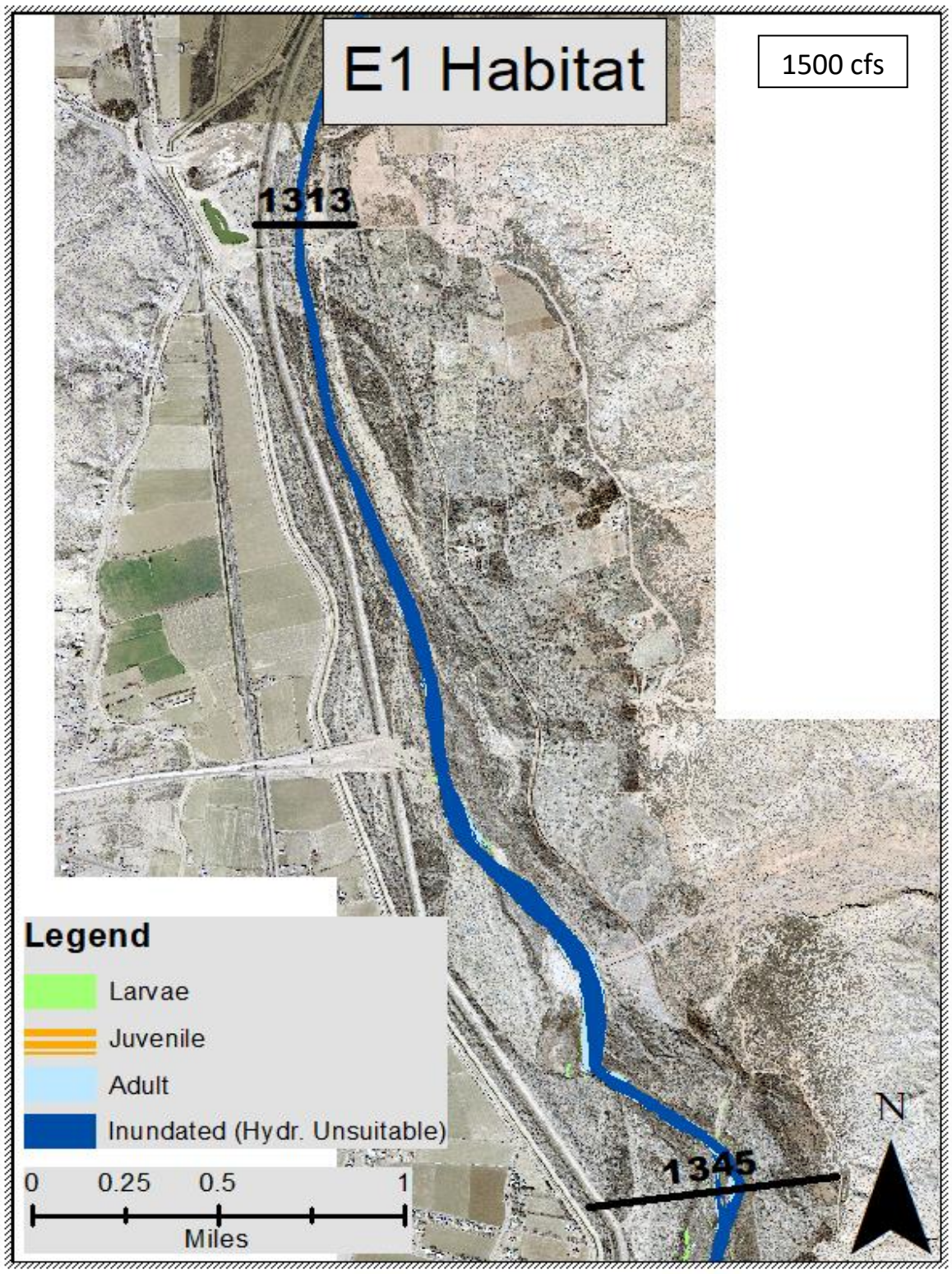

Figure E- 1 RGSM Habitat in subreach E1 at 1500 cfs with hydraulically suitable areas labeled for larvae (green), juvenile (orange), and adult (light blue) and unsuitable inundated areas in dark blue.

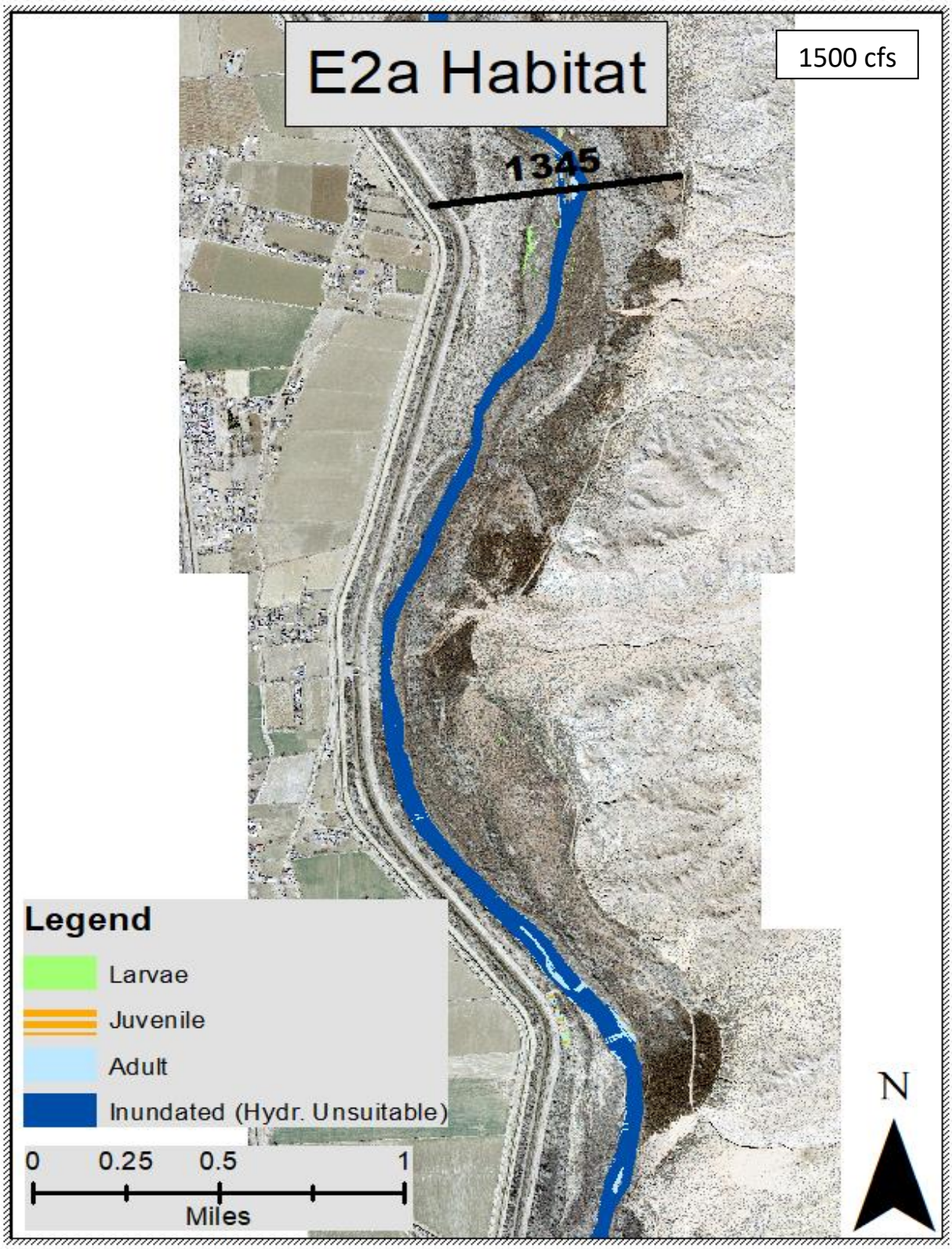

Figure E- 2 RGSM Habitat in subreach E2 (upstream portion part a) at 1500 cfs with hydraulically suitable areas labeled for larvae (green), juvenile (orange), and adult (light blue) and unsuitable inundated areas in dark blue.

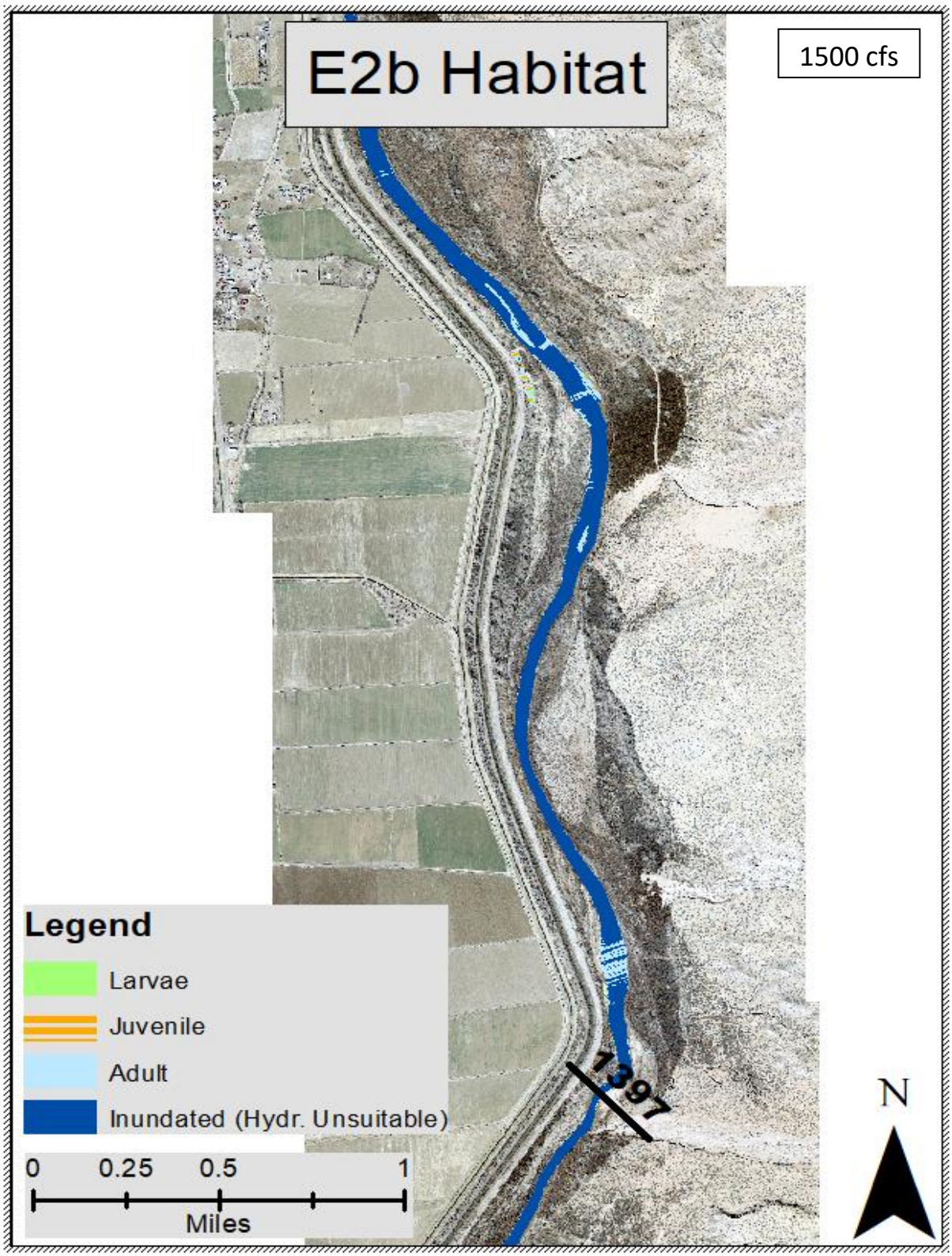

Figure E- 3 RGSM Habitat in subreach E2 (downstream portion part b) at 1500 cfs with hydraulically suitable areas labeled for larvae (green), juvenile (orange), and adult (light blue) and unsuitable inundated areas in dark blue.

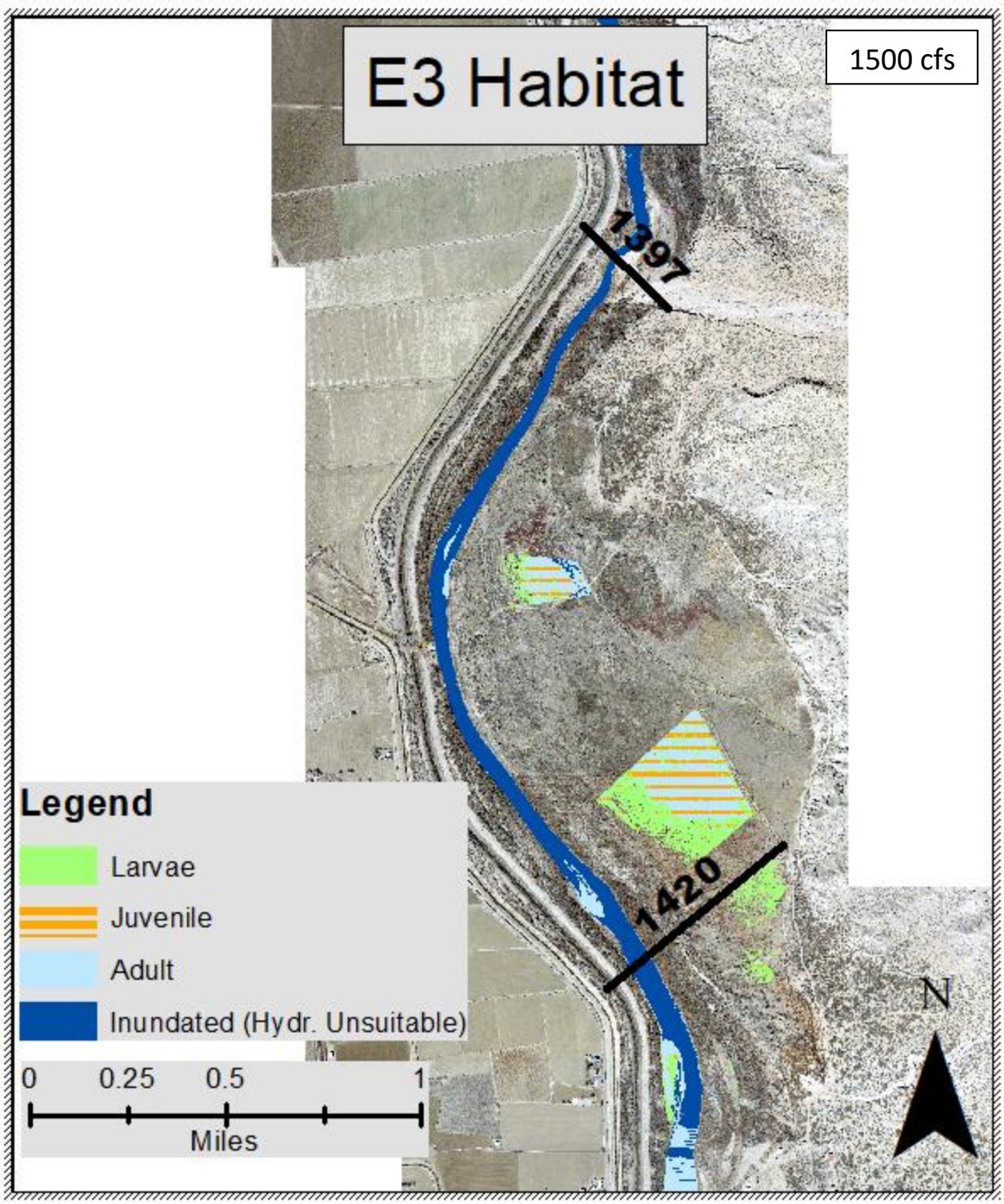

Figure E- 4 RGSM Habitat in subreach E3 at 1500 cfs with hydraulically suitable areas labeled for larvae (green), juvenile (orange), and adult (light blue) and unsuitable inundated areas in dark blue. There should be very little overtopping of the computational levees at 1,500 cfs, which means water inundation is not expected in the floodplains. This may be an issue of the pseudo 2-D model that arises when working with perched channels.

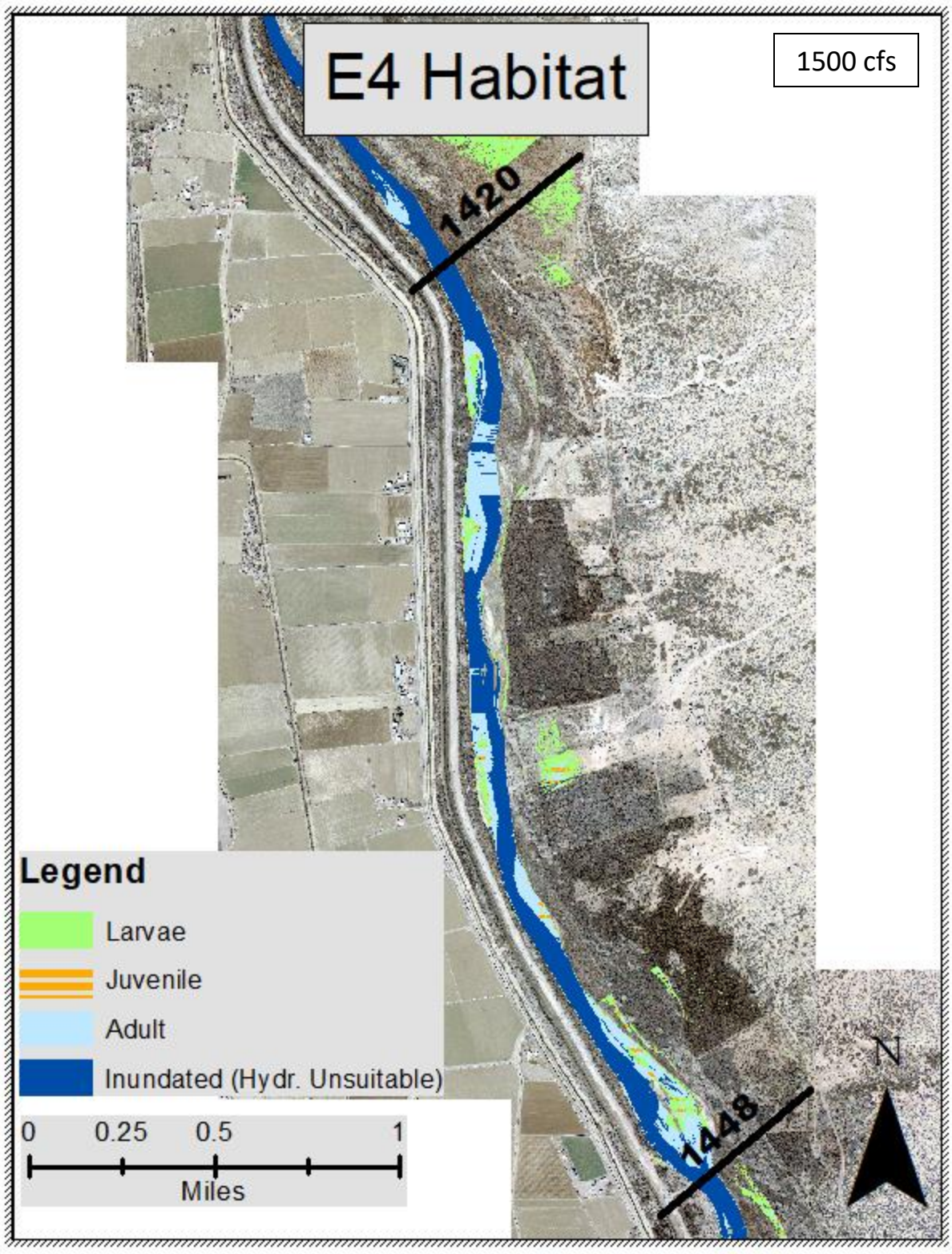

Figure E- 5 RGSM Habitat in subreach E4 at 1500 cfs with hydraulically suitable areas labeled for larvae (green), juvenile (orange), and adult (light blue) and unsuitable inundated areas in dark blue.

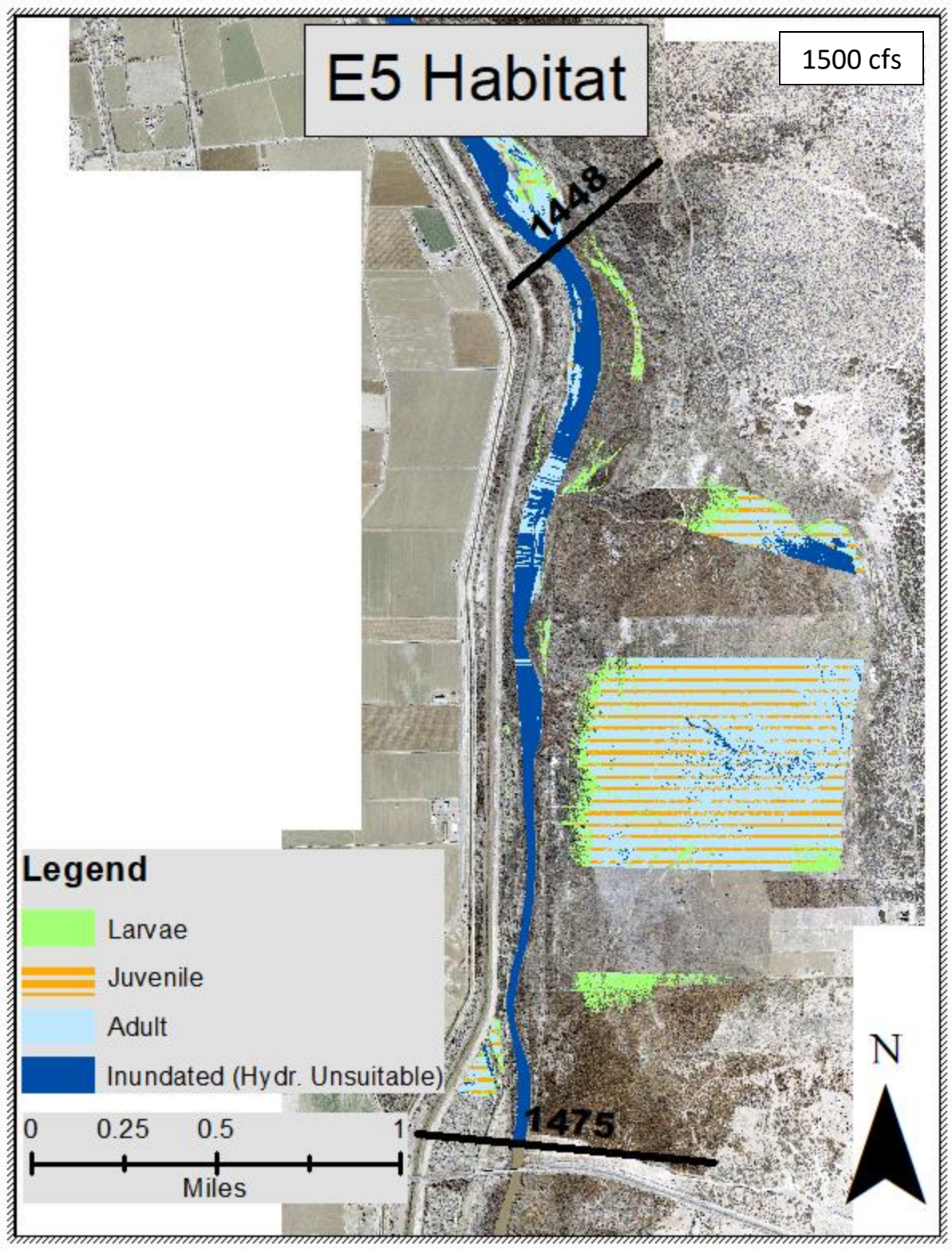

Figure E- 6 RGSM Habitat in subreach E5 at 1500 cfs with hydraulically suitable areas labeled for larvae (green), juvenile (orange), and adult (light blue) and unsuitable inundated areas in dark blue. There should be very little overtopping of the computational levees at 1,500 cfs, which means water inundation is not expected in the floodplains. This may be an issue of the pseudo 2-D model that arises when working with perched channels.

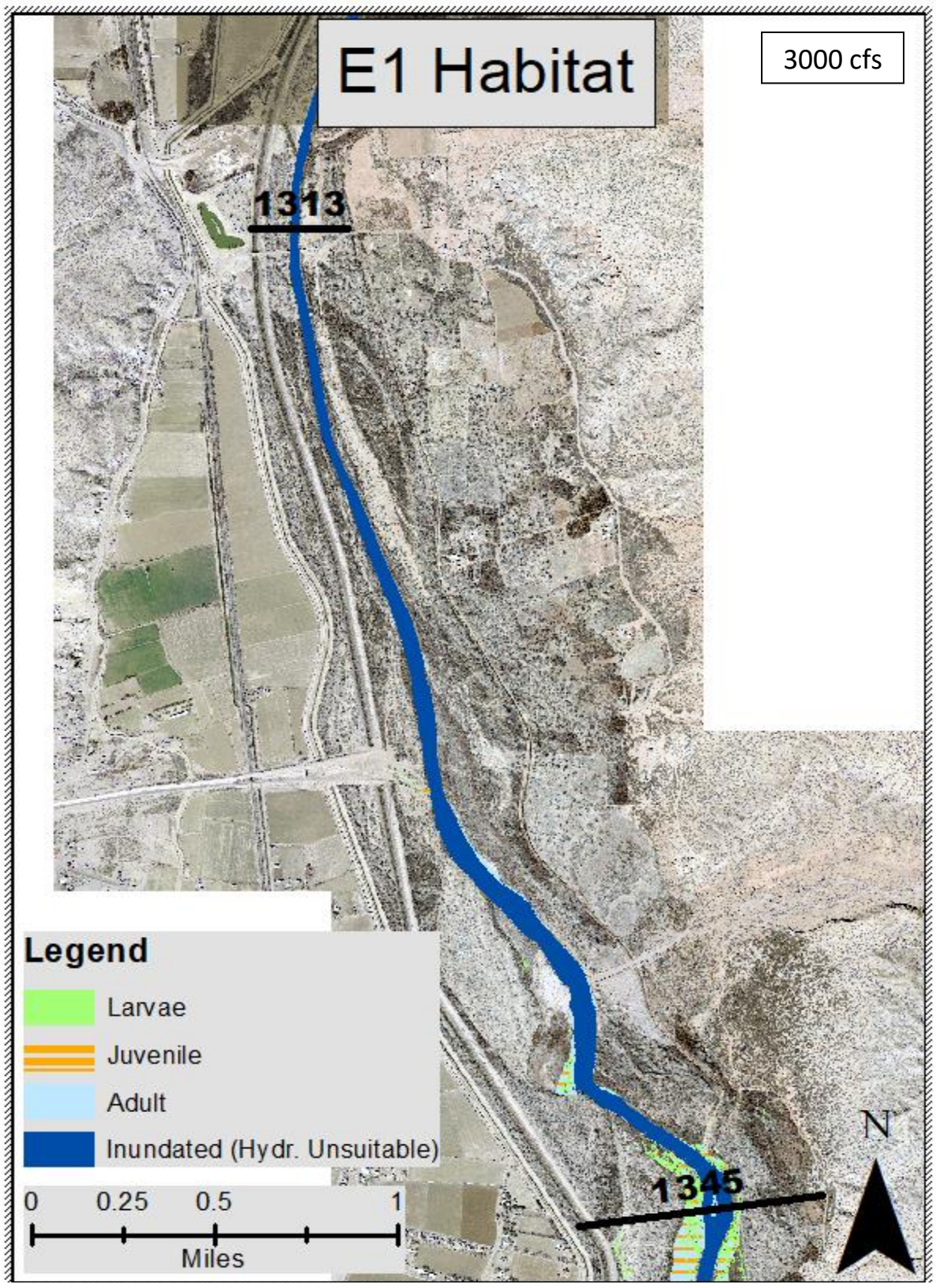

Figure E- 7 RGSM Habitat in subreach E1 at 3000 cfs with hydraulically suitable areas labeled for larvae (green), juvenile (orange), and adult (light blue) and unsuitable inundated areas in dark blue.

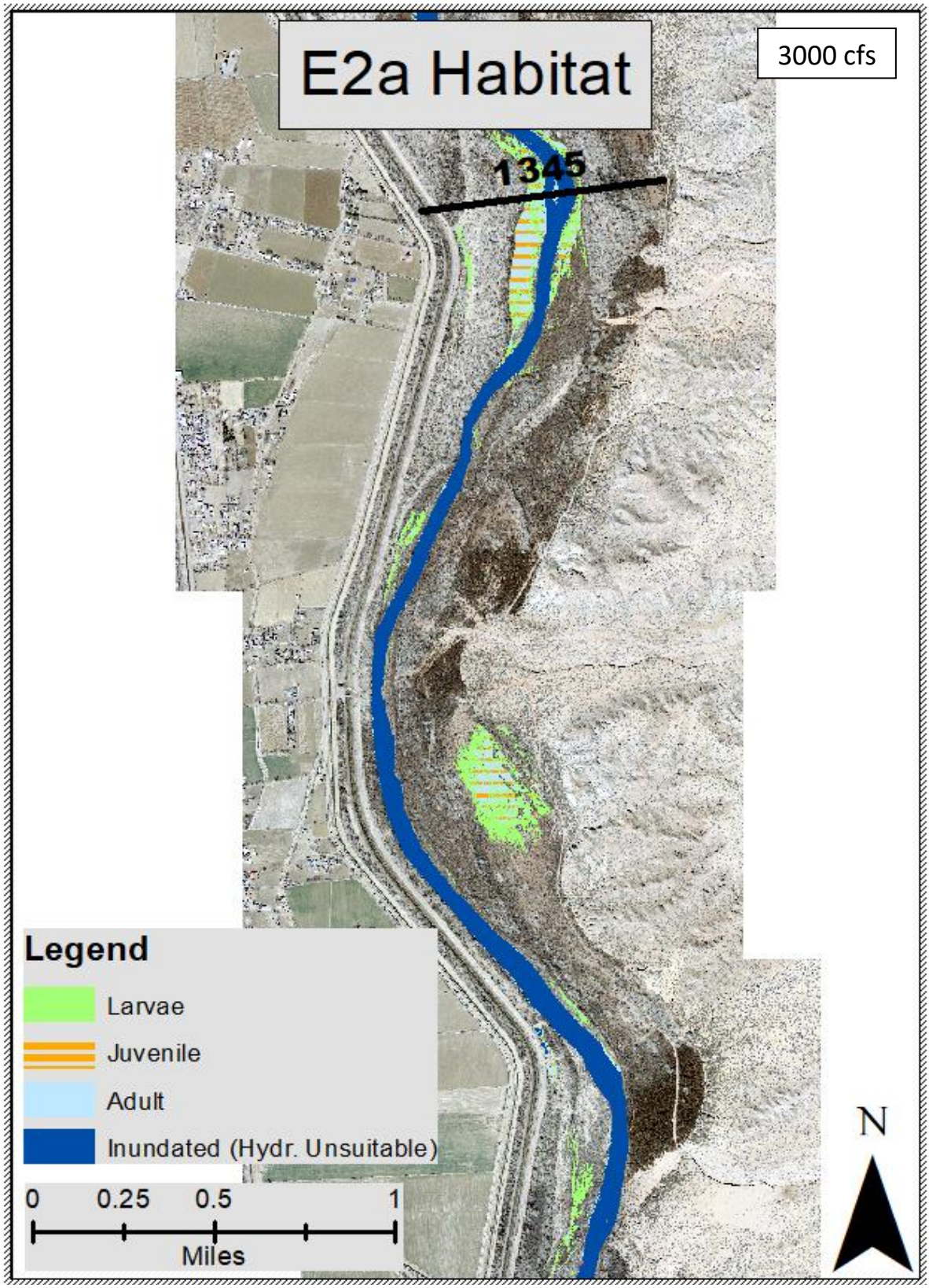

Figure E- 8 RGSM Habitat in subreach E2 (upstream portion part a) at 3000 cfs with hydraulically suitable areas labeled for larvae (green), juvenile (orange), and adult (light blue) and unsuitable inundated areas in dark blue.

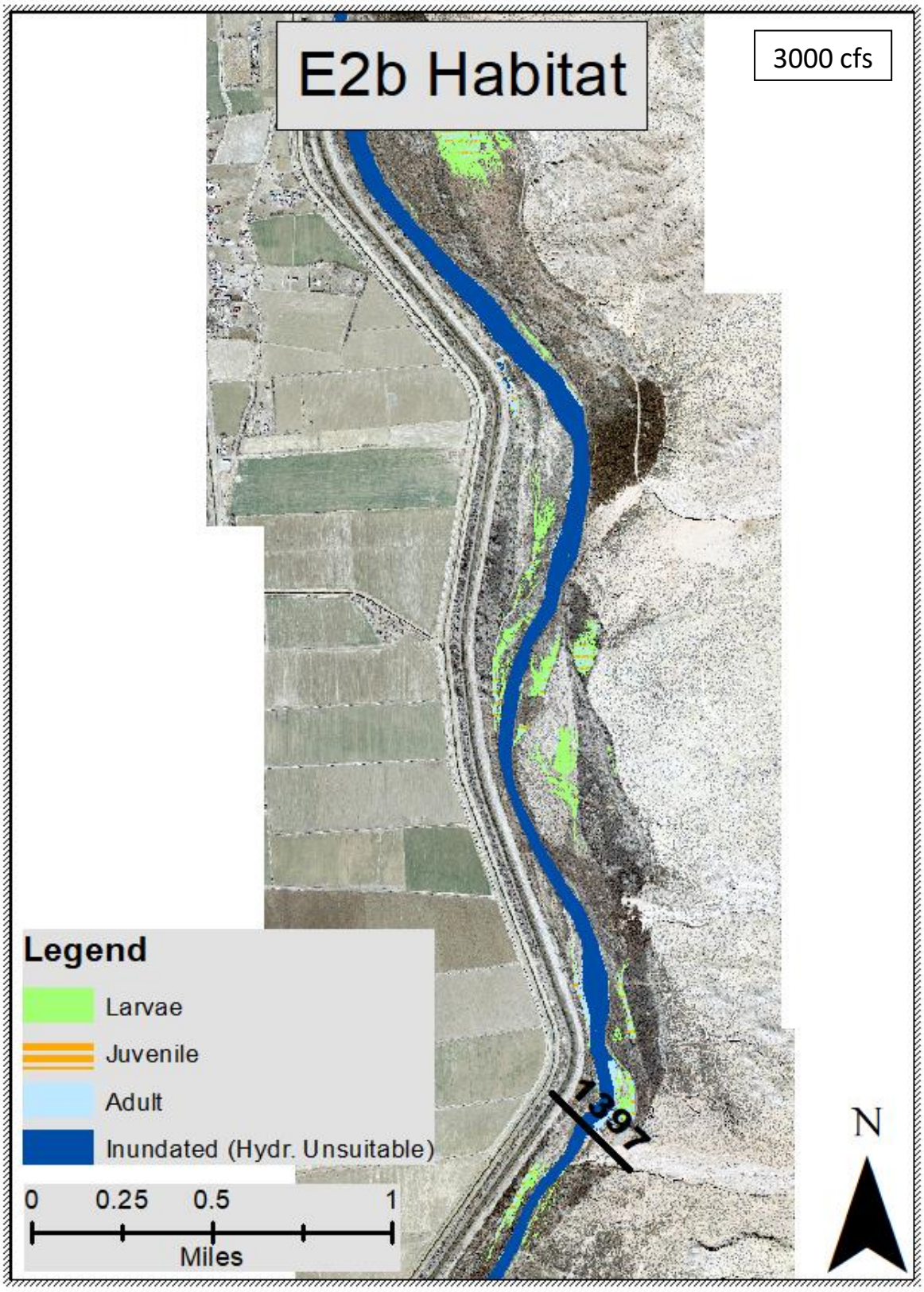

Figure E- 9 RGSM Habitat in subreach E2 (downstream portion part b) at 3000 cfs with hydraulically suitable areas labeled for larvae (green), juvenile (orange), and adult (light blue) and unsuitable inundated areas in dark blue.

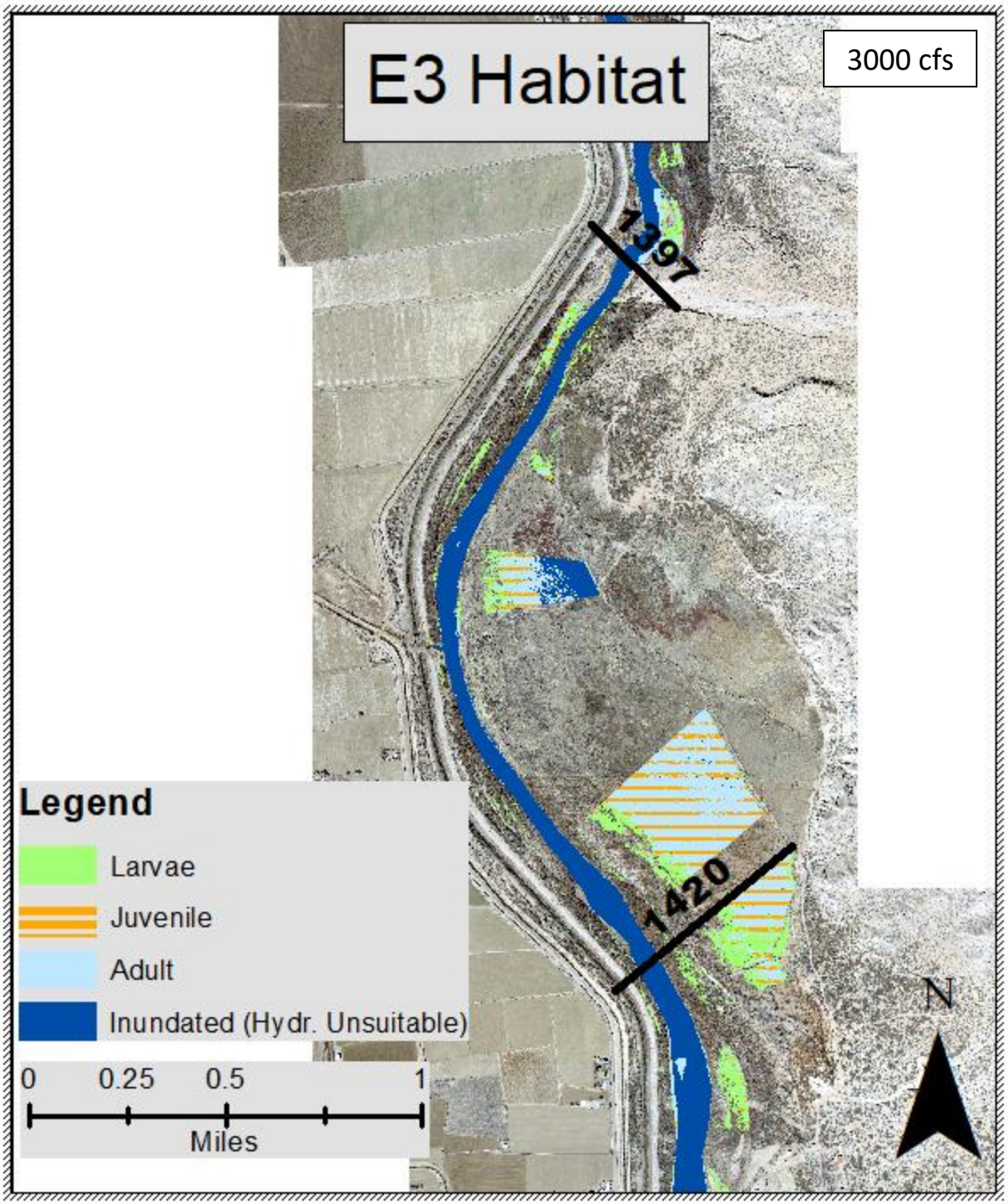

Figure E- 10 RGSM Habitat in subreach E3 at 3000 cfs with hydraulically suitable areas labeled for larvae (green), juvenile (orange), and adult (light blue) and unsuitable inundated areas in dark blue. At 3,000 cfs, computational levees have not been removed from the model, so some cross sections are experiencing overtopping while others are not.

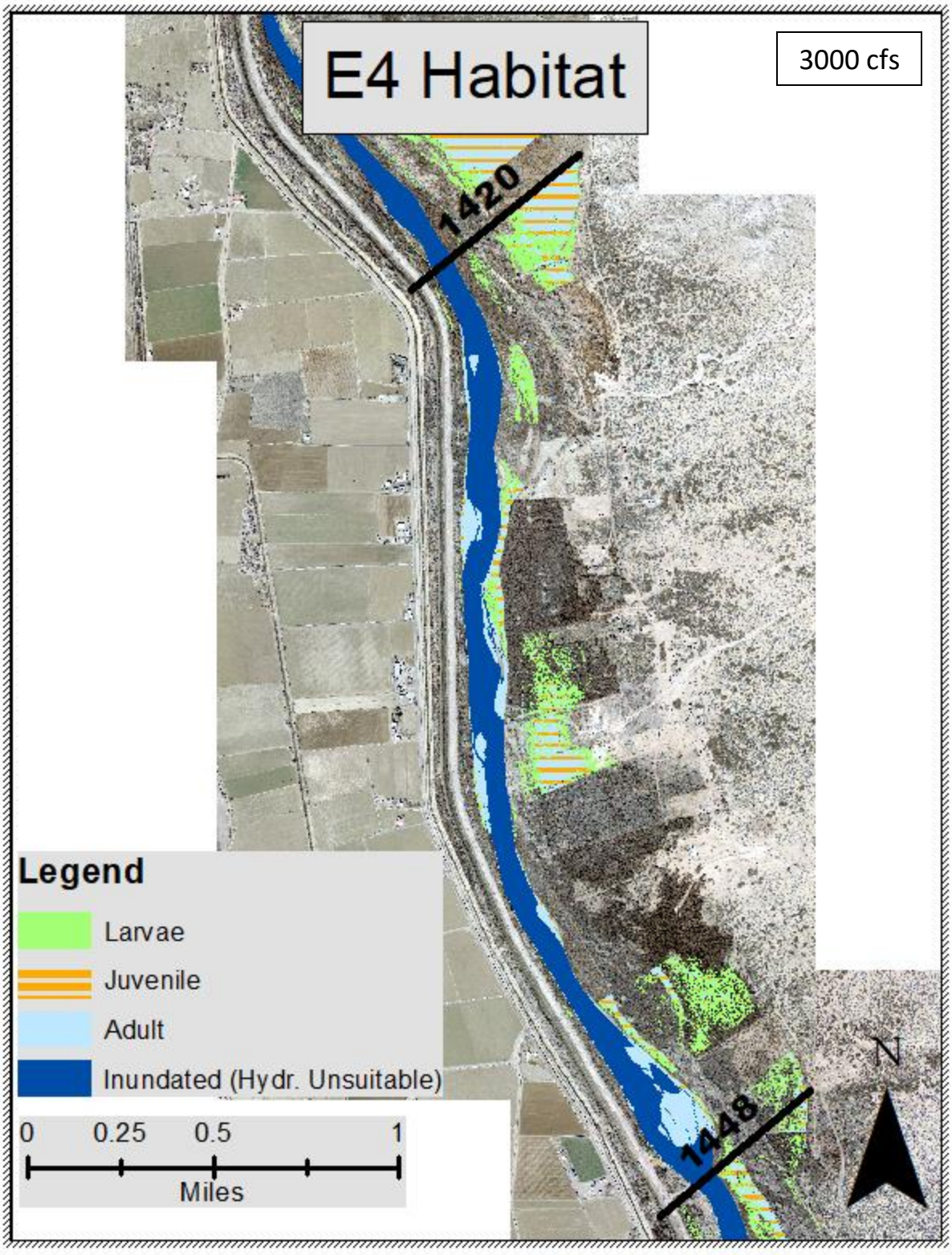

Figure E- 11 RGSM Habitat in subreach E4 at 3000 cfs with hydraulically suitable areas labeled for larvae (green), juvenile (orange), and adult (light blue) and unsuitable inundated areas in dark blue.

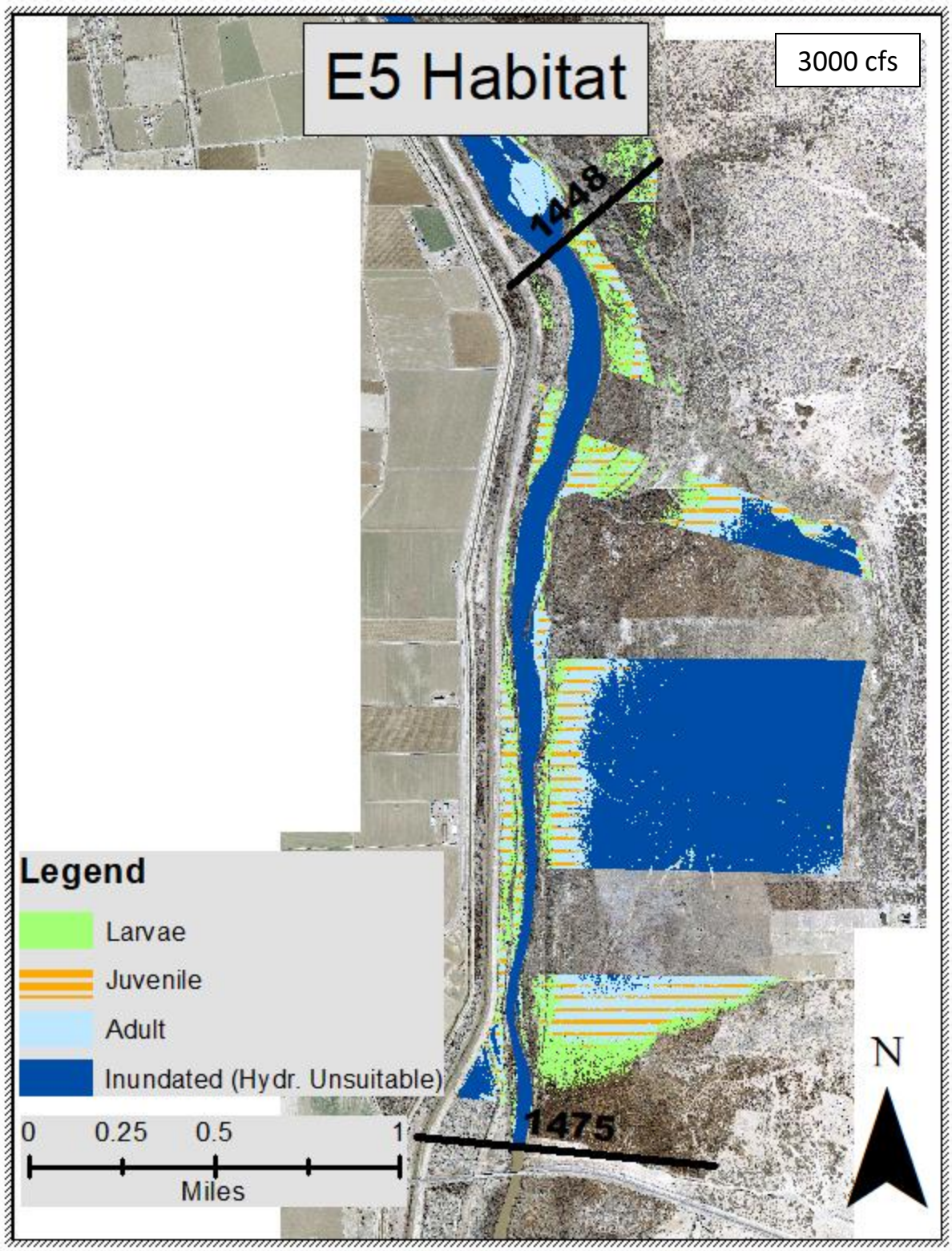

Figure E- 12 RGSM Habitat in subreach E5 at 3000 cfs with hydraulically suitable areas labeled for larvae (green), juvenile (orange), and adult (light blue) and unsuitable inundated areas in dark blue.

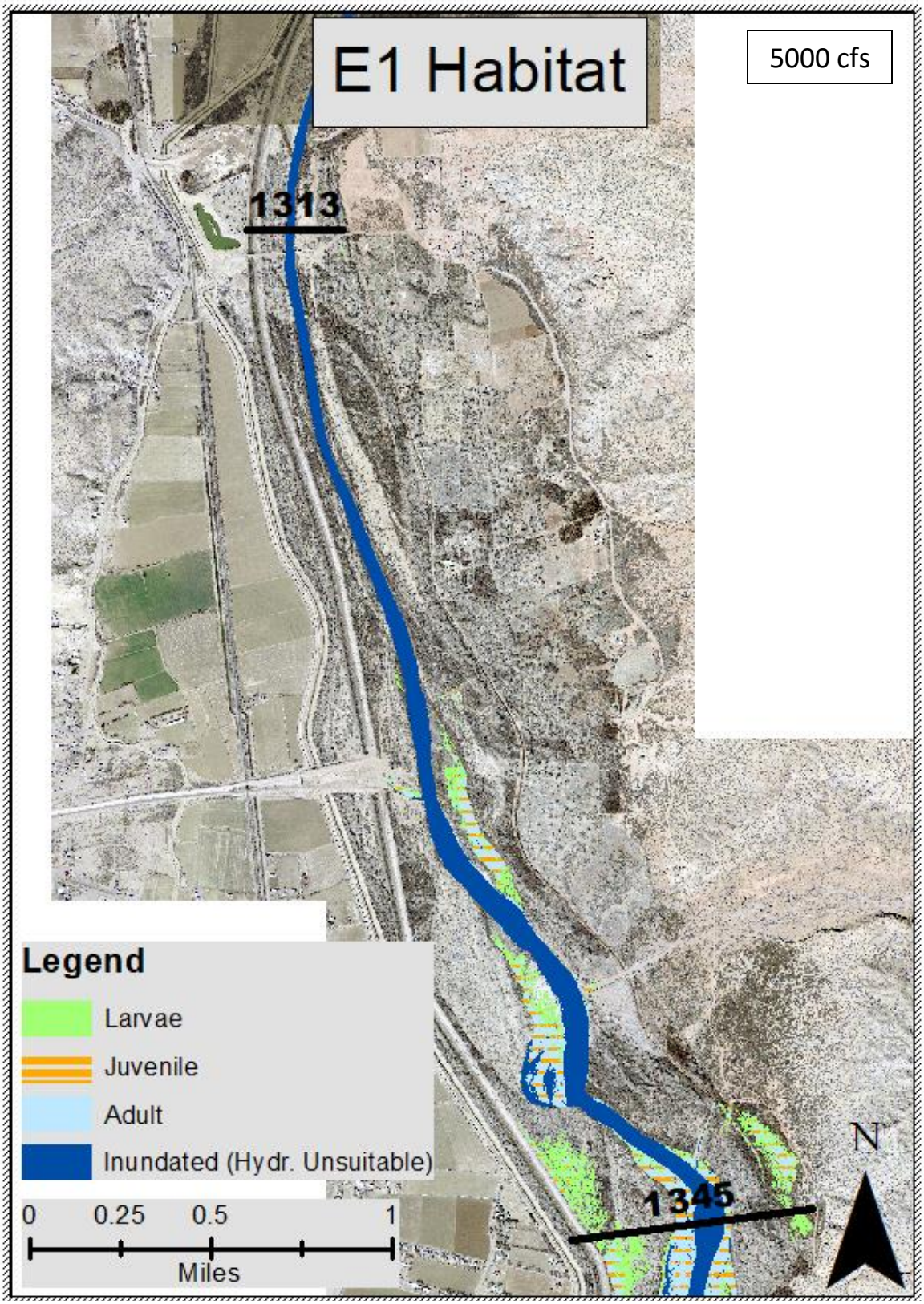

Figure E- 13 RGSM Habitat in subreach E1 at 5000 cfs with hydraulically suitable areas labeled for larvae (green), juvenile (orange), and adult (light blue) and unsuitable inundated areas in dark blue.

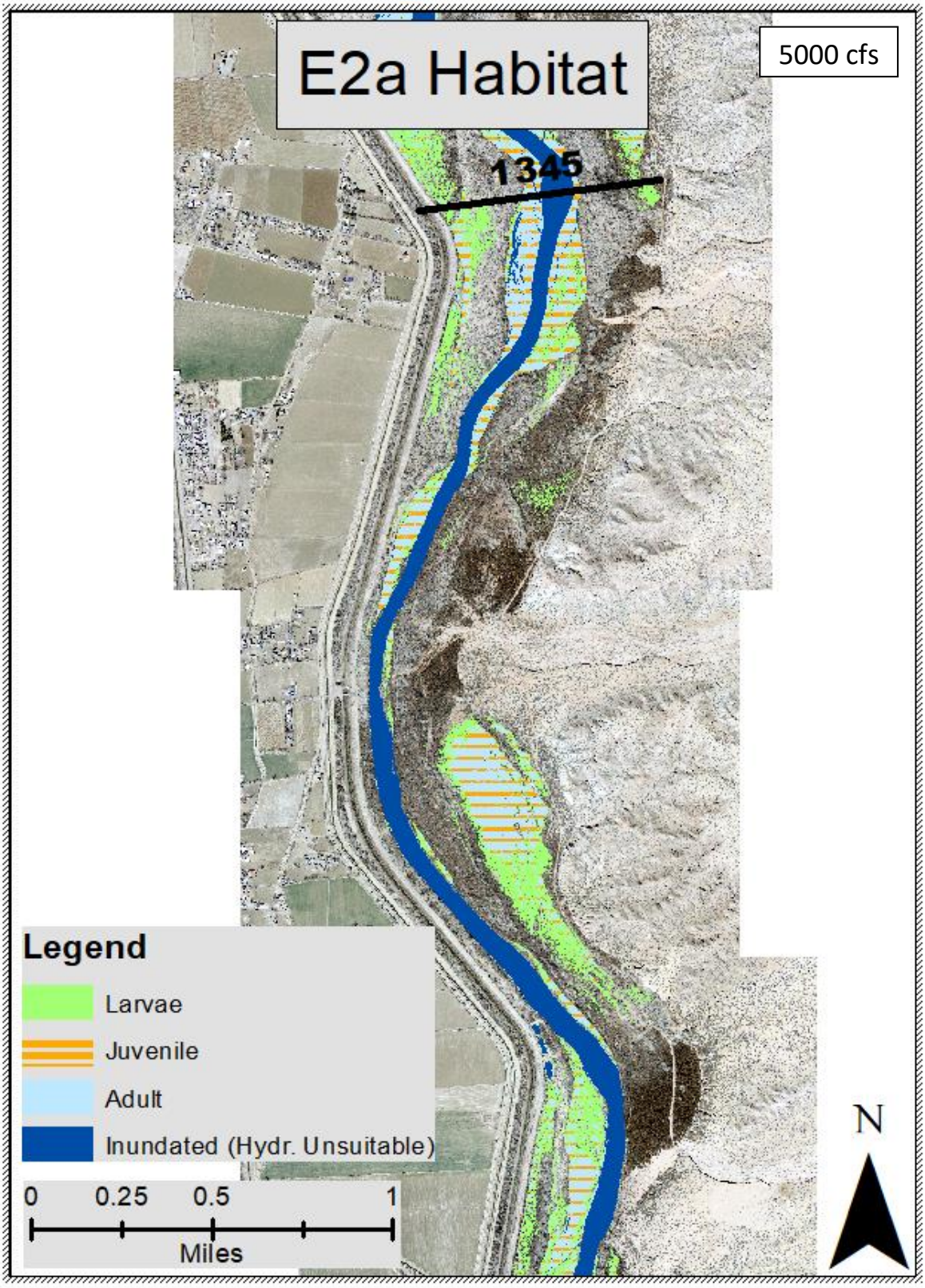

Figure E- 14 RGSM Habitat in subreach E2 (upstream portion part a) at 5000 cfs with hydraulically suitable areas labeled for larvae (green), juvenile (orange), and adult (light blue) and unsuitable inundated areas in dark blue.

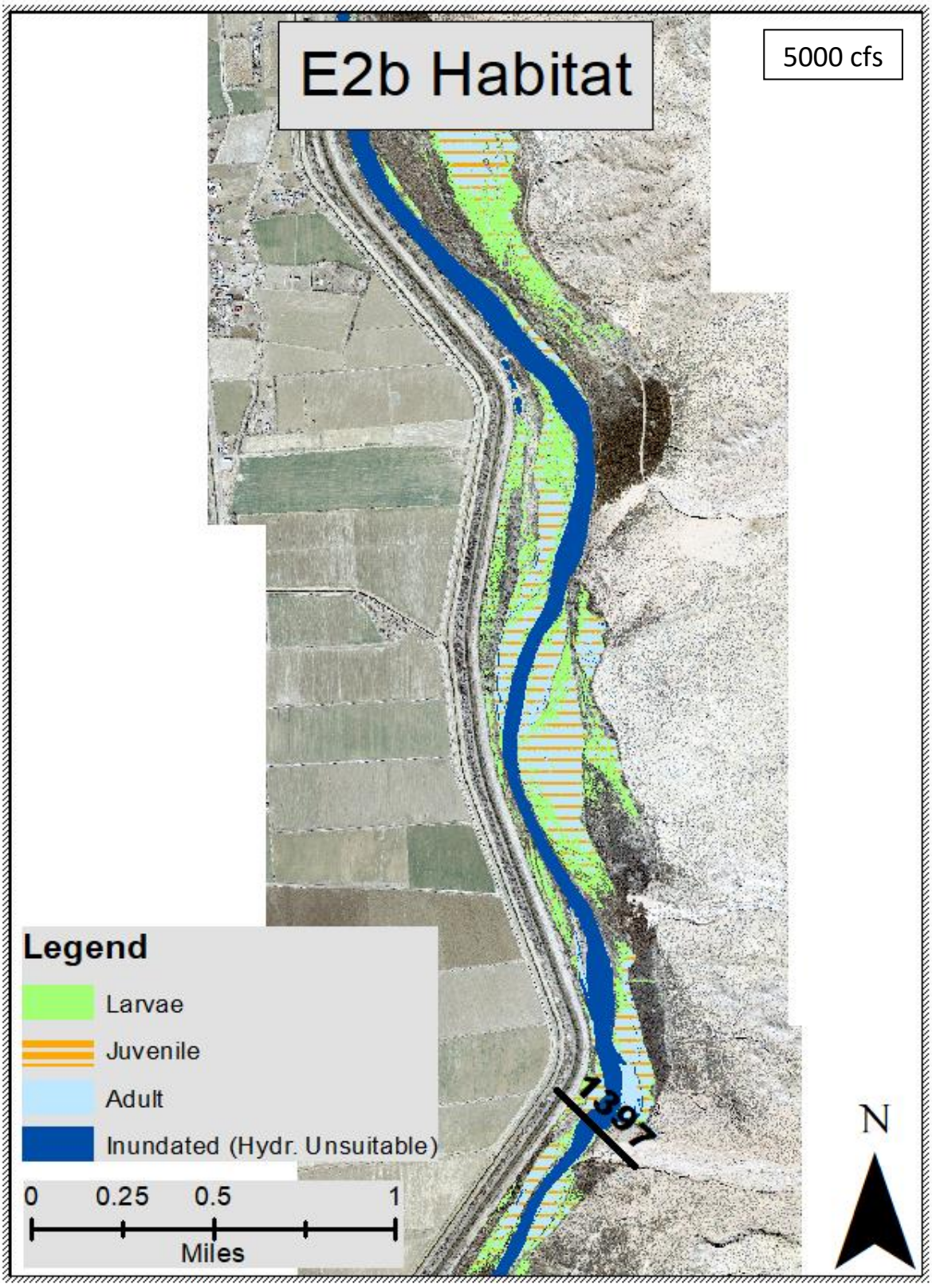

Figure E- 15 RGSM Habitat in subreach E2 (downstream portion part b) at 5000 cfs with hydraulically suitable areas labeled for larvae (green), juvenile (orange), and adult (light blue) and unsuitable inundated areas in dark blue.

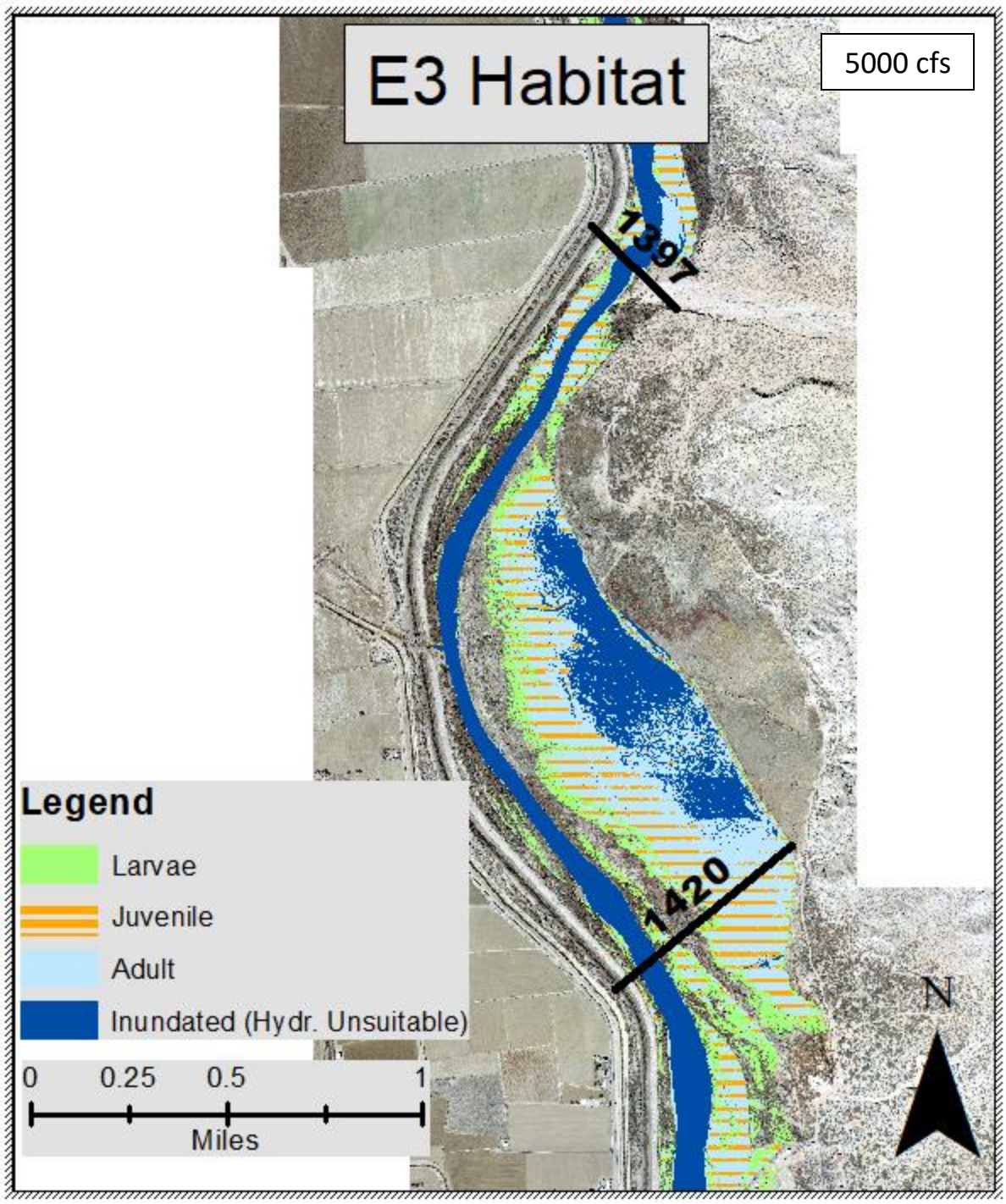

Figure E- 16 RGSM Habitat in subreach E3 at 5000 cfs with hydraulically suitable areas labeled for larvae (green), juvenile (orange), and adult (light blue) and unsuitable inundated areas in dark blue.

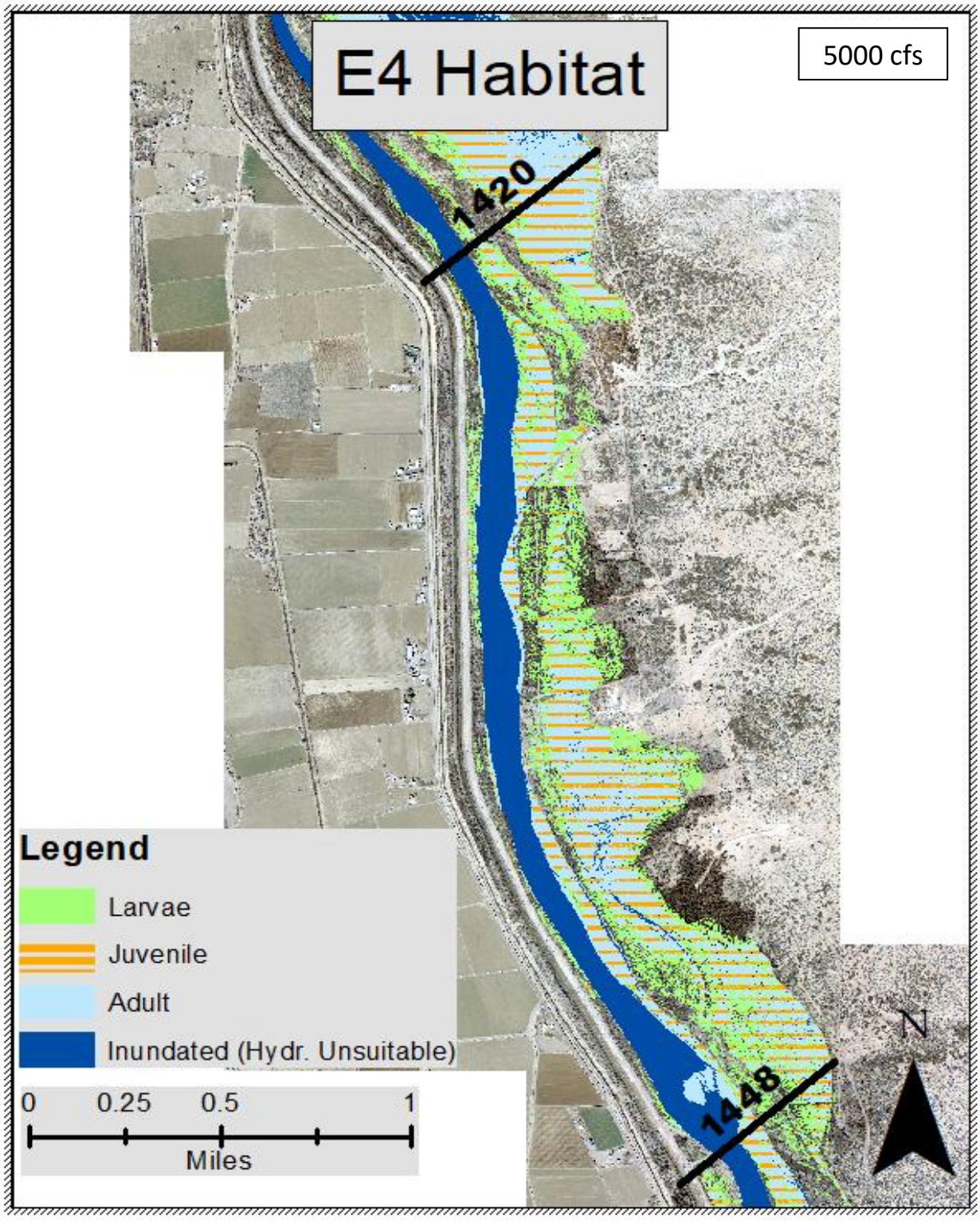

Figure E- 17 RGSM Habitat in subreach E4 at 5000 cfs with hydraulically suitable areas labeled for larvae (green), juvenile (orange), and adult (light blue) and unsuitable inundated areas in dark blue

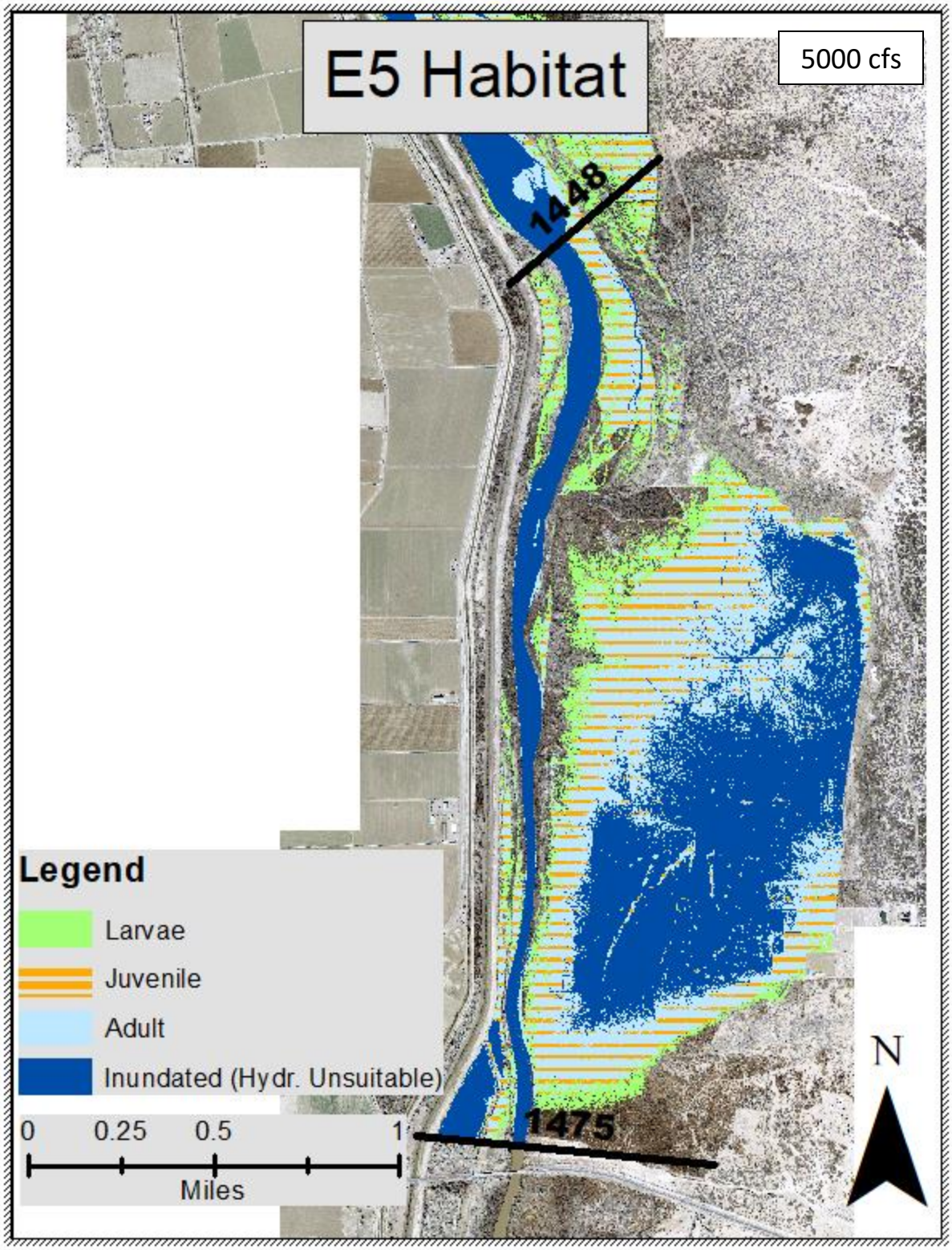

Figure E- 18 RGSM Habitat in subreach E5 at 5000 cfs with hydraulically suitable areas labeled for larvae (green), juvenile (orange), and adult (light blue) and unsuitable inundated areas in dark blue.

Appendix F

Geomorphology/Habitat Connection Figures for Process Linkage Report

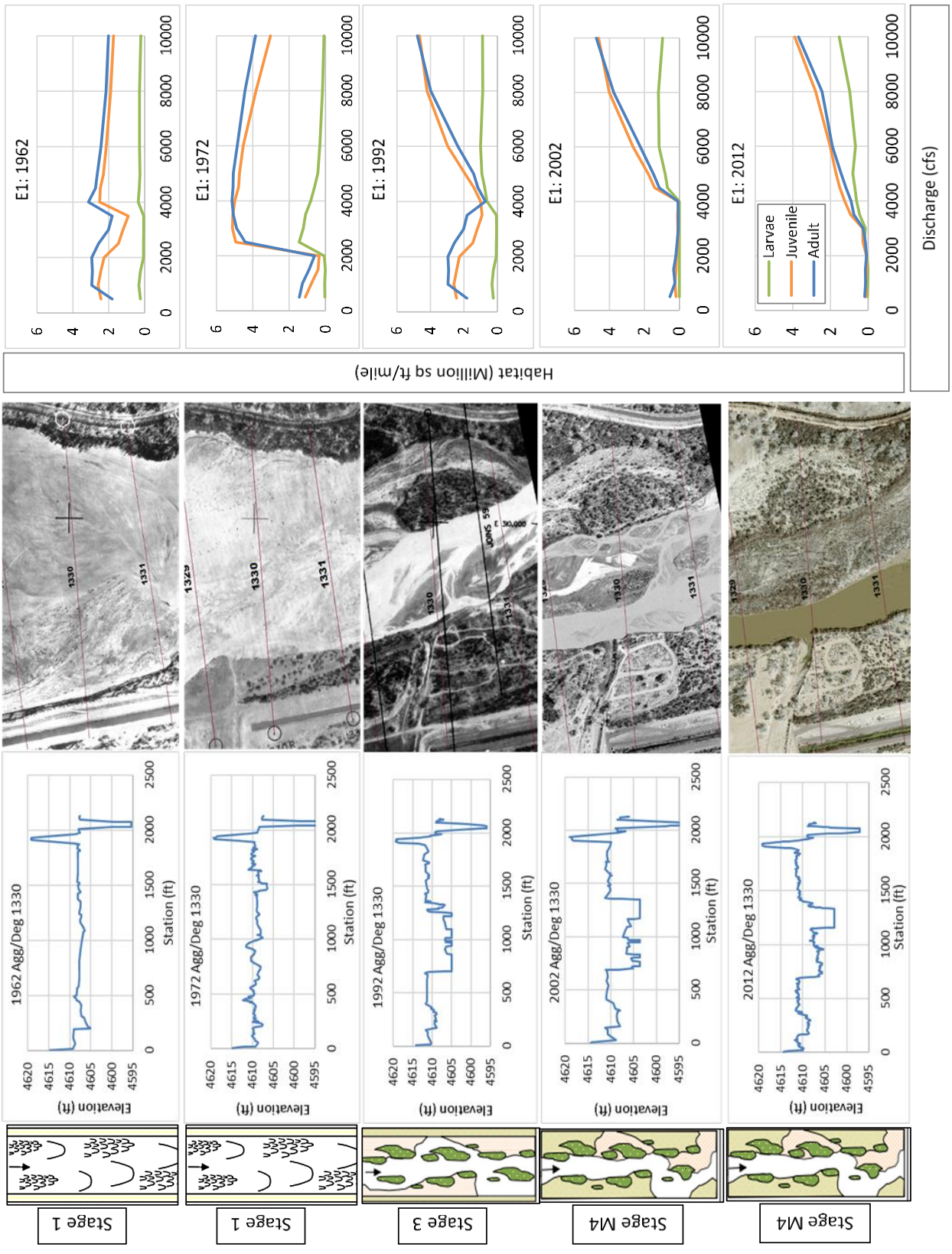

Figure F- 1 Geomorphology and habitat connections collage for subreach E1

Figure F- 2 Geomorphology and habitat connections collage for subreach E2

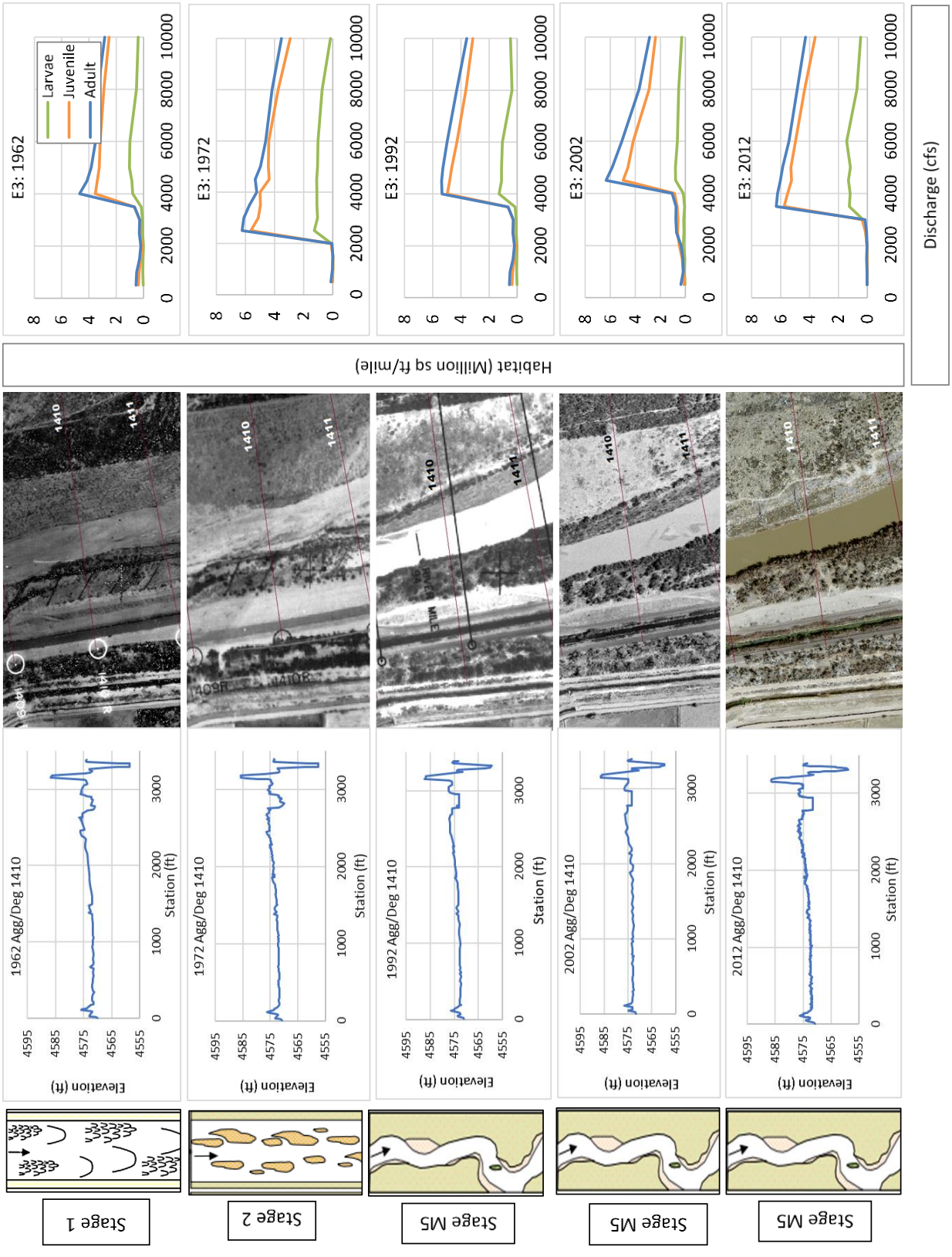

Figure F- 3 Geomorphology and habitat connections collage for subreach E3

Figure F- 4 Geomorphology and habitat connections collage for subreach E4

Figure F- 5 Geomorphology and habitat connections collage for subreach E5